ACHIRAL TEMPLATES IN ASYMMETRIC CATALYSIS: APPLICATIONS IN

CONSTRUCTION OF ALL CARBON QUATERNARY CENTERS

A Dissertation
Submitted to the Graduate Faculty
of the
North Dakota State University
of Agriculture and Applied Science

By

Hariharaputhiran Subramanian

In Partial Fulfillment of the Requirements
for the Degree of
DOCTOR OF PHILOSOPHY

Major Department:
Chemistry and Biochemistry

August 2018

Fargo, North Dakota

North Dakota State University
Graduate School

Title

ACHIRAL TEMPLATES IN ASYMMETRIC CATALYSIS:
APLICATIONS IN CONSTRUCTION OF ALL CARBON QUATERNARY
CENTERS

By

Hariharaputhiran Subramanian

The Supervisory Committee certifies that this ***disquisition*** complies with North Dakota State

University's regulations and meets the accepted standards for the degree of

DOCTOR OF PHILOSOPHY

SUPERVISORY COMMITTEE:

Mukund P. Sibi

Chair

Gregory R. Cook

Dean C. Webster

Christopher Colbert

Approved:

11/14/2018	Gregory R. Cook
Date	Department Chair

ABSTRACT

Conjugated olefins are readily available and inexpensive starting materials and their functionalization offers a rapid access to many important building blocks for organic synthesis. The functionalization of these olefins by asymmetric catalytic methods for the formation of C-C and C-X bonds is an active area of research. Major advances in this field are not only triggered by the development of new catalysts but also by engineering of new acceptor olefins. In our lab we have successfully developed acceptor olefins appended to alkoxyimidazoles as a novel template. Using these templated acceptors, we demonstrated methodologies to construct all carbon-quaternary centers, one of the demanding tasks in synthetic methodology development. We have also made significant efforts towards understanding the solution structures of the intermediates involved in the catalytic asymmetric reactions developed in our lab.

In chapter 1, the importance of templated acceptors in the field of chemical synthesis with special emphasis on acylimidazoles is reviewed. The versatility of the N-alkylimidazole templates is showcased by their utility in several organic transformations.

In chapter 2, modes of activation of acceptor olefins by catalysts, need for templated acceptors and challenges associated with designing an asymmetric catalytic process is described. Our approach in designing novel acceptors based on imidazoles is also described.

In chapter 3 the synthetic utility of these novel N-alkoxyimidazole based acceptors is shown by enantioselective construction of all carbon quaternary centers by Lewis-acid catalysis. We also compare the effectiveness of other templates such as oxazolidinone and N-methylimidazoles in the Lewis-acid catalyzed Friedel-Crafts alkylation reaction. The effect of various parameters such as Lewis acid, chiral ligands, temperature, additives and solvents on the conjugate addition of Friedel-Crafts nucleophiles are presented in this chapter.

In chapter 4, our research efforts toward understanding solution structures of intermediates involved in catalytic asymmetric reactions are presented. A combination of Diffusion Ordered Spectroscopy (DOSY), heteronuclear NMR spectroscopy, mass spectrometry and X-ray crystallography has been used to study the solution structure of intermediates involved in asymmetric catalytic reactions.

In chapter 5, a future outlook on templated chemistry developed in our laboratory is presented. Some preliminary results pertinent to future projects are presented.

DEDICATION

This work is dedicated to

My Family:

Mom and Dad

I would like to thank my family for all of your love and support through the tough times. Thank you for encouraging and supporting me through this whole process; I am very grateful for having such a wonderful family. I dedicate this thesis to you.

TABLE OF CONTENTS

LIST OF TABLES

LIST OF FIGURES

xvi

LIST OF ABBREVIATIONS

Å ....Angstrom

[α] ....Specific rotation (° mL/g dm)

Ac ....Acetyl

ACN...Acetonitrile

Aq ....Aqueous

Ar...Aryl

BA..Brønsted acid

BINOL..1,1'-Bi-2-naphthol

BINAP ....2-2'-Bis(diphenylphosphino)-1,1'-binaphthyl

Boc...tert-Butoxy carbonyl

BOX..Bis(oxazoline)

Bn ....Benzyl

BuLi ....Butyl Lithium

t-Bu ....tert-Butyl

Calcd..Calculated

CBS..Chiral Brønsted acid

CLA ....Chiral Lewis acid

δ ....Chemical shift in parts per million

DABCO ....1,4-Diazabicyclo[2.2.2]octane

DBFOX...4,6-Dibenzofurandiyl-2,2'-bis(oxazoline)

DBU...Diazabicyclo[5.4.0]undec-7-ene

DCM ....Dichloromethane

Dil..Dilute

DIPA...Diisopropylamine

min	Minute(s)
mL	millimeter
mol	Moles
Mol.Wt	Molecular weight
MS	Molecular Seives
n	normal
NaCl	Sodium chloride
$NaHCO_3$	Sodium bicarbonate
Na_2SO_4	Sodium sulfate
NMR	Nuclear magnetic resonance
nOe	Nuclear Overhauser effect
Nu	Nucleophile
NTf_2	Bis(trifluromethane) sulfonimide
o	ortho
OBn	Benzyloxy
OTf	Triflate
p	para
Ph	Phenyl
ppm	Parts per million
i-Pr	Isopropyl
Pybox	Pyridine-2,6-bis(oxazoline)
rt	Room temperature
Si	Silicon
TBDMS	tert-Butyldimethylsilyl
TBDPS	tert-Butyldiphenylsilyl

CHAPTER 1. IMIDAZOLE TEMPLATES IN ASYMMETRIC CATALYTIC REACTIONS

1.1. Introduction

α,β-Unsaturated carbonyl compounds are most important class of organic molecules as they are readily available starting materials. They are important building blocks and relatively inexpensive or can be prepared in few synthetic steps. These substrates are very well suited for asymmetric catalysis. Using catalytic methods, the activated alkenyl fragment, the carbonyl fragment or the whole α,β-unsaturated carbonyl (both alkenyl and C=O fragments) can be functionalized (Scheme 1.1). In asymmetric catalytic reactions a chiral activator activates these compounds. These chiral activators could be a metal/chiral ligand complex acting as a Lewis acid or a chiral small organic molecule such as thioureas or phosphoric acids acting as organocatalysts (Scheme 1.1). The mode of activation assumes either coordination of the Lewis basic O atom of the carbonyl to the chiral Lewis acid, involves in hydrogen bonding interactions or complete protonation.

Diels-Alder reaction

Hetero Diels-Alder reaction

1,3-dipolar cycloaddition reaction

α,β-functionalization

Cyclopropanation, epoxidation, aziridination

X

β-functionalization

1,2- functionalization

Michael reaction

*C

Aldol reaction

Friedel-Crafts reaction

C* - chiral activator

Mukaiyama aldol reaction

Aza-, thio-, phospha- Michael reaction

Chiral metal ligand catalysis

C=O reduction

Conjugate radical addition

Chiral organocatalysis

C=O arylation

Chiral iminium ion catalysis
(applicable only if X = H or C)

Henry aldol reaction

C=O alkylation

Scheme 1.1. Versatility of α,β-unsaturated carbonyl compounds

There is another mode of activation (chiral iminium ion catalysis), which is applicable to aldehydes and ketones, where the carbonyl functionality forms a chiral iminium ion with chiral secondary amine catalyst. The activation is a direct result of lowering the LUMO of the α,β-unsaturated carbonyl compounds thereby a facile reaction can happen with a nucleophile.

The modes of coordination of unsaturated carbonyl compounds to a chiral activator are important when designing a stereoselective reaction. Accordingly several kinds of α,β-unsaturated carbonyl compounds that differ in modes of coordination have been designed and successfully used in asymmetric catalytic reactions.[1] Some of these compounds are shown in figure 1.1. These activators are classified according to the type of chelates they form. Simple ketone such as **1.1** forms a monodentate coordination, which generally leads to poor discrimination. Hence compounds **1.2-1.8** capable of forming bidentate coordination have been developed.[1] Classification of substrates such as **1.2 - 1.4, 1.6, 1.8** has been reviewed.[1]
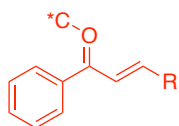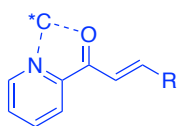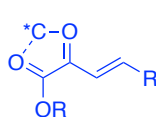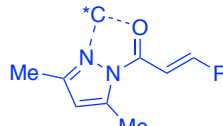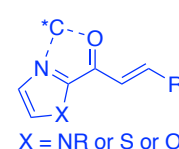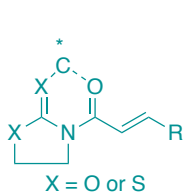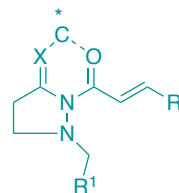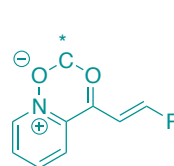
Figure 1.1. α,β-Unsaturated carbonyl compounds showing different modes of coordination

1.2. Acylimidazoles as bidentate coordinating substrates in asymmetric catalytic reactions

As it is directly related to our research and latest developments with compounds of type **1.5** this chapter will focus on recent developments on the use of this class in asymmetric catalysis.

1.2.1. Asymmetric Friedel-Crafts reaction

2-alkylimidazole was used as a masked equivalent of esters, amides aldehydes etc. in the late 1980s.[2] The fact that 2-acylimidazole can be used as latent functionality and also the realization that it can act as a bidentate coordinating substrate led Evans et al. to the development of asymmetric Friedel-Crafts alkylation (Scheme 1.2).[3] In their study, a scandium triflate indane-derived pyridinebisoxazoline ligand combination was used as a catalyst for the Friedel-Crafts alkylation of indoles. As low as 1 mol% of catalyst can effect the reaction with very high selectivity. By comparison the monodentate substrate gave poor yield and enantioselectivity in the reaction.
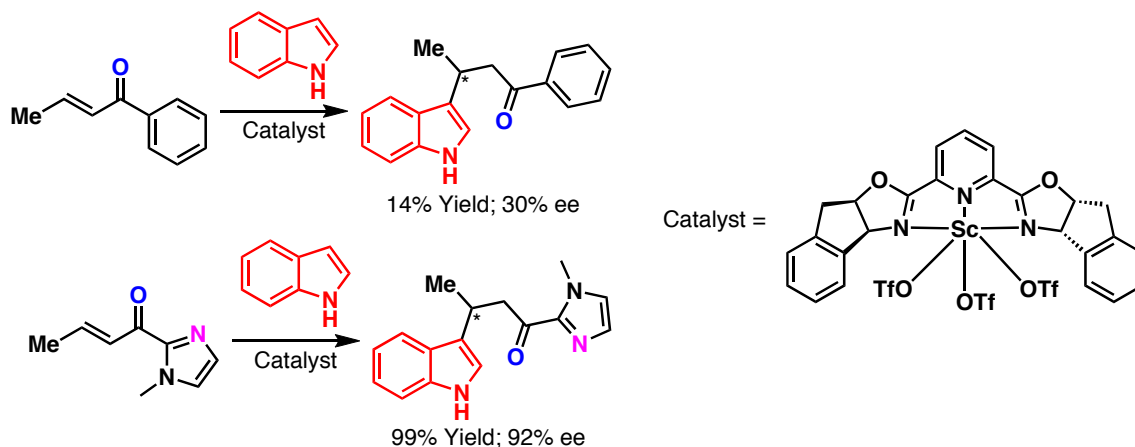
Scheme 1.2. First catalytic asymmetric reaction using N-methylimidazole as template

Evans et al. also reported Friedel-Crafts reaction where pyrroles like **1.8** were competent nucleophiles under Sc(OTf)₃/**1.10** chiral Lewis acid catalysis. The authors used a bulky N-isopropyl group as N-1 substituent instead of an N-methyl group. Good chemical yields and

excellent enantioselectivities were obtained in the asymmetric process.[4] The authors showcased

the methodology by enantioselective synthesis of alkaloid (+)-heliotridane.
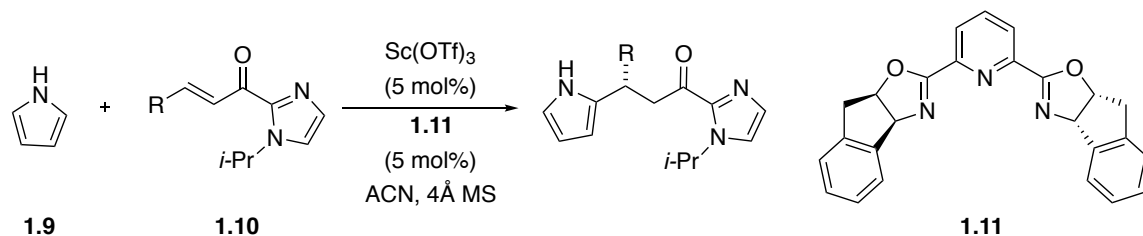
Scheme 1.3. Pyrrole alkylation of N-isopropylacylimidazoles

Recently, Meggers and coworkers reported chiral-at-metal iridium (III) complexes for

Friedel-Crafts alkylation of indole to α,β-unsaturated 2-acylimidazoles (Scheme 1.4).[5] In their

study metal-coordination-based asymmetric catalyst having metal centrochirality is reported. The

reaction showed good acylimidazole scope and good indole scope. Very low catalytic loadings

were required (0.25-2 mol%). The C_2-symmetrical Ir (I) complex activates the α,β-unsaturated

2-acylimidazoles through N,O-coordination and one face of the alkene is shielded by a bulky

tert-butyl group to furnish the product with excellent enantioselectivity. The authors have

extended this protocol to other arenes such as pyrroles, furans and electron-rich benzene

derivatives.
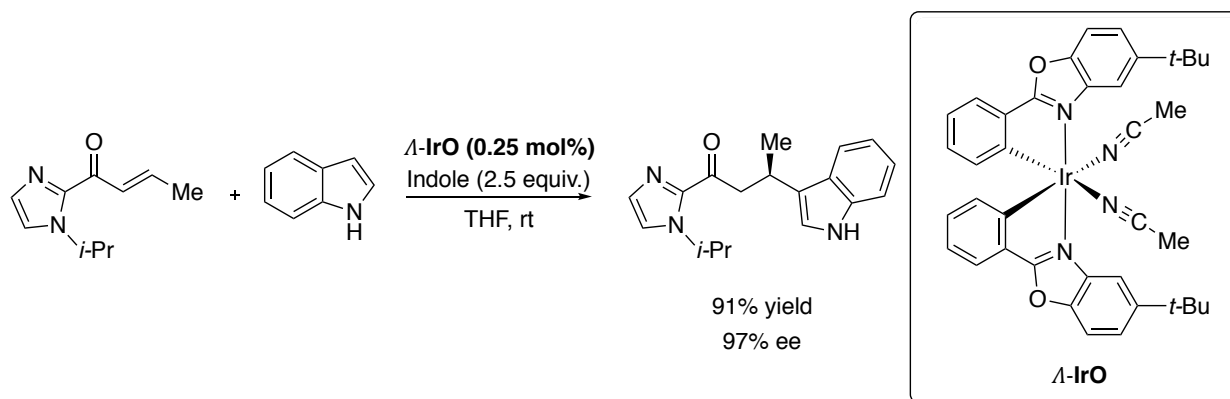
Scheme 1.4. Asymmetric Friedel-Crafts alkylation of indoles catalyzed by chiral-at-iridium
complex

1.2.2. Conjugate addition of silyl ketene acetals: Mukaiyama-Michael reactions

Recently, Singh and co-workers have reported highly diastereoselective and enantioselective addition of 2-silyloxyfuran as pronucleophiles (Scheme 1.5).[7] Scandium triflate/**1.10** combination was found to catalyze the reaction with high diastereoselectivity (>20:1) and high enantioselectivity. 5-methyl-siloxyfurans were also found to be highly competent in the reaction. Hence two contiguous stereocenters with one quaternary substituted center can be synthesized by this methodology with control of relative and absolute stereochemistry.
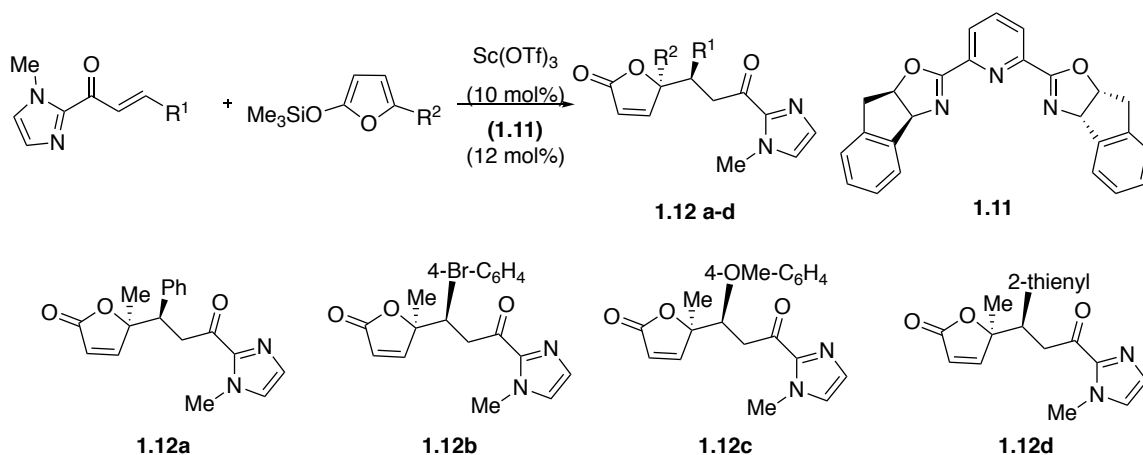
Scheme 1.5. Mukaiyama-Michael addition of 2-siloxyfurans

1.2.3. Cycloaddition reaction

Evans and coworkers have reported the use of imidazole templates in cycloaddition reactions. In a Ce(OTf)$_4$/Desimoni type pyridine bisoxazoline ligand **1.13** combination nitrone (1,3-dipole) added to α,β-unsaturated 2-acylimidazoles form a chiral oxazolidine product in high selectivity. Three contiguous stereocenters are formed in the process with a very high selectivity for endo isomer (dr > 99:1) and high enantioselectivity for isooxazolidine (Scheme 1.6).[8]
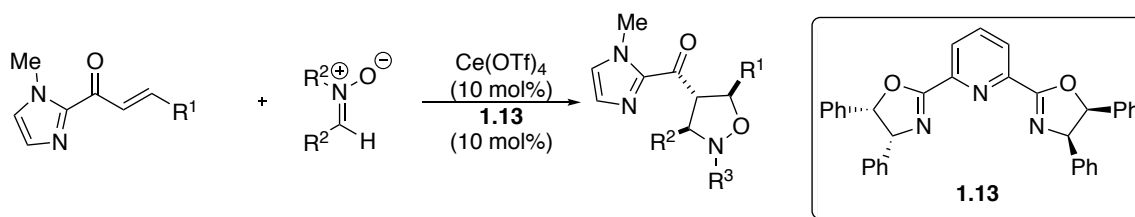
Scheme 1.6. [3+2] nitro cycloaddition to α,β-unsaturated 2-acylimidazoles

Sibi and coworkers have used chiral N-triflyl phosphoramide **1.14** as a Brønsted acid

catalyst to effect nitrone cycloaddition reactions. α,β-Unsaturated 2-acylimidazoles in the

presence of a chiral activator such as **1.14** underwent cycloaddition with nitrones to form

isooxazolidine. Unlike Evans' case they observed the exo-stereoisomer as the major product in

good yield and high enantioselectivity (up to 90:10 er) (Scheme 1.7).[9]
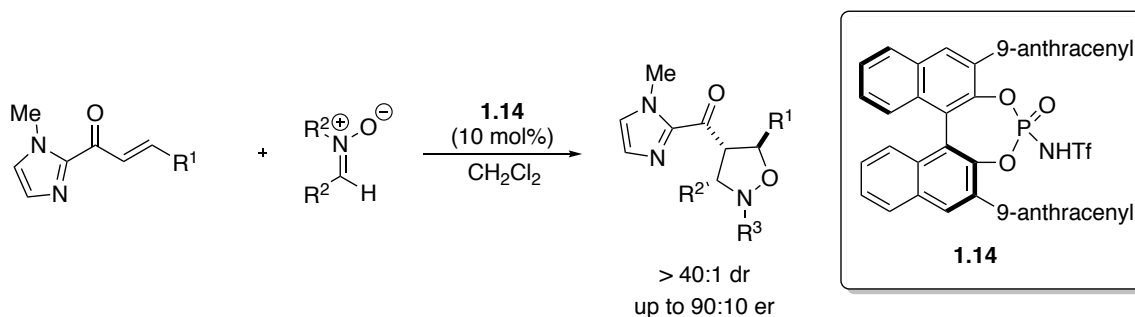
Scheme 1.7. Exo-selective nitrone cycloaddition to α,β-unsaturated 2-acylimidazoles

Yoon and co-workers reported photocatalytic [2+2] cycloaddition of N-methylimidazole

based enones. α,β-Unsaturated 2-imidazolyl ketones underwent [2 + 2] cycloaddition with a

variety of Michael acceptors upon irradiation with visible light in the presence of $Ru(bpy)_3^{2+}$.

Cleavage of the imidazolyl auxiliary from the cycloadducts affords cyclobutane carboxamides,

esters, thioesters, and acids that would not be accessible from direct cycloaddition of the

corresponding unsaturated carbonyl compounds (Scheme 1.8).[10]
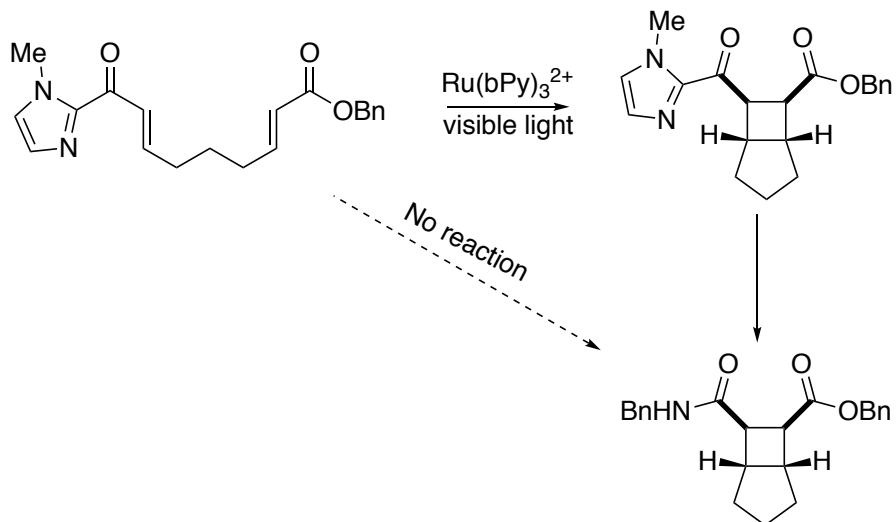
Scheme 1.8. Photocatalytic intramolecular [2+2] cycloaddition

The authors also studied the effect of other bidentate coordinating templates in the reaction. The templated substrates include monodentate n-pyrroloyl enone **1.15**, bidentate acylphosphonates **1.16**, 3,5-dimethylpyrrazolylenone **1.17** and N-methylacylimidazole **1.18** (Scheme 1.9). From the CV studies they showed that compound **1.18** reduced at lower reduction potential and was a successful template under the reaction conditions.

Scheme 1.9. Dimerization of templated enones
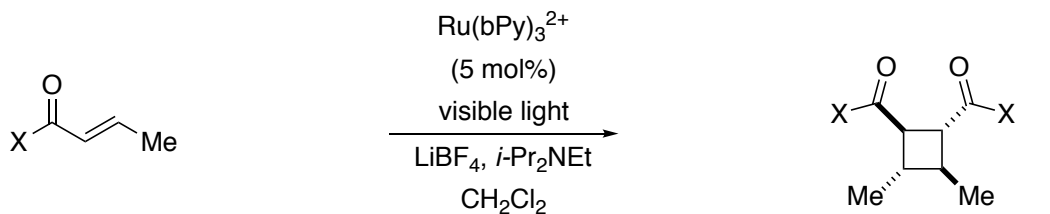
Entry	Substrate	E_{red}	Yield (%)
1.	1.15	-1.80 V	0
2.	1.16	-1.87 V	16
3.	1.17	-2.39 V	<5
4.	1.18	-1.32 V	82%

1.2.4. Asymmetric allylic alkylation

Trost et al. have reported Pd catalyzed asymmetric allylic alkylation of 2-acylimidazoles as ester enolate equivalents. A wide variety of enantioenriched 2-acylimidazoles were synthesized using this decarboxylative asymmetric alkylation. The authors show cased the synthetic utility of this protocol in a short synthesis of cetiedil (Scheme 1.10), an anti-sickling compound.
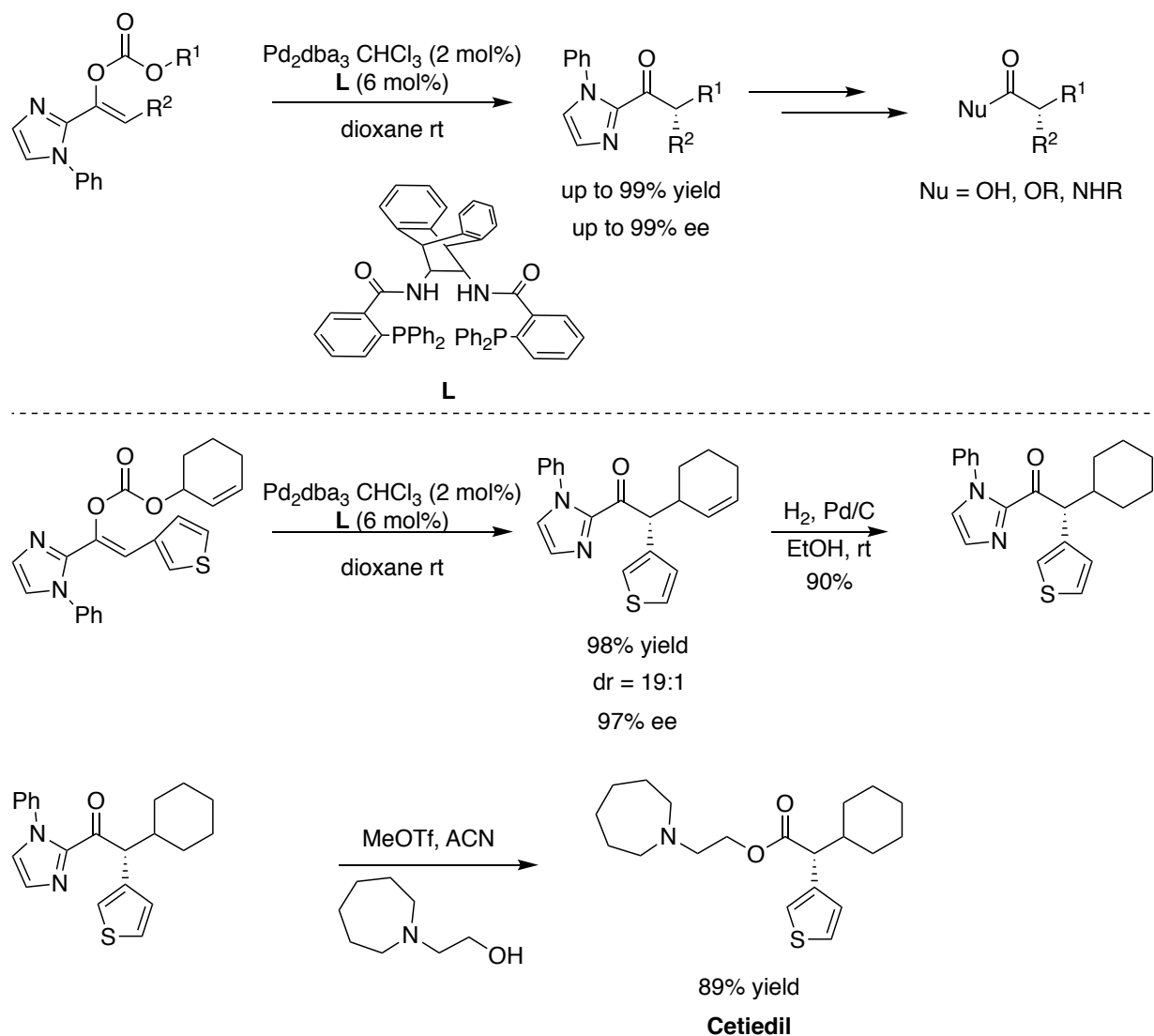
Scheme 1.10. Pd-catalyzed asymmetric allylic alkylation of 2-acylimidazoles

1.2.5. Enolate coupling reactions

The photophysical and photochemical properties of bis-cyclometalated iridium complexes are well precedented.[12] Meggers et al. used these complexes as photocatalysts in enolate coupling reactions. The iridium complexes Λ-IrS and Δ-IrS in presence of visible light, catalyzed the reaction between 2-acylimidazoles **1.19** electron-deficient benzylbromide or phenacyl bromides to give high yields of α-alkylated products with excellent enantioselectivities

(Scheme 1.11).[13] The authors expanded the scope of this reaction to α-trichloromethylation, α-trifluoromethylation and α-perfluoroalkylation of 2-acylimidazoles.[14,15]
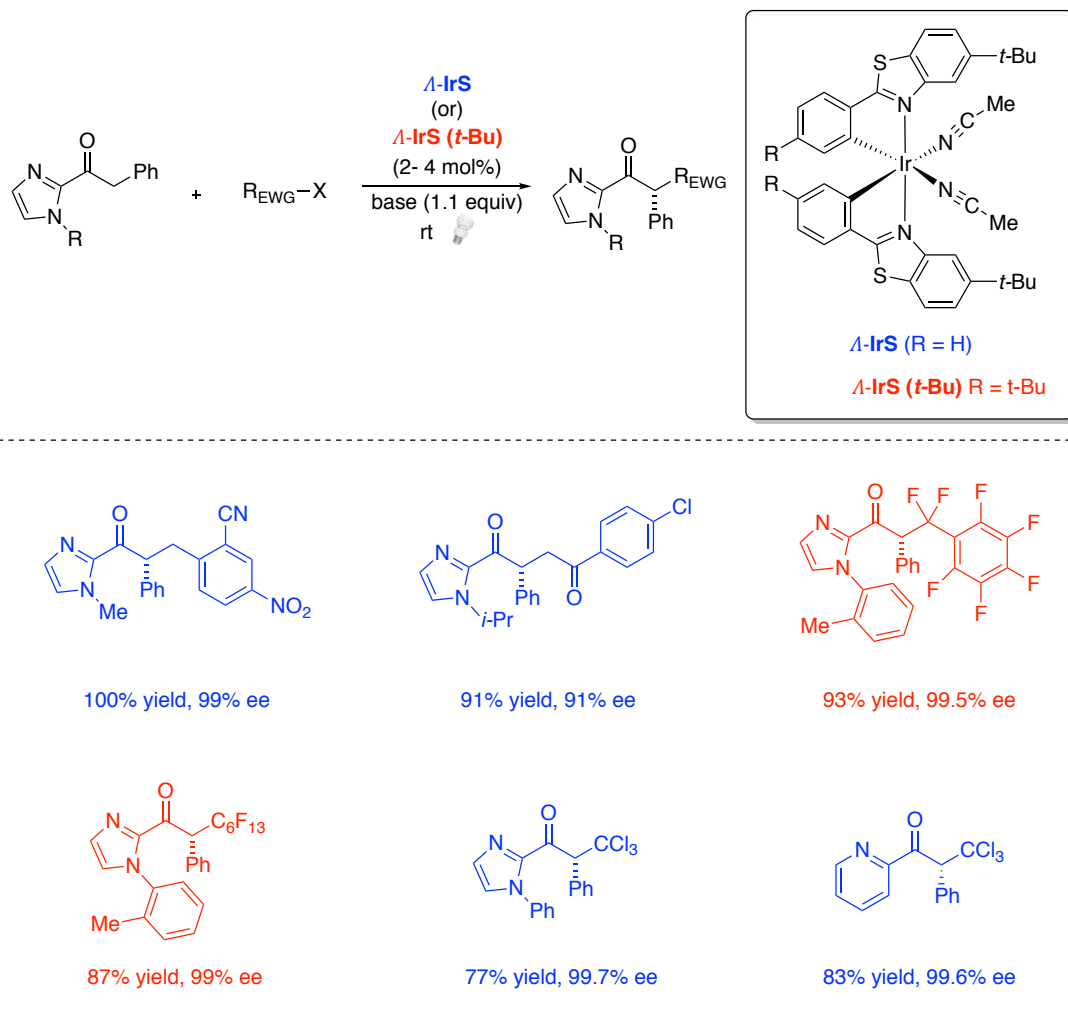
Scheme 1.11. Cooperative asymmetric-photoredox catalysis for enolate coupling

Mechanistic investigations conducted by the authors support the mechanism provided in Scheme 1.12.[13] Asymmetric catalysis starts with replacement of two labile acetonitrile ligands in the catalyst by the substrate 2-acylimidazole in a bidentate fashion to form intermediate **1.20**, which on deprotonation by a base gives iridium enolate **1.21**. In the enantiodetermining step the reductively generated electrophilic radical adds to electron-rich enolate double bond to give iridium-coordinated ketyl radical **1.22**. The following SET oxidation step furnishes product

bound catalyst. Subsequent product release and acylimidazole coordination complete the catalytic cycle. The authors determined that the enolate complex **1.21** acts as a photo-sensitizer, which upon absorption of light transfers an electron to generate a radical species that takes part in the reaction.
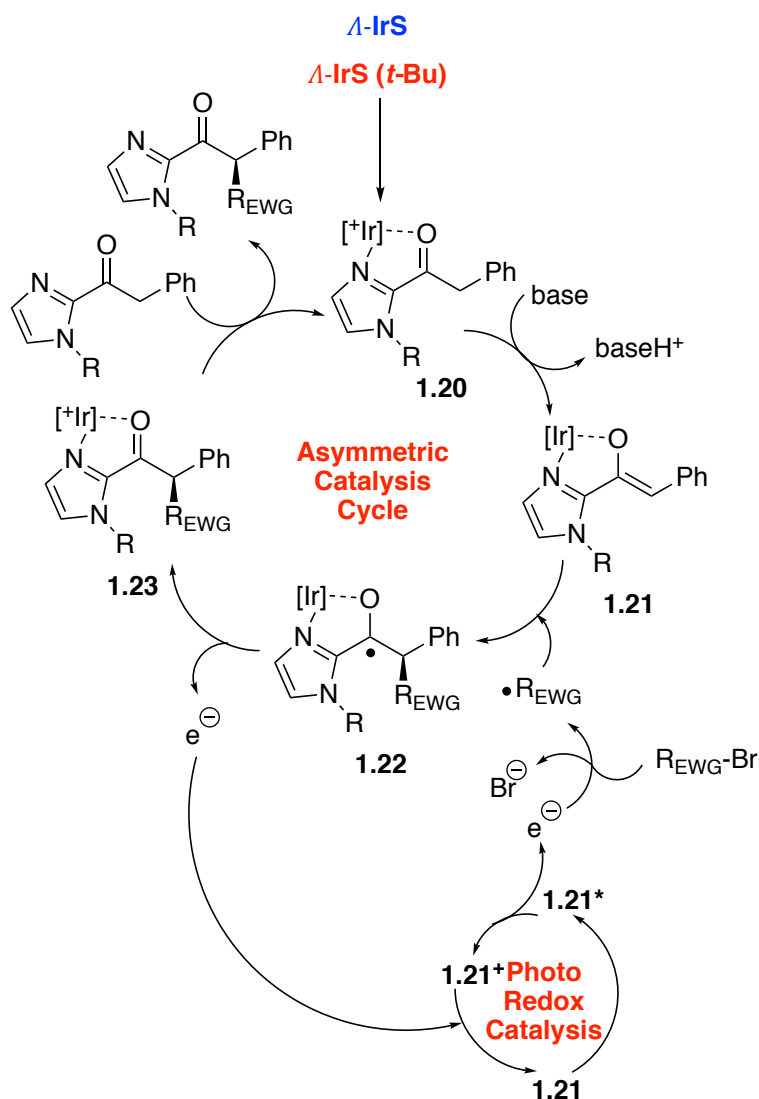
Scheme 1.12. Proposed mechanism for cooperative asymmetric/photoredox catalysis with Ir complex

Meggers et al. also reported photocatalyzed oxidative α-alkylation.[16] The authors chose oxidation of α-silylamines as the model system. When 2-phenylacetyl-1-methylimidazole **1.24a** was treated with N,N-diphenyl-N-(trimethylsilyl)methylamine **1.25a** in presence of Λ-IrO as the

catalyst, visible light irradiation gave the aminoalkylated product **1.26a** in 34% yield and 91%

ee. The reaction depended on N-substitution of the imidazole. **1.24a** gave the product **1.26a** in

34% yield, **1.24c** (R = Ph) gave the product **1.26c** (R = Ph) in 92% yield and 97% ee. When

catalyst Λ-IrS was used instead, the product **1.26c** was obtained only in 51% yield after 20h or

irradiation (Scheme 1.13).

Substrate	R	Product	catalyst	time (h)	yield %	ee (%)
1.24a	Me	**1.26a**	Λ-IrO	20	34	91
1.24b	i-Pr	**1.26b**	Λ-IrO	20	48	90
1.24c	Ph	**1.26c**	Λ-IrO	6.5	92	97
1.24c	Ph	**1.26c**	Λ-IrS	20	51	97
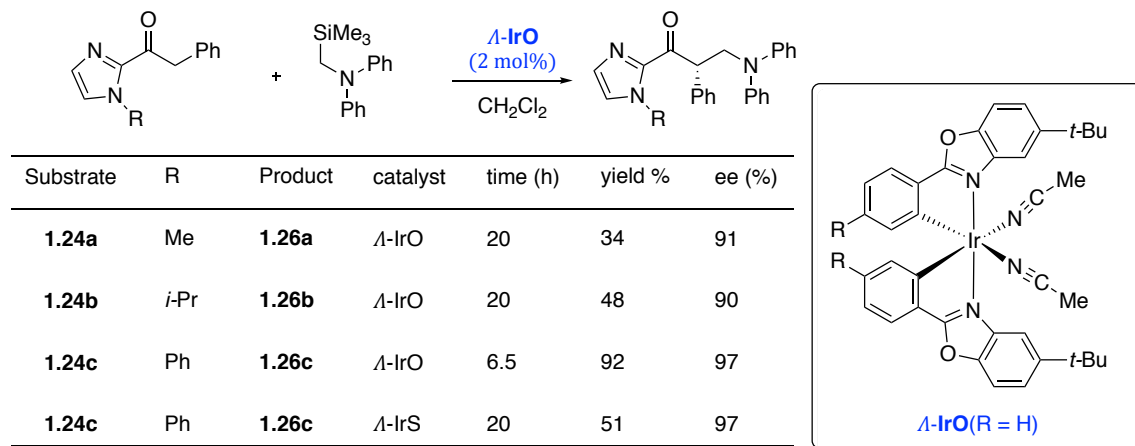
Scheme 1.13. Effect of N-substituent on the oxidative α-aminoalkylation

The reaction showed very good scope with respect to acylimidazole as well as

silylamines (Scheme 1.14). In this case a cationic intermediate formed after chelation to

acylimidazole to act as a weak oxidant.
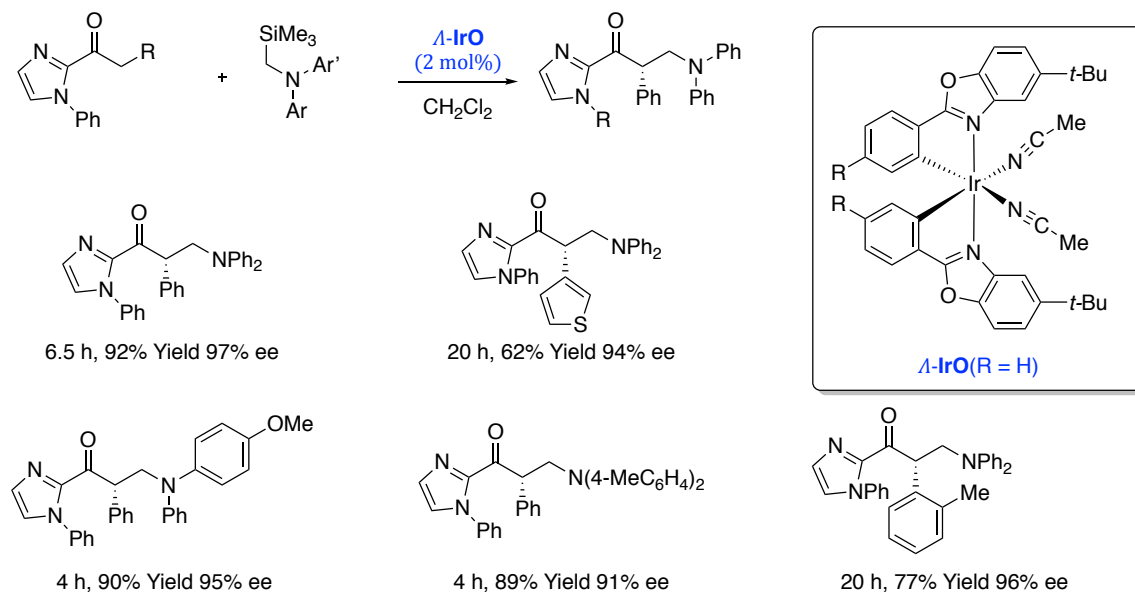
Scheme 1.14. Photoinduced enantioselective α-aminoalkylation

1.3. Conclusions

Although it has been more than a decade since the first use of imidazoles as a template/auxiliary in asymmetric catalytic reaction, there are only very few reports on the use of these templated acceptors in stereoselective transformations. With the advances in multi-catalytic systems the past 5 years have seen the synthetic community using acylimidazole substrates in new catalytic transformations such as enolate couplings. A better understanding of the structural characteristics of the intermediates involved in this reaction will unlock the potential of these substrates towards other reactions.

1.4. References

1. (a) Desimoni, G.; Faita, G.; Quadrelli, P. *Chem. Rev.* **2014**, *114*, 6081. (b) Desimoni, G.; Faita, G.; Quadrelli, P. *Chem. Rev.* **2015**, *115*, 9922.

2. (a) Miyashita, A.; Suzuki, Y.; Nagasaki, I.; Ishiguro, C.; Iwamoto, K.-I.; Higashino, T. *Chem. Pharm. Bull.* **1997**, *45*, 1254-1258. (b) Ohta, S.; Hayakawa, S.; Nishimura, K.; Okamoto, M. *Chem. Pharm. Bull.* **1987**, *35*, 1058-1069.

3. (a) Evans, D. A.; Fandrick, K. R.; Song, H.-J. *J. Am. Chem. Soc.* **2005**, *127*, 8942. (b) Evans, D. A.; Fandrick, K. R.; Song, H.-J.; Scheidt, K. A.; Xu, R. *J. Am. Chem. Soc.* **2007,** *129,* 10029.

4. Evans, D. A.; Fandrick, K. R. *Org. Lett.* **2006**, *8*, 2249.

5. Huo, H.; Fu, C.; Harms, K.; Meggers, E. *J. Am. Chem. Soc.* **2014**, *136*, 2990.

6. Shen, X.; Huo, H.; Wang, C.; Zhang, B.; Harms, K.; Meggers, E. *Chem. – A Eur. J.* **2015**, *21*, 9720.

7. Rout, S.; Das, A.; Singh, V. K. *Chem. Commun.* **2017**, *53*, 5143.

8. Evans, D. A.; Song, H.-J.; Fandrick, K. R. *Org. Lett.* **2006**, *8*, 3351.

9. Rane, D. S.; Sibi, M. P. unpublished data.

10. Tyson, E. L.; Farney, E. P.; Yoon, T. P. *Org. Lett.* **2012**, *14*, 1110.

11. Trost, B. M.; Lehr, K.; Michaelis, D. J.; Xu, J.; Buckl, A. K. *J. Am. Chem. Soc.* **2010**, *132*, 8915.

12. Flamigni, L.; Barbieri, A.; Sabatini, C.; Ventura, B.; Barigelletti, F. Photochemistry and Photophysics of Coordination Compounds Iridium. *Top. Curr. Chem.* **2007,** *281,* 143.

13. Huo, H.; Shen, X.; Wang, C.; Zhang, L.; Röse, P.; Chen, L.-A.; Harms, K.; Marsch, M.; Hilt, G.; Meggers, E. *Nature* **2014**, *515*, 100.

14. Huo, H.; Wang, C.; Harms, K.; Meggers, E. *J. Am. Chem. Soc.* **2015**, *137*, 9551.

15. Huo, H.; Huang, X.; Shen, X.; Harms, K.; Meggers, E. *Synlett* **2016**, *27*, 749.

16. Wang, C.; Zheng, Y.; Huo, H.; Röse, P.; Zhang, L.; Harms, K.; Hilt, G.; Meggers, E. *Chem. – A Eur. J.* **2015**, *21*, 7355.

CHAPTER 2. NOVEL IMIDAZOLE TEMPLATES: CONCEPTS, CHALLENGES AND DESIGN

2.1. Introduction

Conjugated olefins are readily available and inexpensive starting materials, and their functionalization offers a rapid and versatile access to many important building blocks for organic synthesis. The functionalization of these olefins by asymmetric catalytic methods for the formation of C-C and C-X bonds is an active area of research. Reactions involving simple conjugate addition of nucleophiles (both carbon as well as hetero-atoms), as well as reactions utilizing cycloaddition or cyclization strategies have emerged as most useful and atom economical approaches for the construction of carbon-carbon and carbon-heteroatom bonds stereoselectively (Scheme 2.1).[1-8]
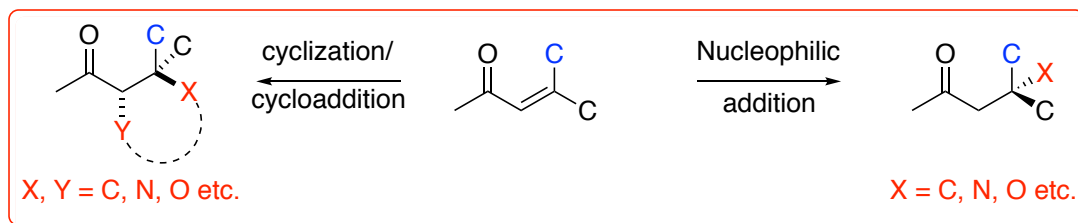
Scheme 2.1. Generic scheme showing functionalization of conjugated olefins

Major advances in this field were not only triggered by the development of new catalysts but also by the engineering of new acceptor templates.[9, 10] In addition to providing chemical versatility to the adducts obtained in the reactions, the template also plays an important role in controlling the reactivity and selectivity. In other words, properly designed templates might be conducive to performing challenging asymmetric transformations such as the construction of all carbon quaternary centers.[11-13]

2.2. α,β-Unsaturated carbonyl compounds as acceptor olefins and modes of activation

Among the several acceptor olefins used, α,β-unsaturated carbonyl compounds (such as conjugated aldehydes, ketones, carboxylic acids and their derivatives such as esters, amides etc.) are significantly important. In a catalytic reaction, the most important step is the activation of the acceptor olefins by a catalyst. Accordingly, three different types of activations have been developed as depicted in Scheme 2.2. In a Lewis acid activation, the electron-deficient metal center coordinates to Lewis basic carbonyl oxygen of the α,β-unsaturated carbonyl compounds. This process enhances the electrophilicity at the carbonyl carbon as well as the β-carbon. Hence the β-position is prone to nucleophilic attack. In a Brønsted acid activation, the Lewis basic oxygen of the carbonyl group gets protonated (if the acid is strong enough) or hydrogen bonds to the acid (if the acid catalyst is not strong enough), which in turn enhances the electrophilicity at the β-position. In another mode of activation namely, iminium ion activation, a secondary amine is used as a catalyst. The amine catalyst condenses with carbonyl compounds to form an intermediate iminium ion, which has a more electrophilic β-carbon center and is susceptible to nucleophilic attack. While the reactions to α,β-unsaturated aldehydes and ketones are well suited for iminium ion catalysis and accordingly several successful asymmetric catalytic reactions have been developed,[14-19] this type of activation is not suited for carboxylic acids and their derivatives.
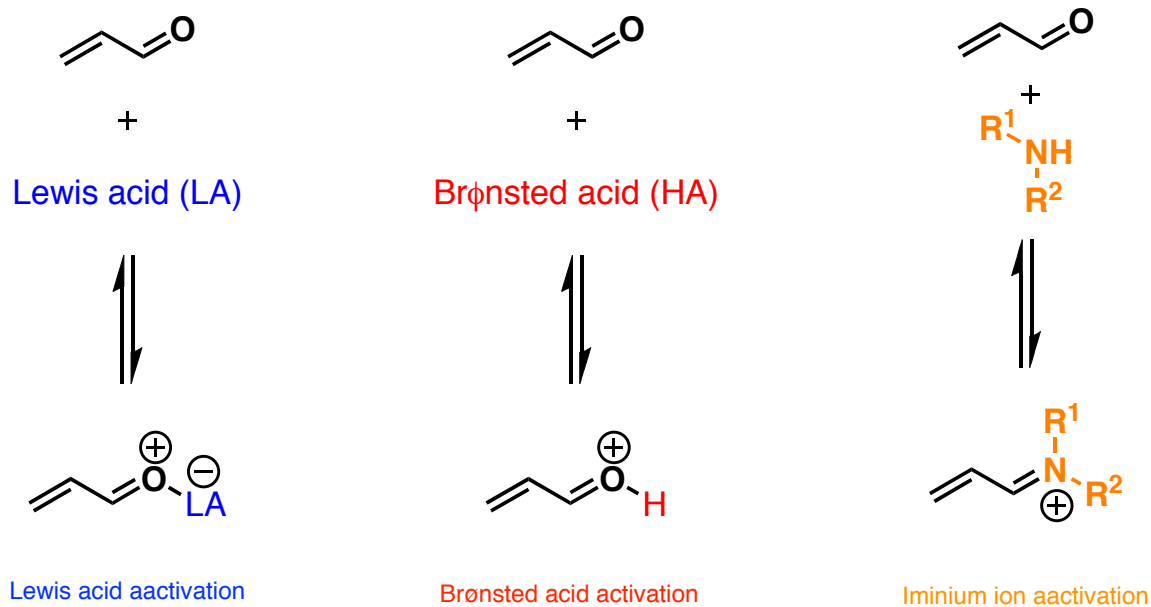
Scheme 2.2. Modes of activation of α,β-unsaturated carbonyl compounds

2.3. Coordination modes and development of templated olefin acceptors

Accordingly, activation of simple conjugate carboxylic acid esters or amides remains a challenging task with only a few successful reports. In this case the most common mode of activation is either by coordination to a Lewis acidic metal (Lewis acid catalysis) or by H-bonding or protonation (Brønsted acid catalysis). In the case of esters or amides, carbonyl coordination to metal (Lewis acid) results in two degenerate C=O··metal complex geometries (Scheme 2.3), thus complicating the stereocontrol of the reaction. One way to circumvent this problem is to develop activated ester surrogates as the masked equivalents of the products. In this context several two-point binding, conjugated systems have been developed. These bidentate systems can form a chelate to the chiral metal complexes that can act as a key activation and organizational element. A series of templated olefin acceptors (bidentate compounds) have been studied extensively in the literature, some of which are shown in Scheme 2.4. These acceptors are classified into two classes depending on where the coordinating groups are appended in the acceptors: class I and class II.

17

Monodentate coordination
(poor stereodiscrimination)

Bidentate coordination
(high stereodiscrimination)
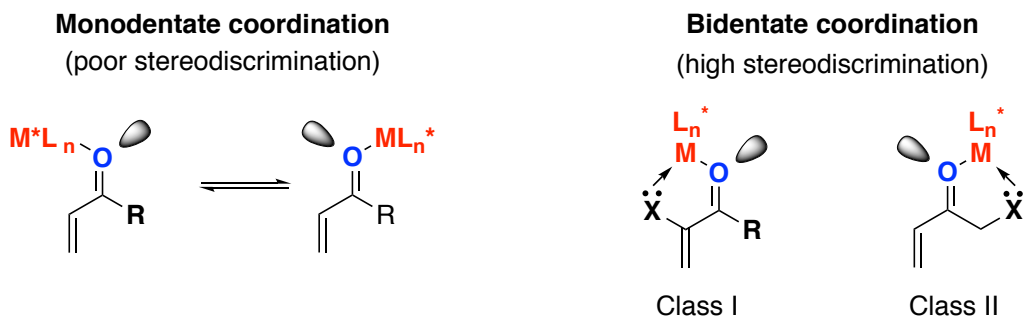
Class I Class II

Scheme 2.3. Coordination patterns of complexes between α,β-unsaturated carbonyl compounds and chiral Lewis acidic metal complexes

Examples of class I acceptors include alkylidene malonates **4.1** and nitroacrylates **4.2** (Scheme 2.4). The class II acceptors are further classified into three types. Type (A) which consists of an acyl-heteroatom linkage. Examples include: α,β-unsaturated acyloxazolidinones (**2.3**),[20-24] α,β-unsaturated acylpyrazolidinones (**2.4**),[25] α,β-unsaturated acylthiazolidinones (**2.5**), α,β-unsaturated thioesters (**2.6**), α,β-unsaturated acylphosphonates (**2.7**),[26,27] α,β-unsaturatedacyl pyrazoles (**2.8**).[28, 29] Type (B) contains an acyl-carbon (sp^2) linkage which includes the following types of compounds: β,γ-unsaturated-α-keto esters (**2.9**),[30] α,β-unsaturated acylimidazoles (**2.10**),[31, 32] α,β-unsaturated acylthiazoles (**2.11**), α,β-unsaturated acylpyridines (**2.12**). Type (C) compounds contain an acyl-carbon (sp^3) linkage. Examples include α'-hydroxyenones (**2.13**)[33] and α'-phosphonate enones (**2.14**).

Examples of Class I bidentate acceptors:

2.1
alkylidene malonate
Evans

2.2
nitroacrylates

Examples of Class II bidentate acceptors:

Type (B)

2.9
**β,γ-unsaturated
-α-ketoesters**
Evans, Jørgensen

2.10
**α,β,-unsaturated
acylimidazoles**
Evans, Sibi

2.11

**α,β,-unsaturated
acylthiazoles**
Evans, Sibi

2.12
**α,β,-unsaturated
acylpyridines**

Examples of Class II bidentate acceptors:

Type (C)

2.14
**α'-hydroxy
enones**

2.15
**α'-phosphonate
enones**

Examples of Class II bidentate acceptors:

Type (A)

2.3
**α,β,-unsaturated
acyloxazolidinones**
Evans

2.4
**α,β,-unsaturated
acyloxazolidinones**
Sibi

2.5
**α,β,-unsaturated
acylthiazolidinone**
Evans

2.6
**α,β,-unsaturated
thioesters**

2.7
**α,β,-unsaturated
acyl phsphonates**
Evans

2.8
**α,β,-unsaturated
acyl pyrazole**
Kanemasa

Scheme 2.4. Different classes of templated acceptor olefins

2.4. Reactivity of templated acceptors for asymmetric catalytic reactions

Although different bidentate conjugate acceptors are available, we know that acceptors

2.3 - **2.6** might be less reactive when challenging asymmetric reactions are performed. These

acceptors might be less reactive than acceptors such as **2.7**, **2.9-2.15**. This is mainly due to the

oxidation state of the acceptors. While **2.3** - **2.6** can be thought of as acid derivatives, compounds **2.7, 2.9** - **2.15** are in the ketone oxidation state. Hence, one expects these substrates to be more reactive (Scheme 2.5).
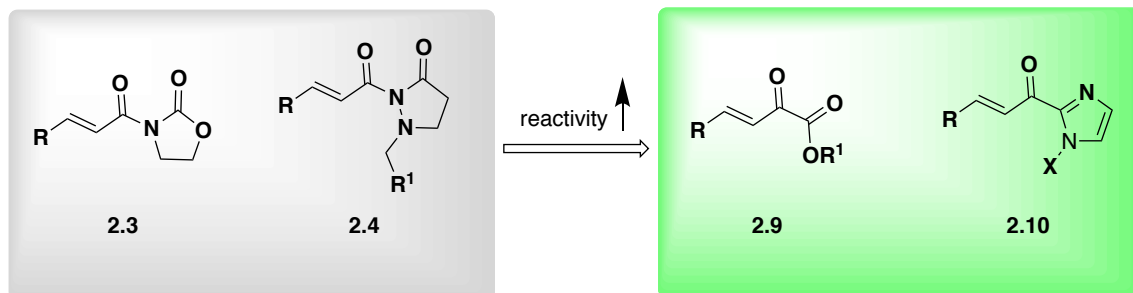
Scheme 2.5. Comparison of reactivity between imide acceptors and ketone acceptors

2.5. Importance of rotomer control during catalytic reactions

A simple conjugate addition of a reactive nucleophile to an oxazolidinone based acceptor olefin is shown in scheme 2.6. Under catalytic conditions, *s*-cis to *s*-trans rotomer equilibrium is possible, which might affect the relative and absolute stereochemistry of the product formed during reactions such as α-protonation. The template chosen should favor one rotomer over the other for an effective asymmetric catalytic process.
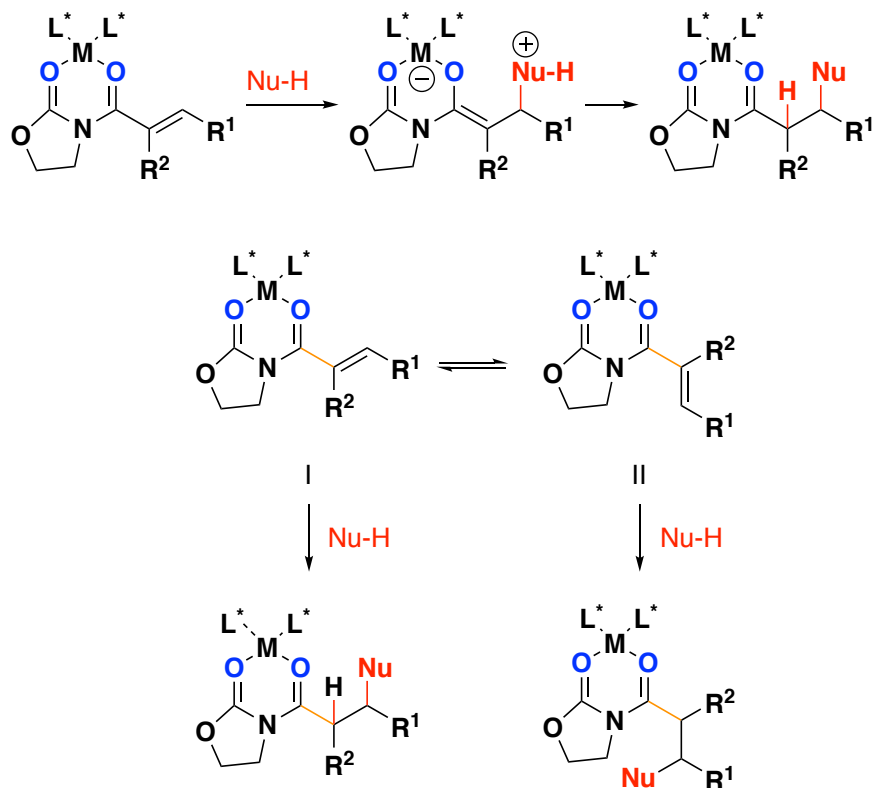
Scheme 2.6. Rotomer control during catalytic reaction

2.6. Design of templates for asymmetric catalytic reaction

We have chosen imidazole-based bidentate olefin acceptors for several projects in our lab for a variety of reasons. First, the N-3 nitrogen on the imidazole ring can act as either a Brønsted or Lewis base. Substituting the 2-position of the imidazole by an acyl group reduces the basic character of the nitrogen (Scheme 2.7). It is still basic enough to interact with a Lewis- or Brønsted acidic catalyst in reactions. Secondly, the N-1 nitrogen offers a handle to change the electronics or the sterics around the N-atom, which can have major impact on the reactivity. Finally, from a structural perspective, the N can be labeled as ^{15}N, which can be very useful while studying the solution structures of intermediates involved in catalytic reactions.
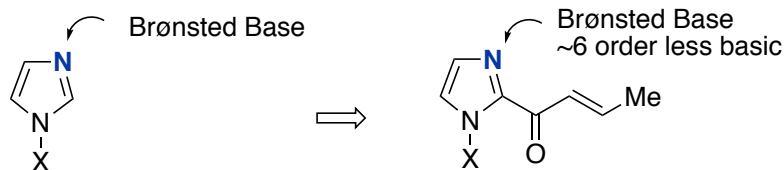
X can be used as a handle to fine tune the reactivity
Possiblity of ^{15}N labeling

Scheme 2.7. Possibility of developing new acceptors with imidazole as templates

2.7. Conclusions

Over the past decade the application of acylimidazoles as a template in catalytic reaction has evolved. They have been used in several catalytic processes ranging from Lewis acid catalysis to photo-redox catalysis. Only N-alkyl/aryl imidazoles such as N-methylimidazoles, N-isopropylimidazoles and rarely N-phenylimidazoles have been used as templates. Our research with substituted imidazoles should expand the repertoire of acceptor olefins used in catalytic reactions.

2.8. References

1. *Catalytic Asymmetric Conjugate Reactions;* Córdova, A., Ed.; Wiley- VCH Verlag GmbH & Co. KgaA: Weinheim, 2010.

2. Nguyen, B. N.; Hii, K. K.; Szymanski, W.; Jansen, D. B. In *Science of Synthesis Houben Weyl, Stereoselective Synthesis 1, Stereoselective Reactions of Carbon-Carbon Double Bonds;* de Vries, J. G., Ed.; Georg Thieme Verlag KG: Stuttgart, NY, 2010; pp 571.

3. Vicario, J. L.; Badía, D.; Carrillo, L.; Reyes, E. *Organocatalytic Enantioselecive Conjugate Addition Reactions;* RSC Publishing: Cambridge, 2010.

4. Tsogoeva, S. B. *Eur. J. Org. Chem.* **2007,** 1701.

5. Almasi, D.; Alonso, D. A.; Nájera, C. *Tetrahedron: Asymmetry* **2007,** *18,* 299.

6.   Vicario, J. L.; Badía, D.; Carrillo, L. *Synthesis* **2007,** 2065.

7.   Zhang, Y.; Wang, W. *Catal. Sci. Technol.* **2012,** *2,* 42.

8.   Zhang, Y.; Wang, W. In *Stereoselective Organocatalysis;* Ríos, R., Ed; Wiley: Hoboken, New Jersey, 2013; pp 147.

9.   *Comprehensive Asymmetric Catalysis;* Jacobsen, E. N., Pfaltz, A., Yamamoto, H., Eds.; Springer: Berlin, 1999; Vol I−III.

10. *Lewis Acids in Organic Synthesis;* Yamamoto, H., Ed.; Wiley-VCH: Weinheim, 2000, Vol 1−3.

11. Corey, E. J.; Guzman-Perez, A. *Angew. Chem., Int. Ed.* **1998**, *37*, 388;

12.   Peterson, E. A.; Overman, L. E. *Proc. Natl. Acad. Sci. U. S. A* **2004**, *101*, 11943.

13. Quaternary Stereocenters; Christoffers, J., Baro, A., Ed.; Wiley-VCH Verlag GmbH & Co. KGaA: 2006.

14. Lelais, G.; MacMillan, D. W. C. *Aldrichimica Acta* **2006,** *39,* 79.

15. Erkkila, A.; Majander, I.; Pihko, P. M. *Chem. Rev.* **2007,** *107,* 5416.

16. Nielsen, M.; Worgull, D.; Zweifel, T.; Gschwend, B.; Bertelsen, S.; Jørgensen, K. A. *Chem.Commun.* **2011,** *47,* 632.

17. Melchiorre, P. *Angew. Chem., Int. Ed.* **2012,** *51,* 9748.

18. Liu, Y.; Melchiorre, P. In Science of Synthesis: Asymmetric Organocatalysis Vol. 1; List, B., Maruoka, K., Eds.; Thieme: Stuttgart, 2012; pp 403− 438.

19. MacMillan, D. W. C.; Watson, A. J. B. In *Science of Synthesis: Asymmetric Organocatalysis Vol. 1;* List, B., Maruoka, K., Eds.; Thieme: Stuttgart, 2012; pp 309−401.

20. Johnson, J.S.; Evans, D. A. *Acc. Chem. Res.* **2000,** *33,* 325.

21. Evans, D. A.; Scheidt, K. A.; Johnston, J. N.; Willis, M. C. *J. Am. Chem. Soc.* **2001,** *123*, 4480.

22. Sibi, M. P.; Manyem, S.; Zimmerman, J. *Chem. Rev.* **2003,** *103,* 3263.

23. Hird, A. W.; Hoveyda, A. M. *Angew. Chem., Int. Ed.* **2003,** *42,* 1276.

24. Zhuang, W.; Hazell, R. G.; Jørgensen, K. A. *Chem. Commun.* **2001,** 1240.

25. Sibi, M. P.; Ma, Z.; Jasperse, C. P. *J. Am. Chem. Soc.* **2004,** *126,* 718.

26. Evans, D. A.; Scheidt, K. A.; Fandrick, K. R.; Law, H. W.; Wu, J. *J. Am. Chem. Soc.* **2003,** *125,* 10780.

27. Evans, D. A.; Fandrick, K. R.; Song, H.-J.; Scheidt, K. A.; Xu, R. *J. Am. Chem. Soc.* **2007,** *129,* 10029.

28. Itoh, K.; Kanemasa, S. *J. Am. Chem. Soc.* **2002,** *124,* 13394.

29. Sibi, M. P.; Shay, J. J.; Liu, M.; Jasperse, C. P. *J. Am. Chem. Soc.* **1998,** *120,* 6615.

30. Jensen, K. B.; Thorhauge, J.; Jørgensen, K. A. *Angew. Chem., Int. Ed.,* **2001,** *40,* 160.

31. Evans, D. A.; Fandrick, K. R.; Song, H.-J. *J. Am. Chem. Soc.* **2005,** *127,* 8942.

32. Coquie re, D.; Feringa, B. L.; Roelfes, G. *Angew. Chem., Int. Ed.* **2007,** *46,* 9308.

33. Palomo, C.; Oiarbide, M.; García, J. M. *Chem. Soc. Rev.* **2012,** *41*, 415.

CHAPTER 3. CONSTRUCTION OF ALL CARBON QUATERNARY CENTERS USING

CHIRAL LEWIS ACID CATALYSIS: FRIEDEL-CRAFTS ALKYLATION OF ARENES

3.1. Introduction

The latter half of the 20th century has seen remarkable advances in stereoselective

synthesis of small organic molecules, and these have been incorporated successfully into the

synthesis of complex organic structures.[1] However, construction of *quaternary stereocenters* -

carbon atoms to which four different carbon substituents are attached - selectively, has been a

daunting task and remains a significant challenge in natural product synthesis. Quaternary carbon

stereocenters are common structural features in organic molecules found in nature, synthetic

pharmaceuticals and agrochemicals (Figure 3.1).
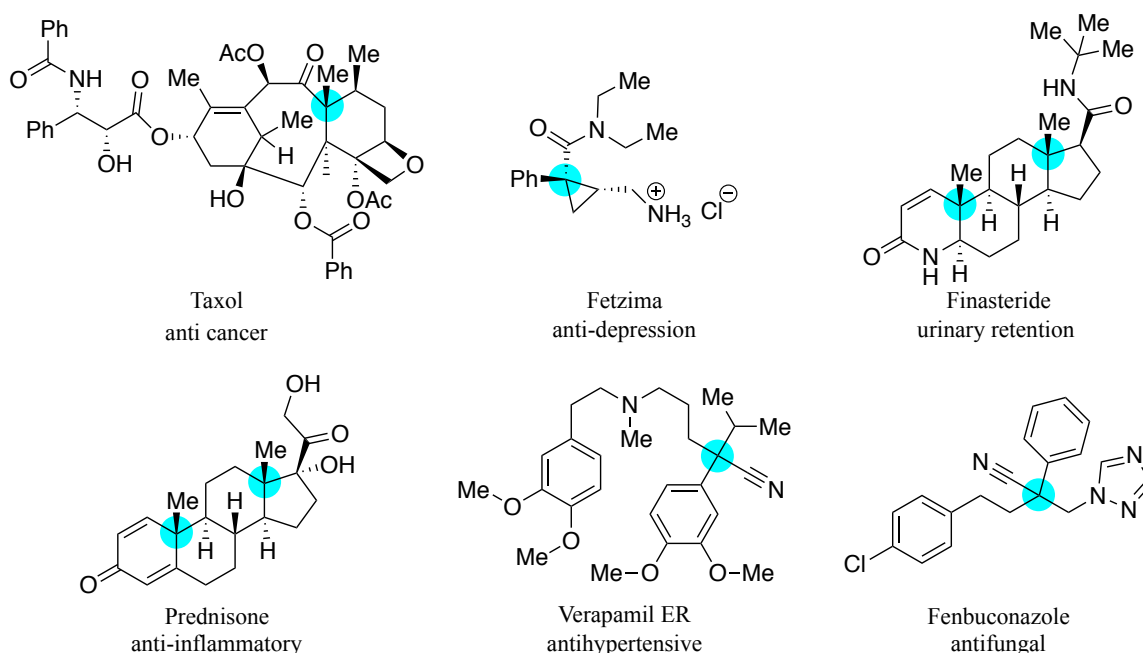
Figure 3.1. Prescribed pharmaceutical products containing all carbon quaternary stereocenters:
blue circle highlights quaternary stereocenters and drugs are administered as racemates when
stereochemistry is not defined.

One of the main challenges in constructing an all carbon-quaternary center is the

congested nature of such center: orbital overlap is tough to achieve and specifically, in an

asymmetric process the approach of the chiral catalyst or reagent is quite challenging. Unlike a carbon stereocenter with one hydrogen substituent, quaternary stereocenters are not amenable to inversion of configuration. In other words, one has to design a C-C bond forming reaction that provides the correct absolute configuration of the stereocenter.[2-7] One fact that highlights the challenges involved in the construction of quaternary centers is the structures of the top 200 prescription drugs sold in 2016.[8] About 13% of these drugs contain all carbon quaternary stereocenters. However, most of the drugs bearing the quaternary stereocenters are derived from natural products such as steroids, terpenoids, opioids etc. The absence of chemically synthesized quaternary stereocenters in these prescription drugs further accentuates the challenges involved in the asymmetric catalytic process.

Although decent progress has been made towards the construction of quaternary stereocenters in the ring system, the corresponding synthesis of acyclic congeners have been relatively limited. This is mainly due to the conformational flexibility of the acyclic systems.[7, 9] In a survey of catalytic enantioselective synthesis of quaternary stereocenters, Overman et al.[5] concluded that transformations such as (a) Diels-Alder reaction (DA), (b) intramolecular Heck reactions, (c) chiral allyl-metal intermediates with carbon nucleophiles and (d) chiral carbon nucleophiles with achiral electrophiles were useful and well documented.

3.2. Addition of chiral organometallics to β,β,α-trisubstituted alkenes

Enantioselective conjugate addition of nucleophiles to activated olefins is an atom-economical process for the construction of C-C bonds. Over the past two decades, advances in the field of asymmetric catalysis have exposed us to effective enantioselective methodologies for the β-functionalization of acceptors such as enals and enones.[10] However, the current protocols are restricted to the addition of organometallic reagents.

Hayashi et al.[11] reported a Rh(I)-chiral diene catalyzed addition of sodium tetraarylborates to β,β-disubstituted enones (Scheme 3.1).

3.1a: R = Me
3.1b: R = Et
3.1c: R = CO$_2$Me
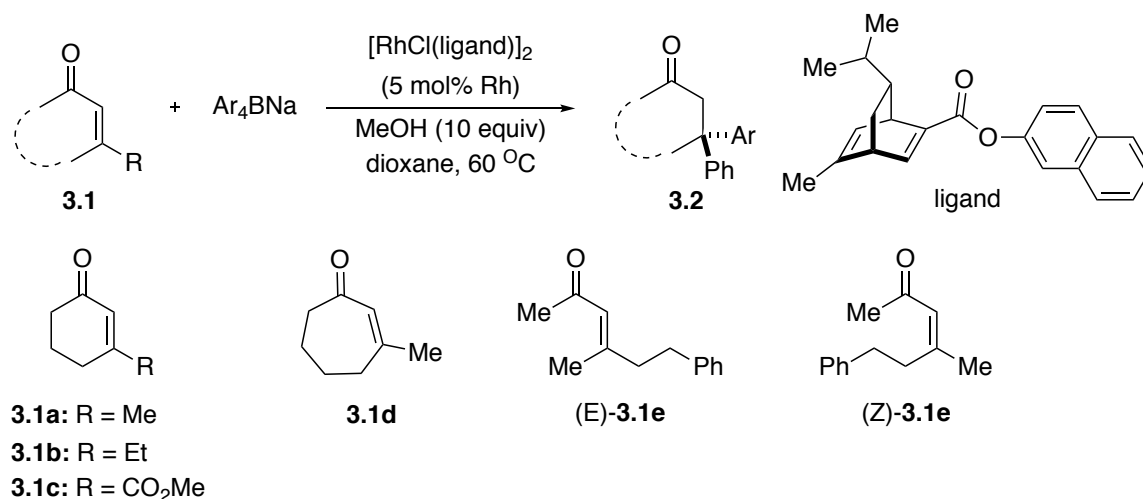
Entry	1	Ar	time (h)	Product	Yield (%)	ee (%)
1	**3.1a**	Ph	24	(R)-**3.2aa**	83	98
2	**3.1b**	Ph	24	(R)-**3.2ba**	79	98
3	**3.1c**	Ph	24	(S)-**3.2ca**	80	98
4	**3.1d**	Ph	48	(R)-**3.2da**	75	89
5	(E)-**3.1e**	Ph	60	(S)-**3.2ea**	92	78
6	(Z)-**3.1e**	Ph	60	(R)-**3.2ea**	94	91
7	**3.1a**	4-MeC$_6$H$_4$	48	(R)-**3.2ab**	73	91
8	**3.1a**	4-FC$_6$H$_4$	60	(R)-**3.2ac**	62	91
9	**3.1a**	3-MeC$_6$H$_4$	24	(R)-**3.2ad**	84	95
10	**3.1a**	3-FC$_6$H$_4$	48	(R)-**3.2ae**	65	97

Scheme 3.1. Asymmetric conjugate addition of sodium tetraarylborates to β,β-disubstituted enones.

Simple boronic acids and boronic acid esters are incompetent nucleophiles in this reaction. Cyclic enones are very competent nucleophiles in the reaction. The acceptor with electron withdrawing group (methoxycarbonyl **3.1c**) gave opposite enantiomer in good yield and high selectivity (89% ee for product **3.2ca**). For acyclic acceptors, the geometry of the double bond is shown to affect the selectivity: while acceptor (E)-**3.1e** gave conjugate adduct (S)-**3.1ea**

in 78% ee, the acceptor (Z)- **3.1e** gave the adduct (R)-**3.1ea** in excellent ee of 91%. Although the selectivity for the catalytic process is very high, the reaction is not atom-economical.

Another example that is very important in the literature for the conjugate addition of arylboronic acids to β,β-disubstituted enones is the Pd^{2+} catalyzed asymmetric transformation reported by Stoltz et al.[12] In this communication, the researchers used commercially available boronic acids as the nucleophile. The transition metal catalyst was derived from a Pd^{2+} source and pyridineoxazoline ligand **3.3**. The advantage of this method over the Hayashi protocol is that it uses commercially available boronic acids rather than sodium tetraarylborate and also the reaction is water tolerant so no special precautions need to be taken. The reaction shows good acceptor scope with respect to the ring size and β-substitution: 5-, 6-, and 7-membered ketones are competent acceptors in the reaction. The reaction also showed good boronic acid scope (Scheme 3.2). The Stoltz group also extended this reaction to other acceptors such as chromenes and quinlolones.[13]
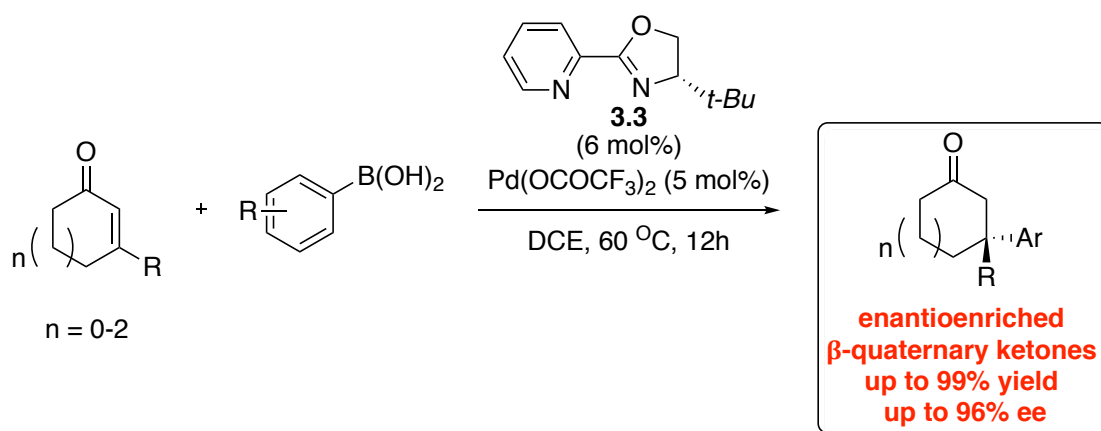
Scheme 3.2. Pd(II)-pyridineoxazoline catalyzed conjugate addition of arylboronic acids to β-substituted cyclic enones.

Alexakis et al. developed a Cu(I) - phosphoramidate catalytic system to add alkylorganometallic reagents to β-trisubstituted enones. Using CuTC as a Cu(I) source and chiral

phosphoramidate **3.4** as a ligand resulted in successful addition of trimethylaluminum to enones (Scheme 3.3 (A)).[14a] On a similar note, Hoveyda et al. used dialkylzinc as a pronucleophile for the copper catalyzed conjugate addition (Scheme 3.3 (B)).[14b]

(A)

(B)
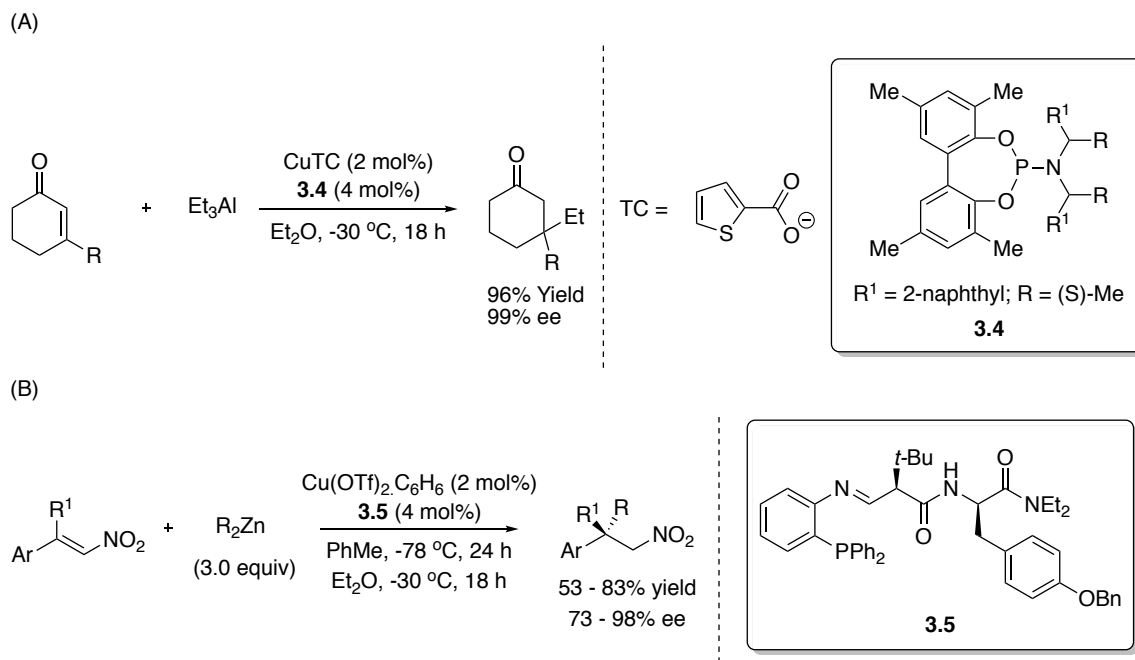
Scheme 3.3. (A) Copper (I) catalyzed asymmetric conjugate addition of trialkylaluminum by Alexakis et al. (B) Copper catalyzed asymmetric conjugate addition of dialkylzinc to nitroolefins by Hoveyda et al.

3.3. Conjugate addition of achiral nucleophiles to β,β,α-trisubstituted alkenes

Aromatic hydrocarbons are the simplest of achiral nucleophiles. In addition, they are inexpensive and readily available starting materials. The direct functionalization of such compounds offers rapid access to important building blocks and core structures of many biologically active natural products. Since its seminal publication in 1877, [15] the Friedel-Crafts reaction (FC) has been one of the most studied reactions.[16] It is a Lewis acid catalyzed reaction between an aromatic hydrocarbon (nucleophile or donor) and an electron deficient species (electrophile or acceptor) as shown in scheme 3.4. Even though the scope and the utility of the reaction has been significantly expanded since its discovery, it took almost a century for the

29

chemists to develop catalytic enantioselective versions of this reaction.[17] The choice of

electrophiles has been limited for catalytic enantioselective FC reactions.

$$E = \qquad \underset{R^1 \quad R^2}{\overset{Y}{\|}} \qquad \underset{R^1 \quad R^2}{\overset{Y}{\triangle}} \qquad \underset{R^1 \quad R^2}{\overset{X}{\diagdown}} \qquad \underset{R^1 \quad X}{\overset{O}{\|}}$$

Y = O, NH, NR^3 Y = O, NH, NR^3 X = halogens, OR etc.   X = R^1, OR^1, NHR^1
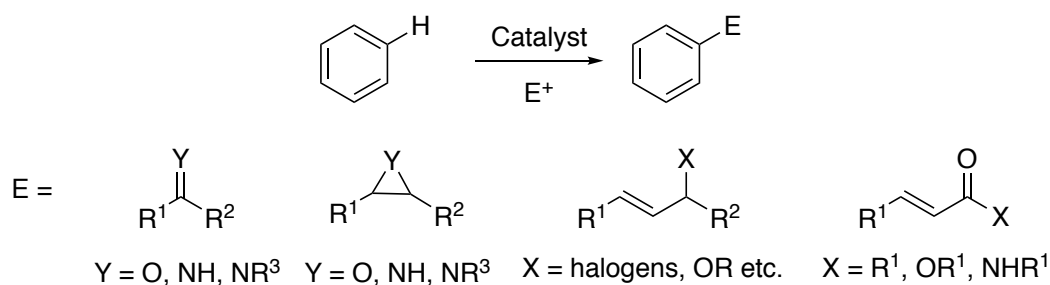
Scheme 3.4. Friedel-Crafts (FC) reaction between donor (aromatic hydrocarbon) and acceptor (electrophile) and different classes of acceptors used in catalytic asymmetric FC reaction.

Although enantioselective variants of FC reactions by Lewis acids[18] and organocatalysts[19]

have been reported for β-monosubstituted-unsaturated carbonyl compounds, it was not until

recently that the FC reaction was used in the stereoselective construction of all carbon quaternary

centers. During the enantioselective synthesis of alkaloids such as (-)-rhazinal, (-)-rhazinilam, (-

)-leuconolam and (+)-*epi*-leuconolam, Banwell et al. first reported an intramolecular FC

alkylation to construct an all carbon quaternary center with moderate ee of 74%. This was

achieved using chiral secondary amine based organocatalysis.[20] Recently, Kwiatkowski and

coworkers reported high-pressure accelerated organocatalytic FC alkylation of indoles.[21]

Primary chiral amine salts such as **3.6** was found to catalyze indole addition to β,β-disubstituted

enones (Scheme 3.5). The enones used in this study contained an electron withdrawing ester

group at the β-position. Hence, the protocol has limited substrate scope, however, good

selectivities (72-80% ee) were obtained. The 2- and 5-substitution (2-Me and 5-OMe) on the

indole were also tolerated (entry # 4 and # 5, Scheme 3.5).

3.7 (10 mol%)

Salicylic acid (25 mol%)

PhMe

10 kbar, 50 °C, 20h

3.6a: R = Bn
3.6b: R = Me
3.6c: R = Et

3.8aa: R = Bn, $R^1 = R^2$ = H
3.8ba: R = Me, $R^1 = R^2$ = H
3.8ca: R = Et, $R^1 = R^2$ = H
3.8ab: R = Et, R^1 = OMe, R^2 = H
3.8ac: R = Et, R^1 = H, R^2 = Me
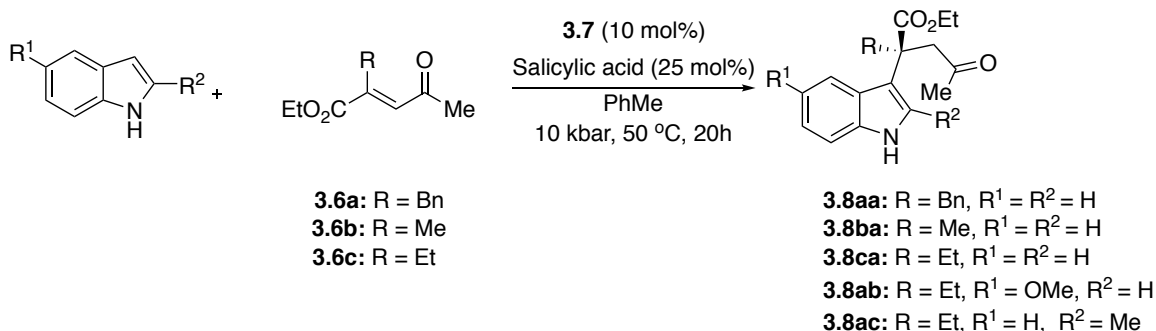
Entry	R	R^1	R^2	Product	Yield (%)	ee (%)
1	Bn	H	H	**3.8aa**	75	72
2	Me	H	H	**3.8ba**	70	74
3	Et	H	H	**3.8ca**	67	68
4	Bn	OMe	H	**3.8ab**	72	80
5	Bn	H	Me	**3.8ac**	66	74

3.7
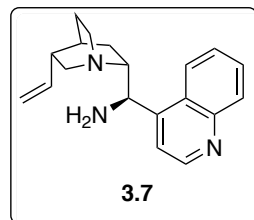
Scheme 3.5. High-pressure accelerated organocatalytic FC alkylation of indoles with β,β-disubstituted enones.

Chiral imidazoline-aminophenol ligand **3.9** developed by Arai and coworkers was used in the copper catalyzed FC reaction of indoles with isatin-derived nitroolefins (Scheme 3.6).[22] The reaction showed good scope with respect to nitroolefin and also indoles.

3.9 (11 mol%)

Cu(OTf)$_2$ (10 mol%)

HFIP (2.0 equiv)

PhMe, rt

3.9
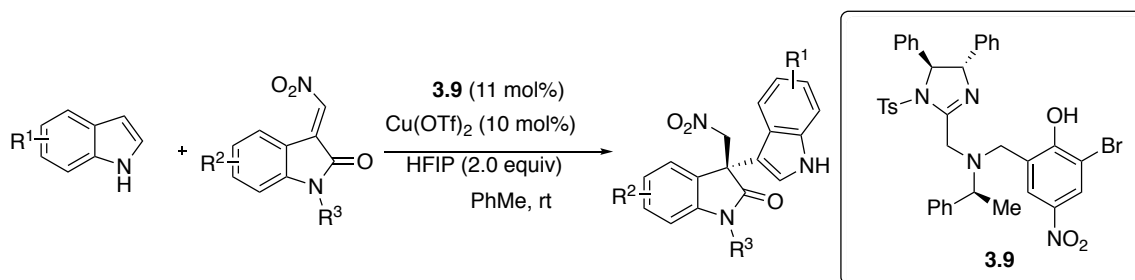
Scheme 3.6. Asymmetric FC reaction of indoles with isatin-derived nitroolefins for the construction of quaternary stereocenters.

Recently, the Jia group reported asymmetric FC alkylation of indoles with β,β-disubstituted nitroolefins containing a trifluoromethyl group (Scheme 3.7).[23] The FC alkylation process reported in this communication was catalyzed by the Ni(ClO$_4$)·6H$_2$O chiral bisoxazoline **3.10** complex. Substitutions at 5-, 6-, and 7- positions of indoles were very well tolerated.

However, N-substituted indoles were not competent under the reaction conditions. Using this methodology, indoles bearing all carbon quaternary stereogenic centers were synthesized in good yields and very high selectivities (up to 97% ee).
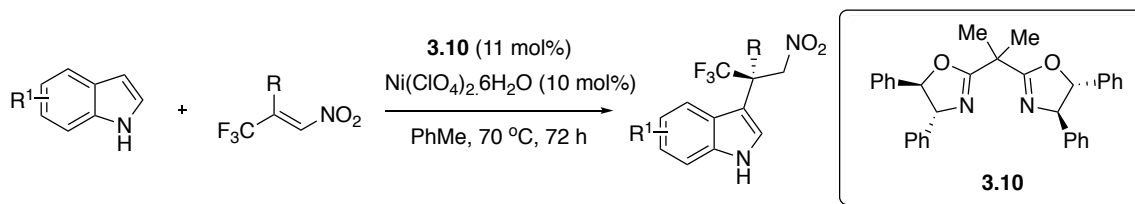
Scheme 3.7. Ni-catalyzed asymmetric FC reaction of indoles with β-CF$_3$-β-disubstituted nitroolefins.

In spite of these advances, stereoselective functionalization of α,β-unsaturated carboxylic acids and their derivatives such as esters and amides are notoriously difficult. One way to circumvent this problem is to use templated acceptors. In addition to controlling the rate and stereoselectivity of conjugate addition, templates also increase the structural versatility of the conjugate adducts.[24] Our group has shown that a judicious choice of template and chiral catalyst is essential for increased reactivity and high levels of stereoinduction.[25] Hence, there is a constant motivation towards the design of novel templated acceptors that might be conducive when performing challenging asymmetric transformations such as the construction of all carbon-quaternary centers[2-7] by the addition of carbon nucleophiles.

3.4. Chiral Lewis acid catalyzed FC reaction between indoles and β,β,α-trisubstituted-α,β-unsaturated enones

The reactivity of α,β-unsaturated carbonyl compounds towards a nucleophile decreases with β-substitution. Hence β-unsubstituted-α,β-unsaturated carbonyl compounds **3.11** (acrylate and related compounds) are the most reactive. β-Substituted unsaturated carbonyl compounds **3.12** (crotonates, cinnamates and related compounds) are less reactive than compounds of type

3.11. The least reactive among the series is β,β-disubstituted unsaturated carbonyl compounds

3.13 (Scheme 3.8). In order to make compounds of type **3.13** amenable to reactions with

nucleophiles, it is essential to systematically vary the Z group and study its effect on the reaction

rate and selectivity of the asymmetric process. The Z group not only influences the reactivity and

selectivity but also control the rotomer geometry, which is a major challenge in acyclic systems.
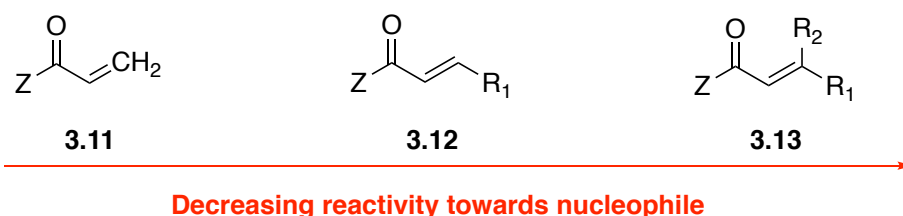
Figure 3.2. Methodology development for the identification of achiral templates for the selective construction of all carbon quaternary stereocenter.

3.4.1. Results and discussion

3.4.1.1. Survey of achiral templates in chiral Lewis acid catalyzed asymmetric FC reaction

We undertook our objective of determining the optimal template for β,β-disubstituted

system in FC alkylation of indoles. The β-substitutions were chosen to be a trifluoromethyl

group and a methyl group. There are several reasons for selecting a trifluoromethyl group: (a)

construction of quaternary stereocenter bearing CF_3 group is challenging (b) helps minimizing

the E/Z isomerization of the double bond (c) increases the electrophilicity at the β-position and

(d) ^{19}F aids in reaction monitoring by NMR. We initiated our research by subjecting different

template appended β,β-disubstituted unsaturated carbonyl compounds to FC alkylation with N-

methylindole using ytterbium triflate and chiral pyridinebisoxazoline ligand **3.14**. Simple β,β-

disubstituted ester **3.15** (where Z = OEt) is not a competent electrophile in the asymmetric FC

reaction (Table 3.1, entry # 1). Weinreb amide **3.16** (Z = N(OMe)Me) is also an unreactive

substrate (Table 3.1, entry # 2). Changing Z to 2-oxazolidinonyl group results in an imide

acceptor **3.17**, which is also unreactive under the reaction condition (Table 3.1, entry # 3). The

corresponding N-benzyloxy-2-acylimidazole substrate **3.20** reacted with indole **3.21a** to give the

alkylated product **3.22f** in 95% yield and 98% ee (Table 3.1, entry # 6).

Table 3.1. Comparison of different templates in chiral Lewis acid catalyzed FC alkylation of N-methylindole and β,β-disubstituted enones.
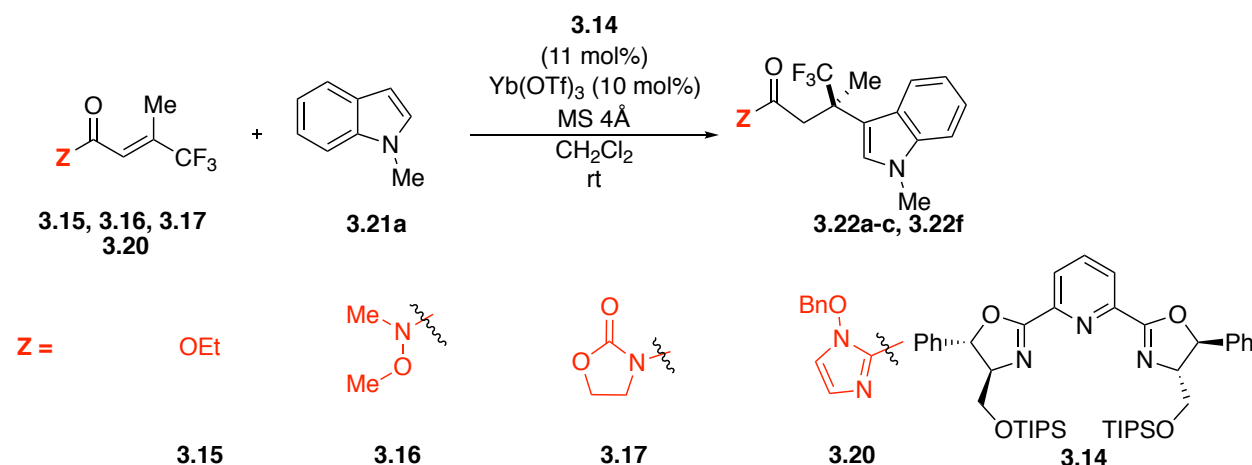
Entry	Z	time	product	yield (%)[a]	ee (%)[b]
1	**3.15**	48 h	**3.22a**	nr	-
2	**3.16**	48 h	**3.22b**	nr	-
3	**3.17**	48 h	**3.22c**	nr	-
4	**3.20**	48 h	**3.22f**	95	98

Reaction conditions: **3.15-3.20** (0.1 mmol), **3.21** (0.2 mmol), Yb(OTf)$_3$ (0.01 mmol), **3.14** (0.011 mmol) MS 4Å (0.10 g) DCM (2 mL) were stirred at rt. [a] isolated yield. [b] determined by chiral HPLC. nr = no reaction.

3.4.1.2. Survey of chiral Lewis acids for the asymmetric FC reaction of β,β-disubstituted enones

Having identified templated substrate **3.20** as the optimal substrate for FC reaction, we focused on other chiral Lewis acids in catalyzing the reaction. The results are summarized in Table 3.2. Magnesium triflate bisoxazoline ligand **3.23** combination doesn't catalyze the reaction (Table 3.2, entry # 1). Magnesium triflimide - bisoxazoline **3.23** complex gave product **3.22f** as racemate in 55% yield (Table 3.2, entry # 2). Zinc triflate/**3.23** and copper triflate/**3.23** complexes catalyzed the FC reaction to give product in 65% yield, 30% ee and 60% yield, 65% ee, respectively (Table 3.2, entry # 3 and # 4). Nickel triflimide /dibenzofuran-derived bisoxazoline ligand **3.24** gave the product in 29% yield and poor enantioselectivity (6% ee) (Table 3.2, entry # 5). Cobalt triflimide /dibenzofuran-derived bisoxazoline ligand **3.24** combination gave the product in 71% yield and 40% ee (Table 3.2, entry # 6). Cobalt triflimide /**3.14** combination gave the product in 93% yield and 53% ee (Table 3.2, entry # 7). We also used scandium triflate/pyridine bisoxazoline **3.14** complex as a catalyst in the FC reaction. Although, the reaction is chemically efficient (76% yield), there is no selectivity (0% ee) (Table 3.2, entry # 8). Chiral Lewis acid formed from Ytterbium triflate/**3.14** combination was able to catalyze the FC reaction and gave the product **3.22f** bearing quaternary center in very high yield (95%) and excellent enantioselectivity (98%) (Table 3.2, entry # 9).

Table 3.2. Chiral Lewis acid survey for asymmetric indole alkylation with β,β-disubstituted enones.
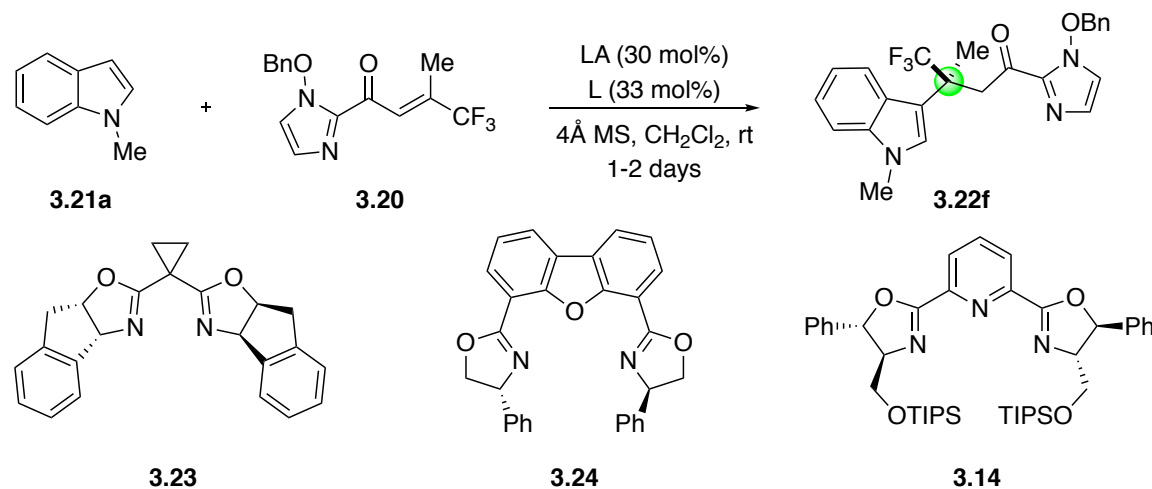
Entry	LA	L	Yield of **3.22f** (%)[a]	ee of **3.22f** (%)[b]
1	Mg(OTf)$_2$	**3.23**	0	nd
2	Mg(NTf$_2$)$_2$	**3.23**	55	0
3	Zn(OTf)$_2$	**3.23**	65	30
4	Cu(OTf)$_2$	**3.23**	60	65
5	Ni(NTf$_2$)$_2$	**3.24**	29	6
6	Co(NTf$_2$)$_2$	**3.24**	71	40
7	Co(NTf$_2$)$_2$	**3.14**	93	53
8	Sc(OTf)$_3$	**3.14**	76	0
9	Yb(OTf)$_3$	**3.14**	95	98

Reaction conditions: **3.20** (0.1 mmol), **3.21** (0.2 mmol), LA (0.03 mmol), **L** (0.033 mmol) MS 4Å (0.10 g) DCM (2 mL) were stirred at rt. [a] isolated yield. [b] determined by chiral HPLC. nd = not determined.

3.4.1.3. Effect of catalyst loading, temperature and additives on the FC reaction

Having identified the optimal template and catalytic system we studied the effect of other parameters on the efficiency of the catalytic process. Initially, we studied the effect of catalytic loading on the FC alkylation process. Reducing the catalytic loading to 15 mol% reduced the rate of the reaction without affecting the enantioselectivity (98% ee, Table 3.3, compare entry # 1 and # 2). Reducing the loading to 10 mol% reduced the yield of the product **3.22f** to 70% (compare

entry # 3 with entry # 2, Table 3.3) but there is no erosion of enantioselectivity. Further reduction in catalytic loading was not pursued. The effect of temperature on rate and selectivity of FC reaction was studied. Reducing the temperature to 0 °C reduced the rate of the reaction. After 7 days only 30% of **3.22f** was formed without any change to enantioselectivity (entry # 4, Table 3.3). When the temperature was further reduced to -20 °C, only trace amount of product was formed after 7 days (entry # 5, Table 3.3). Next we also studied the effect of the additive namely, 4 Å molecular sieves (MS) on the reaction. To our surprise we found that MS reduced the rate of the reaction. The reaction was completed in 48 h with MS as opposed to just 6h for the reaction without additive. The yield and enantioselectivity were similar to the one observed with MS but in a shorter amount of time (entry # 6, Table 3.3). Finally, we also studied the effect of solvent. The reaction failed in solvents such as acetonitrile and DME ((entry # 6 and # 7 Table 3.3). DCE gave results similar to DCM (entry # 8, Table 3.3). The reaction was completed in 2h when toluene was used as the solvent (entry # 9, Table 3.3).

Table 3.3. Effect of catalytic loading, temperature, additive and solvent on FC reaction.
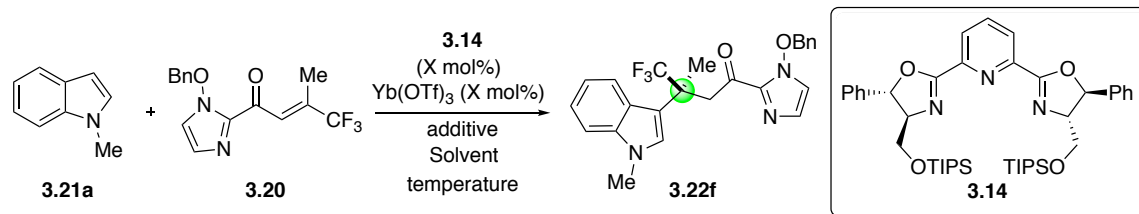
Entry	X	T (°C)	additive	solvent	time	yield (%)[b]	ee of **3.22f** (%)[c]
1	30	rt	MS	DCM	2d	95	98
2	15	rt	MS	DCM	5d	95	98
3	10	rt	MS	DCM	5d	70	98
4	10	0	MS	DCM	7d	30	98
5	10	-20	MS	DCM	7d	trace	nd
6	10	rt	-	DCM	8h	95	98
7	10	rt	-	ACN	2d	nr	-
8	10	rt	-	DME	2d	nr	-
9	10	rt	-	PhMe	2h	95	98

Reaction conditions: **3.20** (0.1 mmol), **3.21** (0.2 mmol), LA (X mmol), **L** (X mmol) Additive: 4Å MS (0.10 g) Solvent (2 mL) were stirred at rt. [a] isolated yield. [b] determined by chiral HPLC. nr = no reaction. nd = not determined.

3.4.1.4. Indole scope in asymmetric FC alkylation

With optimized conditions in hand, we started examining the scope of indoles in FC alkylation. N-methylindole **3.21a** reacted with N-benzyloxy-2-acylimidazole **3.20** to furnish alkylated product **3.22f** in very good yield (95%) and excellent enantioselectivity (98% ee) (entry # 1, Table 3.4). When parent indole **3.21b** was used, the reaction was completed in 2h with 99% yield and 99% ee for the product **3.22g** (entry # 2, Table 3.4). 2-methylindole **3.21c**, when used as a nucleophile, furnished the product **3.22h** in 97% yield and 99% ee (entry # 3, Table 3.4). N-methyl-2-methyl indole **3.21d** is also a competent nucleophile in the reaction, providing **3.22i** in 90% yield and 99% ee (entry # 4, Table 3.4). Next, we used 5-substituted indoles in the reaction. When 5-halogenated indoles **3.21e, 3.21f, 3.21g** were used, the products **3.22j** (92% yield and

99% ee), **3.22k** (99% yield, 98% ee), and **3.22l** (97% yield, 99% ee) were obtained in high yields

and excellent enantioselectivity (entry # 5, #6, and #7, Table 3.4). The electron withdrawing

group (CO$_2$Me) in the 5-position of the indole **3.21h** is competent enough to give product **3.22m**

in 82% yield and 99% ee (entry # 8, Table 3.4). Electron donating groups (OMe and Me) at the

5-position of the indole **3.21i, 3.21j** were also tolerated in the reaction providing products **3.22n**

(97% yield, 99% ee) and **3.22o** (97% yield, 99% ee) in very high yields and excellent

enantioselectivities (entry # 9 and # 10, Table 3.4). 4-methoxyindole **3.21k** furnished the

alkylated product **3.22p** in 99% yield and 99% ee (entry # 11, Table 3.4).

Table 3.4. Indole scope in asymmetric FC reaction.
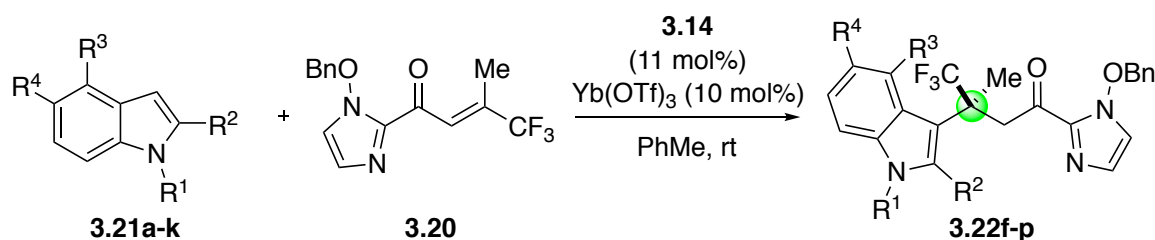
Entry	Indole	R^1	R^2	R^3	R^4	Product	time (h)	yield (%)[a]	ee (%)[b]
1	**3.21a**	Me	H	H	H	**3.22f**	2	95	98
2	**3.21b**	H	H	H	H	**3.22g**	2	99	99
3	**3.21c**	H	Me	H	H	**3.22h**	2	97	99
4	**3.21d**	Me	Me	H	H	**3.22i**	2	90	99
5	**3.21e**	H	H	H	F	**3.22j**	2	92	99
6	**3.21f**	H	H	H	Cl	**3.22k**	2	99	98
7	**3.21g**	H	H	H	Br	**3.22l**	2	97	99
8	**3.21h**	H	H	H	CO$_2$Me	**3.22m**	2	82	99
9	**3.21i**	H	H	H	OMe	**3.22n**	2	97	99
10	**3.21j**	H	H	H	Me	**3.22o**	2	97	99
11	**3.21k**	H	H	OMe	H	**3.22p**	2	99	99

Reaction conditions: **3.20** (0.1 mmol), **3.21a-k** (0.2 mmol), Yb(OTf)$_3$ (10 mmol), **3.14** (11 mmol), PhMe (3 mL) were stirred at rt. [a] isolated yield. [b] determined by chiral HPLC.

3.4.1.5. Acylimidazole scope in asymmetric FC alkylation of indoles

3.4.1.5.1. β,β-Acylimidazoles containing trifluoromethyl group at β-position

Next, we studied the scope of acylimidazoles in the asymmetric FC alkylation of indoles. Initially, we studied β,β-disubstituted enones containing a trifluoromethyl group at the β-position, while systematically changing the second substituted β-position (Table 3.5). Acylimidazole **3.20** containing a CF$_3$ group and a methyl group in the β-position reacted smoothly with indole **3.21b** to furnish the alkylated product **3.22g** in 95% yield and 99% ee. When the R group on the acylimidazole was changed to an ethyl group the corresponding acylimidazole **3.20a** gave the alkylated product **3.25a** 92% yield and 94% ee (entry # 2, Table 3.5). Substrate **3.20b** (R = Bn) underwent FC alkylation to give product **3.25b** in 99% yield and 88% ee (entry # 3, Table 3.5). Acylimidazole **3.20c** furnished FC alkylated product **3.25c** in 88% yield and 85% ee in 48 h (entry # 4, Table 3.5). The FC alkylation reactions proceeded smoothly when electron withdrawing ester groups were present in the β-position of the electrophiles **3.20d** (R = CO$_2$Me) and **3.20e** (R = CO$_2$Et). The products **3.25d** (99% yield, 90% ee) and **3.25e** (97% yield, 91% ee) were obtained in excellent yields and enantioselectivities (entry # 5 and # 6, Table 3.5). When the β-substituent on the acylimidazole was changed to a phenyl group **3.20f** (R = Ph), the reaction failed (entry # 7, Table 3.5).

Table 3.5. Scope of acylimidazoles containing β-trifluoromethyl group.
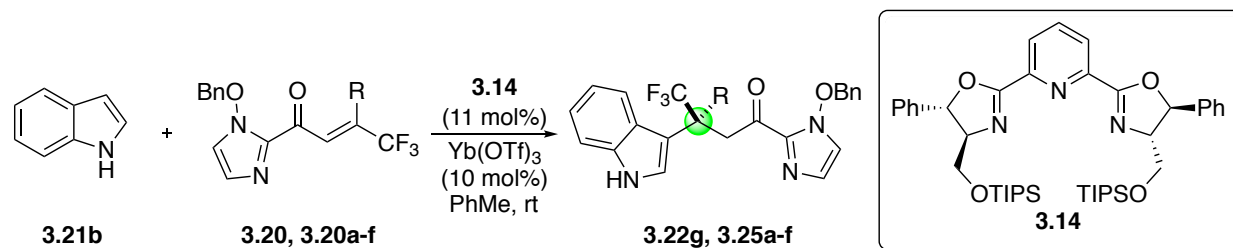
Entry	Substrate	R	Time	Product	Yield (%)[a]	ee (%)[b]
1	**3.20**	Me	2 h	**3.22g**	95	99
2	**3.20a**	Et	24 h	**3.25a**	92	94
3	**3.20b**	Bn	24 h	**3.22b**	99	88
4	**3.20c**	CH$_2$Bn	48 h	**3.25c**	88	85
5	**3.20d**	CO$_2$Et	24 h	**3.22d**	99	90
6	**3.20e**	CO$_2$Me	24 h	**3.25e**	97	91
7	**3.20f**	Ph	7d	**3.25f**	nr	-

Reaction conditions: **3.20, 3.20a-f** (0.1 mmol), **3.21b** (0.2 mmol), Yb(OTf)$_3$ (10 mmol), **3.14** (11 mmol) PhMe (3 mL) were stirred at rt. [a] isolated yield. [b] determined by chiral HPLC.

3.4.1.5.2. *β,β-Acylimidazoles containing β-substituents other than CF$_3$*

One main advantage of acylimidazole acceptors bearing β-CF$_3$ substituent is that these are configurationally stable. But when other substituents such as two alkyl groups for instance, are present at the β-position of the acylimidazoles, they might not be configurationally stable: E/Z isomerization is possible under reaction conditions as depicted in Scheme 3.8. Hence acylimidazole **3.26a** will give a stereoisomer (enantiomer) of the product that is exactly the mirror image of the product obtained from **3.26b**. Hence, this type of isomerization will result in a decrease in the enantioselectivity of the asymmetric process. Also the electrophilicity at the β-carbon is substantially reduced when compared to its CF$_3$ counterpart. In addition, it is really challenging to develop an asymmetric process for molecules with configurational mobility.

3.26a   **3.26b**

R^1, R^2 = alkyl, aryl R^1, R^2 = alkyl, aryl
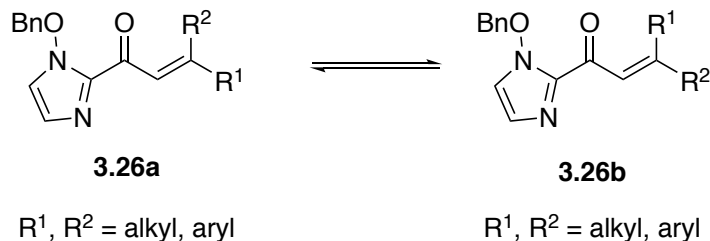
Scheme 3.8. Possible E/Z isomerization under catalytic conditions.

We started our investigation of acylimidazoles of type **3.26** in asymmetric FC alkylation of indoles. When acylimidazole containing alkyl groups at the β-position such as in **3.27a** (R^1 = Me, R^2 = CH$_2$Bn) is subjected to FC reaction conditions alkylated product **3.28a** is obtained in 97% yield and 90% ee (entry # 1, Table 3.6). When acylimidazole **3.27b** (R^1 = Me, R^2 = (CH$_2$)$_2$CH=CMe$_2$) derived from geranial and N-benzyloxyimidazole is used as the substrate in FC reaction with **3.21a** the alkylated product **3.28b** was obtained in 93% yield and 92% ee (entry # 2, Scheme 3.6). Substrate **3.27c** (R^1 = Me, R^2 = CO$_2$Me) gave product **3.28c** in 92% yield and 90% ee on reaction with indole **3.21a**. When the β-positions of the benzyloxy acylimidazoles were substituted by an alkyl and aryl group (R^1 = Me; R^2 = Ar), the reactions became sluggish furnishing moderate to good yield of the product. For instance, compound **3.27d** (R^1 = Me, R^2 = 4-NO$_2$C$_6$H$_4$) on reaction with indole **3.21b** gave product **3.28d** 83% yield and 90% ee (entry # 3, Table 3.6). Substrate **3.27e** (R^1 = Me, R^2 = 4-Cl-C$_6$H$_4$) on reaction with indole **3.21b** gave product **3.28e** 63% yield and 80% ee (entry # 4, Table 3.6).

Table 3.6. Scope of acylimidazoles containing substituents other than β-trifluoromethyl group.
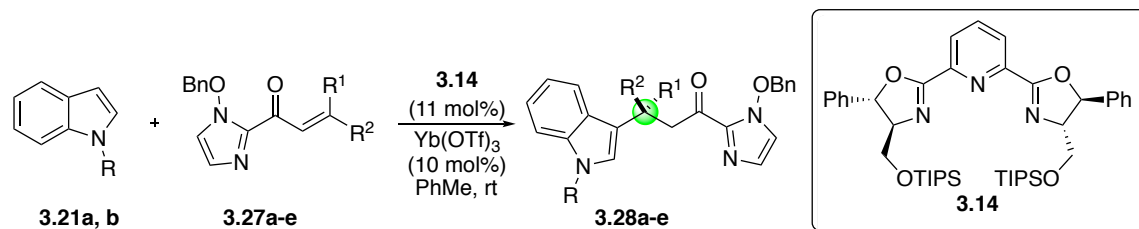
Entry	Indole	R^1	R^2	Substrate	time	Product	yield (%)[a]	ee (%)[b]
1	**3.21a**	Me	CH_2Bn	**3.27a**	2d	**3.28a**	97	90
2	**3.21a**	Me	$(CH_2)_2CH=CMe_2$	**3.27b**	1d	**3.28b**	93	92
3	**3.21a**	Me	CO_2Me	**3.27c**	2d	**3.28c**	92	90
4	**3.21b**	Me	$4\text{-}NO_2\text{-}C_6H_4$	**3.27d**	5d	**3.28d**	83	90
5	**3.21b**	Me	$4\text{-}Cl\text{-}C_6H_4$	**3.27e**	5d	**3.28e**	63	80

Reaction conditions: **3.27a-e** (0.1 mmol), **3.21a-b** (0.2 mmol), Yb(OTf)$_3$ (10 mmol), **3.14** (11 mmol) PhMe (3 mL) were stirred at rt. [a] isolated yield. [b] determined by chiral HPLC.

3.4.1.6. Template cleavage

The N-benzyloxy-2-acylimidazoles can be transformed to carboxylic acid derivatives. The removal of N-benzyloxyimidazole can be accomplished by methylation followed by nucleophilic conditions to yield carboxylic acid derivatives such as esters (Scheme 3.9).
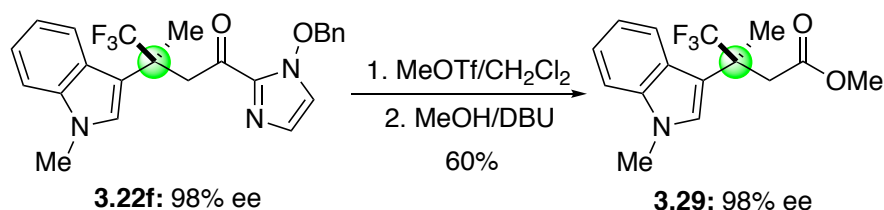
Scheme 3.9. Conversion of benzyloxy acylimidazoles to esters.

3.5. Chiral Lewis acid catalyzed FC reaction between pyrroles and β,β,α-trisubstituted-α,β-unsaturated enones

Although the FC reaction has been used as a powerful C-C bond forming process in synthetic organic chemistry, not all types of aromatic compounds have been employed in

43

stereoselective FC alkylation. The well-studied class of compounds that accounts for about 65%

of the published methodologies is indoles (Figure 3.3). Another nitrogen containing heterocycle

that is equally important but received much less attention compared to indoles is pyrroles. They

constitute about 15% of the reported methodologies. Other FC nucleophiles such as anilines,

furans, phenols, naphthols constitute about 20% of the reported stereoselective methodologies

(Scheme 3.10).

Distribution of arenes in stereoselective FC alkylation

- Misc 1%
- aniline/phenol 17%
- furan/benzene 5%
- Pyrrole 14%
- indole 63%
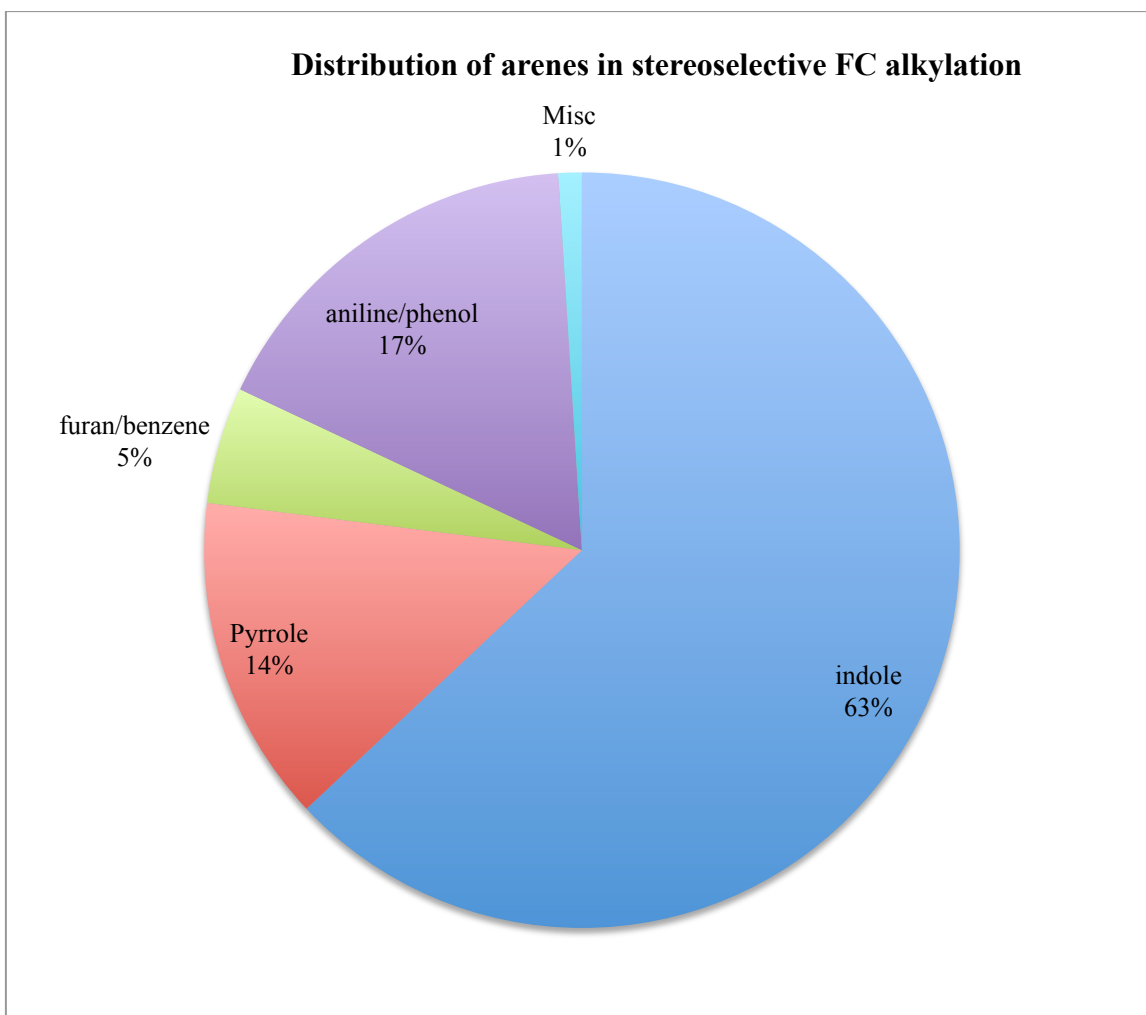
Figure 3.3. Distribution of arenes in catalytic stereoselective FC alkylation.

The huge difference in such distribution is due to the nature of the aromatic compounds.

The substituents (electron donating and electron withdrawing) are very well tolerated in

heteroaromatic systems and the regiochemistry could also be controlled. In fact, the alkylation of indole generally leads to C-3 functionalization while in pyrrole alkylation happens at the C-2 position.
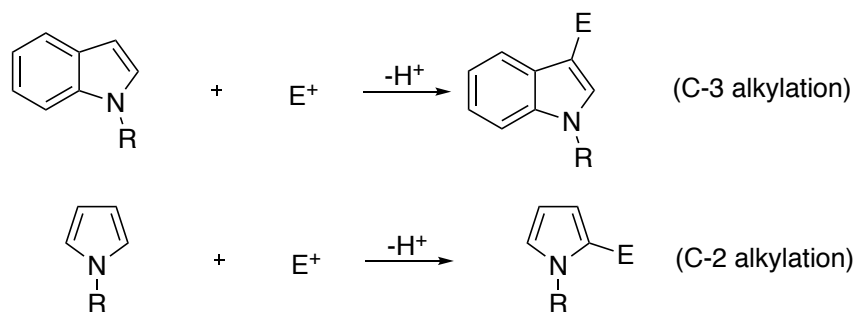
Scheme 3.10. Regioselectivity of alkylation indole vs pyrrole.

Pyrrolyl core is prevalent in many biologically active natural products and in pyrrolidine and pyrrolizidine alkaloids. Some representative natural products that contain a pyrrole core are shown in Figure 3.4. Hence pyrroles can be valued as very useful synthons and pyrrolidine surrogates.[26, 27]

(-)-tashiromine   (-)-razhinilam   (-)-leuconolam   (+)-heliotridane
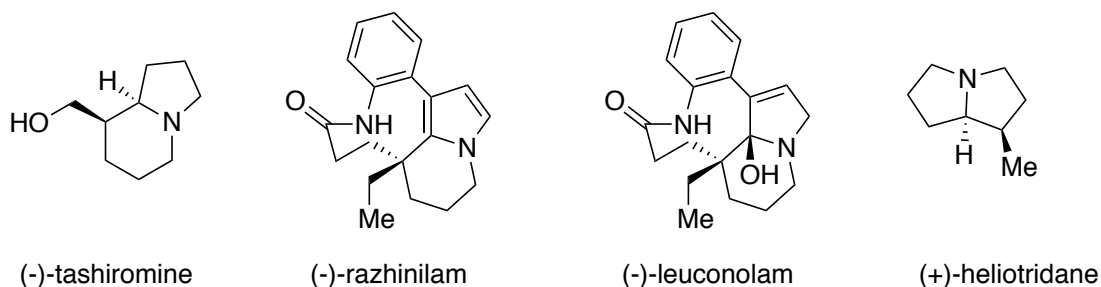
Figure 3.4. Some representative examples of pyrrole natural products.

Macmillan et al. were the first to report enantioselective conjugate addition of pyrroles to α,β-unsaturated carbonyl compounds. The reaction proceeds through iminium ion activation of α,β-unsaturated aldehydes by chiral imidazolidinone catalyst **3.30** (Scheme 3.11). The reaction showed very good scope with respect to the unsaturated aldehydes used and also the pyrroles. The 2-alkylated pyrroles are obtained effectively, with high enantioselectivity.
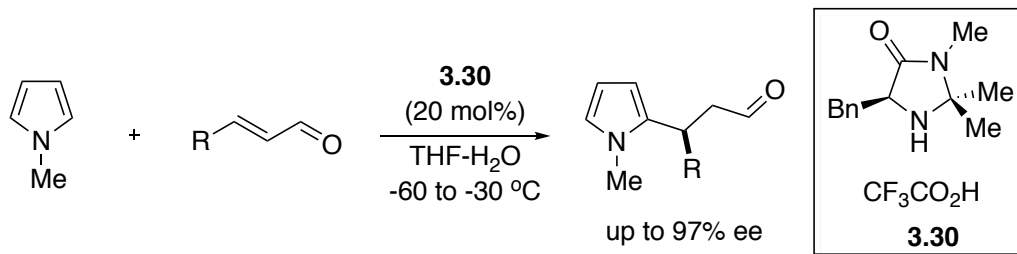
Scheme 3.11. Enantioselective addition of pyrroles to α,β-unsaturated aldehydes using organocatalysis.

Palomo used α'-hydroxyenones as templated substrates in asymmetric FC alkylation of pyrroles. Copper triflate/bisoxazoline **3.31** or **3.32** combination acted as the chiral Lewis acid catalyst in the process. Good chemical efficiency and selectivities are obtained for the catalytic process (Scheme 3.12).
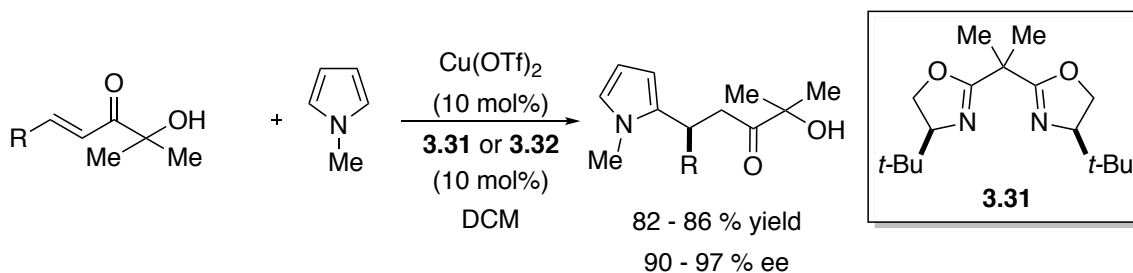
Scheme 3.12. Asymmetric conjugate addition of pyrrole to α'-hydroxyenones.

3.5.1. Results and discussion

3.5.1.1. Survey of chiral Lewis acids for the asymmetric FC alkylation of pyrroles with β,β-disubstituted enones

We have identified N-benzyloxyimidazole as an optimal template for the construction of all carbon quaternary centers using chiral Lewis acid catalyzed FC alkylation of indoles. We surmised that the same template could be successful in constructing quaternary centers using pyrrole as the nucleophile. Initially, we surveyed chiral Lewis acids in effecting the Friedel-Crafts reaction of N-methylpyrrole **3.32a** with β-methyl-β-trifluoromethyl-α,β-unsaturated acylimidazole **3.20**. Copper triflate/bisoxazoline **3.23** complex did not catalyze the reaction even

after 4 days (entry # 1, Table 3.7). Similarly, Zinc triflate/bisoxazoline **3.23** combination did not catalyze the reaction (entry # 2, Table 3.7). Cobalt triflimide/dibenzofuran based bisoxazoline **3.24** gave alkylated product **3.33a** in 80% yield and no selectivity (0% ee) (entry # 3, Table 3.7). Chiral Lewis acid formed from nickel triflimide/**3.24** gave alkylated product **3.33a** in 36% yield and very poor enantioselectivity of 2% ee (entry # 4, Table 3.7). Next, we tried our successful Lewis acid ytterbium triflate with chiral pyridine bisoxazoline ligand **3.34** in FC alkylation of pyrrole **3.32a**. The alkylated product was obtained in 85% yield and 97% ee after 8 hours (entry # 5, Table 3.7). Evans' chiral scandium Lewis acid formed from Sc(OTf)₃/**3.34** gave no alkylated product (entry # 6, Table 3.7).

Table 3.7. Chiral Lewis acid survey for asymmetric pyrrole alkylation with β,β-disubstituted enones.
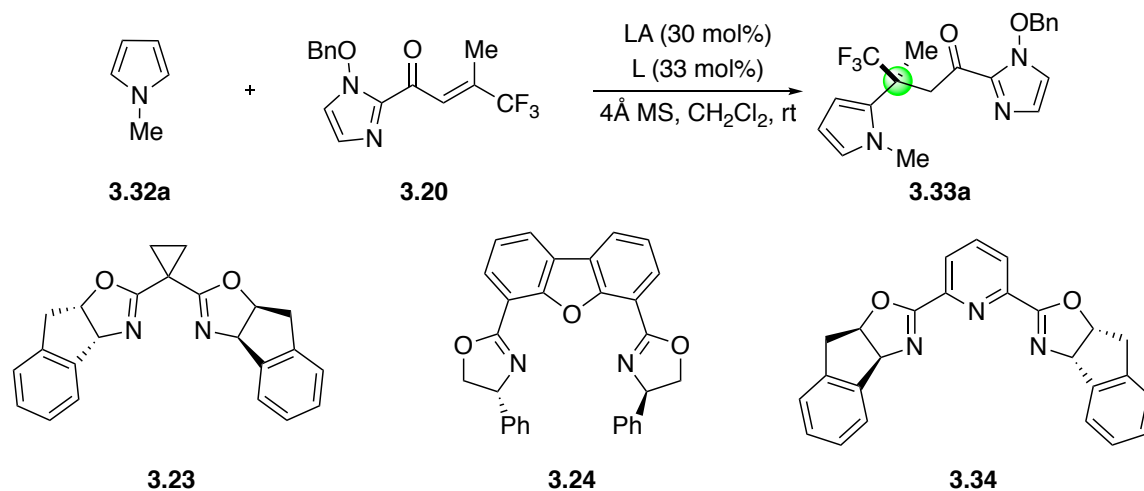
| entry	LA	L	time	**3.33a** yield (%)[a]	**3.33a** ee(%)[b]
1	Cu(OTf)$_2$	**3.23**	4 d	nr	-
2	Zn(OTf)$_2$	**3.23**	4 d	nr	-
3	Co(NTf$_2$)$_2$	**3.24**	4 d	80	0
4	Ni(NTf$_2$)$_2$	**3.24**	4 d	36	2
5	Yb(OTf)$_3$	**3.34**	8 h	85	97
6	Sc(OTf)$_3$	**3.34**	8 h	nr	-

Reaction conditions: **3.20** (0.1 mmol), **3.33a** (0.2 mmol), LA (0.03 mmol), **L** (0.033 mmol) MS 4Å (0.10 g) DCM (2 mL) were stirred at rt. [a] isolated yield. [b] determined by chiral HPLC. nr = no reaction.

3.5.1.2. Survey of chiral ligands for the asymmetric FC alkylation of pyrroles with β,β-disubstituted enones

We surveyed pyridine bisoxazoline ligands for the ytterbium triflate catalyzed FC alkylation of pyrroles. The indane-derived pyridine bisoxazoline **3.34** gave the alkylated product in 85% yield and 97% ee (entry # 1, Table 3.8). The pyridine bisoxazoline ligand **3.35a** gave the pyrrole alkylated product as a racemate in about 16 hours (entry # 2, Table 3.8). Chiral ligand **3.35b** gave 2-alkylated pyrrole **3.33a** in 82 % yield and 45% ee (entry # 3, Table 3.7). The Desimoni type ligand **3.14, 3.14a-b** when used in combination with Yb(OTf)$_3$ gave **3.33a** in high

yields (95% 99%, and 85% yield) and high enantioselectivities (95% , 95%, and 90% ee) (entry

4 - # 6, Table 3.8). The pybox ligand **3.36** gave FC alkylated product **3.33a** in 78% yield and -

65% ee.

Table 3.8. Ligand screening in asymmetric FC alkylation of pyrrole.

3.20   **3.32a**   **3.33a**

3.34

3.35a: R^1 = H, R^2 = t-Bu
3.35b: R^1 = H, R^2 = Ph
3.14: R^1 = Ph, R^2 = CH$_2$OTIPS
3.14a: R^1 = Ph, R^2 = CH$_2$OTBS
3.14b: R^1 = Ph, R^2 = CH$_2$OMs

3.36
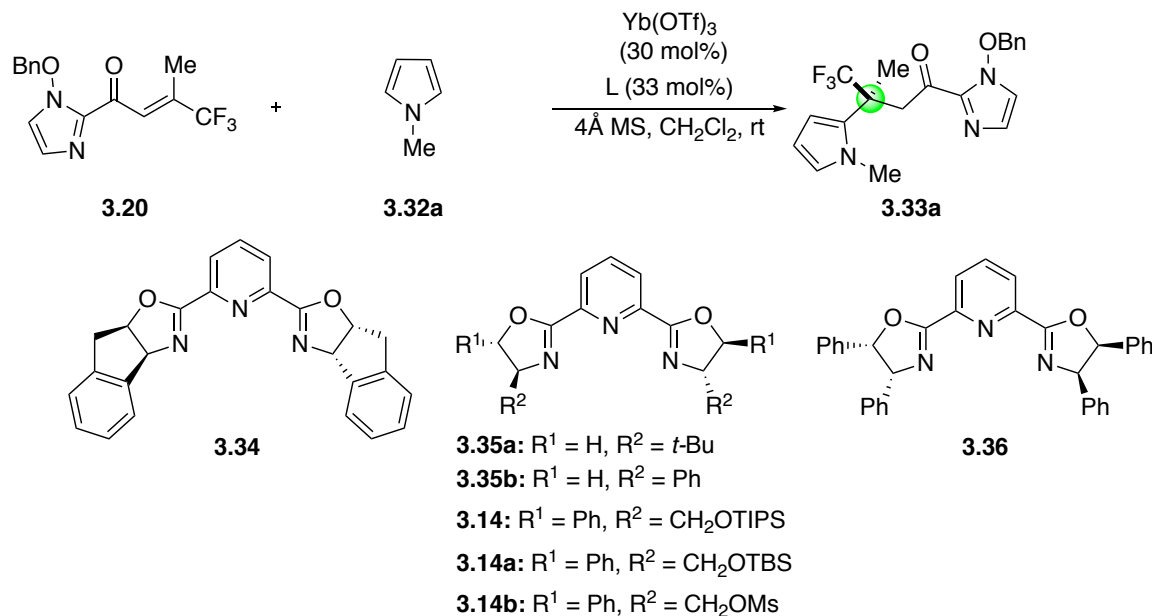
Entry	ligand	time (h)	**3.33a** yield (%)[a]	**3.33a** ee (%)[b]
1	**3.34**	8	85	97
2	**3.35a**	16	85	0
3	**3.35b**	16	82	45
4	**3.14**	24	95	95
5	**3.14a**	16	90	95
6	**3.34b**	24	78	90
7	**3.34**	16	85	-65

Reaction conditions: **3.20** (0.1 mmol), **3.33a** (0.2 mmol), Yb(OTf)$_3$ (0.03 mmol), **L** (0.033 mmol) MS 4Å (0.10 g) DCM (2 mL) were stirred at rt. [a] isolated yield. [b] determined by chiral HPLC.

3.5.1.3. Effect of catalyst loading, temperature on the FC reaction of pyrrole

Having identified the optimal catalytic system we studied the effect of other parameters

on the efficiency of the catalytic process. Initially, we studied the effect of catalytic loading on

the asymmetric FC alkylation process. Reducing the catalytic loading to 15 mol% did not affect the chemical efficiency or the enantioselectivity (compare entry # 1 and # 2, Table 3.9). Reducing the loading all the way to 5% did not have any effect on the yield and selectivity of the FC alkylated product (entry # 3 and # 4, Table 3.9). The temperature didn't have much effect on the enantioselectivity of the reaction but it had a profound effect on reducing the rate of the reaction (entry # 5 and # 6, Table 3.9). We also did solvent screening (results not shown in the table). We found that toluene, benzene, DCM and DCE were the best solvent for the asymmetric FC alkylation of pyrrole. Solvents such as THF and acetonitrile were inefficient.

Table 3.9. Effect of catalyst loading, temperature and additives on the FC reaction of pyrrole.
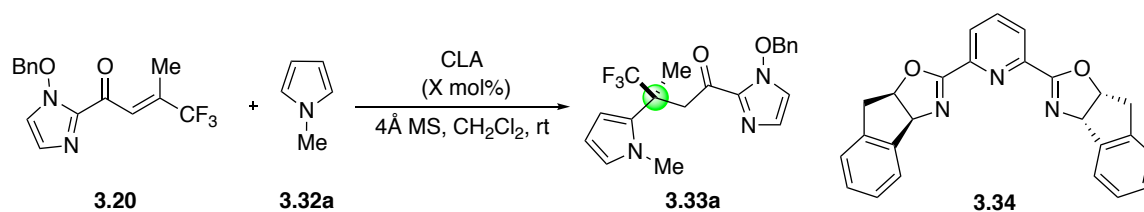
Entry	time (h)	Temp (°C)	X	**3.33a** yield (%)[a]	**3.33a** ee (%)[b]
1	8	rt	30	85	97
2	24	rt	15	82	97
3	24	rt	10	85	98
4	24	rt	5	82	97
5	24	0	30	80	97
6	48	-20	30	81	97

Reaction conditions: **3.20** (0.1 mmol), **3.33a** (0.2 mmol), Yb(OTf)$_3$/L (X mmol), MS 4Å (0.10 g) DCM (2 mL) were stirred at rt. [a] isolated yield. [b] determined by chiral HPLC.

3.5.1.4. Acylimidazole scope in asymmetric FC alkylation of pyrroles

With optimized reaction conditions we studied the scope of acylimidazoles in the FC alkylation of pyrroles and the results are summarized in Table 3.10. Substrate **3.20** (R^1 = CF$_3$, R^2 = Me) reacted with N-methylpyrrole using the catalytic condition given in Table 3.10 gave product **3.33a** in 70% yield and 97% ee (entry # 1, Table 3.10). Acylimidazole **3.20a** (R^1 = CF$_3$,

R^2 = Et) gave 2-alkylated-N-methylpyrrole **3.33b** in 89% yield and 97% ee (entry # 2, Table

3.10). When the β,β-disubstituted enone had two electron withdrawing groups in the β-position

as in **3.20d** (R^1 = CF$_3$, R^2 = CO$_2$Et), and **3.20d** (R^1 = CF$_3$, R^2 = CO$_2$Me) the alkylated product

3.33c-d was obtained in 95% yield and 97% ee (entry # 3 and # 4, Table 3.10). Acylimidazole

substrate **3.20b** (R^1 = CF$_3$, R^2 = Bn), on reaction with pyrrole **3.32a** furnished product **3.33e** in

60% yield and 99% ee (entry # 5, Table 3.10). Similar to our studies on indole alkylation,

substrate **3.20f** was unreactive under the reaction conditions (entry # 6, Table 3.10).

Table 3.10. Acylimidazole scope in FC alkylation of pyrrole.
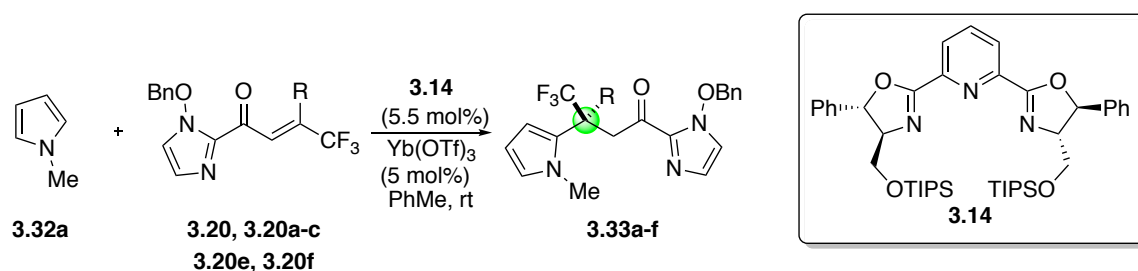
Entry	R	Substrate	time	Product	yield (%)[a]	ee (%)[b]
1	Me	**3.20**	1 h	**3.33a**	70	97
2	Et	**3.20a**	8 h	**3.33b**	88	97
3	CO$_2$Et	**3.20d**	10 h	**3.33d**	95	97
4	CO$_2$Me	**3.20e**	10 h	**3.33e**	95	97
5[c]	Bn	**3.20c**	48 h	**3.33c**	60	99
6	Ph	**3.20f**	7 d	**3.33f**	nr	-

Reaction conditions: **3.20, 3.20a-c, 3.20e-f** (0.1 mmol), **3.33a** (0.2 mmol), Yb(OTf)$_3$/L (5 mmol), PhMe (2 mL) were stirred at rt. [a] isolated yield. [b] determined by chiral HPLC. [c] 30 mol% of chiral Lewis acid used.

3.5.1.5. Pyrrole scope in asymmetric FC alkylation of pyrroles

Finally, we studied the scope of substituted pyrroles in the asymmetric FC alkylation

reaction. Pyrrole **3.32a** reacted with acylimidazole **3.20** to give product **3.33a** in 85% yield and

97% ee (entry # 1, Table 3.11). Initially, we observed the effect of the N-alkyl substitution on the

FC alkylation of pyrrole: N-ethylpyrrole **3.32b** gave the alkylated product **3.33g** in 89% yield

and 94% ee (entry # 3, Table 3.11). N-benzylpyrrole **3.32c** gave the product **3.33h** in moderate

yield of 54% and high enantioselectivity of 94% (entry # 3, Table 3.11). The effects of electron

withdrawing substituents on the N were also studied: *tert*-butyloxycarbonyl- (BOC),

phenylsulfonyl- (PhSO$_2$) groups were detrimental to the reaction. N-TIPSpyrrole was also

unreactive under the reaction conditions (These results are not shown in the table). Parent pyrrole

3.32d, however, is very reactive and gave the alkylated product **3.33i** in 82% yield and 84% ee

(entry # 4, Table 3.11). 2-ethylpyrrole **3.32e** was also a competent nucleophile and furnished the

product **3.33j** in 90% yield and 66% ee (entry # 5, Table 3.11). Disubstituted pyrroles: 2,4-

dimethylpyrrole **3.32f** and trisubstituted pyrroles: 2-ethyl-3,4-dimethylpyrrole **3.32g** are very

reactive nucleophiles under the current conditions: high yields of the products were obtained

albeit no selectivity (not shown in the table).

Table 3.11. Pyrrole scope in asymmetric FC alkylation.
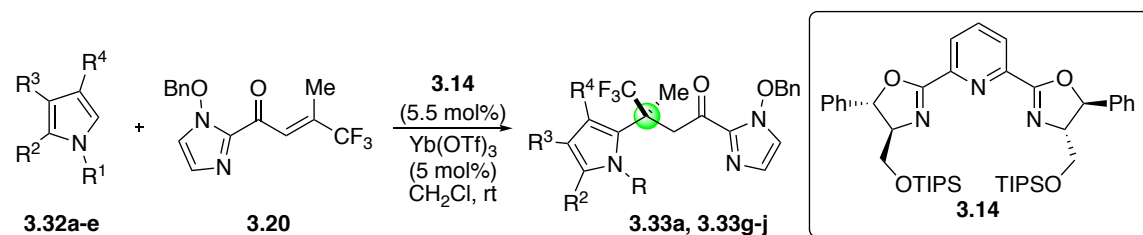
Entry	R^1	R^2	pyrrole	time (h)	yield(%)^a	ee (%)^b
1	Me	H	**3.32a**	1	85	97
2	Et	H	**3.32b**	8	89	94
3	Bn	H	**3.32c**	18	51	94
4	H	H	**3.32d**	4	82	84
5	H	Et	**3.32e**	4	90	66

Reaction conditions: **3.20** (0.1 mmol), **3.33a-e** (0.2 mmol), Yb(OTf)$_3$/L (5 mmol), DCM (2 mL) were stirred at rt. ^{a} isolated yield. ^{b} determined by chiral HPLC.

3.5.1.6. Template cleavage

The N-benzyloxy-2-acylimidazoles can be transformed to carboxylic acid derivatives. The removal of N-benzyloxyimidazole can be accomplished by the methylation followed by nucleophilic conditions to yield carboxylic acid derivatives such as esters (Scheme 3.13).
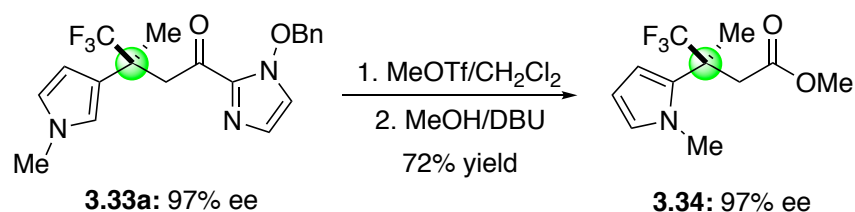
Scheme 3.13. Conversion of benzyloxy acylimidazoles to esters.

3.6. Conclusions

In conclusion we have disclosed a highly enantioselective protocol based on conjugate Friedel-Crafts addition to β,β-disubstituted-α,β-unsaturated acylimidazoles. In this study we have compared the effect of different templates in successfully constructing all carbon quaternary centers. We have shown that a lanthanide Lewis acid/pyridine bisoxazoline combination can be used as a chiral Lewis acid catalyst for the construction of quaternary centers using asymmetric Friedel-Crafts reaction. We have successfully demonstrated that indoles and pyrroles are competent nucleophiles in these reactions. Through this study we have identified 1-benzyloxyimidazole as a novel template that can be used in several challenging asymmetric transformations. Finally N-benzyloxyimidazole could be transformed to carboxylic acid derivatives such as esters which can be useful building blocks. Further use of this achiral template in other organic transformations is underway in our laboratory.

3.7. Experimental section and supporting information

All solvents were dried and degassed by standard methods and stored under nitrogen. Flash chromatography was performed using EM Science silica gel 60 (230-400 mesh). ^{1}H NMR

spectra were recorded on Varian Unity/Inova-400 NB (400 MHz) and Bruker (400 MHz) spectrometer. ^{13}C NMR spectra were recorded on Bruker (100 MHz) spectrometer. HPLC analyses were carried out with Waters 515 HPLC pumps and a 2487 dual wavelength absorbance detector connected to a PC with Empower workstation. Rotations were recorded on a JASCO-DIP-370 polarimeter. High-resolution mass spectra were obtained using Waters SYNAPT-G2-Si-HDMS spectrometer.

3.7.1. General procedure for catalytic asymmetric alkylation of indoles

In a flame-dried 6-dram vial with magnetic stirbar was added Yb(OTf)$_3$ (0.01 mmol), ligand (0.011 mmol) and toluene (4 ml). The mixture was stirred for 30 minutes after which appropriate acylimidazole substrate (0.1 mmol) was added. After 5 minutes, indole (0.2 mmol) was added and the mixture was stirred. After the completion of reaction the mixture was directly loaded on to silica gel column and the product was separated.

3.22f
C$_{24}$H$_{22}$F$_3$N$_3$O$_2$
M. Wt.: 441.45
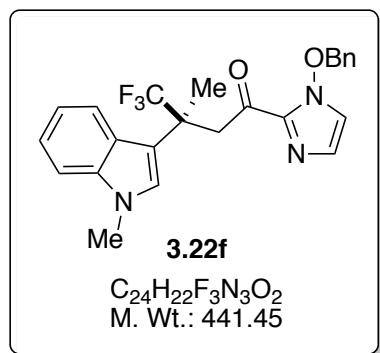
(3R3S)-4,4,4-Trifluoro-1-(1-benzyloxy-1H-imidazol-2-yl)-3-methyl-3-(1-methyl-1H-indol-3-yl)butan-1-one (3.22f): ^{1}H NMR (400 MHz, CDCl$_3$) δ 7.85 (d, J = 8.1 Hz, 1H), 7.45 – 7.13 (m, 6H), 7.11 – 7.02 (m, 3H), 6.93 (d, J = 0.9 Hz, 1H), 6.73 (d, J = 0.9 Hz, 1H), 4.85 – 4.58 (m, 3H), 3.73 (s, 3H), 3.46 (d, J = 16.7 Hz, 1H), 2.05 (s, 3H). ^{13}C NMR (101 MHz, CDCl$_3$) δ δ 185.0, 153.1, 138.2, 135.9, 128.4, 128.0, 127.4, 126.9, 124.7, 124.4, 123.9, 122.1, 121.5, 120.5,

119.4, 111.8, 109.8, 93.5, 72.6, 48.1, 44.8, 44.5, 33.5, 19.0. ^{19}F NMR (376 MHz, CDCl$_3$) δ -76.01. HRMS: Calcd for C$_{24}$H$_{23}$F$_3$N$_3$O$_2$ [M+H$^+$]: 442.1737; Found: 442.1729.

The ee value was determined by HPLC analysis using a CHIRALPAK IC column (1 mL/min, 5%, i-PrOH in hexane); retention times: 18.34 min (min enantiomer) and 28.91 min (maj enantiomer).

3.22g
C$_{23}$H$_{20}$F$_3$N$_3$O$_2$
M. Wt.: 427.43
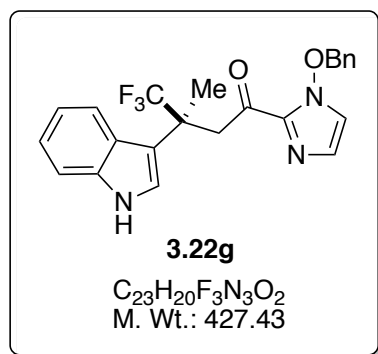
(3R3S)-4,4,4-Trifluoro-3-(1H-indol-3-yl)-1-(1-benzyloxy-1H-imidazol-2-yl)-3-methylbutan-1-one (3.22 g): ^{1}H NMR (400 MHz, CDCl$_3$) δ 8.19 (s, 1H), 7.86 (d, *J* = 8.1 Hz, 1H), 7.39 – 7.26 (m, 5H), 7.19 – 7.13 (m, 1H), 7.11 – 7.03 (m, 2H), 6.93 (d, *J* = 0.9 Hz, 1H), 6.73 (d, *J* = 1.0 Hz, 1H), 4.84 (d, *J* = 10.8 Hz, 1H), 4.72 (d, *J* = 10.8 Hz, 1H), 4.66 (d, *J* = 16.8 Hz, 1H), 3.55 – 3.40 (m, 1H), 2.05 (s, 3H). ^{13}C NMR (101 MHz, CDCl$_3$) δ 186.4, 138.1, 136.8, 133.0, 132.5, 130.0, 129.7, 129.5, 128.6, 126.9, 125.8, 125.0, 124.5, 122.3, 121.8, 121.6, 119.7, 111.4, 81.9, 77.4, 77.1, 76.7, 44.8, 44.5, 44.2, 44.0, 41.5, 20.1, 20.1. ^{19}F NMR (376 MHz, CDCl$_3$) δ -76.0. HRMS: Calcd for C$_{23}$H$_{21}$F$_3$N$_2$O$_2$ [M+H$^+$]: 428.1580; Found: 428.1567.

The ee value was determined by HPLC analysis using a CHIRALPAK IC column (1 mL/min, 5%, i-PrOH in hexane); retention times: 13.69 min (min enantiomer) and 23.39 min (maj enantiomer).
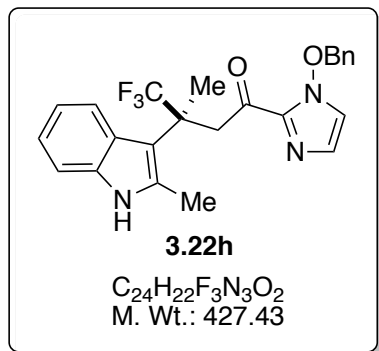
(3R3S)-4,4,4-Trifluoro-1-(1-benzyloxy-1H-imidazol-2-yl)-3-methyl-3-(2-methyl-1H-indol-3-yl)butan-1-one (3.22h): ^{1}H NMR (400 MHz, CDCl$_3$) δ 7.86 (s, 1H), 7.77 (d, *J* = 8.2 Hz, 1H), 7.40 – 7.27 (m, 3H), 7.20 (d, *J* = 8.0 Hz, 1H), 7.05 (td, *J* = 8.5, 1.3 Hz, 3H), 6.97 (ddd, *J* = 8.2, 7.1, 1.2 Hz, 1H), 6.93 (d, *J* = 1.1 Hz, 1H), 6.72 (d, *J* = 1.1 Hz, 1H), 5.01 (d, *J* = 18.4 Hz, 1H), 4.77 (d, *J* = 10.9 Hz, 1H), 4.65 (d, *J* = 10.9 Hz, 1H), 3.35 (d, *J* = 18.3 Hz, 3H), 2.60 (s, 3H), 2.15 (s, 1H). ^{13}C NMR (101 MHz, CDCl$_3$) δ 185.9, 137.8, 134.8, 133.7, 133.1, 130.3, 130.0, 129.4, 128.6, 128.3, 127.5, 124.9, 122.1, 121.1, 120.7, 119.4, 110.4, 107.5, 81.8, 77.4, 77.0, 76.7, 45.5, 45.3, 45.0, 44.8, 43.6, 22.4, 22.3, 16.1. ^{19}F NMR (376 MHz, CDCl$_3$) δ -76.4. HRMS: Calcd for C$_{24}$H$_{23}$F$_3$N$_3$O$_2$ [M+H^{+}]: 442.1737; Found: 442.1724.

The ee value was determined by HPLC analysis using a CHIRALPAK IC column (1 mL/min, 5%, i-PrOH in hexane); retention times: 13.8 min (min enantiomer) and 28.95 min (maj enantiomer).

(3R3S)-3-(1,2-Dimethyl-1H-indol-3-yl)-4,4,4-trifluoro-1-(1-benzyloxy-1H-imidazol-2-yl)-3-methylbutan-1-one (3.22i): ^{1}H NMR (400 MHz, CDCl$_3$) δ 7.88 (d, J = 4.7 Hz, 1H), 7.63 – 7.59 (m, 1H), 7.53 (m, 1H), 7.38 – 7.24 (m, 6H), 7.14 – 7.06 (m, 2H), 6.95 (d, J = 4.5 Hz, 1H), 5.01 (dd, J = 10, 10 Hz 2H), 4.25 (d, J = 17.1 Hz, 1H), 3.75 (d, J = 17.1 Hz, 1H), 3.40 (s, 3H), 2.60 (s, 3H), 2.03 (s, 3H). ^{13}C NMR (101 MHz, CDCl$_3$) δ 153.1, 138.7, 138.6, 135.9, 129.4, 128.4, 128.0, 127.2, 125.4, 122.9, 122.7, 120.2, 120.1, 117.4, 111.8, 110.4, 87.1, 72.6, 47.4, 29.4, 19.6, 11.6. ^{19}F NMR (376 MHz, CDCl$_3$) δ -75.4. HRMS: Calcd for C$_{25}$H$_{25}$F$_3$N$_3$O$_2$ [M+H$^+$]: 456.1893; Found: 456.1899.

The ee value was determined by HPLC analysis using a CHIRALPAK IC column (1 mL/min, 5%, i-PrOH in hexane); retention times: 31.87 min (min enantiomer) and 49.14 min (maj enantiomer).

3.22j
C$_{23}$H$_{19}$F$_4$N$_3$O$_2$
M. Wt.: 445.42
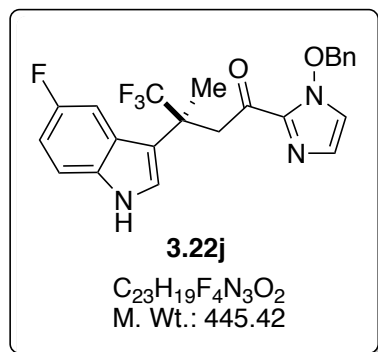
(3R3S)-4,4,4-Trifluoro-3-(5-fluoro-1H-indol-3-yl)-1-(1-benzyloxy-1H-imidazol-2-yl)-3-methylbutan-1-one (3.22j): ^{1}H NMR (400 MHz, CDCl$_3$) δ 7.64 (d, J = 7.6 Hz, 1H), 7.39 – 7.25 (m, 7H), 7.22 (d, J = 7.3 Hz, 1H), 7.15 (d, J = 7.5 Hz, 1H), 6.96 – 6.87 (m, 2H), 4.98 (dd, J = 9.0, 9.0 2H), 3.83 (d, J = 17.3 Hz, 1H), 3.33 (d, J = 17.4 Hz, 1H), 2.21 (s, 3H). ^{13}C NMR (101 MHz, CDCl$_3$) δ 199.7, 157.3, 154.8, 153.1, 135.9, 135.0, 135.0, 128.8, 128.7, 128.4, 128.0, 124.4, 123.4, 121.9, 114.2, 114.0, 112.9, 112.8, 111.8, 106.2, 106.0, 72.6, 70.7, 70.6, 48.2, 45.3, 19.0. HRMS: Calcd for C$_{23}$H$_{20}$F$_4$N$_3$O$_2$ [M+H$^+$]: 446.1486; Found:446.1492.

The ee value was determined by HPLC analysis using a CHIRALPAK IC column (0.5 mL/min, 1%, i-PrOH in hexane); retention times: 24.19 min (min enantiomer) and 27.52 min (maj enantiomer).
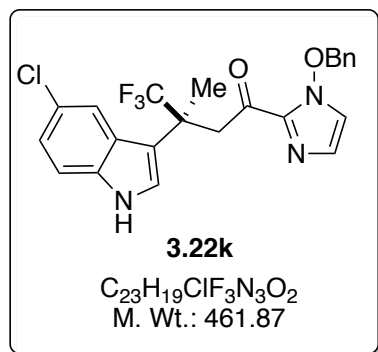
(3R)-3-(5-Chloro-1H-indol-3-yl)-4,4,4-trifluoro-1-(1-benzyloxy-1H-imidazol-2-yl)-3-methylbutan-1-one (3.22k): ^{1}H NMR (400 MHz, CDCl$_3$) δ 7.64 (d, J = 7.6 Hz, 1H), 7.50 (s, 1H), 7.38 – 7.20 (m, 8H), 7.15 (d, J = 7.5 Hz, 1H), 7.05 (d, J = 7.3 Hz, 1H), 4.98 (dd, J = 10.9, 10.9 Hz, 1H), 3.83 (d, J = 17.3 Hz, 1H), 3.33 (d, J = 17.4 Hz, 1H), 2.06 (s, 3H). ^{13}C NMR (101 MHz, CDCl$_3$) δ 186.2, 153.1, 137.0, 135.9, 129.4, 128.4, 128.0, 127.4, 127.3, 124.7, 124.4, 122.0, 121.9, 121.9, 120.4, 119.4, 112.8, 111.8, 72.6, 70.7, 48.1, 45.5, 19.1. ^{19}F NMR (376 MHz, CDCl$_3$) δ -75.8. HRMS: Calcd for C$_{23}$H$_{20}$F$_3$N$_3$O$_2$Cl [M+H$^+$]: 462.1191; Found: 462.1173.

The ee value was determined by HPLC analysis using a CHIRALPAK IC column (1 mL/min, 5%, i-PrOH in hexane); retention times: 10.03 min (min enantiomer) and 14.82 min (maj enantiomer).

3.22l
$C_{23}H_{19}BrF_3N_3O_2$
M. Wt.: 506.32

(3R)-3-(5-Bromo-1H-indol-3-yl)-4,4,4-trifluoro-1-(1-benzyloxy-1H-imidazol-2-yl)-3-methylbutan-1-one (3.22l): ^{1}H NMR (400 MHz, CDCl$_3$) δ 7.74 – 7.57 (m, 2H), 7.45 – 7.05 (m, 10H), 5.12 (dd, J = 10.7, 10.7 Hz, 2H), 3.83 (d, J = 17.3 Hz, 2H), 3.33 (d, J = 17.4 Hz, 2H), 2.06 (s, 3H). ^{13}C NMR (101 MHz, CDCl$_3$) δ 186.4, 153.1, 137.0, 135.9, 128.4, 128.0, 127.4, 127.0, 124.7, 124.4, 123.6, 123.1, 122.0, 121.9, 119.4, 114.7, 113.5, 111.8, 72.6, 70.6, 48.2, 45.7, 45.5, 45.2, 44.9, 19.1. ^{19}F NMR (376 MHz, CDCl$_3$) δ -76.1. HRMS: Calcd for $C_{23}H_{20}F_3N_3O_2Cl$ [M+H$^+$]: 506.0686; Found: 506.0668.

The ee value was determined by HPLC analysis using a CHIRALPAK IC column (1 mL/min, 5%, i-PrOH in hexane); retention times: 9.99 min (min enantiomer) and 14.72 min (maj enantiomer).

3.22m
$C_{25}H_{22}F_3N_3O_4$
M. Wt.: 485.46

Methyl 3-[(2R)-1,1,1-trifluoro-4-(1-benzyloxy-1H-imidazol-2-yl)-2-methyl-4-oxobutan-2-yl]-1H-indole-5-carboxylate (3.22m): ^{1}H NMR (400 MHz, CDCl$_3$) δ 8.39 – 8.35 (s, 1H), 7.76 (d, J = 7.5 Hz, 1H), 7.64 (d, J = 7.6 Hz, 1H), 7.50 – 7.46 (m, 1H), 7.43 (d, J = 7.3

Hz, 1H), 7.39 – 7.27 (m, 6H), 7.24 (d, J = 7.3 Hz, 1H), 7.15 (d, J = 7.5 Hz, 1H), 4.98 (dd, J =

10.6 Hz, 2H), 3.93 (s, 1H), 3.83 (d, J = 17.3 Hz, 1H), 3.33 (d, J = 17.4 Hz, 1H), 2.13 (s, 1H). [13]C

NMR (101 MHz, CDCl$_3$) δ 187.2, 167.8, 153.1, 136.1, 135.9, 129.3, 128.4, 128.0, 127.4, 124.7,

124.4, 123.7, 123.6, 122.9, 122.0, 121.9, 119.4, 111.8, 110.7, 72.6, 70.6, 52.0, 48.1, 45.7, 45.5,

45.2, 44.9, 19.0. HRMS: Calcd for C$_{25}$H$_{23}$F$_3$N$_3$O$_2$ [M+H$^+$]: 486.1635; Found: 486.1652.

The ee value was determined by HPLC analysis using a CHIRALPAK IC column (0.5

mL/min, 1%, i-PrOH in hexane); retention times: 24.19 min (min enantiomer) and 27.52

min (maj enantiomer).

3.22n
C$_{24}$H$_{22}$F$_3$N$_3$O$_3$
M. Wt.: 457.45
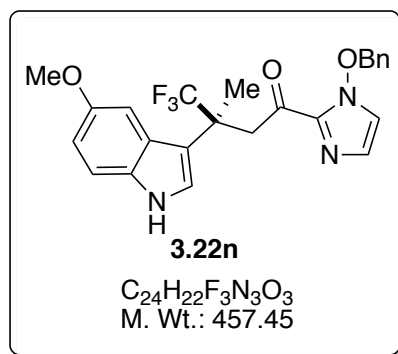
(3R3S)-4,4,4-Trifluoro-1-(1-benzyloxy-1H-imidazol-2-yl)-3-(5-methoxy-1H-indol-3-

yl)-3-methylbutan-1-one (3.22n): ^{1}H NMR (400 MHz, CDCl$_3$) δ 7.64 (d, J = 7.6 Hz, 1H), 7.38

– 7.26 (m, 6H), 7.21 (d, J = 7.3 Hz, 1H), 7.15 (d, J = 7.5 Hz, 1H), 7.10 – 7.03 (m, 2H), 6.81

(dd, J = 7.5, 1.5 Hz, 1H), 4.98 (s, 2H), 3.92 – 3.72 (m, 4H), 3.33 (d, J = 17.4 Hz, 2H), 1.91 (s,

3H). ^{13}C NMR (101 MHz, CDCl$_3$) δ 184.9, 154.7, 153.1, 135.9, 134.7, 129.1, 128.4, 128.0,

127.4, 124.7, 124.4, 122.0, 121.9, 119.4, 112.4, 112.1, 111.8, 105.0, 72.6, 70.6, 55.8, 48.1, 45.7,

45.5, 45.2, 44.9, 19.1. ^{19}F NMR (376 MHz, CDCl$_3$) δ -76.4. HRMS: Calcd for C$_{24}$H$_{23}$F$_3$N$_3$O$_3$

[M+H$^+$]: 458.1686; Found: 458.1672.

The ee value was determined by HPLC analysis using a CHIRALPAK IC column (1

mL/min, 5%, i-PrOH in hexane) retention times: 12.46 min (min enantiomer) and 18.02

min (maj enantiomer).

Me

F₃C **Me** **O** **OBn**

3.22o

$C_{24}H_{22}F_3N_3O_2$

M. Wt.: 441.45
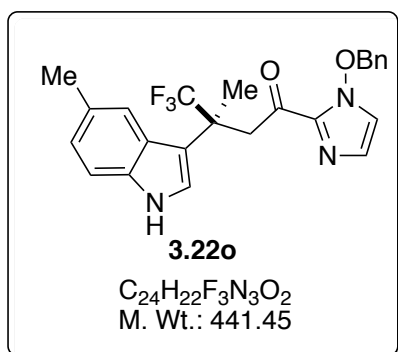
(3R3S)-4,4,4-Trifluoro-1-(1-benzyloxy-1H-imidazol-2-yl)-3-methyl-3-(5-methyl-1H-indol-3-yl)butan-1-one (3.22o): ^{1}H NMR (400 MHz, CDCl₃) δ 7.86 (s, 1H), 7.77 (d, J = 8.2 Hz, 1H), 7.40 – 7.27 (m, 3H), 7.20 (d, J = 8.0 Hz, 1H), 7.05 (td, J = 8.5, 1.3 Hz, 3H), 6.97 (ddd, J = 8.2, 7.1, 1.2 Hz, 1H), 6.93 (d, J = 1.1 Hz, 1H), 6.72 (d, J = 1.1 Hz, 1H), 5.01 (d, J = 18.4 Hz, 1H), 4.77 (d, J = 10.9 Hz, 1H), 4.65 (d, J = 10.9 Hz, 1H), 3.35 (d, J = 18.3 Hz, 3H), 2.60 (s, 3H), 2.15 (s, 1H). ^{13}C NMR (101 MHz, CDCl₃) δ 185.9, 137.8, 134.8, 133.7, 133.1, 130.3, 130.0, 129.4, 128.6, 128.3, 127.5, 124.9, 122.1, 121.1, 120.7, 119.4, 110.4, 107.5, 81.8, 77.4, 77.0, 76.7, 45.5, 45.3, 45.0, 44.8, 43.6, 22.4, 22.3, 16.1. ^{19}F NMR (376 MHz, CDCl₃) δ -76.4. HRMS: Calcd for $C_{24}H_{23}F_3N_3O_2$ [M+H^{+}]: 442.1737; Found: 442.1724.

The ee value was determined by HPLC analysis using a CHIRALPAK IC column (1 mL/min, 5%, i-PrOH in hexane); retention times: 17.65 min (min enantiomer) and 28.90 min (maj enantiomer).

Me
F₃C, Me O OBn
N
N
H
3.22p
C₂₄H₂₂F₃N₃O₂
M. Wt.: 441.45
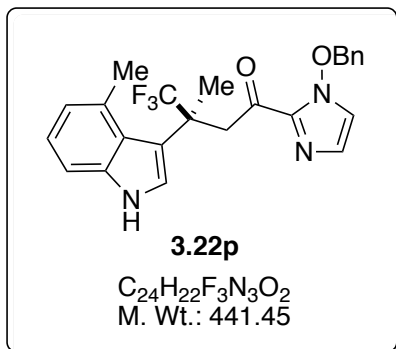
(3R3S)-4,4,4-Trifluoro-1-(1-benzyloxy-1H-imidazol-2-yl)-3-methyl-3-(4-methyl-1H-indol-3-yl)butan-1-one (3.22p): ^{1}H NMR (400 MHz, CDCl$_3$) δ 7.86 (s, 1H), 7.77 (d, J = 8.2 Hz, 1H), 7.40 – 7.27 (m, 3H), 7.20 (d, J = 8.0 Hz, 1H), 7.05 (td, J = 8.5, 1.3 Hz, 3H), 6.97 (ddd, J = 8.2, 7.1, 1.2 Hz, 1H), 6.93 (d, J = 1.1 Hz, 1H), 6.72 (d, J = 1.1 Hz, 1H), 5.01 (d, J = 18.4 Hz, 1H), 4.77 (d, J = 10.9 Hz, 1H), 4.65 (d, J = 10.9 Hz, 1H), 3.35 (d, J = 18.3 Hz, 3H), 2.60 (s, 3H), 2.15 (s, 1H). ^{13}C NMR (101 MHz, CDCl$_3$) δ 185.9, 137.8, 134.8, 133.7, 133.1, 130.3, 130.0, 129.4, 128.6, 128.3, 127.5, 124.9, 122.1, 121.1, 120.7, 119.4, 110.4, 107.5, 81.8, 77.4, 77.0, 76.7, 45.5, 45.3, 45.0, 44.8, 43.6, 22.4, 22.3, 16.1. ^{19}F NMR (376 MHz, CDCl$_3$) δ -76.4. HRMS: Calcd for C₂₄H₂₃F₃N₃O₂ [M+H^{+}]: 442.1737; Found: 442.1724.

The ee value was determined by HPLC analysis using a CHIRALPAK IC column (1 mL/min, 5%, i-PrOH in hexane); retention times: 10.03 min (min enantiomer) and 14.82 min (maj enantiomer).

(3R3S)-3-(1H-indol-3-yl)-1-(1-benzyloxy-1H-imidazol-2-yl)-3-(trifluoromethyl)pentan-1-one (3.25a): ^{1}H NMR (400 MHz, CDCl$_3$) δ 7.69 – 7.61 (m, 2H), 7.40 – 7.27 (m, 6H), 7.24 – 7.10 (m, 5H), 4.98 (dd, J = 10.9 Hz, 1H), 3.83 (d, J = 17.6 Hz, 1H), 3.33 (d, J = 17.4 Hz, 1H), 2.12 (m, 2H), 1.53 (t, J = 8.1 Hz, 1H). ^{13}C NMR (101 MHz, CDCl$_3$) δ 184.5, 152.6, 135.8, 134.5, 128.4, 128.0, 127.3, 126.9, 125.2, 124.6, 123.0, 122.9, 121.9, 121.7, 119.2, 112.5, 111.3, 72.4, 71.2, 54.1, 53.8, 53.5, 53.3, 47.0, 27.0, 11.3. ^{19}F NMR (376 MHz, CDCl$_3$) δ -76.1. HRMS: Calcd for C$_{24}$H$_{23}$F$_3$N$_3$O$_2$ [M+H$^+$]: 442.1737; Found: 442.1746.

The ee value was determined by HPLC analysis using a CHIRALPAK IC column (1 mL/min, 5%, i-PrOH in hexane); retention times: 12.48 min (min enantiomer) and 25.38 min (maj enantiomer).
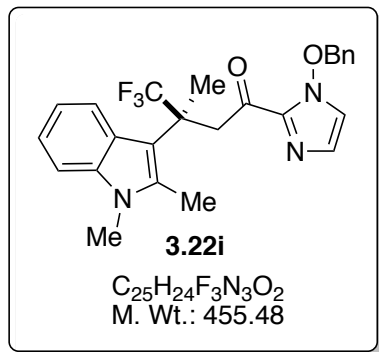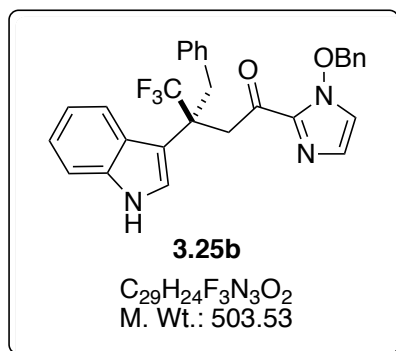

(3R3S)-3-(1H-Indol-3-yl)-1-(1-benzyloxy-1H-imidazol-2-yl)-3-(trifluoromethyl)-4-phenylbutan-1-one (3.25b): ^{1}H NMR (400 MHz, CDCl$_3$) δ 7.69 – 7.60 (m, 2H), 7.39 – 7.10 (m, 14H), 6.74 (m, 2H), 4.98 (dd, J = 9.9 Hz, 2H), 3.88 (d, J = 17.6 Hz, 1H), 3.52 – 3.33 (m, 2H),

2.95 (dt, $J = 13.0, 1.0$ Hz, 1H). ^{13}C NMR (101 MHz, CDCl$_3$) δ 186.1, 152.6, 135.8, 135.1, 134.8, 134.5, 134.2, 130.9, 128.4, 128.3, 128.0, 126.9, 126.8, 126.5, 125.2, 123.8, 122.9, 121.7, 121.2, 120.7, 120.1, 118.5, 112.5, 111.3, 73.1, 72.4, 52.8, 52.5, 52.3, 52.0, 46.6, 38.5. ^{19}F NMR (376 MHz, CDCl$_3$) δ -76.4. HRMS: Calcd for C$_{29}$H$_{25}$F$_3$N$_3$O$_2$ [M+H^{+}]: 504.1893; Found: 504.1904.

The ee value was determined by HPLC analysis using a CHIRALPAK IC column (1 mL/min, 5%, i-PrOH in hexane); retention times: 18.62 min (min enantiomer) and 35.55 min (maj enantiomer).

3.25c
C$_{30}$H$_{26}$F$_3$N$_3$O$_2$
M. Wt.: 517.55
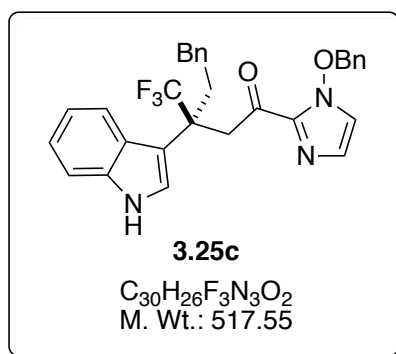
(3R3S)-3-(1H-Indol-3-yl)-1-(1-methoxy-1H-imidazol-2-yl)-3-(trifluoromethyl)-5-phenylpentan-1-one (3.25c): ^{1}H NMR (400 MHz, CDCl$_3$) δ 7.70 – 7.61 (m, 2H), 7.42 – 7.06 (m, 16H), 4.98 (dd, $J = 10.7$ Hz, 2H), 3.85 (d, $J = 17.6$ Hz, 1H), 3.35 (d, $J = 17.4$ Hz, 1H), 2.83 (dtt, $J = 13.9, 7.1, 1.0$ Hz, 1H), 2.75 – 2.65 (m, 1H), 2.54 (dt, $J = 14.1, 7.1$ Hz, 1H), 2.04 (dt, $J = 14.0, 7.1$ Hz, 1H). ^{13}C NMR (101 MHz, CDCl$_3$) δ 185.9, 153.1, 141.4, 137.1, 135.9, 128.4, 128.3, 128.3, 128.0, 127.1, 126.1, 126.0, 124.4, 122.9, 122.1, 121.7, 120.1, 119.0, 112.5, 111.8, 72.6, 70.8, 52.4, 52.1, 51.8, 51.6, 46.8, 35.9, 29.9. ^{19}F NMR (376 MHz, CDCl$_3$) δ -76.4. HRMS: Calcd for C$_{30}$H$_{27}$F$_3$N$_3$O$_2$ [M+H^{+}]: 518.2050; Found: 518.2061.

The ee value was determined by HPLC analysis using a CHIRALPAK IC column (1 mL/min, 5%, i-PrOH in hexane); retention times: 18.62 min (min enantiomer) and 35.55 min (maj enantiomer).

3.25d
C24H20F3N3O4
M. Wt.: 471.44
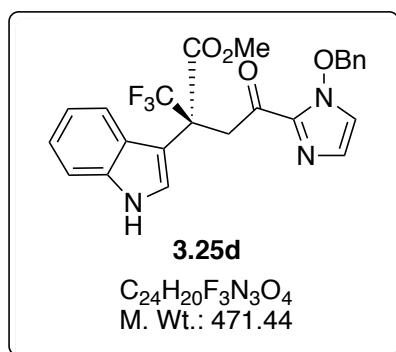
Methyl (2R)-2-(1H-indol-3-yl)-4-(1-methoxy-1H-imidazol-2-yl)-4-oxo-2-(trifluoromethyl)butanoate (3.25d): ^{1}H NMR (400 MHz, CDCl$_3$) δ 7.69 – 7.62 (m, 2H), 7.39 – 7.26 (m, 7H), 7.24 – 7.10 (m, 4H), 4.98 (dd, *J* = 10.9 Hz, 2H), 4.18 (d, *J* = 17.7 Hz, 1H), 3.68 (d, *J* = 17.9 Hz, 1H), 3.58 (s, 3H). ^{13}C NMR (101 MHz, CDCl$_3$) δ 188.6, 173.2, 152.6, 135.8, 134.5, 128.4, 128.1, 128.0, 127.9, 125.9, 125.2, 123.0, 122.5, 121.7, 120.1, 119.9, 112.7, 111.3, 77.6, 72.4, 52.3, 49.8, 49.5, 49.2, 49.0, 41.0. HRMS: Calcd for C24H21F3N3O4 [M+H^{+}]: 472.1479; Found: 472.1473.

The ee value was determined by HPLC analysis using a CHIRALPAK IC column (0.5 mL/min, 1%, i-PrOH in hexane); retention times: 24.19 min (min enantiomer) and 27.52 min (maj enantiomer).


3.25e
C25H22F3N3O4
M. Wt.: 485.46
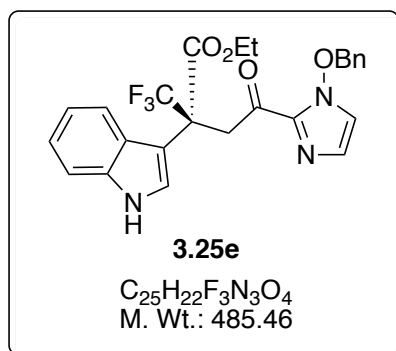
Ethyl (2R)-2-(1H-indol-3-yl)-4-(1-methoxy-1H-imidazol-2-yl)-4-oxo-2-(trifluoromethyl)butanoate (3.25d): ^{1}H NMR (400 MHz, CDCl$_3$) δ 7.70 – 7.61 (m, 2H), 7.41 – 7.26 (m, 7H), 7.24 – 7.09 (m, 4H), 4.98 (dd, *J* = 10.6 Hz, 2H), 4.35 – 4.06 (m, 3H), 3.68 (d, *J* =

17.9 Hz, 1H), 1.57 (t, J = 8.0 Hz, 3H). ^{13}C NMR (101 MHz, CDCl$_3$) δ 188.6, 173.3, 152.6, 135.8, 134.5, 128.4, 128.1, 128.0, 127.9, 125.9, 125.2, 123.0, 122.5, 121.7, 120.1, 119.9, 112.7, 111.3, 77.6, 72.4, 62.5, 50.5, 50.3, 50.0, 49.7, 41.0, 14.1.

^{19}F NMR (376 MHz, CDCl$_3$) δ -76.4. HRMS: Calcd for C$_{25}$H$_{23}$F$_3$N$_3$O$_4$ [M+H$^+$]: 486.1635; Found: 486.1648.

The ee value was determined by HPLC analysis using a CHIRALPAK IC column (0.5 mL/min, 1%, i-PrOH in hexane); retention times: 24.19 min (min enantiomer) and 27.52 min (maj enantiomer).
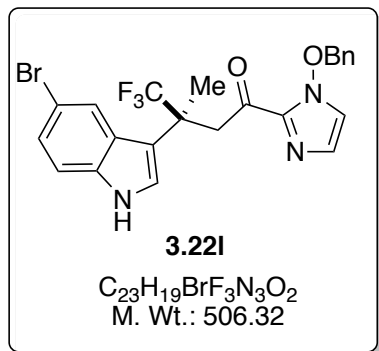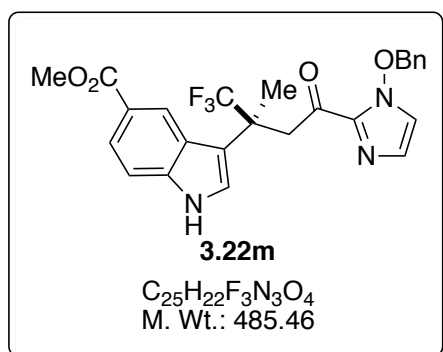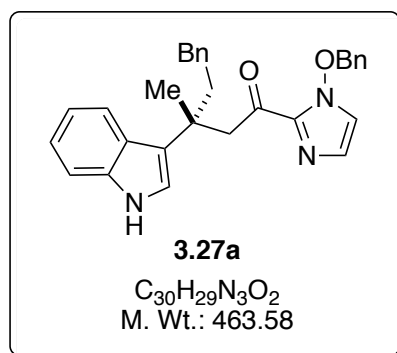

(3R)-3-(1H-Indol-3-yl)-1-(1-benzyloxy-1H-imidazol-2-yl)-3-(methyl)-4-phenylbutan-1-one (3.27a): ^{1}H NMR (400 MHz, CDCl$_3$) δ 7.64 (d, J = 7.6 Hz, 1H), 7.56 (ddt, J = 7.2, 1.7, 0.9 Hz, 2H), 7.41 – 7.22 (m, 10H), 7.17 – 7.08 (m, 2H), 7.01 (s, 1H), 5.06 – 4.90 (m, 2H), 3.70 (s, 3H), 3.43 – 3.17 (m, 2H), 2.74 – 2.50 (m, 2H), 2.14 – 1.84 (m, 2H), 1.44 (s, 3H). ^{13}C NMR (101 MHz, CDCl$_3$) δ 187.1, 153.1, 141.4, 138.0, 135.9, 128.4, 128.3, 128.3, 128.0, 126.0, 124.4, 124.0, 122.1, 122.0, 121.4, 119.4, 111.8, 110.2, 51.9, 42.6, 39.2, 33.5, 30.4, 20.4. HRMS: Calcd for C$_{31}$H$_{31}$N$_3$O$_2$ [M+H$^+$]: 478.2489; Found: 478.2496.

The ee value was determined by HPLC analysis using a CHIRALPAK IC column (1 mL/min, 5%, i-PrOH in hexane); retention times: 45.64 min (min enantiomer) and 63.59 min (maj enantiomer).

Me―C(Me)=... structure label:

3.27b

$C_{28}H_{31}N_3O_2$
M. Wt.: 441.58
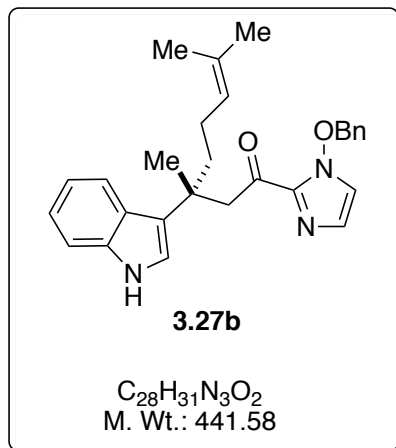
(3S3R)-3-(1H-Indol-3-yl)-1-(1-benzyloxy-1H-imidazol-2-yl)-3,7-dimethyloct-6-en-1-one (3.27b): ^{1}H NMR (400 MHz, CDCl$_3$) δ 7.64 (d, J = 7.6 Hz, 1H), 7.56 (ddt, J = 7.2, 1.7, 0.9 Hz, 2H), 7.41 – 7.26 (m, 7H), 7.15 (d, J = 7.5 Hz, 1H), 7.01 (s, 1H), 5.19 – 5.07 (m, 1H), 4.98 (dt, J = 7.2, 0.9 Hz, 2H), 3.70 (s, 3H), 3.38 – 3.16 (m, 2H), 2.18 – 2.00 (m, 1H), 1.93 – 1.71 (m, 2H), 1.63 (m, 6H), 1.40 (s, 3H). ^{13}C NMR (101 MHz, CDCl$_3$) δ 186.7, 153.1, 138.0, 135.9, 131.5, 128.4, 128.0, 127.6, 124.8, 124.4, 124.0, 122.1, 122.0, 121.4, 119.4, 111.8, 110.2, 51.9, 43.1, 37.5, 33.5, 25.7, 23.3, 20.4, 17.8. HRMS: Calcd for $C_{29}H_{23}N_3O_2$ [M+H$^+$]: 456.2646; Found: 456.2658.

The ee value was determined by HPLC analysis using a CHIRALPAK IC column (0.5 mL/min, 1%, i-PrOH in hexane); retention times: 24.19 min (min enantiomer) and 27.52 min (maj enantiomer).

3.27c
C$_{24}$H$_{23}$N$_3$O$_4$
M. Wt.: 417.47

Methyl (2S)-2-(1H-indol-3-yl)-4-(1-methoxy-1H-imidazol-2-yl)-2-methyl-4-oxobutanoate (3.27c): ^{1}H NMR (400 MHz, CDCl$_3$) δ 7.69 – 7.63 (m, 2H), 7.39 – 7.26 (m, 6H), 7.23 – 7.09 (m, 5H), 5.06 – 4.86 (m, 2H), 3.88 – 3.72 (m, 2H), 3.70 (s, 3H), 1.81 (s, 3H). ^{13}C NMR (101 MHz, CDCl$_3$) δ 186.9, 176.4, 152.6, 135.8, 134.3, 128.4, 128.4, 128.0, 127.7, 125.2, 125.1, 122.8, 121.6, 119.9, 115.7, 112.3, 111.3, 72.4, 52.2, 50.9, 44.8, 21.3. HRMS: Calcd for C$_{24}$H$_{24}$N$_3$O$_2$ [M+H$^+$]: 418.1761; Found: 418.1764.

The ee value was determined by HPLC analysis using a CHIRALPAK IC column (0.5 mL/min, 1%, i-PrOH in hexane); retention times: 24.19 min (min enantiomer) and 27.52 min (maj enantiomer).

3.27d
C$_{28}$H$_{24}$N$_4$O$_4$
M. Wt.: 480.52
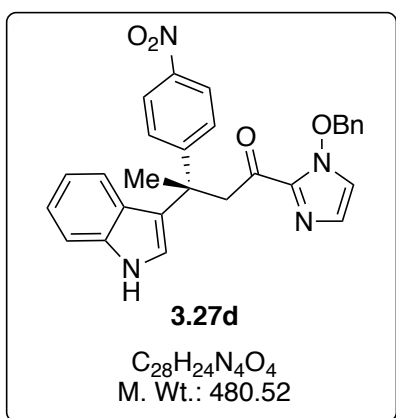
(3R3S)-3-(1H-Indol-3-yl)-1-(1-benzyloxy-1H-imidazol-2-yl)-3-(4-nitrophenyl)butan-1-one (3.27d): ^{1}H NMR (400 MHz, CDCl$_3$) δ 8.16 – 8.11 (m, 2H), 7.98 (dd, *J* = 7.5, 1.5 Hz, 1H), 7.64 (d, *J* = 7.6 Hz, 1H), 7.47 – 7.41 (m, 3H), 7.39 – 7.26 (m, 5H), 7.19 – 6.98 (m, 5H), 5.05 – 4.92 (m, 2H), 3.76 – 3.49 (m, 2H), 1.79 (s, 3H). ^{13}C NMR (101 MHz, CDCl$_3$) δ 188.4,

68

153.2, 150.2, 136.9, 135.9, 128.4, 128.0, 127.1, 126.5, 124.4, 124.4, 124.2, 123.3, 122.9, 121.6, 120.0, 112.4, 111.8, 72.6, 47.4, 41.4, 22.9. HRMS: Calcd for $C_{28}H_{25}N_4O_4$ [M+H$^+$]: 481.1870; Found:481.1882.

The ee value was determined by HPLC analysis using a CHIRALPAK IC column (1 mL/min, 5%, i-PrOH in hexane); retention times: 57.86 min (min enantiomer) and 92.55 min (maj enantiomer).

3.27e
$C_{28}H_{24}ClN_3O_2$
M. Wt.: 469.97
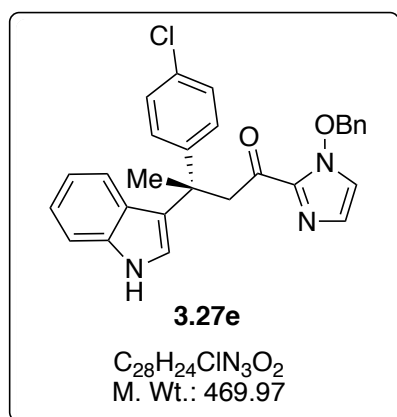
(3R3S)-3-(1H-Indol-3-yl)-1-(1-methoxy-1H-imidazol-2-yl)-3-(4-chlorophenyl)butan-1-one (3.27e): ^{1}H NMR (400 MHz, CDCl$_3$) δ 7.98 (dd, J = 7.5, 1.5 Hz, 1H), 7.64 (d, J = 7.6 Hz, 1H), 7.45 – 7.24 (m, 8H), 7.21 – 6.98 (m, 7H), 4.98 (dt, J = 7.3, 0.9 Hz, 2H), 3.75 – 3.51 (m, 2H), 1.79 (s, 3H). ^{13}C NMR (101 MHz, CDCl$_3$) δ 187.4, 153.1, 144.9, 136.9, 135.9, 135.0, 128.5, 128.4, 128.0, 127.4, 126.5, 124.4, 124.4, 123.3, 122.9, 121.6, 120.0, 112.4, 111.8, 72.6, 47.4, 41.4, 22.9. HRMS: Calcd for $C_{28}H_{25}ClN_3O_2$ [M+H$^+$]: 470.1630; Found:470.1638.

The ee value was determined by HPLC analysis using a CHIRALPAK IC column (0.5 mL/min, 1%, i-PrOH in hexane); retention times: 24.19 min (min enantiomer) and 27.52 min (maj enantiomer).
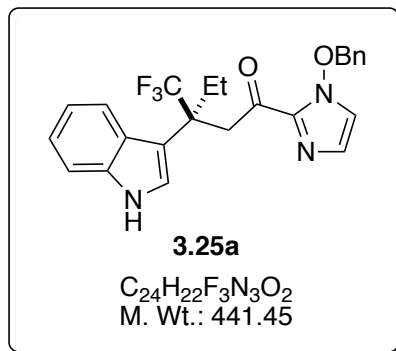
3.33a

$C_{20}H_{20}F_3N_3O_2$
M. Wt.: 391.39
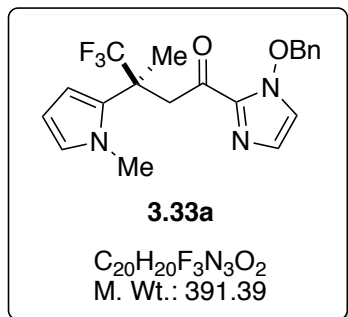
(3R3S)-4,4,4-Trifluoro-1-(1-benzyloxy-1H-imidazol-2-yl)-3-methyl-3-(1-methyl-1H-pyrrol-2-yl)butan-1-one (3.33a): ^{1}H NMR (400 MHz, CDCl$_3$) δ 7.64 (d, J = 7.6 Hz, 1H), 7.43 – 7.24 (m, 5H), 7.15 (d, J = 7.5 Hz, 1H), 6.88 (ddq, J = 7.6, 1.5, 0.7 Hz, 1H), 5.67 (t, J = 7.5 Hz, 1H), 5.50 (dd, J = 7.5, 1.6 Hz, 1H), 4.98 (dd, J = 10.9 Hz, 2H), 3.65 (d, J = 16.8 Hz, 1H), 3.55 (s, 3H), 3.15 (d, J = 16.8 Hz, 1H), 1.48 (s, 3H). ^{13}C NMR (101 MHz, CDCl$_3$) δ 185.5, 152.6, 135.8, 128.4, 128.0, 125.2, 124.5, 123.9, 121.2, 118.5, 115.9, 115.2, 112.7, 111.3, 92.9, 72.4, 47.8, 40.8, 40.5, 40.3, 40.0, 34.4, 15.9. ^{19}F NMR (376 MHz, CDCl$_3$) δ -73.8. HRMS: Calcd for $C_{20}H_{23}F_3N_3O_2$ [M+H$^+$]: 392.1580; Found: 392.1588.

The ee value was determined by HPLC analysis using a CHIRALPAK IC column (0.5 mL/min, 1%, i-PrOH in hexane); retention times: 26.86 min (maj enantiomer) and 36.46 min (min enantiomer).

3.33b

$C_{21}H_{22}F_3N_3O_2$
M. Wt.: 405.42
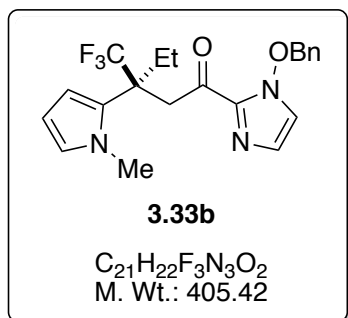
(3R3S)-1-(1-Benzyloxy-1H-imidazol-2-yl)-3-(1-methyl-1H-pyrrol-2-yl)-3-(trifluoromethyl)pentan-1-one (3.33b): ^{1}H NMR (400 MHz, CDCl$_3$) δ 7.64 (d, J = 7.6 Hz, 1H), 7.44 – 7.24 (m, 5H), 7.15 (d, J = 7.5 Hz, 1H), 6.93 – 6.82 (m, 1H), 5.67 (t, J = 7.5 Hz, 1H), 5.47

(dd, J = 7.5, 1.4 Hz, 1H), 4.98 (dd, J = 10.9 Hz, 1H), 3.66 (d, J = 16.8 Hz, 1H), 3.55 (s, 3H), 3.16 (d, J = 17.0 Hz, 1H), 2.17 (dq, J = 12.7, 8.0 Hz, 1H), 1.67 (dq, J = 12.9, 8.0 Hz, 1H), 1.02 (t, J = 8.0 Hz, 3H). ^{13}C NMR (101 MHz, CDCl$_3$) δ 185.6, 152.6, 135.8, 128.4, 128.0, 125.2, 124.5, 123.9, 121.2, 118.5, 115.8, 114.9, 112.7, 111.3, 86.1, 72.4, 51.1, 50.9, 50.6, 50.3, 46.4, 34.4, 27.2, 8.3. ^{19}F NMR (376 MHz, CDCl$_3$) δ -68.2. HRMS: Calcd for C$_{21}$H$_{23}$F$_3$N$_3$O$_2$ [M+H$^+$]: 406.1737; Found: 442.1729.

The ee value was determined by HPLC analysis using a CHIRALPAK IA column (0.5 mL/min, 1%, i-PrOH in hexane); retention times: 22.51 min (maj enantiomer) and 24.4 min (min enantiomer).


3.33c

C$_{26}$H$_{24}$F$_3$N$_3$O$_2$
M. Wt.: 467.49
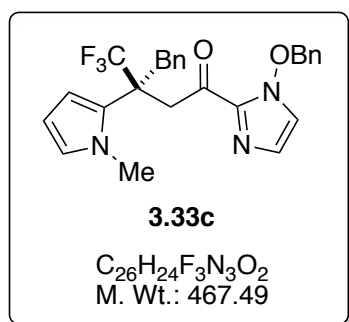
(3R3S)-3-Benzyl-4,4,4-trifluoro-1-(1-benzyloxy-1H-imidazol-2-yl)-3-(1-methyl-1H-pyrrol-2-yl)butan-1-one (3.33c): ^{1}H NMR (400 MHz, CDCl$_3$) δ 7.64 (d, J = 7.6 Hz, 1H), 7.39 – 7.21 (m, 8H), 7.15 (d, J = 7.5 Hz, 1H), 6.88 (ddd, J = 7.5, 1.6, 0.8 Hz, 1H), 6.74 (ddq, J = 6.3, 1.9, 1.0 Hz, 2H), 5.67 (t, J = 7.5 Hz, 1H), 5.48 (dd, J = 7.5, 1.5 Hz, 1H), 4.98 (dd, J = 10.9 Hz, 2H), 3.70 (d, J = 17.0 Hz, 1H), 3.55 (s, 3H), 3.34 (dt, J = 12.6, 0.9 Hz, 1H), 3.20 (d, J = 17.0 Hz, 1H), 2.83 (dt, J = 12.6, 0.9 Hz, 1H). ^{13}C NMR (101 MHz, CDCl$_3$) δ 185.6, 152.6, 135.8, 134.8, 130.9, 128.4, 128.3, 128.0, 126.8, 125.2, 124.5, 122.2, 119.6, 116.9, 114.2, 112.7, 111.3, 110.3, 90.8, 72.4, 47.7, 47.4, 47.1, 46.9, 46.5, 41.2, 34.4. ^{19}F NMR (376 MHz, CDCl$_3$) δ -68.2. HRMS: Calcd for C$_{26}$H$_{25}$F$_3$N$_3$O$_2$ [M+H$^+$]: 468.1893; Found: 468.1889.

The ee value was determined by HPLC analysis using a CHIRALPAK IC column (0.5

mL/min, 1%, i-PrOH in hexane); retention times: 24.19 min (maj enantiomer) and 27.52

min (min enantiomer).
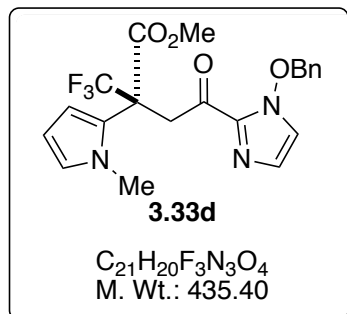
Methyl (2R2S)-4-(1-benzyloxy-1H-imidazol-2-yl)-2-(1-methyl-1H-pyrrol-2-yl)-4-oxo-2-(trifluoromethyl)butanoate (3.33d): ^{1}H NMR (400 MHz, CDCl$_3$) δ 7.64 (d, J = 7.6 Hz, 1H), 7.41 – 7.24 (m, 5H), 7.15 (d, J = 7.5 Hz, 1H), 6.89 (ddt, J = 7.5, 1.2, 0.7 Hz, 1H), 5.72 (t, J = 7.5 Hz, 1H), 5.48 (dd, J = 7.5, 1.6 Hz, 1H), 5.04 – 4.88 (m, 2H), 3.88 – 3.66 (m, 2H), 3.63 – 3.52 (m, 6H). ^{13}C NMR (101 MHz, CDCl$_3$) δ 185.6, 169.0, 152.6, 135.8, 128.4, 128.0, 125.2, 124.5, 122.5, 119.8, 117.1, 116.5, 114.4, 112.7, 111.3, 91.9, 72.4, 54.9, 54.6, 54.4, 54.1, 52.3, 43.5, 34.4. ^{19}F NMR (376 MHz, CDCl$_3$) δ -68.8. HRMS: Calcd for C$_{21}$H$_{21}$F$_3$N$_3$O$_2$ [M+H$^+$]: 436.1479; Found: 436.1484.

The ee value was determined by HPLC analysis using a CHIRALPAK IC column (0.5 mL/min, 1%, i-PrOH in hexane); retention times: 24.19 min (maj enantiomer) and 27.52 min (min enantiomer).

3.33e

C$_{22}$H$_{22}$F$_3$N$_3$O$_4$
M. Wt.: 449.43
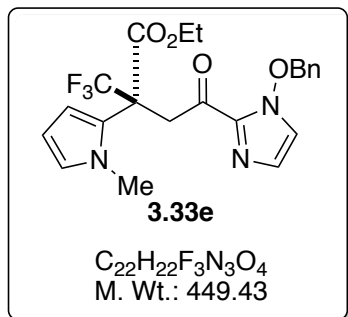
Ethyl (2R2S)-4-(1-benzyloxy-1H-imidazol-2-yl)-2-(1-methyl-1H-pyrrol-2-yl)-4-oxo-2-(trifluoromethyl)butanoate (3.33e): ^{1}H NMR (400 MHz, CDCl$_3$) δ 7.64 (d, *J* = 7.6 Hz, 1H), 7.44 – 7.28 (m, 4H), 7.15 (d, *J* = 7.5 Hz, 1H), 6.89 (ddt, *J* = 7.5, 1.3, 0.7 Hz, 1H), 5.72 (t, *J* = 7.5 Hz, 1H), 5.48 (dd, *J* = 7.5, 1.6 Hz, 1H), 5.07 – 4.91 (m, 2H), 4.25 (qd, *J* = 8.1, 3.9 Hz, 2H), 3.86 – 3.66 (m, 2H), 3.57 (s, 3H), 1.17 (t, *J* = 8.0 Hz, 3H). ^{13}C NMR (101 MHz, CDCl$_3$) δ 185.6, 168.6, 152.6, 135.8, 128.4, 128.0, 125.2, 124.5, 122.5, 119.8, 117.1, 116.5, 114.4, 112.7, 111.3, 91.9, 72.4, 62.5, 55.5, 55.2, 54.9, 54.7, 43.5, 34.4, 14.1. ^{19}F NMR (376 MHz, CDCl$_3$) δ -68.8. HRMS: Calcd for C$_{22}$H$_{23}$F$_3$N$_3$O$_2$ [M+H^{+}]: 4501635; Found: 450.1642.

The ee value was determined by HPLC analysis using a CHIRALPAK IC column (0.5 mL/min, 1%, i-PrOH in hexane); retention times: 24.19 min (maj enantiomer) and 27.52 min (min enantiomer).


3.33g

C$_{21}$H$_{22}$F$_3$N$_3$O$_2$
M. Wt.: 405.42
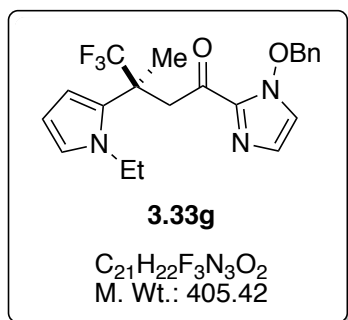
(3R3S)-3-(1-Ethyl-1H-pyrrol-2-yl)-4,4,4-trifluoro-1-(1-benzyloxy-1H-imidazol-2-yl)-3-methylbutan-1-one (3.33g): ^{1}H NMR (400 MHz, CDCl$_3$) δ 7.64 (d, *J* = 7.6 Hz, 0H), 7.43 – 7.23 (m, 2H), 7.15 (d, *J* = 7.5 Hz, 0H), 6.89 (dd, *J* = 7.4, 1.5 Hz, 0H), 5.80 – 5.59 (m, 1H), 4.98

(t, J = 0.9 Hz, 1H), 3.76 – 3.51 (m, 1H), 3.15 (d, J = 16.8 Hz, 0H), 1.48 (s, 1H), 1.33 (t, J = 8.0

Hz, 1H). ^{13}C NMR (101 MHz, CDCl$_3$) δ 185.6, 152.6, 135.8, 128.4, 128.0, 125.2, 124.7, 123.9,

121.2, 118.5, 115.9, 114.6, 111.8, 111.3, 92.9, 72.4, 47.9, 44.1, 40.8, 40.5, 40.2, 40.0, 15.9, 14.9.

^{19}F NMR (376 MHz, CDCl$_3$) δ -73.8. HRMS: Calcd for C$_{21}$H$_{23}$F$_3$N$_3$O$_2$ [M+H$^+$]: 406.1737;

Found: 406.1742.

The ee value was determined by HPLC analysis using a CHIRALPAK IC column (0.5

mL/min, 1%, i-PrOH in hexane); retention times: 24.78 min (maj enantiomer) and 32.53

min (min enantiomer).

3.33h
C$_{26}$H$_{24}$F$_3$N$_3$O$_2$
M. Wt.: 467.49
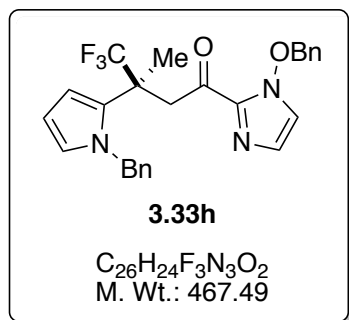
(3R)-3-(1-Benzyl-1H-pyrrol-2-yl)-4,4,4-trifluoro-1-(1-benzyloxy-1H-imidazol-2-yl)-

3-methylbutan-1-one (3.33h): ^{1}H NMR (400 MHz, CDCl$_3$) δ 7.64 (d, J = 7.6 Hz, 1H), 7.38 –

7.24 (m, 8H), 7.15 (d, J = 7.5 Hz, 1H), 7.11 (ddt, J = 7.6, 1.8, 1.0 Hz, 2H), 6.87 (dd, J = 7.4, 1.5

Hz, 1H), 5.76 (t, J = 7.5 Hz, 1H), 5.67 (dd, J = 7.5, 1.6 Hz, 1H), 5.06 (dt, J = 5.3, 1.0 Hz, 2H),

4.98 (t, J = 0.9 Hz, 2H), 3.65 (d, J = 16.8 Hz, 1H), 3.15 (d, J = 16.8 Hz, 1H), 1.48 (s, 3H). ^{13}C

NMR (101 MHz, CDCl$_3$) δ 185.6, 152.6, 136.2, 128.6, 128.5, 128.4, 128.1, 128.0, 127.4, 125.2,

123.9, 121.2, 118.5, 115.9, 114.5, 111.6, 111.3, 93.7, 72.4, 50.6, 47.9, 40.8, 40.5, 40.2, 40.0,

15.9. ^{19}F NMR (376 MHz, CDCl$_3$) δ -73.8. HRMS: Calcd for C$_{26}$H$_{25}$F$_3$N$_3$O$_2$ [M+H$^+$]: 468.1893;
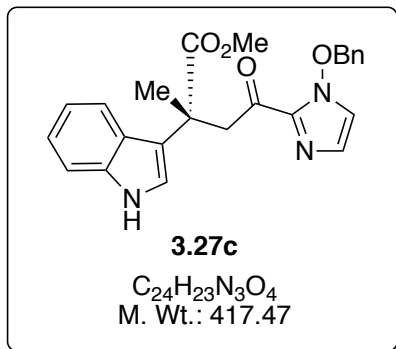
Found: 468.1882.The ee value was determined by HPLC analysis using a CHIRALPAK IC

column (0.5 mL/min, 1%, i-PrOH in hexane); retention times: 29.27 min (maj enantiomer) and

43.02 min (min enantiomer).

3.33i

$C_{19}H_{18}F_3N_3O_2$
M. Wt.: 377.37
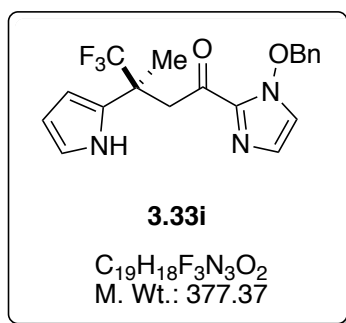
(3R)-3-(5-Ethyl-1H-pyrrol-2-yl)-4,4,4-trifluoro-1-(1-methoxy-1H-imidazol-2-yl)-3-methylbutan-1-one (3.33i): ^{1}H NMR (400 MHz, CDCl$_3$) δ 7.64 (d, J = 7.6 Hz, 1H), 7.39 – 7.25 (m, 5H), 7.13 (dd, J = 20.9, 7.5 Hz, 2H), 6.87 (td, J = 7.5, 1.5 Hz, 1H), 6.30 (dd, J = 7.6, 1.5 Hz, 1H), 6.06 (t, J = 7.5 Hz, 1H), 4.98 (t, J = 0.9 Hz, 2H), 3.73 (d, J = 17.0 Hz, 1H), 3.23 (d, J = 17.0 Hz, 1H), 1.59 (s, 3H). ^{13}C NMR (101 MHz, CDCl$_3$) δ 185.6, 152.6, 135.8, 128.4, 128.0, 125.2, 125.1, 123.3, 122.4, 119.7, 117.1, 111.3, 108.2, 98.6, 72.4, 47.4, 41.7, 41.4, 41.1, 40.9, 14.4. ^{19}F NMR (376 MHz, CDCl$_3$) δ -73.8. HRMS: Calcd for C$_{19}$H$_{19}$F$_3$N$_3$O$_2$ [M+H$^+$]: 378.1424; Found: 378.1427.

The ee value was determined by HPLC analysis using a CHIRALPAK IC column (0.5 mL/min, 1%, i-PrOH in hexane); retention times: 19.17 min (maj enantiomer) and 22.39 min (min enantiomer).


3.33j

$C_{21}H_{22}F_3N_3O_2$
M. Wt.: 405.42
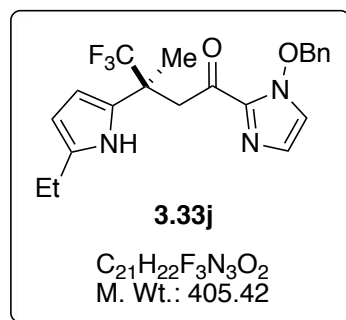
(3R3S)-3-(3,5-Dimethyl-1H-pyrrol-2-yl)-4,4,4-trifluoro-1-(1-benzyloxy-1H-imidazol-2-yl)-3-methylbutan-1-one (3.33j): ^{1}H NMR (400 MHz, CDCl$_3$) δ 7.64 (d, J = 7.6 Hz, 1H), 7.41 – 7.25 (m, 5H), 7.15 (d, J = 7.5 Hz, 1H), 6.49 (s, 1H), 6.13 – 5.99 (m, 2H), 4.98 (t, J = 0.9

75

Hz, 2H), 3.75 (d, J = 17.0 Hz, 1H), 3.24 (d, J = 17.0 Hz, 1H), 2.39 (q, J = 8.2 Hz, 2H), 1.61 (s, 3H), 1.25 (t, J = 8.0 Hz, 3H). ^{13}C NMR (101 MHz, CDCl$_3$) δ 185.6, 152.6, 141.1, 135.8, 128.4, 128.0, 125.2, 125.1, 122.4, 119.7, 117.1, 111.6, 111.3, 109.3, 99.4, 72.4, 47.4, 41.6, 41.3, 41.1, 40.8, 20.0, 14.4, 12.1. ^{19}F NMR (376 MHz, CDCl$_3$) δ -73.8. HRMS: Calcd for $C_{21}H_{23}F_3N_3O_2$ [M+H$^+$]: 406.1737; Found: 406.1729.

The ee value was determined by HPLC analysis using a CHIRALPAK IC column (0.5 mL/min, 1%, i-PrOH in hexane); retention times: 24.19 min (maj enantiomer) and 27.52 min (min enantiomer).

3.7.2. Synthesis of starting materials

The compounds *3.20, 3.20a, b, 3.20d, e, 3.27c* were synthesized in 4 steps according to scheme 3.14.
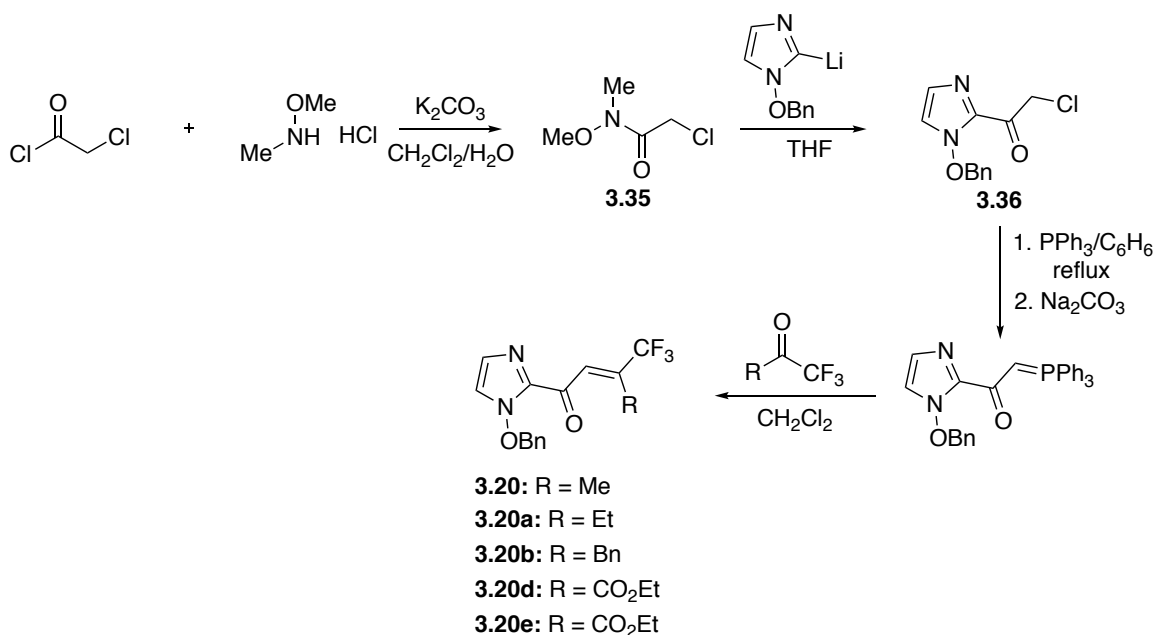
Scheme 3.14. Synthetic scheme for β,β-acylimidazoles containing trifluoromethyl group and alkyl group at β-position.

76

3.7.2.1. Procedure for synthesis of 2-chloro-N-methoxy-N-methylacetamide 3.35

3.35
$C_4H_8ClNO_2$
Mol. Wt.:137.56
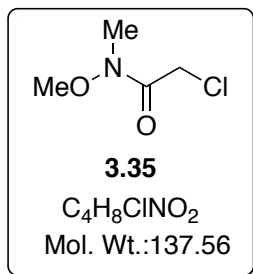
N,O-dimethylhydroxylamine hydrochloride (100 mmol) was dissolved in 100 mL water. To this solution was added a solution of chloroacetyl chloride (120 mmol) in 100 ml CH_2Cl_2. To the biphasic mixture was added potassium carbonate at 0 °C and the mixture was stirred for another 16 h at room temperature. After the reaction, the organic layer was separated and the aqueous layer was washed with CH_2Cl_2 (3x100 mL). The combined organic layers were dried over sodium sulfate and the solvent was removed in vacuo to give **3.35** as a white solid. (13.7 g, quantitative yield).

^{1}H NMR (400 MHz, CDCl$_3$): δ 4.15 (s, 2H), 3.64 (s, 3H), 3.11 (s, 3H). ^{13}C NMR (101 MHz, CDCl$_3$): δ 167.1, 61.4, 40.6, 32.3.

3.7.2.2. Procedure for synthesis of 1-[1-(benzyloxy)-1H-imidazol-2-yl]-2-chloroethanone 3.36

3.36
$C_{12}H_{11}ClN_2O_2$
Mol. Wt: 250.68
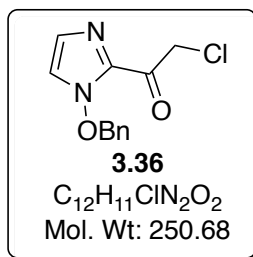
To a flame-dried flask N-benzyloxyimidazole (4.35 g, 25 mmol) and THF (100 mL) were added under Ar atmosphere. The reaction mixture was cooled to -78 °C and then *n*-BuLi (2.5 M in hexanes) (10 mL, 25 mmol) was added over 10 minutes and the mixture was stirred at -78 °C for 30 minutes. 2-chloro-N-methoxy-Nmethylacetamide (3.4 g, 25 mmol) dissolved in another

25 mL of THF was added slowly at -78 °C. The reaction was monitored by TLC. Upon completion of the reaction, the reaction was warmed to rt and then quenched using glacial acetic acid (6 equivalents). The reaction was diluted with ethyl acetate and washed with saturated NaHCO$_3$ (3x100 mL), washed with brine (100 mL). The combined organic layers were dried over sodium sulfate, filtered and the filtrate was concentrated in vacuum to give the crude solid, which was then purified by flash chromatography to give 5.14 g of white solid Yield = 82%. M.P: 85-88 °C.

^{1}H NMR (400 MHz, CDCl$_3$): δ 7.49-7.38 (m, 6H), 7.03 (d, J = 1.1 Hz, 1H), 7.00 (d, J = 1.1 Hz, 1H), 5.29 (s, 2H), 4.91 (s, 2H). ^{13}C NMR (101 MHz, CDCl$_3$): δ 180.6, 136.1, 132.8, 130.1 (CH, 2C), 129.7, 128.8 (CH, 2C), 126.0, 122.7, 82.6, 46.6. HRMS: Calcd for C$_{12}$H$_{12}$ClN$_2$O$_2$ [M+H$^+$]: 251.0587; Found: 251.0594.

3.7.2.3. Synthesis of 3.20, 3.20a, b, 3.20d, e, 3.27c

To a flame-dried 250 mL round bottom flask fitted with a condenser was added 1-[1-(benzyloxy)-1H-imidazol-2-yl]-2-chloroethanone **3.36** (2.5 g, 10 mmol), triphenylphosphine (2.62 g, 10 mmol) and benzene (50 mL) under Ar atmosphere. The mixture was refluxed overnight. The solid phosphonium salt was filtered off from the reaction mixture, dissolved in CH$_2$Cl$_2$, washed with saturated Na$_2$CO$_3$ (3x50 mL), washed with brine (100 mL), dried over sodium sulfate and filtered. The organic layer was concentrated in vacuo to give a brownish foamy solid. This was used without purification in the next step.

The ylide prepared in the last step was dissolved in 30 ml of CH$_2$Cl$_2$. Trifluoromethyl ketone (20 mmol) was added to this mixture and stirred for 48 hours to give β,β-disubstituted enones.
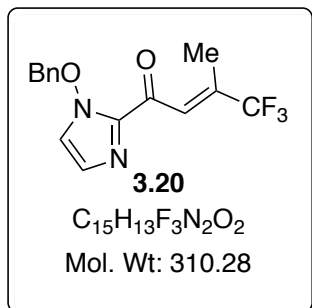
(2E)-1-[1-(Benzyloxy)-1H-imidazol-2-yl]-4,4,4-trifluoro-3-methylbut-2-en-1-one

(3.20): White solid. M.P: 35-38 ºC. (2.0 g, 65%). ^{1}H NMR (400 MHz, CDCl$_3$): δ 7.77 (hept, J = 1.4 Hz, 1H), 7.55-7.35 (m, 5H), 7.02 (d, J = 1.1 Hz, 1H), 6.96 (d, J = 1.1 Hz, 1H), 5.31 (s, 2H), 2.38 (d, J = 1.5 Hz, 3H). ^{13}C NMR (101 MHz, CDCl$_3$): δ 178.4, 141.3 (q), 138.9, 133.0, 130.0 (CH, 2C), 129.6, 128.7 (CH, 2C), 125.6 (CH, 2C), 124.4 (q), 123.6 (q), 82.3, 12.6. ^{19}F NMR (376 MHz, CDCl$_3$): δ -71.05. HRMS: Calcd for C$_{15}$H$_{14}$F$_3$N$_2$O$_2$ [M+H$^+$]: 311.1007; Found: 311.1009.
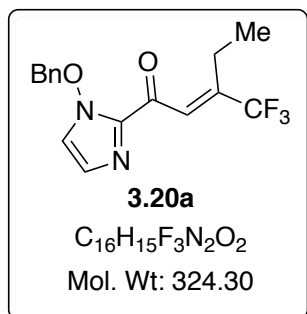
(2E)-1-[1-(Benzyloxy)-1H-imidazol-2-yl]-3-(trifluoromethyl)pent-2-en-1-one (3.20a):

Yellow solid. M.P: 35-38 ºC. (1.13 g, 34%). ^{1}H NMR (400 MHz, CDCl$_3$): δ 7.76 (q, J = 1.4 Hz, 1H), 7.43 (s, 5H), 7.00 (d, J = 1.1 Hz, 1H), 6.94 (d, J = 1.1 Hz, 1H), 5.30 (s, 2H), 2.81 (q, J = 7.5 Hz, 2H), 1.29 (t, J = 7.5 Hz, 3H). ^{13}C NMR (101 MHz, CDCl$_3$): δ178.1, 147.3 (q), 138.9, 133.0, 130.0 (CH, 2C), 129.6, 128.7 (CH, 2C), 125.5, 124.4 (q), 123.6 (q), 122.6, 82.3, 20.4, 13.2. ^{19}F

NMR (376 MHz, CDCl$_3$): δ -69.01. HRMS: Calcd for C$_{16}$H$_{16}$F$_3$N$_2$O$_2$ [M+H$^+$]: 325.1164; Found: 325.1177.

3.20b
C$_{21}$H$_{17}$F$_3$N$_2$O$_2$
Mol. Wt: 386.37
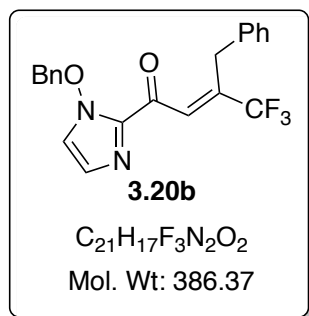
(2E)-3-Benzyl-1-[1-(benzyloxy)-1H-imidazol-2-yl]-4,4,4-trifluorobut-2-en-1-one

(3.20b): Yellow solid. M.P: 55-58 ºC. (1.5g, 78%). ^{1}H NMR (400 MHz, CDCl$_3$): δ 7.91.7.85 (m, 1H), 7.44-7.14 (m, 10H), 6.99 (d, J = 1.1 Hz, 1H), 6.91 (d, J = 1.1 Hz, 1H), 5.18 (s, 2H), 4.18 (s, 2H). ^{13}C NMR (101 MHz, CDCl$_3$): δ 178.0, 143.2 (q), 138.8, 136.8, 132.9, 130.1 (CH, 3C), 129.7, 128.8 (CH, 3C), 128.4 (CH, 2C), 126.6, 126.5 (q), 125.8, 123.4 (q), 122.8, 82.4, 32.1. ^{19}F NMR (376 MHz, CDCl$_3$): δ -67.43. HRMS: Calcd for C$_{21}$H$_{18}$F$_3$N$_2$O$_2$ [M+H$^+$]: 387.1320; Found: 387.1327.

3.20d
C$_{17}$H$_{15}$F$_3$N$_2$O$_4$
Mol. Wt: 368.31
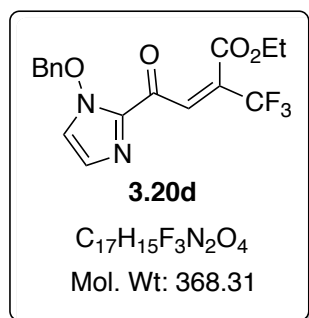
Ethyl-(2E)-4-[1-(benzyloxy)-1H-imidazol-2-yl]-4-oxo-2-(trifluoromethyl)but-2-

enoate (3.20d): Yellow solid. M.P: 45-48 ºC. (2.76 g, 75%). ^{1}H NMR (400 MHz, CDCl$_3$): δ 7.75(q, J = 1.4 Hz, 1H), 7.61-7.29 (m, 5H), 7.02 (d, J = 1.1 Hz, 1H), 6.96 (d, J = 1.1 Hz, 1H), 5.29 (s, 2H), 4.36 (q, J = 7.1 Hz, 2H), 1.33 (t, J = 7.1 Hz, 3H). ^{13}C NMR (101 MHz, CDCl$_3$): δ

176.7, 161.8, 137.5, 134.8 (q), 132.9, 132.2 (q), 130.1 (CH, 2C), 129.7, 128.8, (CH, 2C), 126.5, 123.2, 121.0 (q), 82.4, 62.5, 13.7. ^{19}F NMR (376 MHz, CDCl$_3$): δ -65.11. HRMS: Calcd for C$_{17}$H$_{16}$F$_3$N$_2$O$_4$ [M+H$^+$]: 369.1062; Found: 369.1077.

BnO

O

CO$_2$Me

N

N

CF$_3$

3.20e

C$_{16}$H$_{13}$F$_3$N$_2$O$_4$

Mol. Wt: 354.29
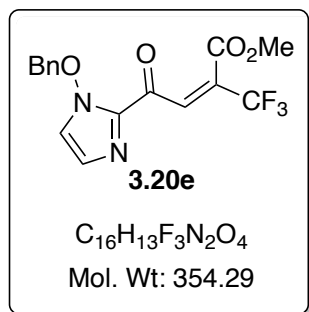
Methyl-(2E)-4-[1-(benzyloxy)-1H-imidazol-2-yl]-4-oxo-2-(trifluoromethyl)but-2-enoate (3.20d): White solid. M.P: 45-48 ºC. (2.4 g, 75%). ^{1}H NMR (400 MHz, CDCl$_3$): δ 7.75(q, J = 1.4 Hz, 1H), 7.61-7.29 (m, 5H), 7.02 (d, J = 1.1 Hz, 1H), 6.96 (d, J = 1.1 Hz, 1H), 5.29 (s, 2H), 4.36 (q, J = 7.1 Hz, 2H), 1.33 (t, J = 7.1 Hz, 3H). ^{13}C NMR (101 MHz, CDCl$_3$): δ 176.7, 161.8, 137.5, 134.8 (q), 132.9, 132.2 (q), 130.1 (CH, 2C), 129.7, 128.8, (CH, 2C), 126.5, 123.2, 121.0 (q), 82.4, 62.5, 13.7. ^{19}F NMR (376 MHz, CDCl$_3$): δ -65.11. HRMS: Calcd for C$_{17}$H$_{16}$F$_3$N$_2$O$_4$ [M+H$^+$]: 369.0827; Found: 369.0835.

BnO

O

Me

N

N

CO$_2$Me

3.20c

C$_{16}$H$_{16}$N$_2$O$_4$

Mol. Wt: 300.3
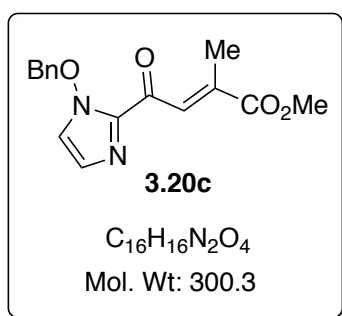
Chemical Formula: C$_{16}$H$_{16}$N$_2$O$_4$
Molecular Weight: 300.3140

Methyl-(2E)-4-[1-(benzyloxy)-1H-imidazol-2-yl]-2-methyl-4-oxobut-2-enoate (3.27c):
Yellow solid. M.P: 55-58 ºC. (1.5g, 50%). ^{1}H NMR (400 MHz, CDCl$_3$): δ 8.14 (q, J = 1.6 Hz,

1H), 7.48-7.37 (m, 5H), 7.00 (d, J = 1.1 Hz, 1H), 6.95 (d, J = 1.1 Hz, 1H), 5.31 (s, 2H), 2.41 (s, 3H), 1.37 (t, J = 7.1 Hz, 3H). ^{13}C NMR (101 MHz, CDCl$_3$): δ 179.8, 167.5, 143.5, 139.2, 133.1, 130.1 (CH, 2C), 129.6, 129.6, 128.7 (CH, 2C), 125.5, 122.4, 82.3, 61.6, 14.8. HRMS: Calcd for C$_{17}$H$_{19}$N$_2$O$_4$ [M+H$^+$]: 300.3140; Found: 300.3150.

3.7.2.4. Synthesis of compounds 3.27 a, b, 3.27d, e

These compounds are synthesized in two steps according to Scheme 3.15.
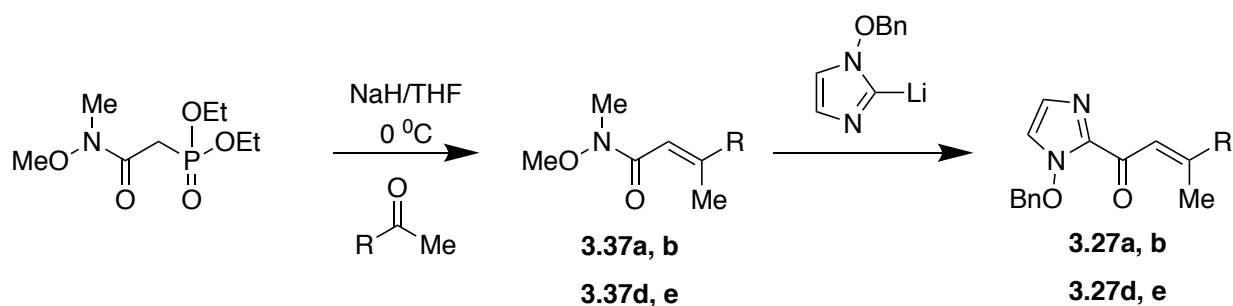
Scheme 3.15. Synthesis of substrates **3.27a-b** and **3.27d-e**

3.7.2.5. Procedure for synthesis of 3.37a-b and 3.37d-e

To a flame-dried 250 mL flask 250 mL round-bottom flask were added NaH (20 mmol, 2.0 equiv) and THF (80 mL). The suspension was then cooled to 0 ^{0}C. Now, *N*-Methoxy-*N*-methyl-phosphonoacetamide diethyl ester (20 mmol, 2.0 equiv) dissolved in THF (10 mL) was added dropwise. The resulting mixture was allowed to stir at 0 ^{0}C for 15 minutes and at room temperature for 45 minutes. Then corresponding ketone (10 mmol, 1.0 equiv) was dissolved in THF (10 mL) was added. The solution was refluxed for 12 hours. The reaction was cooled to rt, quenched with NH$_4$Cl, extracted with ethyl acetate (3x100 mL). The combined organic layers were washed with brine, dried over MgSO$_4$, filtered and the solvent was removed in vacuo to give a crude product, which on purification by column chromatography gave 75 - 80% of **3.37**.

3.37a
C₁₄H₁₉NO₂
Mol. Wt.: 233.31

(2E)-N-Methoxy-N,3-dimethyl-5-phenylpent-2-enamide(3.37a): ^{1}H NMR (400 MHz, CDCl₃) δ 7.31 – 7.19 (m, 2H), 7.19 – 7.08 (m, 3H), 6.03 (s, 1H), 3.49 (s, 3H), 3.13 (s, 3H), 2.77 (dd, J = 8.8, 6.8 Hz, 2H), 2.51 – 2.38 (m, 2H), 2.14 (d, J = 1.1 Hz, 3H). ^{13}C NMR (101 MHz, CDCl₃) δ 167.7, 155.0, 141.0, 128.2, 125.8, 114.4, 61.1, 42.4, 33.7, 18.5. HRMS: Calcd for $C_{14}H_{20}NO_2$ [M+H⁺]: 234.1416; Found: 234.1408.

3.37b
C₁₂H₂₁NO₂
Mol. Wt.: 211.31
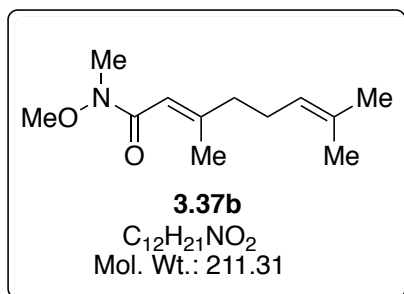
(2E)-N-Methoxy-N,3,7-trimethylocta-2,6-dienamide (3.37b): ^{1}H NMR (400 MHz, CDCl₃) δ 6.06 (s, 1H), 5.05 (dd, J = 2.7, 1.3 Hz, 1H), 3.62 (s, 3H), 3.16 (s, 3H), 2.13 (d, J = 3.1 Hz, 5H), 2.08 (d, J = 1.2 Hz, 3H), 1.67 – 1.61 (m, 7H), 1.57 (s, 3H). ^{13}C NMR (101 MHz, CDCl₃) δ 168.1, 156.1, 132.1, 123.3, 113.9, 61.3, 41.0, 26.1, 25.6, 18.6, 17.6. HRMS: Calcd for $C_{12}H_{22}NO_2$ [M+H⁺]: 251.0954; Found: 251.0962.
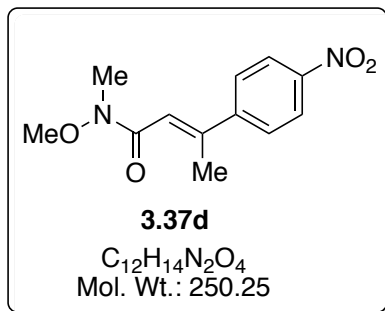
(2E)-N-Methoxy-N-methyl-3-(4-nitrophenyl)but-2-enamide (3.37d): ^{1}H NMR (400

MHz, CDCl$_3$) δ 8.35 – 7.99 (m, 1H), 7.69 – 7.40 (m, 1H), 6.59 (s, 0H), 3.69 (s, 2H), 3.24 (s, 2H),

2.49 (s, 2H). ^{13}C NMR (101 MHz, CDCl$_3$) δ 167.3, 149.5, 147.9, 127.4, 124.0, 119.3, 61.9, 18.1.

HRMS: Calcd for C$_{12}$H$_{15}$N$_2$O$_4$ [M+H$^+$]: 212.1572; Found: 212.1580.
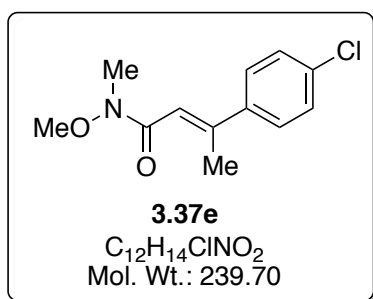
(2E)-3-(4-4hlorophenyl)-N-methoxy-N-methylbut-2-enamide (3.37d): ^{1}H NMR (400

MHz, CDCl$_3$) δ 7.38, 7.38, 7.37, 7.36, 7.36, 7.35, 7.31, 7.31, 7.30, 7.29, 7.29, 3.67, 3.23, 2.46,

2.46. ^{13}C NMR (101 MHz, CDCl$_3$) δ 167.9, 1501.0, 141.5, 134.7, 128.8, 127.8, 116.6, 61.8, 18.1.

HRMS: Calcd for C$_{12}$H$_{15}$ClNO$_2$ [M+H$^+$]: 240.0713; Found: 240.0725.

3.7.2.6. Synthesis of 3.27a, b and 3.27c, d

To a flame-dried flask N-benzyloxyimidazole (6 mmol) and THF (40 mL) were added

under Ar atmosphere. The reaction mixture was cooled to -78 °C and then *n*-BuLi (2.5 M in

hexanes) (6 mL, 25 mmol) was added over 10 minutes and the mixture was stirred at -78 °C for

30 minutes. Weinreb amide **3.37a,b,d,e** (6 mmol) dissolved in another 5 mL of THF was added

slowly at -78 °C. The reaction was monitored by TLC. Upon completion of the reaction, the

reaction was warmed to rt and then quenched using glacial acetic acid (6 equivalents). The

reaction was diluted with ethyl acetate and washed with saturated NaHCO$_3$ (3x50 mL), washed

with brine (50 mL). The combined organic layers were dried over sodium sulfate, filtered and the

filtrate was concentrated in vacuum to give the crude solid, which was then purified by flash

chromatography to give N-benzyloxy acylimidazoles **3.27a,b,d,e.**

3.27a
C$_{22}$H$_{22}$N$_2$O$_2$
Mol. Wt.: 346.43
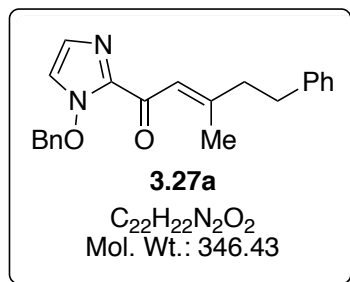
(2E)-1-[1-(Benzyloxy)-1H-imidazol-2-yl]-3-methyl-5-phenylpent-2-en-1-one (3.27a):
^{1}H NMR (400 MHz, CDCl$_3$) δ 7.47 – 7.33 (m, 5H), 7.33 – 7.13 (m, 5H), 6.90 (d, J = 1.0 Hz,

1H), 6.82 (d, J = 1.0 Hz, 1H), 5.29 (s, 2H), 2.86 (dd, J = 9.7, 6.7 Hz, 2H), 2.56 (dd, J = 9.8, 6.6

Hz, 2H), 2.35 (s, 1H). ^{13}C NMR (101 MHz, CDCl$_3$) δ 179.6, 161.3, 141.1, 139.6, 133.5, 130.0,

129.4, 128.7, 128.4, 128.3, 126.0, 124.5, 121.6, 120.7, 43.7, 34.2, 20.0. HRMS: Calcd for

C$_{22}$H$_{22}$N$_2$O$_2$ [M+H$^+$]: 347.1681; Found: 347.1686.

3.27b
C$_{20}$H$_{24}$N$_2$O$_2$
Mol. Wt.: 324.42
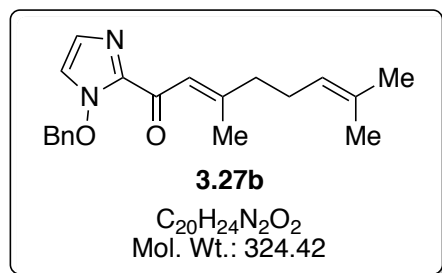
(2E)-1-[1-(Benzyloxy)-1H-imidazol-2-yl]-3,7-dimethylocta-2,6-dien-1-one (3.27b): ^{1}H

NMR (400 MHz, CDCl$_3$) δ 7.44 – 7.28 (m, 5H), 7.17 (s, 1H), 6.87 (s, 1H), 6.83 – 6.77 (m, 1H),

5.27 (s, 1H), 2.36 – 2.15 (m, 7H), 1.65 (s, 3H), 1.59 (s, 3H). ^{13}C NMR (101 MHz, CDCl$_3$) δ

179.9, 162.5, 139.9, 133.8, 132.7, 130.3, 129.6, 128.9, 124.7, 123.3, 121.8, 120.7, 82.3, 42.1,

26.6, 25.9, 20.09, 17.9. HRMS: Calcd for $C_{20}H_{25}N_2O_2$ [M+H$^+$]: 325.1838; Found: 325.1850.

3.27d

$C_{20}H_{17}N_3O_4$
Mol. Wt.: 363.37
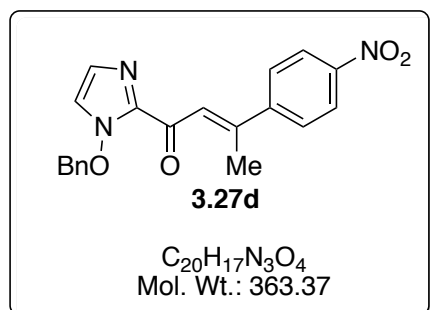
(2E)-1-[1-(Benzyloxy)-1H-imidazol-2-yl]-3-(4-nitrophenyl)but-2-en-1-one (3.27d): [1]H

NMR (400 MHz, CDCl$_3$) δ 8.28 – 8.15 (m, 1H), 7.79 – 7.65 (m, 2H), 7.47 – 7.41 (m, 1H), 7.41 –

7.36 (m, 2H), 6.94 (d, J = 1.1 Hz, 0H), 6.90 (d, J = 1.1 Hz, 0H), 5.31 (s, 1H), 2.70 (d, J = 1.3 Hz,

2H). ^{13}C NMR (101 MHz, CDCl$_3$) δ 179.3, 153.5, 149.2, 148.2, 139.9, 133.5, 130.3, 129.8,

129.0, 127.8, 125.3, 124.4, 124.0, 122.4, 82.5, 18.7. HRMS: Calcd for $C_{20}H_{18}N_3O_4$ [M+H$^+$]:

364.1219; Found: 364.1234.

3.27e

$C_{20}H_{17}ClN_2O_2$
Mol. Wt.: 352.82
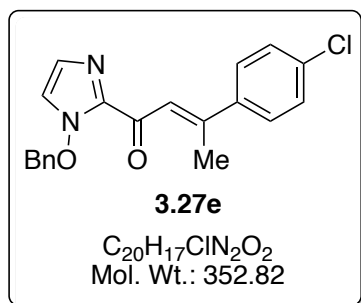
(2E)-1-[1-(Benzyloxy)-1H-imidazol-2-yl]-3-(4-chlorophenyl)but-2-en-1-one (3.27e):

^{1}H NMR (400 MHz, CDCl$_3$) δ 7.65 (d, J = 1.2 Hz, 1H), 7.58 – 7.50 (m, 2H), 7.47 – 7.30 (m,

7H), 6.92 (d, J = 0.9 Hz, 1H), 6.86 (d, J = 0.7 Hz, 1H), 5.31 (s, 2H), 2.68 (d, J = 1.1 Hz, 3H). [13]C

NMR (101 MHz, CDCl$_3$) δ 179.7, 155.2, 141.1, 140.1, 135.5, 133.7, 130.3, 129.7, 129.0, 128.9,

128.2, 125.0, 122.1, 122.0, 82.4, 18.7. Calcd for $C_{20}H_{18}ClN_2O_2$ [M+H$^+$]: 353.0979; Found: 353.0968.

3.8. References

1. Carriera, E. M.; Kvaerno, L. *Classics in Stereoselective Synthesis*; Wiley-VCH Verlag GmbH & Co. KGaA: 2009.

2. Quaternary Stereocenters; Christoffers, J., Baro, A., Ed.; Wiley-VCH Verlag GmbH & Co. KGaA: 2006.

3. Corey Elias, J.; Guzman-Perez, A. *Angew. Chem., Int. Ed.* **1998**, *37*, 388.

4. Peterson, E. A.; Overman, L. E. *Proc. Natl. Acad. Sci.* **2004**, *101*, 11943.

5. Douglas, C. J.; Overman, L. E. *Proc. Natl. Acad. Sci.* **2004**, *101*, 5363.

6. Quasdorf, K. W.; Overman, L. E. *Nature* **2014**, *516*, 181.

7. Feng, J.; Holmes, M.; Krische, M. J. *Chem. Rev.* **2017**, *117*, 12564.

8. (a) McGrath, N. A.; Brichacek, M.; Njardarson, J. T. *J. Chem. Ed.* **2010**, *87*, 1348-1349. (b) Qureshi, M. H.; Smith, D. T.; Delost, M. D.; Njardarson, J. T. *Top 200 Pharmaceutical Products by Prescriptions in* 2016 https://njardarson.lab.arizona.edu/sites/njardarson.lab.arizona.edu/files/2016Top200Pharma ceuticalPrescriptionSalesPosterLowResV2.pdf (accessed July 20, 2018).

9. Marek, I.; Minko, Y.; Pasco, M.; Mejuch, T.; Gilboa, N.; Chechik, H.; Das, J. P. *J. Am. Chem. Soc.* **2014**, *136*, 2682.

10. For recent reviews on Asymmetric conjugate addition reactions in general see: (a) Sibi, M. P; Manyem, S. *Tetrahedron* **2000**, *56*, 8033; (b) Catalytic Asymmetric Conjugate Reactions; Córdova, A., Ed.; Wiley- VCH Verlag GmbH & Co. KgaA: Weinheim, 2010. For metal catalyzed asymmetric conjugate additions see: (c) Harutyunyan, S. R.; den

Hartog, T.; Geurts, K.; Minnaard, A. J.; Feringa, B. L. *Chem. Rev.* **2008**, *108*, 2824; (d) Alexakis, A.; Bäckvall, J. E.; Krause, N.; Pàmies, O.; Diéguez, M. *Chem. Rev.* **2008**, *108*, 2796; (e) Adachi, S.; Moorthy, R.; Sibi, M. P. In *Copper-Catalyzed Asymmetric Synthesis*; Wiley-VCH Verlag GmbH & Co. KGaA: 2014, p 283-324. For reviews on organocatalytic asymmetric conjugate additions see: (f) Rios, R.; Companyó, X. In *Comprehensive Enantioselective Organocatalysis*; Wiley-VCH Verlag GmbH & Co. KGaA: 2013, p 975-1012; (g) Roux, C.; Bressy, C. In *Comprehensive Enantioselective Organocatalysis*; Wiley-VCH Verlag GmbH & Co. KGaA: 2013, p 1013-1042. (h) Marcia de Figueiredo, R.; Campagne, J.-M. In *Comprehensive Enantioselective Organocatalysis*; Wiley-VCH Verlag GmbH & Co. KGaA: 2013, p 1043-1066.

11. Shintani, R.; Tsutsumi, Y.; Nagaosa, M.; Nishimura, T.; Hayashi, T. *J. Am. Chem. Soc.* **2009**, *131,* 13588.

12. Kikushima, K.; Holder, J. C.; Gatti, M.; Stoltz, B. M. *J. Am. Chem. Soc.* **2011**, *133,* 6902.

13. Holder J. C.; Marziale A. N.; Gatti, M.; Mao, B.; Stoltz B. M. *Chem. – A Eur. J.* **2012**, *19*, 74.

14. (a) d' Augustine, M.; Palais, L.; Alexakis, A. *Angew. Chem., Intl. Ed.* **2005**, 44, 1376; (b) Wu, J.; Mampreian, D. W.; Hoveyda, A. H. *J. Am. Chem. Soc.* **2005**, *127,* 4584.

15. Friedel, C.; Crafts, J. M. Comptes Rendus de l'Academie des Sciences Paris **1877**, *84,* 1450.

16. (a) Catalytic Asymmetric Friedel–Crafts Alkylations; Bandini, M., Umani-Ronchi, A., Ed.; Wiley-VCH Verlag GmbH & Co. KGaA: 2009. (b) Poulsen, T. B.; Jørgensen, K. A. *Chem. Rev.* **2008**, *108*, 2903. (c) Terrasson, V.; Marcia de Figueiredo, R.; Campagne, J. M. *Eur. J. Org. Chem.* **2010**, *2010*, 2635. (d) Zeng, M.; You, S.-L. *Synlett* **2010**, *2010*, 1289. (e)

Montesinos-Magraner, M.; Vila, C.; Blay, G.; Pedro, J. R. *Synthesis* **2016**, *48*, 2151.

17. Erker, G.; van der Zeijden Adolphus, A. H. *Angew. Chem., Intl. Ed.* **1990**, *29*, 512.

18. (a) Jensen, K. B.; Thorhauge, J.; Hazell, R. G.; Jørgensen, K. A. *Angew. Chem., Int. Ed.* **2001**, *40*, 160; (b) Evans, D. A.; Fandrick, K. R.; Song, H.-J. *J. Am. Chem. Soc.* **2005**, *127*, 8942. (c) Evans, D. A.; Fandrick, K. R.; Song, H.-J.; Scheidt, K. A.; Xu, R. *J. Am. Chem. Soc.* **2007**, *129*, 10029. (d) Evans, D. A.; Fandrick, K. R. *Org. Lett.* **2006**, *8*, 2249.

19. (a) Austin, J. F.; MacMillan, D. W. C. *J. Am. Chem. Soc.* **2002**, *124*, 1172. (b) Paras, N. A.; MacMillan, D. W. C. *J. Am. Chem. Soc.* **2001**, *123*, 4370.

20. Banwell, M. G.; Beck, D. A. S.; Willis, A. C. ARKIVOC **2006**, No. iii, 163.

21. Lyzwa, D.; Dudzinski, K.; Kwiatkowski, P. *Org. Lett.* **2012**, *14*, 1540.

22. Arai, T.; Yamamoto, Y.; Awata, A.; Kamiya, K.; Ishibashi, M.; Arai, M. A. *Angew. Chem., Int. Ed.* **2013**, *52*, 2486.

23. Gao, J.-R.; Wu, H.; Xiang, B.; Yu, W.-B.; Han, L.; Jia, Y.- X. *J. Am. Chem. Soc.* **2013**, *135*, 2983.

24. Achiral template mediated asymmetric reactions, see: (a) Desimoni, G.; Faita, G.; Quadrelli, P. *Chem. Rev.* **2014**, *114*, 6081. (b) Desimoni, G.; Faita, G.; Quadrelli, P. *Chem. Rev.* **2015**, *115*, 9922.

25. (a) Sibi, M. P.; Ji, J. *J. Am. Chem. Soc.* **1996,** *118*, 3063. (b) Sibi, M. P.; Stanley, L. M.; Xiaoping, N.; Venkatraman, L.; Liu, M.; Jasperse, C. P. *J. Am. Chem. Soc.* **2007,** *129*, 395. (c) Sibi, M. P.; Gustafson, B.; Coulomb, J. *Bull. Korean Chem. Soc.* **2010,** *31,* 341.

26. Kaiser, H. P.; Muchowski, J. M. *J. Org. Chem.* **1984**, *49*, 4203.

27. L. Gilchrist, T.; Lemos, A.; J. Ottaway, C. *J. Chem. Soc., Perkin Trans. 1* **1997**, 3005.

CHAPTER 4. UNDERSTANDING SOLUTION STRUCTURES OF INTERMEDIATES INVOLVED IN ASYMMETRIC CATALYTIC REACTIONS: CHARACTERIZATION OF INTERMEDIATES BY DOSY AND VT NMR TECHNIQUES

4.1. Introduction

The development of an efficient asymmetric catalytic process is laborious, challenging unpredictable and so often empirical. Over the past two decades the field of asymmetric catalysis has seen unprecedented surge in development of successful organic reactions.[1-5] Despite this progress, the demand for enantioenriched compounds such as natural products, synthetic pharmaceuticals etc. is on the rise. However, technical scale up process has been applied only to a handful of asymmetric reactions.[6] This enormous offset between the advances in asymmetric catalysis in an academic setting and inability to emulate these reaction in a process environment is mainly due to our lack of understanding reaction mechanism. In other words, principles of reactivity gleaned do not have adequate mechanistic support. Hence to rationally develop an asymmetric process, a clear understanding of solution structure of intermediates involved in catalytic reaction is crucial. In the high-stakes world of industrial research, understanding solution structures of catalytic intermediates and mechanism of asymmetric reactions are taking a center-stage.

"I believe that, for those who seek to discover new reactions, the most insightful lessons come from trying to trace important reactivity principles back to their origin"

-Barry K. Sharpless[7]

With in situ spectroscopic techniques, X-ray crystallographic data and powerful computational methods to access experimentally elusive details, physical organic chemistry today is in the midst of renaissance. Although there has been an outburst in studying the

structure-activity relations, our understanding of the solution structures and reactivities of the intermediates involved in the reaction lags behind. Hence a detailed study on solution structures of intermediates will improve our understanding of the reaction mechanisms and enable the development of robust catalysts for the enantioselective process.

4.2. Diffusion ordered spectroscopy as technique for characterizing reactive intermediates

Nuclear Magnetic Resonance (NMR) spectroscopy is the powerful technique that is routinely used to characterize the structure of molecules. Traditionally, this is done by correlation of chemical shifts, coupling constants and NOE signals specific to certain structural features. One of the most important experiments that is often overlooked was the gradient spin-echo experiment (or PFGSE - Pulse Field Gradient Spin-Echo) introduced by Stejskal and Tanner in 1965.[8] Although invented four decades ago, its potential as an analytical tool in various chemical and biological applications has been realized only recently. The PFGSE experiments measure diffusion coefficients of molecules in solution, thus providing information about relative particle sizes. Diffusion coefficient is closely related to molecular size, molar mass, solvation etc. Hence it is recognized as a tool to study solution structure of aggregates and ionic interactions.[9]

4.2.1. Pulse field gradient spin echo for measurement of diffusion coefficients

Diffusion is defined as the random translational motion of molecules that is mainly due to thermal energy under the conditions of thermodynamic equilibrium (Figure 4.1).
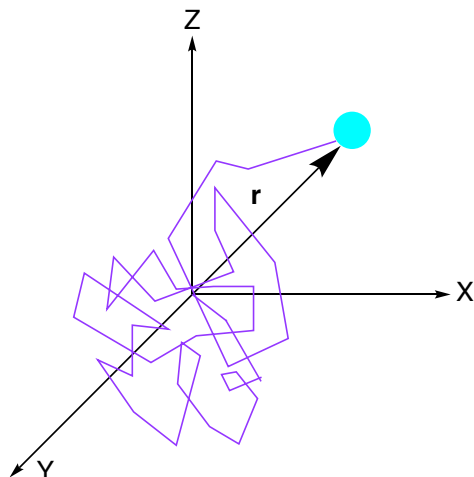
Figure 4.1. Self-diffusion (Brownian motion) of a molecule.

The Einstein-Smoluchowski equation to define diffusion coefficient (D) is given by,

$$<r^2> = 6 \, D \, T \qquad \text{(eq. 4.1)}$$

where r is the RMS distance and T is the temperature. For a sphere diffusing in an isotropic medium of viscosity η, diffusion coefficient is given by Stokes-Einstein equation:

$$D = K_B T/f \qquad \text{(eq. 4.2)}$$

$f = 6\pi\eta r_H$; where D is the diffusion coefficient, K_B is the Boltzmann constant, T is the temperature, f is the frictional factor, η is the viscosity of the medium and r_H is the hydrodynamic radius.

In NMR, each nuclear spin is defined by its precession frequency known as Larmor frequency (ω), which is given by eq. 4.3.

$$\omega = \gamma B_0 \qquad \text{(eq. 4.3)}$$

where ω is the Larmor frequency in rad s^{-1}; γ- gyromagnetic ratio in rad s^{-1} T^{-1}; B_0- static magnetic field. In order observe diffusion, another gradient magnetic field of constant strength is applied along the z-direction. This extra magnetic field strength is given by eq. 4.4.

$$\vec{g} = g_z\vec{z} \qquad \text{(eq. 4.4)}$$

Hence, the total magnetic field experienced by a nuclear spin is given by eq. 4.5.

$$B = B_0 + gz \qquad \text{(eq. 4.5)}$$

Each gradient pulse is characterized by its strength and the duration of time it is applied (δ). If a gradient field is applied for δ amount of time, it causes nuclear spin to change its phase angle. The phase angle, which is related to, the signal intensity of space occupied by the nuclear spins along the z-axis is given by eq. 4.6.

$$\phi(z) = -\gamma(B_0+gz)\cdot\delta = -\gamma B_0\delta - \gamma gz\delta \qquad \text{(eq. 4.6)}$$

This basic idea was used in Stejskal and Tanner pulse sequence, which is given in Figure 4.2. This modified pulse sequence derived from Hahn spin-echo sequence with introduction of gradient pulses. The net magnetization before the application of RF pulses is along z-axis under thermal equilibrium. The phase angle experienced by the spins at the beginning of the experiment is given by eq. 4.7.
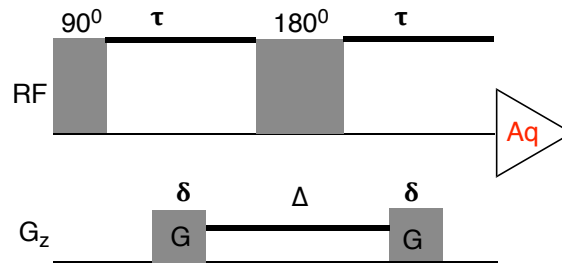
Figure 4.2. Stejskal and Tanner PGSE sequence.

$$\phi(z) = -\gamma B_0 t \qquad \text{(eq. 4.7)}$$

After the application of 90° pulse the spins are in X-Y plane along +X-axis. A pulsed gradient defined by its strength (g) and duration (δ) is applied at time say t_1. The phase angle is given by eq. 4.8.

$$\phi(z) = -\gamma B_0 t_1 - \gamma gz\delta \qquad \text{(eq. 4.8)}$$

After a time period of τ 180° pulse is applied which rotates the magnetization to -X direction. Phase angle after the application of 180° pulse is given by eq. 4.9.

$$\phi(z_1) = \gamma g z \delta \qquad \text{(eq. 4.9)}$$

When second pulse field gradient is applied, the phase-angle change becomes spatially labeled and the phase difference is given by eq. 4.10. From eq. 4.10 it becomes clear that if there is change in position the signal intensity will decrease.

$$/\phi(z_2) = -\gamma g z_3 \delta + \gamma g z \delta = \gamma g \delta (z-z_2) \qquad \text{(eq. 4.10)}$$

So a series of experiments can be performed where the gradient field strength is varied and the corresponding intensity is observed for each experiment. To measure the diffusion constant (D) a decay curve (Figure 4.3) is fitted to eq. 4.11.

$$I(2\tau)/I_0 = \exp(-2\tau/T_2) \cdot \exp(-\gamma^2 G^2 \delta^2 D_t (\Delta - \delta/3)) \qquad \text{(eq. 4.11)}$$

I = intensity of echo signals with gradients; I_0 = intensity of signals without gradients; γ = gyromagnetic ratio; G = Gradient strength; δ = pulse-width; D = diffusion coefficient and Δ = diffusion time.
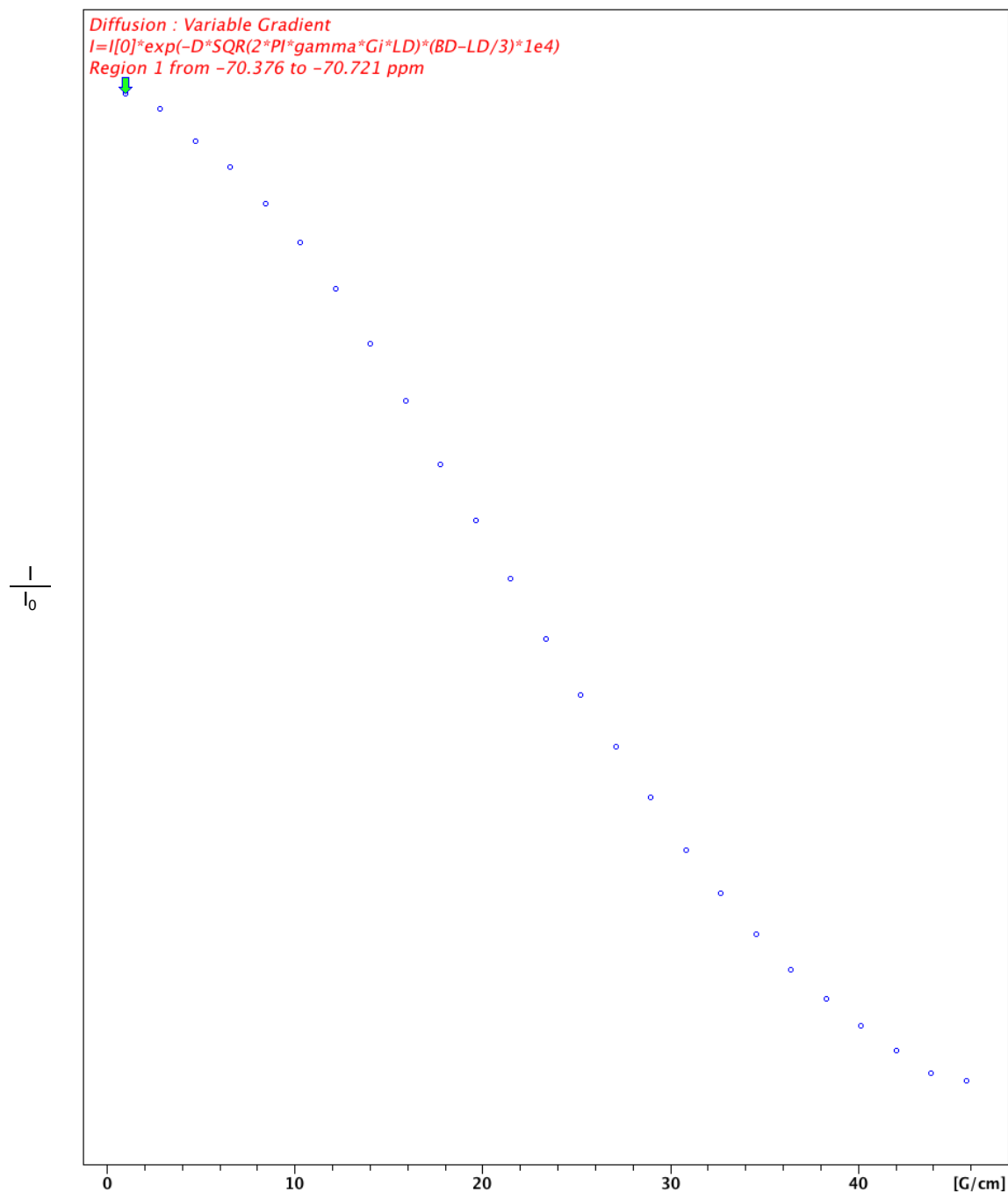
Figure 4.3. The decay curve.

Methods such as SPLMOD[10], CONTIN[11], DECRA[12] (direct exponential curve resolution algorithm), MCR[13] (multivariate curve resolution), Maxent[14] (max entropy), HNN[15] (Hopfield neutral network), post-Widder Laplace inversion[16] and Zhuang's phase function method[17] can be utilized to recover the diffusion coefficient in a specific chemical shift by a fitting procedure.

In 1992, the diffusion coefficients were incorporated into a 2D-NMR experiment, which is called "*DOSY (Diffusion Ordered Spectroscopy*) has been introduced by C. S. Johnson[18] in which the F2 dimension represent chemical shift while the other dimension is represented by diffusion coefficient (Figure 4.4). Hence a mixture of compounds can be resolved by its diffusion properties. Due to its ability to separate different components of a mixture by diffusion constants, DOSY is otherwise known as "*chromatography by NMR*".
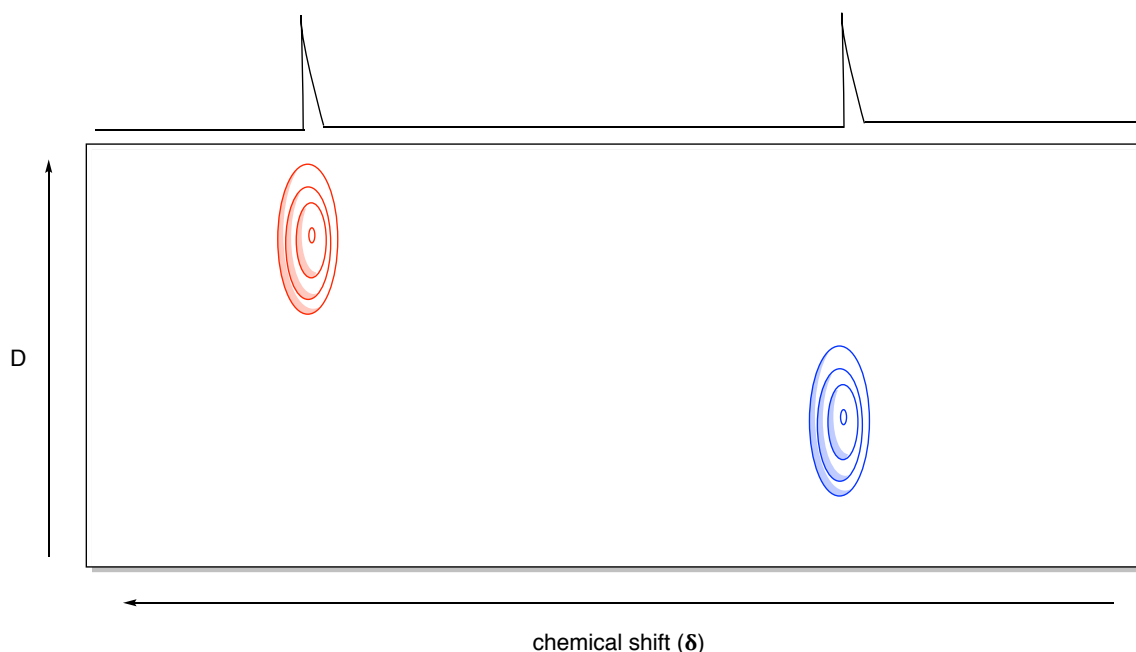
Figure 4.4. Typical DOSY spectrum of a two-component mixture moving with different diffusion coefficients.

4.3. Applications of diffusion ordered spectroscopy to determine solution structures of intermediates

As a powerful analytical tool DOSY technique has been used as a supplement to mass spectroscopy. The diffusion NMR has several advantages: (a) it is a non-invasive technique, which can be applied to unstable complexes and aggregates, (b) require only very small amount of sample, (c) various diffusion NMR experiments based on several nuclei such as ^{1}H, ^{19}F, [19, 20]

[31]P,[21] [28]Si,[22] [2]D,[23] [7]Li,[24] [35]Cl,[25] [195]Pt,[26] [13]C,[27] have been developed. (d) takes short amount of time.

Berger et al. applied DOSY NMR technique to successfully to study the molecularity of an intermediate in the reaction depicted in Scheme 4.1.[28] The zirconium complex [Cp$_2$Zr(H) Cl] **4.1** reacts with carbondioxide to form the formiato complex **4.2** formed by the insertion of CO_2 into the Zr-H bond of **4.1**. They also observed binuclear diolato complex **4.3**, which is formed by the reaction of **4.1** with **4.2**. Although the complex **4.2** was synthesized the existence of **4.3** was only postulated, as it is very unstable and couldn't be characterized completely. In this study the authors used DOSY NMR study to characterize binuclear zirconium complex **4.3**. The DOSY NMR studies were initiated by examining the behavior of two model compounds: **4.4**, a binuclear Zr complex that is close in molar mass to **4.3** and zirconium dichloride complex **4.6**.
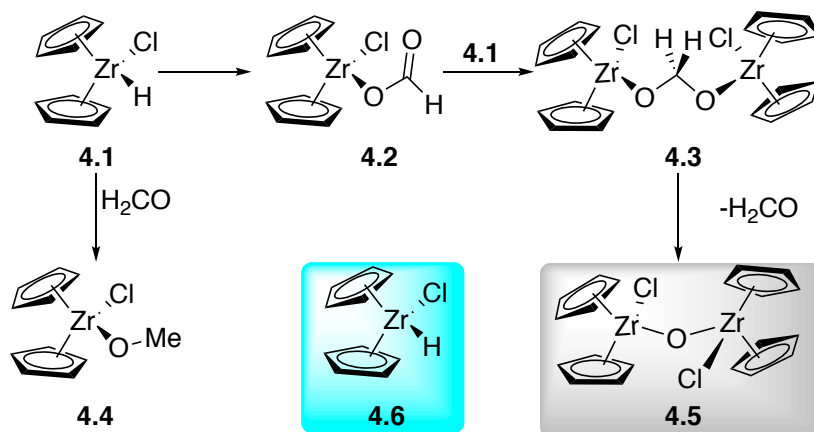
Scheme 4.1. Characterization of intermediates involved in reaction between Zr hydride complex **4.1** and CO_2 by DOSY NMR.

A ^{13}C INEPT DOSY experiment was performed on the mixture of **4.5** and **4.6**. The DOSY spectrum shown in Figure 4.5 shows resolved Cp signals two complexes in the diffusion dimension. The heavier binuclear Zr complex has the smaller diffusion coefficient, which allowed the assignment of signals to the corresponding complexes. Also the hydrodynamic radii

calculated from diffusion measurement and the one obtained from X-ray crystallographic data

are in excellent agreement (Figure 4.5).

Complex	Experimental		Calculated	
	r_H [Å]	D (m^2 s^{-1})	r_H [Å]	D (m^2 s^{-1})
4.6	3.0	1.61×10^{-9}	3.1	1.55×10^{-9}
4.4	3.7	1.31×10^{-9}	3.7	1.30×10^{-9}
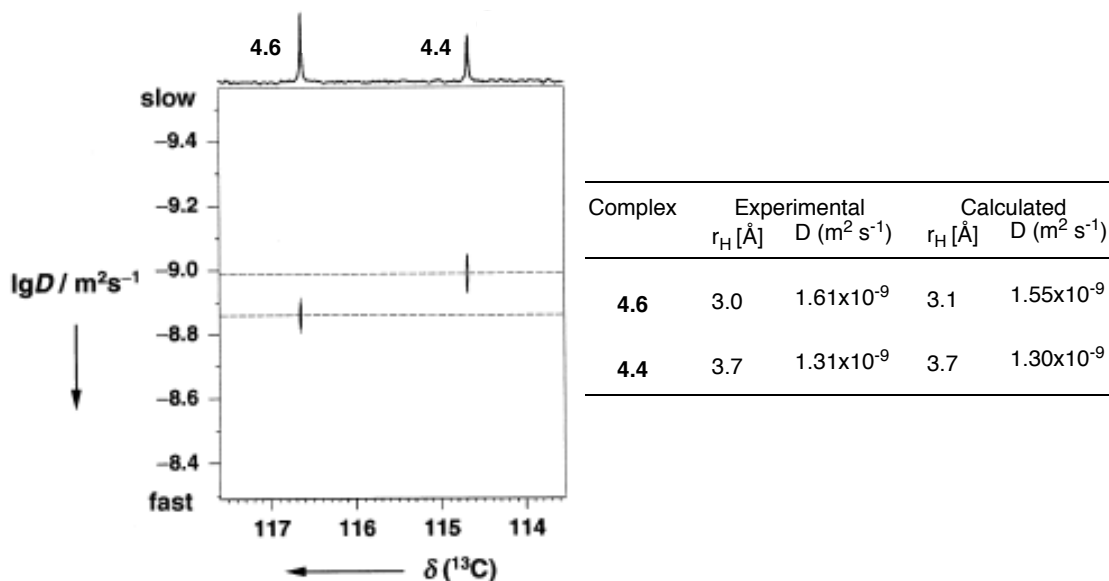
Figure 4.5. ^{13}C INEPT DOSY experiments on model compounds and comparison of experimental hydrodynamic radii (r_H from DOSY studies) and calculated hydrodynamic radii (r_H from X-ray structure). The DOSY spectrum is taken from Schlörer, et al. *Angew. Chem., Int. Ed.* **2002**, *41*, 107-109.

After the studies on model compounds, complex **4.3** was prepared by the reaction

between **4.1** and ^{13}CO$_2$. Once sufficient amount of binuclear complex is formed cooling the

probe to -78 ^{0}C stopped the reaction and ^{13}C INEPT DOSY experiments were performed. As in

the case of model compounds a clear separation was achieved in the diffusion dimension (Figure

4.6). This allowed the assignment of Cp signal of **4.3**, which was not possible by simple ^{13}C

NMR spectra. Signals from methoxy carbon and Cp of **4.5** diffused with same rate and Cp of **4.3**

and methylene (CH$_2$) carbon atom on **4.3** diffused together. Also, the experimentally determined

r_H and the calculated r_H agreed well similar to the model compounds (Figure 4.6).

98
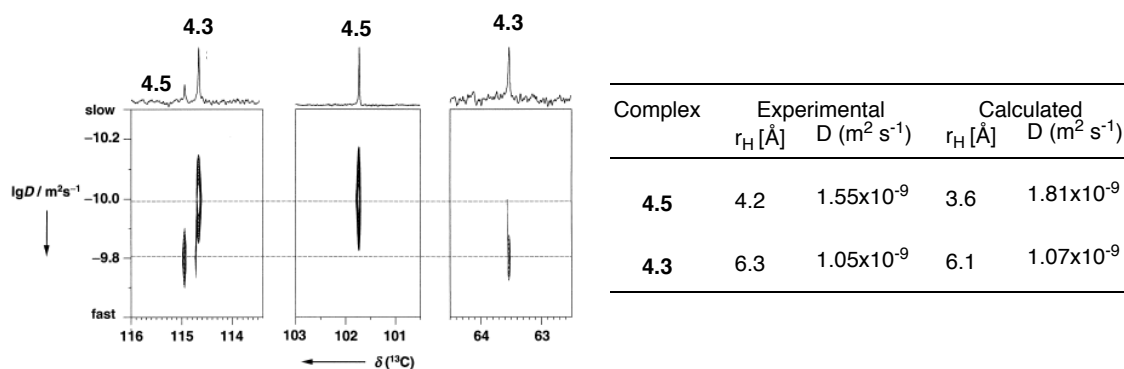
Figure 4.6. ^{13}C INEPT DOSY experiments on reaction mixture and comparison of experimental hydrodynamic radii (r$_H$ from DOSY studies) and calculated hydrodynamic radii (r$_H$ from X-ray structure). The DOSY spectrum is taken from Schlörer, et al. *Angew. Chem., Int. Ed.* **2002**, *41*, 107-109.

Asymmetric addition of organolithium reagents to aldehydes results in formation of chiral alcohol. Owing to the high reactivity, propensity to form aggregates organolithiums give modest enantioselectivities in asymmetric 1,2-addition reactions. 1,2-addition of butyllithium **4.7** to pivalylaldehyde **4.8** in presence of amino ether ligand **4.9** was studied (Scheme 4.2).[29] The enantioinduction of the reaction depended on the solvent used, ether substituents (alkyl and silyl) and also the rate of addition of the electrophile (aldehyde in this case). The inconsistent observation in ee for the rate of addition made the authors to study the reaction in detail. DOSY NMR was used to characterize the intermediates involved in the reaction. They characterized a new trimeric complex **4.12** formed by 2 equivalents of lithium amide and 1 equivalent of lithium alkoxide. This observation strongly suggested product-induced chirality inhibition that is detrimental to enantioselectivity of 1,2-addition. This conclusion was based on the reactions outlined in Scheme 4.2. Formation of **4.12** completely destroys the chiral integrity of aggregate **4.10**, which is responsible for enantioinduction.
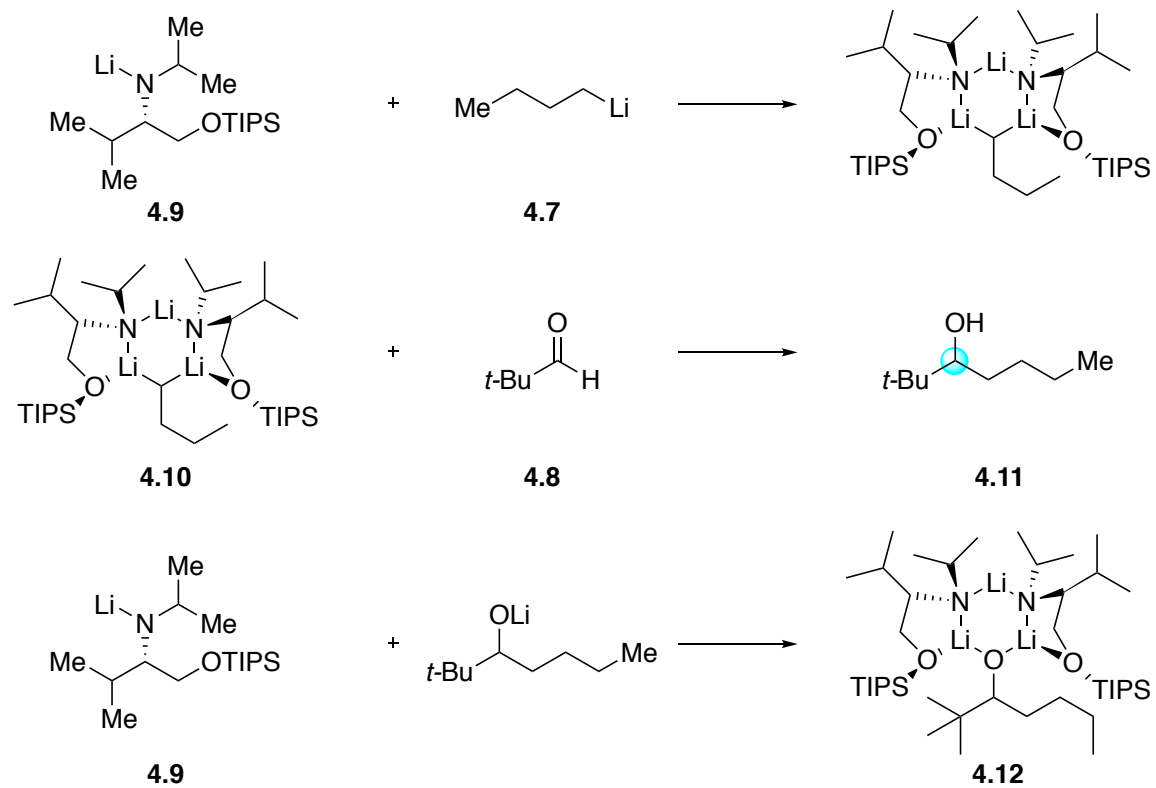
Scheme 4.2. Aggregates formed during asymmetric 1,2-addition reaction.

The DOSY spectrum of trimer **4.12** with ODE (1-octadecene) as internal standard separates into two species in the diffusion dimension (Figure 4.7). A linear correlation of log D and log FW is obtained with extremely high r^2.
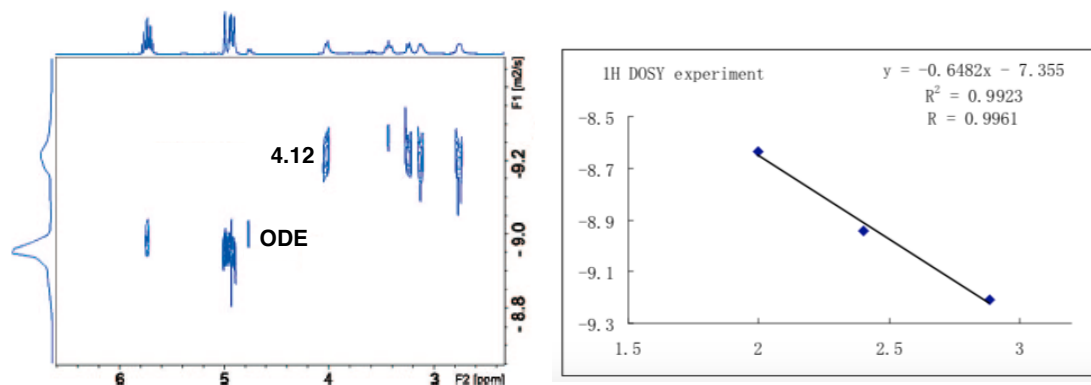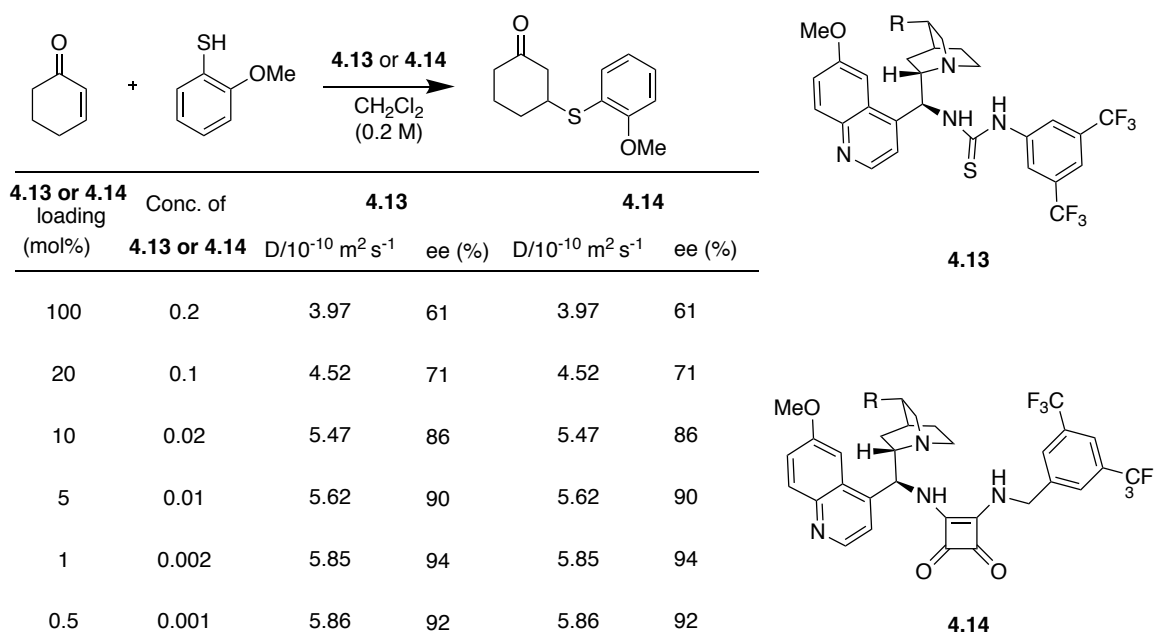
Figure 4.7. DOSY of trimeric complex and ODE in toluene-d_8 and log D vs log FW analysis taken from Guang et al. *J. Org. Chemistry* **2015**, *80*, 9102-9107.

DOSY technique is used in bifunctional organocatalysis to study the aggregation of catalysts. Song and coworkers demonstrated that self-aggregation is an intrinsic problem in bifunctional organocatalysts such as chiral thioureas (**4.13**) and squarimides (**4.14**) where substrates doesn't have functional group that binds to the catalyst effectively. The process of self-aggregation increases with decrease in temperature or increase in concentration. The ee value increases with increase in the value of diffusion coefficient suggesting that degree of self-association plays crucial role in inducing the enantioselectivity (Scheme 4.3).[30]

4.13 or 4.14 loading (mol%)	Conc. of 4.13 or 4.14	4.13		4.14	
		D/10^{-10} m^2 s^{-1}	ee (%)	D/10^{-10} m^2 s^{-1}	ee (%)
100	0.2	3.97	61	3.97	61
20	0.1	4.52	71	4.52	71
10	0.02	5.47	86	5.47	86
5	0.01	5.62	90	5.62	90
1	0.002	5.85	94	5.85	94
0.5	0.001	5.86	92	5.86	92

Scheme 4.3. Correlation between organocatalyst aggregation and enantioselectivity in conjugate addition of heteronucleophiles.

4.4. Results and discussion

4.4.1. Characterization of Brønsted acid-base complexes by ^{19}F DOSY

Achiral templates play influential roles in stereoselective organic transformations.[31] We have demonstrated that judicious choice of template in conjunction with chiral catalyst (Lewis or Brønsted acid) can affect both reactivity and stereoselectivity.[32] Chiral Brønsted acids, particularly phosphoric acids, have emerged as powerful asymmetric catalysts in a plethora of

organic transformations,[33] activating substrates via hydrogen bonding or by complete

protonation[34] (Scheme 4.4). For effective enantioselectivity, proximity between the reactive site

and the catalyst chirality is crucial.[35] If an ion pair is solvent-separated, for example, high

enantioselectivity is unlikely. In the context of understanding and developing asymmetric

Brønsted acid catalysis, we became interested in studying Brønsted acid-base interactions in

solution.

Diffusion ordered NMR spectroscopy (DOSY) has emerged as an effective tool for

studying non-covalent interactions in solution. Since diffusion depends on size, coordination

reduces diffusion rates. The pulse field gradient spin- echo diffusion method has been used

extensively to study ion-pairing, aggregation, hydrogen bonding, π-π stacking in supramolecular

systems[36] and transition metal catalysis.[37] Diffusion constants (D) can be used to determine

formula weights (FW) using the relationship log D $\propto$ log FW. Williard[38] and others[39] have used

DOSY to determine formula weights of polymers and solution structures of organometallic

complexes. While ^{1}H DOSY has been used most extensively, peak overlap is problematic. Thus

several heteronuclear (^{13}C, ^{31}P, ^{6}Li, etc.) DOSY methods have been developed.[40]

We envisaged that applying DOSY to complexes between basic substrates and Brønsted

acids would help understand ion-pairing and aggregation (Scheme 4.4). Solvent-separated ion

pairs should show different diffusion profiles from contact ion pairs. Likewise, aggregates

should be distinguishable from 1:1 complexes. Unfortunately our initial attempts using ^{1}H

DOSY were somewhat discouraging due to signal overlap.

We reasoned that ^{19}F DOSY might be a very practical alternative, due to its well-resolved

signals and high sensitivity, which facilitate peak picking and curve-fitting analysis.

Conceptually the ^{19}F can be present in the acid, the substrate, or both (Scheme 4.4). Brønsted

acid catalysts such as chiral N-triflylphosphoramides and chiral thioureas contain fluorine atoms, as do several Lewis acid counterions such as BF_4^-, $CF_3SO_3^-$, $(CF_3SO_2)_2N^-$, PF_6^-, and SbF_6^-. Many of the substrates that we use in catalytic reactions also contain fluorines (see **4.22a**, Scheme 4.5). Dual labeling should also be possible, in which both substrate and acid are fluorinated; if complexation occurs, then fluorine signals associated with both substrate and acid should show the same diffusion rates. Here we disclose the development and effectiveness of ^{19}F DOSY for successful formula weight determination in simple acid base complexes.
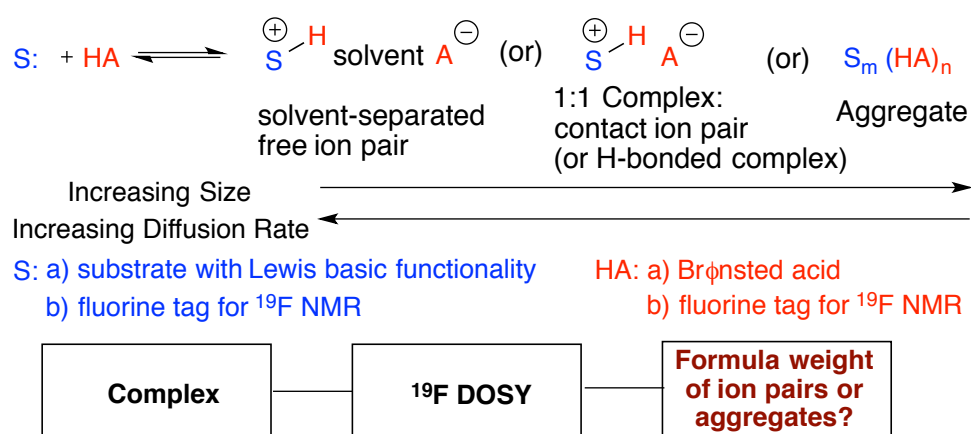
Scheme 4.4. Reaction scheme for ^{19}F DOSY experiments.

The internal standards and the analytes chosen for the initial ^{19}F DOSY experiments are shown in Figure 4.8. They are as follows: benzotrifluoride **4.15** (146 g mol^{-1}), 1,4-bis(trifluoromethyl)benzene **4.16** (214 g mol^{-1}) and 1,3,5-tris(trifluoromethyl)benzene **4.17** (282 g mol^{-1}). Trifluoroacetic acid **4.18** (114 g mol^{-1}) was used as the test Brønsted acid to check the validity of formula weight analysis by ^{19}F DOSY. Benzene-d$_6$ was used as the solvent. The standard Bruker pulse sequence (ledbpgp2s) incorporating longitudinal eddy current delay was used for ^{19}F DOSY experiments.[41]
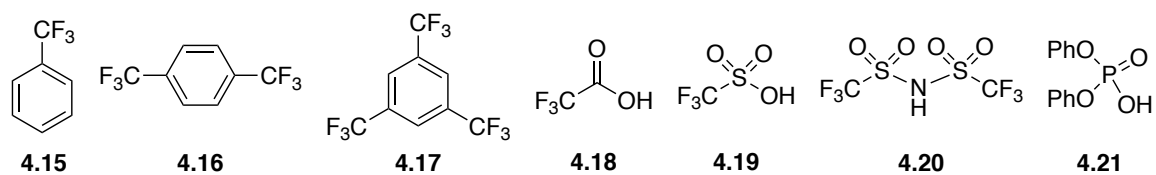
Figure 4.8. Internal standards and analytes chosen for initial ^{19}F DOSY studies.

The resulting DOSY spectrum is shown in Figure 4.9 and is consistent with what is expected: the diffusion coefficient decreases in the order **4.18**>**4.15**>**4.16**>**4.17**. Of the three internal standards, the smallest one diffuses fastest and the heaviest diffuses slowest, and the smaller CF_3CO_2H diffuses fastest of all.[42] The D value for a particular species was obtained using curve fitting of signal attenuation data for the corresponding resonance in the DOSY experiment.
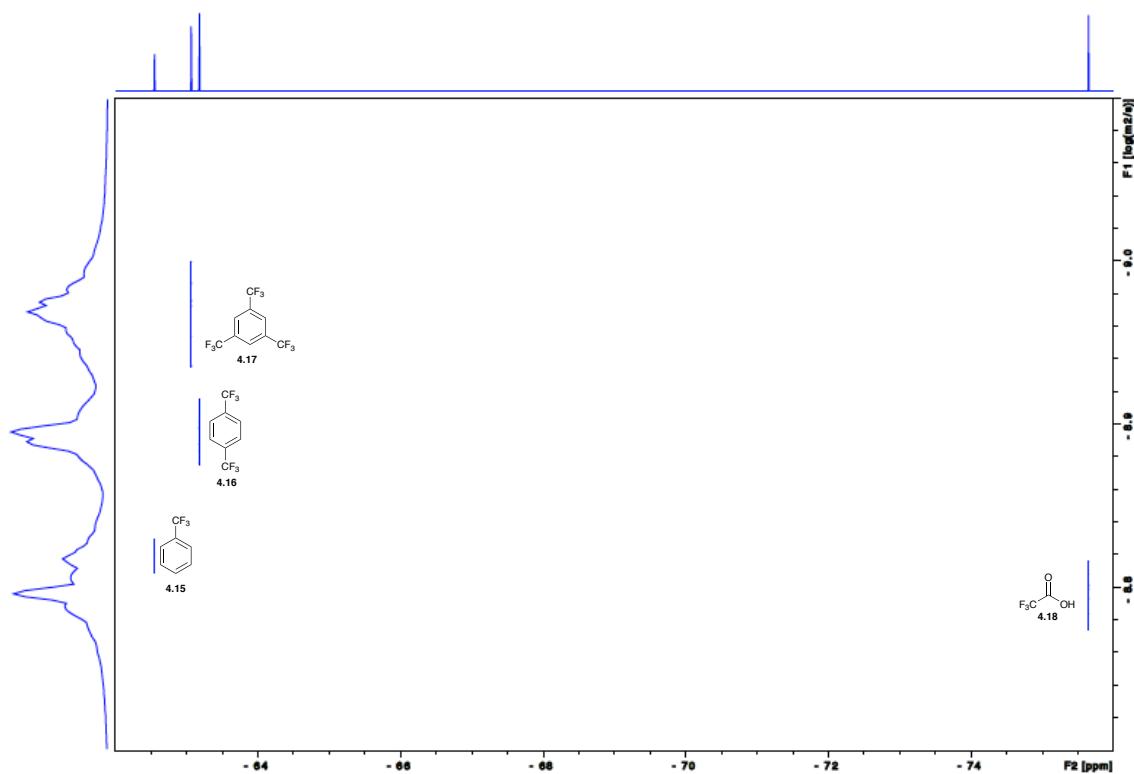
Figure 4.9. ^{19}F DOSY spectrum of a mixture of internal standards **1-3** and trifluoroacetic acid **4** in C$_6$D$_6$.

To check the validity of the formula weight (FW) analysis by diffusion experiments, we performed a linear regression analysis of log D versus log FW for the mixture of compounds **4.15-4.18** (Figure 4.10). The graph shows a very good correlation of the internal references selected and the predicted formula weight of 4.18 from DOSY studies with a very high r^2 value of 0.982.
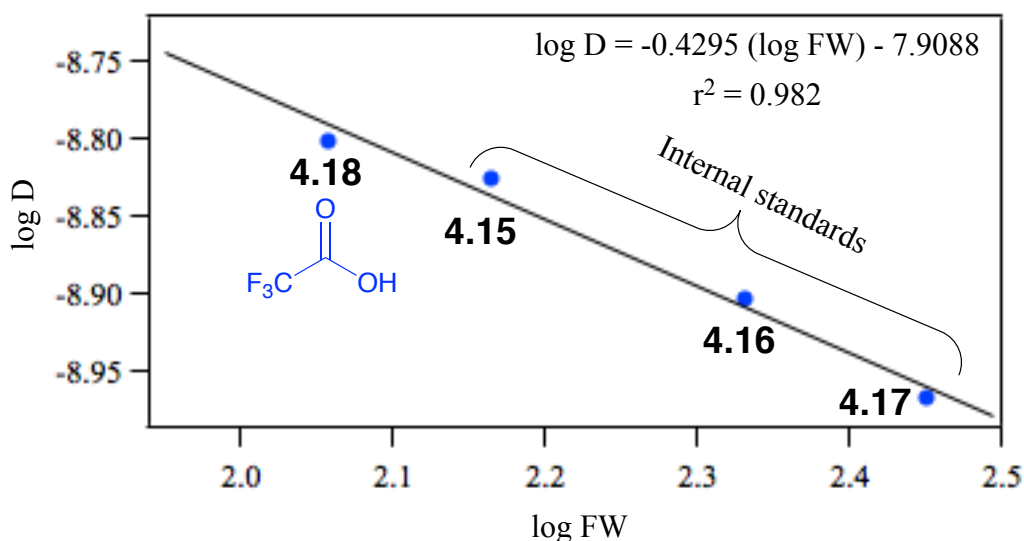
Figure 4.10. log D versus log FW analysis of ^{19}F DOSY of a mixture of **4.15-4.18** in benzene-d_6.

The formula weight of **4.18** from the diffusion studies is calculated to be 120 g mol^{-1} as compared to the actual formula weight of 114 g mol^{-1} (Table 4.1) with only about 5% error.

Table 4.1. D-FW analysis of ^{19}F DOSY spectrum of compounds **4.15-4.18** in C_6D_6.

compound	FW (g mol^{-1})	D (m^2 s^{-1})	FW$_{DOSY}$ (g mol^{-1})^a	error %
4.15	146	1.489 x 10^{-9}	137	6.2
4.16	214	1.265 x 10^{-9}	201	6.1
4.17	282	1.071 x 10^{-9}	295	4.6
4.18	114	1.595 x 10^{-9}	120	5.1

^{a} log D = -0.4295(log FW) – 7.9088.

Analogous formula weight analysis by ^{19}F DOSY evaluated the formula weight of triflic

acid **4.19** to be 154 g mol^{-1} and bis(trifluoromethane)sulfonimide **4.20** to be 287 g mol^{-1}. The

DOSY-estimated formula weights are within 10% of the actual formula weights (Table 4.2).

Table 4.2. [19]F DOSY-estimated formula weights of other fluorinated Brønsted acids.

analyte	FW_{Actual} (g mol^{-1})	FW_{DOSY} (g mol^{-1})[a]	error %
4.18	114	120	5.1
4.19	150	155	3.3
4.20	281	287	2.1

[a] calculated from the plot of log D Vs log FW.

Having confirmed the feasibility of using ^{19}F DOSY for formula weight determination,

we next applied these experiments to Brønsted acid-basic substrate complexes. Determining the

formula weight of these complexes can give useful insights into the stoichiometry of complexes

involved in catalytic reactions. Acylimidazoles (**4.22**) have been used extensively in asymmetric

transformations.[43] We applied our ^{19}F DOSY method to determine the formula weights of the

complexes formed between Brønsted acids and acylimidazoles **4.22** (Scheme 4.5). Fluorine-

labeled substrate **4.22a** is amenable to ^{19}F DOSY using unlabeled phosphoric acids.

Alternatively, double-labeling studies using 7a in combination with fluorinated acids **4.18-4.20**

are also possible. Substrate **4.22b** is itself not labeled, but can be studied with the fluorinated

acids.
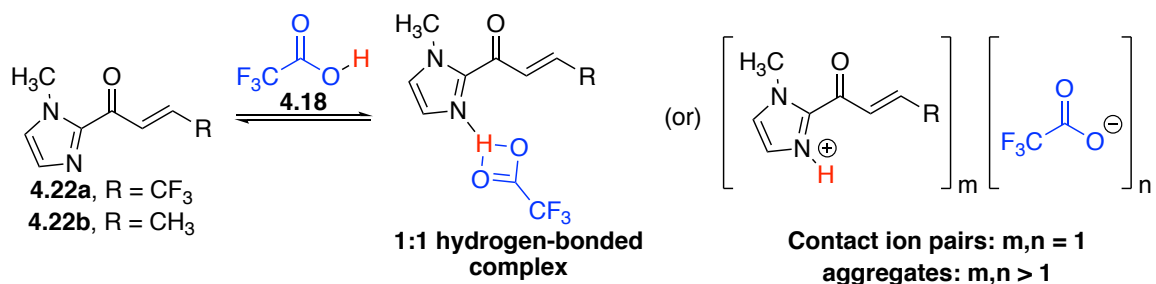
Scheme 4.5. Interaction between trifluoroacetic acid (Brønsted acid) and acylimidazole substrates.

^{19}F DOSY was conducted on a solution containing internal standards **4.15**-**4.17**, trifluoroacetic acid **4.18**, and fluorinated substrate **4.22a**. A remarkable difference is seen in the DOSY spectrum (Figure 4.11). In the absence of a nitrogenated substrate, acid 4 had been faster moving than any of the three internal standards **4.15**-**4.17** (Figures 4.9 and 4.10). But in the presence of acylimidazole **4.22a**, trifluoroacetic acid 4 now moves slower than all of the three internal standards, indicating complexation and significant formula weight increase. Further, the labeled substrate **4.22a** and acid **4.18** move with equivalent diffusion coefficients, again indicating that they are complexed to each other. In the presence of acid **4.18** there is also a considerable change in the ^{19}F chemical shift of **4.22a** (δ^{19}F ~ 64.4 ppm in absence of acid, δ^{19}F ~ 65.4 ppm in presence of acid), again indicating complexation.
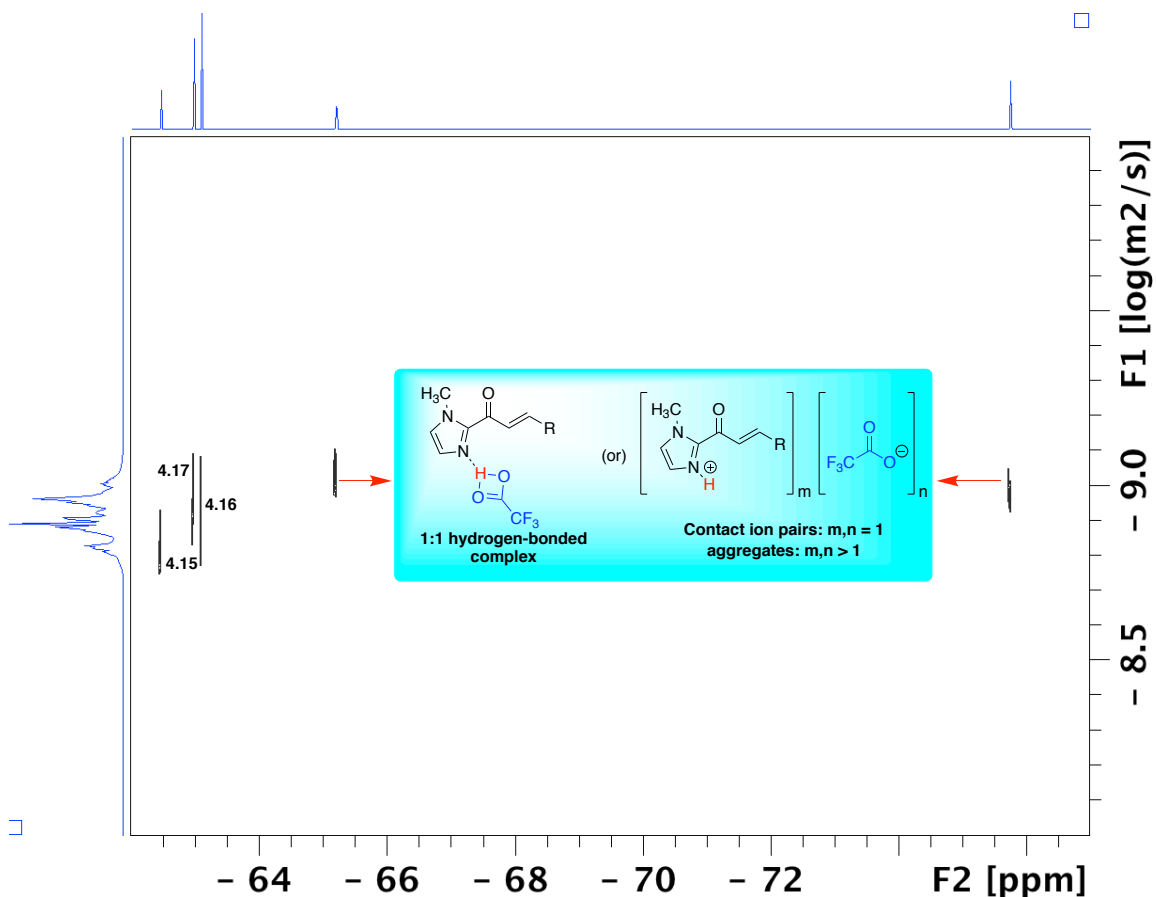
Figure 4.11. ^{19}F DOSY spectrum of compounds **4.15-4.18** and acylimidazole **4.22a** in C$_6$D$_6$.

The formula weight analysis graph is shown in Figure 4.12. Based on the experimentally obtained D value of 9.993 x 10^{-10}, a very good correlation is obtained for the internal references (r^2 = 0.9996) and a formula weight of 343 g mol^{-1} is obtained for the complex. This 343 g mol^{-1} estimation is relatively close (7.8% error) to what would be expected for a 1:1 acid-base complex between substrate **4.22a** and trifluoroacetic acid **4.18** (actual FW = 318 g mol^{-1}). Thus chemical shift change, change in diffusion rates, and matching diffusion rates for substrate and acid clearly show complexation, with the actual diffusion rate suggesting 1:1 complexation.
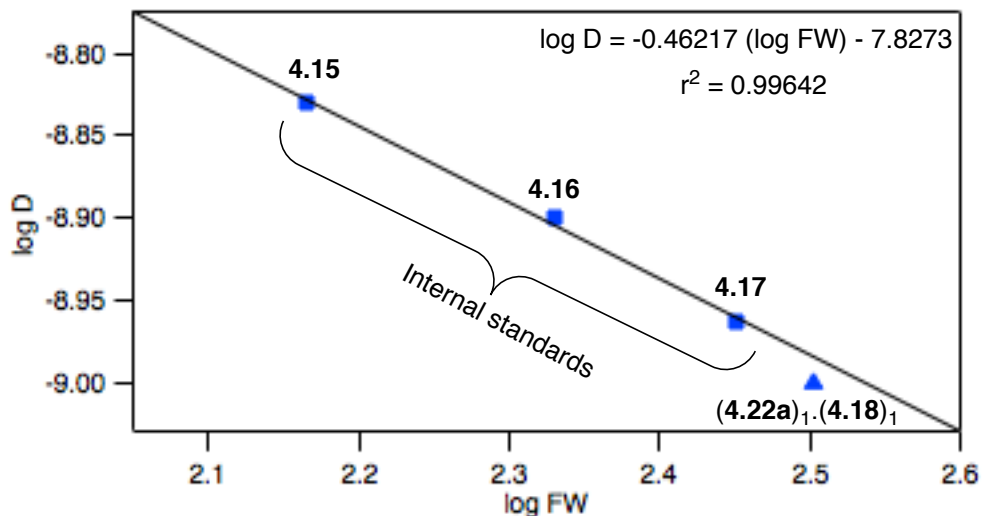
Figure 4.12. Analysis of ^{19}F DOSY for a mixture of **4.15-4.18** and **4.22a** in C_6D_6..

We next performed analogous ^{19}F DOSY experiments using both labelled and unlabelled

substrates **4.22a** and **4.22b** and two stronger Brønsted acids **4.19** and **4.20**. The results are

shown in Table 4.3. Interestingly, while trifluoroacetic acid gave a 1:1 complex with **4.22a**, the

strongly acidic bis(trifluoromethane)sulfonimide **4.20** gave a 2:2 complex. We were unable to

determine the formula weight of the complex of **4.22a** with triflic acid **4.19** due to precipitation

of the complex. Unlabeled acylimidazole **4.22b** formed a 2:2 complexes with both triflic acid

4.19 and bis(trifluoromethane)sulfonimide **4.20**. While the interactions of **4.22a** with acids **4.18**

and **4.20** represent double-labeling experiments, the interaction of **4.22b** with acids **4.19** and **4.20**

demonstrates the utility of the ^{19}F DOSY approach for unlabeled substrates reacting with

fluorine-tagged acids. The predicted formula weights of these higher molecular weight

complexes are well within the experimental error (Table 4.3).

We also studied the complexation between fluorine-tagged acylimidazole **4.22a** and

unlabeled phosphoric acid **4.21**, which is representative of the types of chiral Brønsted acids used

in asymmetric reactions. When ^{19}F DOSY was conducted on a solution containing internal

109

references (**4.15-4.17**) acylimidazole **4.22a** and phosphoric acid **4.21** (Table 4.3, last entry) a

formula weight of 429 g mol^{-1} corresponding to a 1:1 complex (454 g mol^{-1}) was obtained. This

result shows promise towards the characterization of complexes in chiral Brønsted acid-mediated

transformations.

Table 4.3. Predicted formula weights of various acylimidazole-Brønsted acid complexes

acid	FW$_{Calc}$ (g mol^{-1})	complex	FW$_{DOSY}$ (g mol^{-1})[a]	error %
4.18	318	(**4.22a**)$_1$.(**4.18**)$_1$	343	7.8
4.19	708	(**4.22a**)$_m$.(**4.19**)$_n$	-[b]	-[b]
4.20	970	(**4.22a**)$_2$.(**4.20**)$_2$	950	2.1
4.19	600	(**4.22b**)$_2$.(**4.19**)$_2$	624	4.0
4.20	862	(**4.22b**)$_2$.(**4.20**)$_2$	847	1.7
4.23	454	(**4.22a**)$_1$.(**4.21**)$_1$	429	5.5

[a] calculated from the plot of log D Vs log FW. [b] the complex precipitates and no fluorine peaks corresponding to **4.22a** and **4.19** were observed.

4.5. Brønsted acid catalysis in template mediated asymmetric synthesis: understanding solution structure of intermediates

Organocatalysts such as chiral Brønsted acids and hydrogen bond donors such as chiral

thioureas, squarimides etc. have been used in plethora of stereoselective organic

transformations.[33-35] From the perspective of templated acceptor chemistry, these catalysts (vide

supra) activates the acceptors by complete protonation or by hydrogen bonding to the carbonyl

group of the acceptor. There are a handful of structural and mechanistic details are available in

the literature for the activation of imines by chiral phosphoric acids,[44-49] these are just the tip of

the iceberg when compared to the volume of work reported on the synthetic utility of Brønsted

acid catalysis.

Over the past decade Sibi group has used Brønsted acids as catalyst in several

asymmetric transformations. In 2009, Norihiko and Sibi reported enantioselective α-oxygenation

using TEMPO (Scheme 4.6).[50] In this study several ketones of type **4.23** in presence of catalytic amount of chiral H_8-binaphthol derived phosphoric acid **4.24** and a single electron transfer agent such as ferrocenium hexafluorophosphate (**4.25**) gave enantioenriched α-oxygenated product. Norihiko appended various templates as R group and found that N-methylimidazole or thiazole template performed well. The reaction is believed to go through an enol-intermediate which on SET oxidation gives α-keto radical **4.27** that can be trapped by TEMPO to form the product.
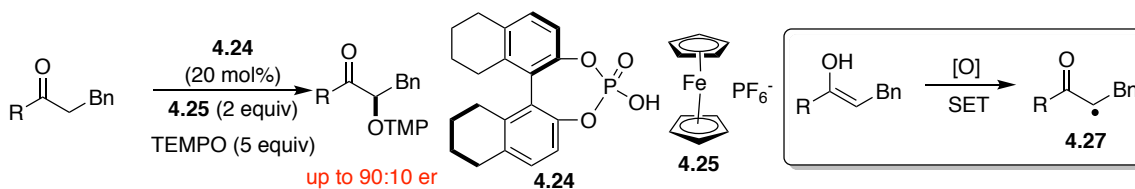
Scheme 4.6. H_8-BINOL-derived phosphoric acid catalyzed enantioselective α-oxygenation reaction by Sibi et al.

Dr. Rane, from Sibi group reported [3+2] cycloaddition between nitrones and β,β-disubstituted-α,β,-unsaturated acylimidazoles using chiral Brønsted acid catalysis (Table 4.4).[51] The phosphoric acid catalyzed reaction gave exo-products in high diasteroselectivity (> 40:1) were obtained in high chemical yield and high enantioselectivities (90-97% ee).

Table 4.4. Chiral phosphoric acid catalyzed nitrone cycloaddition by Sibi et al.
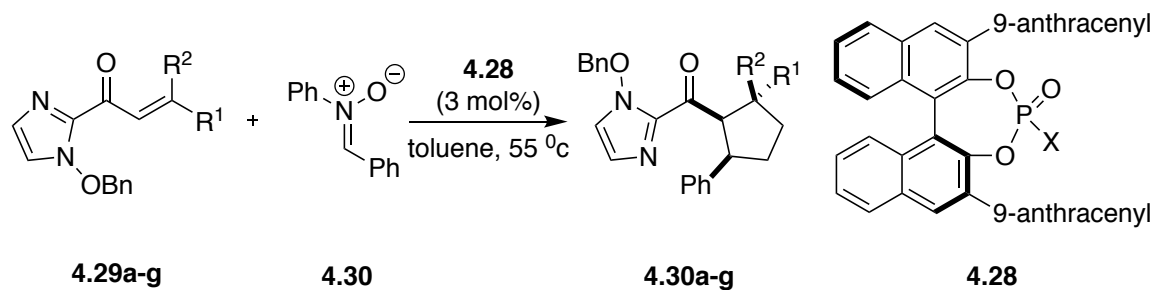
Entry	SM	R^1	R^2	Product	Time (d)	Yield (%)	*exo* ee (%)
1	**4.29a**	CF$_3$	CH$_3$	**4.30a**	0.5	94	96
2	**4.29b**	CF$_3$	Ph	**4.30b**	3	89	95
3	**4.29c**	CF$_3$	*p*-FC$_6$H$_4$	**4.30c**	3	98	93
4	**4.29d**	CF$_3$	*p*-ClC$_6$H$_4$	**4.30d**	3	98	97
5	**4.29e**	CF$_3$	*m*-FC$_6$H$_4$	**4.30e**	3	87	91
6	**4.29f**	CF$_3$	*m*-CF$_3$C$_6$H$_4$	**4.30f**	3	83	90
7	**4.29g**	CH$_3$	CH$_3$	**4.30g**	6	92	94

4.5.1. Results and discussion

Another example from Sibi group is Brønsted acid catalyzed [3+2] cycloaddition of cyclic azomethine imines to α,β,-unsaturated acylimidazoles.[52] The *N,N'*-cyclic azomethine imines shown in Figure 4.12 are attractive dipoles due to their stability.[53] Cycloaddition to alkenes produces diazabicycloalkanes, which have been evaluated as biologically active peptidomimetics.[54] Hence, enantioselective catalytic methods aimed at developing such scaffolds are warranted. Enantioselective catalytic azomethine imine cycloadditions are known in the literature,[55] but a main drawback has been the problem associated with synthesizing molecules bearing multiple stereocenters. During the course of developing chiral Lewis acid catalyzed azomethine imine cycloadditions to α,β-unsaturated pyrazolidinone imides, we found that the reaction is *exo* selective with good levels of enantioselectivity.[55e] The selectivity achieved in the methodology was attributed to two-point binding enoyl templates that bear an additional

coordinating group tethered to the α,β-unsaturated system. However, the reaction was found to be intolerant towards substitution at either α or β position. A stoichiometric catalyst loading was required, and the product was obtained with poor stereoselectivity (Figure 4.13). Is it possible to improve the reactivity? If so, is it also possible to access all stereoisomers of the cycloadducts, both *exo* and *endo,* with relative and absolute stereocontrol from the same set of starting materials?

4.5.1.1. Design of templates to control the stereoselectivity

In an ongoing research program that primarily focuses on development of novel template based acceptors for complex enantioselective transformations, we became interested in mode of activation of these substrates and how it affects the stereoselective outcome of the reaction. We chose to pursue *N*-alkylimidazoles as templates, as the reactions with enoyl acceptors bearing oxazolidinone and pyrazolidinone templates were unreactive. We envisaged that going from an imide oxidation state to a ketone oxidation state would increase the reactivity of the acceptors dramatically, and also the appended imidazole group with N-atoms would serve as a second point of coordination to a Lewis acid catalyst or H-bond donor catalyst. Bidentate enoyl systems are known to form chelates III (Figure 4.13B) with Lewis acid catalytic systems. Alternately, H-bond donor catalytic systems such as Brønsted acids can form two kinds of complex with the same substrates: I (protonated, open form) (Figure 4.13B) and II (bifurcated H-bonding, similar to chelated system III) (Figure 4.13B).

We also envisaged that difference in the catalyst-substrate structure should yield different stereochemical outcomes in the reaction. Such catalytic stereodivergent cycloaddition strategies are scarce.[56] Here we disclose chiral Brønsted acid catalyzed *exo* selective dipolar cycloaddition

and chiral Lewis acid catalyzed *endo* selective dipolar cycloaddition with good levels of

diastereo- and enantioselectivity (Figure 4.13A).
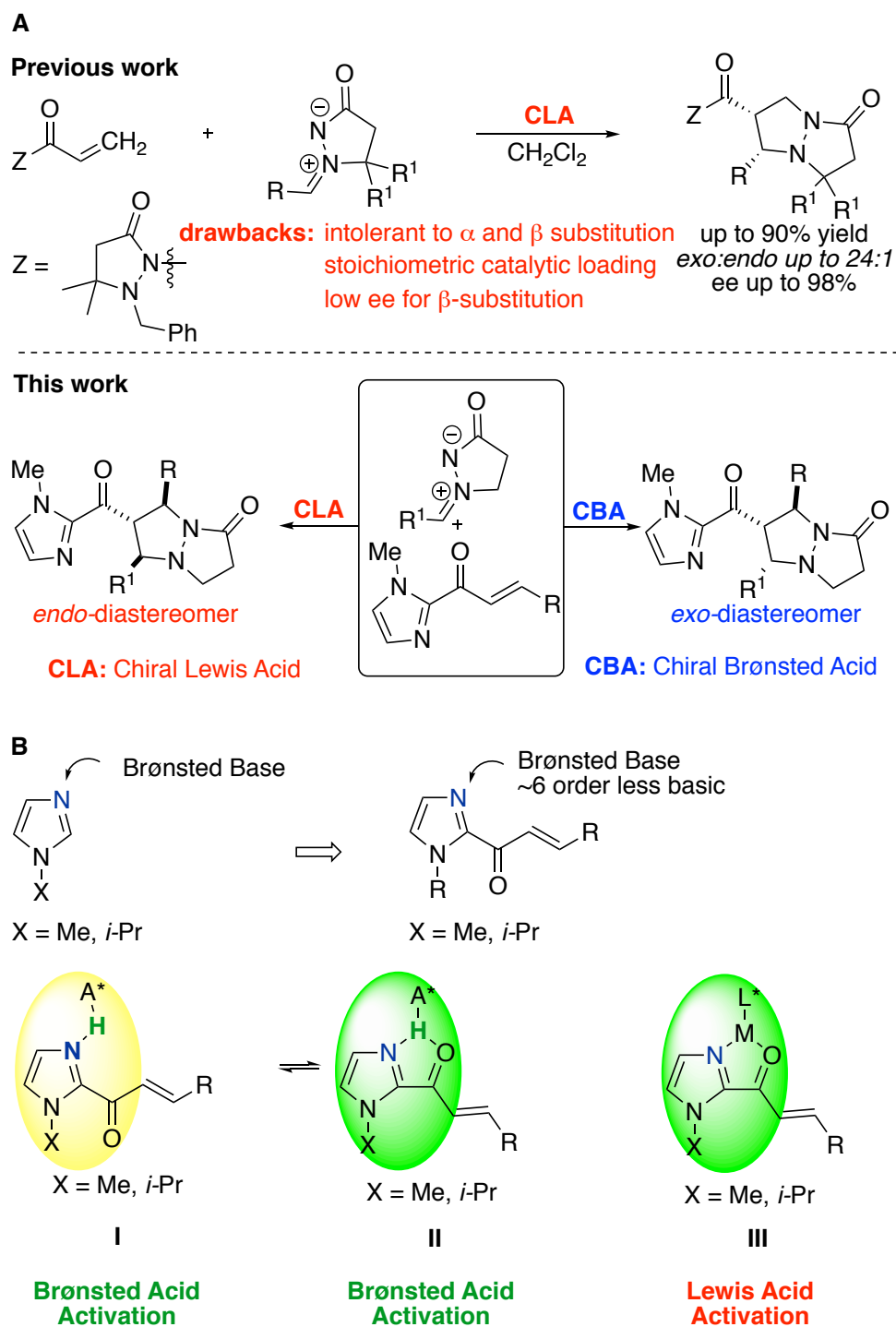
Figure 4.13. A) Stereodivergent synthesis of exo and endo cycloadducts of azomethine imine cycloaddition. B) Different modes of activation of enoylimidazoles: non-chelated (I) vs chelated intermediates (II & III).

4.5.1.2. Optimization of Brønsted acid catalyzed azomethine imine cycloaddition

Initially, we focused our attention on developing highly selective Brønsted acid catalyzed azomethine imine cycloadditions. Our working hypothesis was that Brønsted acid would be able to activate α,β-unsaturated acylimidazoles by protonation or hydrogen bonding[57] or activate azomethine imines[58] or both.[59] There was no cycloaddition between crotonate **4.31a** and dipole **4.32a** in the uncatalyzed reaction (entry 1, Table 4.5). During initial screening of achiral Brønsted acids (entries 2–4, 30 mol%), cycloaddition occurred with high selectivity for the *exo* isomer **4.33a** (*exo:endo* > 40:1). These data suggested the possibility of enantioselective *exo* selective azomethine imine cycloaddition reaction. We found that chiral *N*-triflylphosphoramides **4.28** involving large anthracene substituents gave an excellent yield (93%) of the *exo* cycloadduct **4.33aa** with high enantioselectivity (93% ee) (entry 8, Table 4.5). Reducing the catalyst loading to 10 mol% did not erode the diastereoselectivity (*exo:endo* > 40:1) and enantioselectivity (92% ee) of **4.33aa** (entries 9–10, Table 4.5).

Table 4.5. Evaluation of Brønsted acids in azomethine imine cycloaddition.
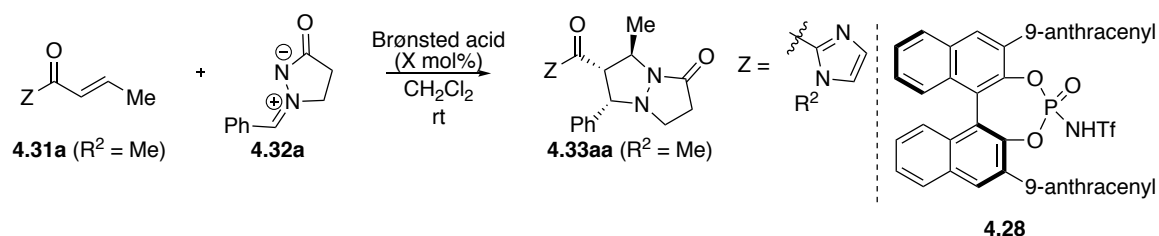
entry	Brønsted Acid	X	time (d)	yield (%)[a]	exo:endo[b]	ee (%)[c]
1	none	-	1	0	00	-
2	AcOH	30	1	15	>40:1	-
3	CF$_3$CO$_2$H	30	1	83	>40:1	-
4	(PhO)$_2$PO$_2$H	30	1	76	>40:1	-
5	**4.28**	10	2	93	>40:1	92

[a] Isolated yield. [b] Calculated from ^{1}H NMR of crude reaction mixture. [c] Determined by chiral HPLC analysis.

4.5.1.3. Substrate scope of Brønsted acid catalyzed azomethine imine cycloaddition

With optimized conditions in hand, we examined the scope of acylimidazoles (**4.31a-g**) in azomethine imine cycloadditions (Table 4.6). The reactions were performed using 10 mol% of **4.28**. β-Alkyl substituents on the acylimidazoles (**4.31b**, **4.31c**, **4.31d)** are well tolerated in the reaction giving the cycloadduct (**4.33ba**, **4.33ca**, **4.33da**) in very high yield (89-93%) and very high enantioselectivity (92-99% ee). The reaction also proceeded smoothly when a β-benzyloxymethyl substituent was present: the cycloadduct **4.33ea** was formed in high yield (93%) and ee (88% ee, Table 4.6). The superior reactivity of these acylimidazole templates in Brønsted acid catalyzed azomethine imine cycloadditions were highlighted by using electron-rich β-heteroaryl substituted acylimidazole (**4.31f)** and β-aryl substituted acylimidazole (**4.31g**). Both substrates provided the *exo* cycloadducts in good yield and good levels of enantioselectivity. By changing the methyl substituent on the acylimidazole to an isopropyl moiety no dramatic change in the outcome the reaction is observed: the cycloadduct **3ha** is obtained in very high yield and high levels of enantioinduction (92% ee). These results are highly noteworthy since reports on exo selective azomethine imine cycloaddition to sterically and electronically challenging substrates are rare. We were able to build three contiguous centers with very high level of relative and absolute stereocontrol. These results also highlight the robustness of chiral binol derived N-triflylphosphoramide catalysts in template chemistry. We also studied the scope of cyclic N,N'-azomethine imines **4.32a-d** in Brønsted acid **4.28** catalyzed cycloadditions to **4.31a** (Table 4.6). Azomethine imines (**4.32a-d**) gave exo cycloadducts **4.33aa-4.33ad** in very good yields and good levels of enantioselectivity ranging from 80-93% ee (Table 4.6).

Table 4.6. Acylimidazole and azomethine imine scope in chiral phosphoramide catalyzed azomethine imine cycloaddition.
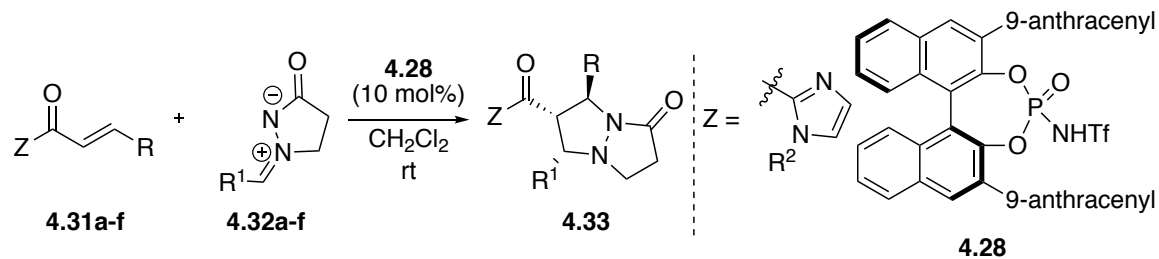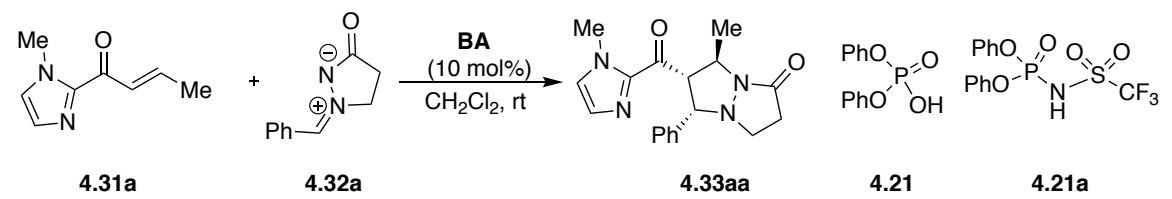
Entry	R	R^1	adduct	yield (%)	ee (%)
1	Me	Ph	**4.33aa**	93	92
2	Et	Ph	**4.33ba**	93	95
3	*i*-Pr	Ph	**4.33ca**	92	99
4	CH$_2$Bn	Ph	**4.33da**	89	93
5	CH$_2$OBn	Ph	**4.33ea**	81	88
6	2-furanyl	Ph	**4.33fa**	63	86
7	Ph	Ph	**4.33ga**	93	98
8	Me	4-Br-C$_6$H$_4$	**4.33ab**	93	86
9	Me	4-OMe-C$_6$H$_4$	**4.33ac**	93	93
10	Me	2-F-C$_6$H$_4$	**4.33ad**	93	80

4.5.1.4. NMR studies on acylimidazole acceptor phosphoric acid complex

An important interaction in catalytic reaction is how the catalyst (activator) activates the substrate. Since the azomethine imine cycloaddition is catalyzed by Brønsted acid we started our investigation by using diphenyl phosphate **4.21** and the corresponding N-triflyl phosphoramide **4.21a** as the catalyst (Table 4.7). Both **4.21** and **4.21a** catalyzed the [3+2] cycloaddition reaction giving high selectivity for the exo product.

Table 4.7. Achiral Brønsted acid catalyzed exo-selective [3+2] azomethine imine cycloaddition.

Entry	BA	Yield (%)	exo:endo
1	**4.21**	76	>40:1
2	**4.21a**	87	>40:1

4.5.1.5. DOSY studies on acylimidazole-phosphoric acid complex

We used the DOSY protocol that we developed to acylimidazole phosphoric acid complex. The DOSY spectrum of internal standards and acylimidazole-catalyst complex is shown in Figure 4.14.
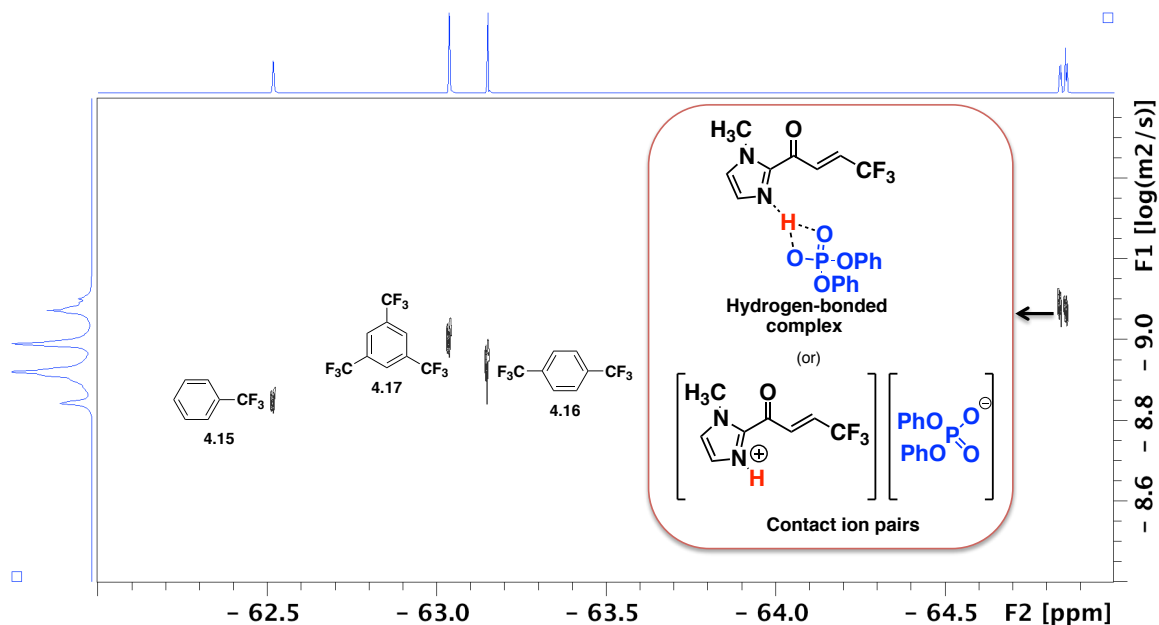
Figure 4.14. ^{19}F DOSY spectrum of a mixture of internal standards **4.15-4.17**, **4.21** and acylimidazole **4.22a** in C_6D_6.

The formula weight analysis is shown in figure 4.13. A very good correlation (with $r^2 =$ 0.99853) is obtained between the internal standards used and the phosphoric acid-acylimidazole complex formed (figure 4.15).
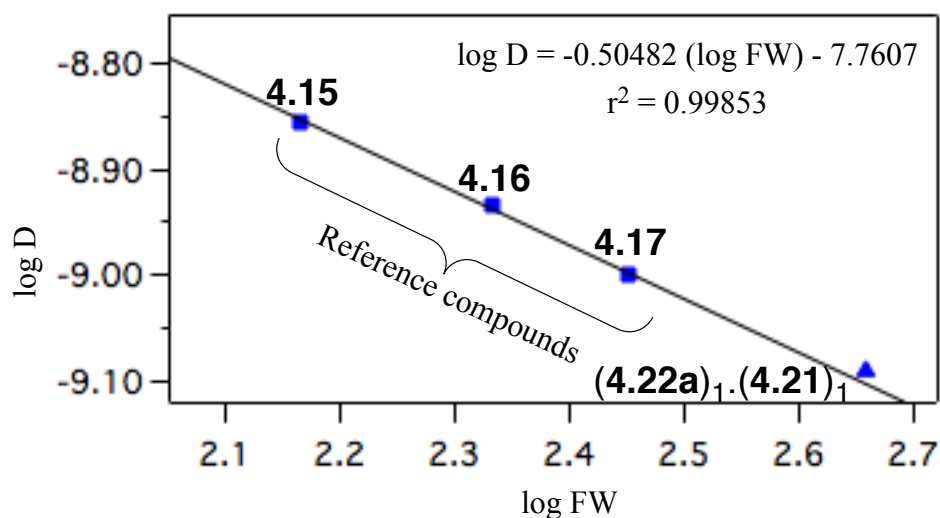
Figure 4.15. log D versus log FW analysis of ^{19}F DOSY of a mixture of **4.15-4.17**, **4.21** and acylimidazole **4.22a** in benzene-d_6.

The formula weight of the complex obtained from the DOSY experiment was found out to be 429 g mol^{-1} as opposed to 454 g mol^{-1} with only about 5.5% error (Table 4.8). Hence the composition of catalyst-substrate intermediate is 1:1 and no higher aggregates are formed.

Table 4.8. D-FW analysis of ^{19}F DOSY spectrum of compounds **4.15-4.17**, **4.21** and acylimidazole **4.22a** in C_6D_6.

Compound	FW (g mol^{-1})	$\delta(^{19}F)$ (ppm)	D (m^2 s^{-1})	FW$_{DOSY}$ (g mol^{-1})[a]	% error
4.15	146	-62.5	1.397 x 10^{-9}	147	0.7
4.16	214	-63.1	1.164 x 10^{-9}	211	1.4
4.17	282	-63.0	1.001 x 10^{-10}	284	0.7
(4.22a)$_m$.(4.21)$_n$	454	-64.9	8.139 x 10^{-10}	429	5.5

[a] log D = -0.50482 (log FW) -7.7607.

4.5.1.6. Observation of catalyst-substrate complex by mass spectrometry

The acylimidazole-substrate complex was also studied by mass spectrometry. When HRMS was recorded in the positive mode protonate form of acyl imidazole was obtained and in the negative mode the counter anion of phosphoric acid or the N-triflyl phosphoramide was obtained. But this doesn't confirm the formation of the complex as the acyl imidazole and the Brønsted acid should give these results individually. We also observed the [M-H$^+$] for the complex [(**4.31a**)$_1$.(**4.21a**)$_1$-H$^+$] (Figure 4.16). These mass specrometric studies corroborate the results obtained in our DOSY experiments.
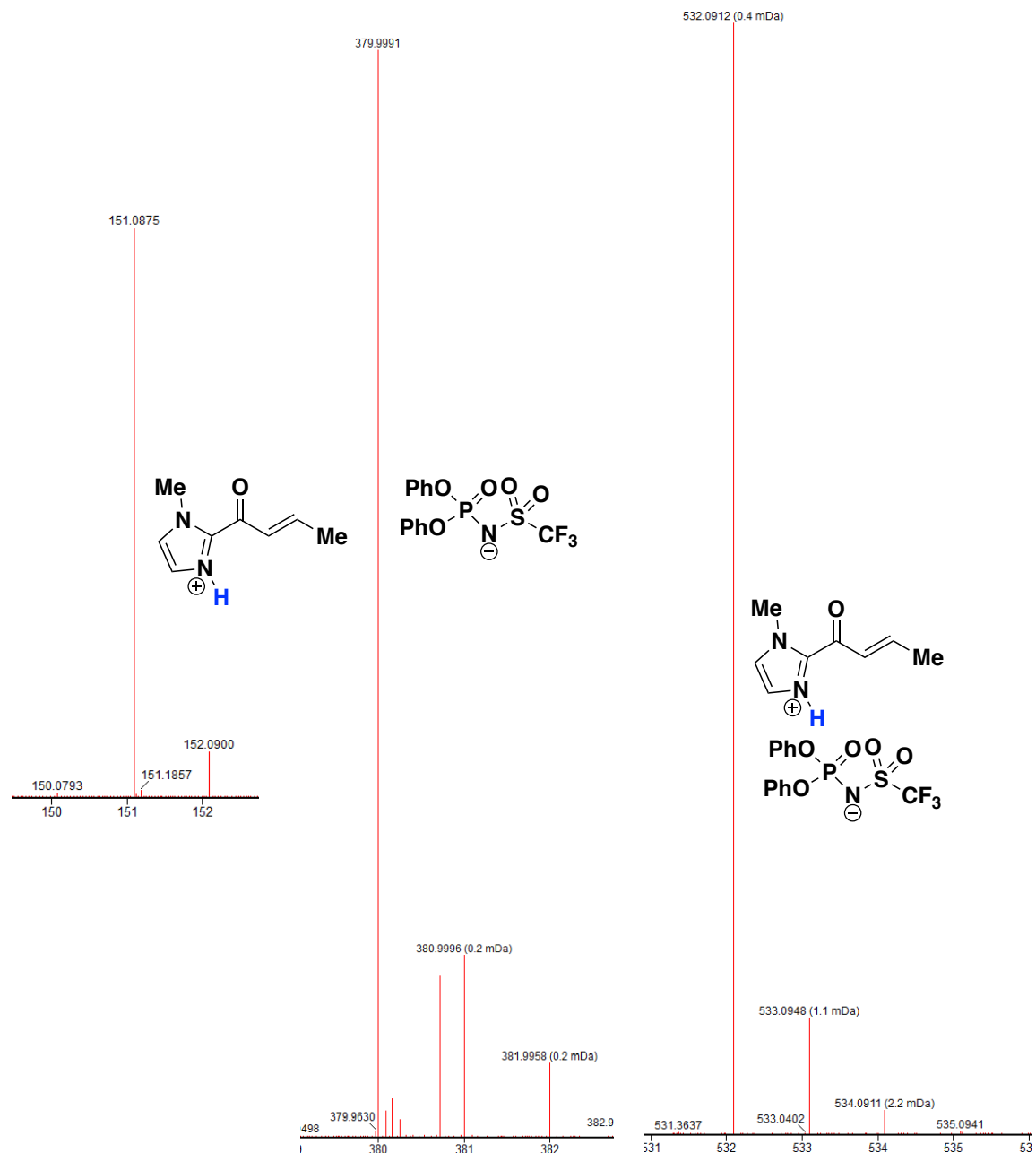
Figure 4.16. Mass spectrometric studies on acylimidazole (**4.31a**) and N-triflyl phosphoramide (**4.21a**) complex.

4.5.1.7. *Variable temperature NMR studies on acylimidazole-Brønsted acid complexes*

The DOSY NMR experiments or mass spectrometric studies never really tells us what the structure of the complex is other than the formula weight of the complex (which provides information about aggregation). Initial NMR studies (^{1}H NMR) on the complex showed NMR

signal >10 ppm. This might be due to protonation (of N or O) or hydrogen bonding (to N or O) (Scheme 4.7)

ion-pairs
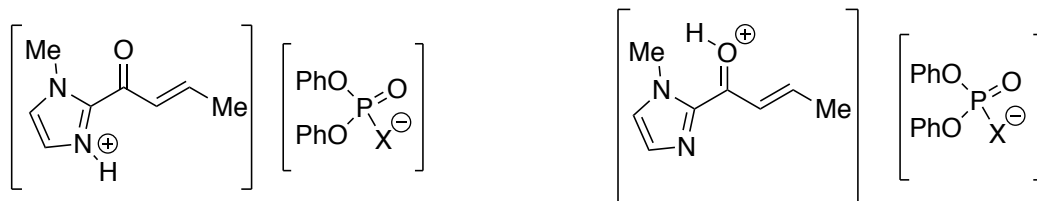
H-bonded complex
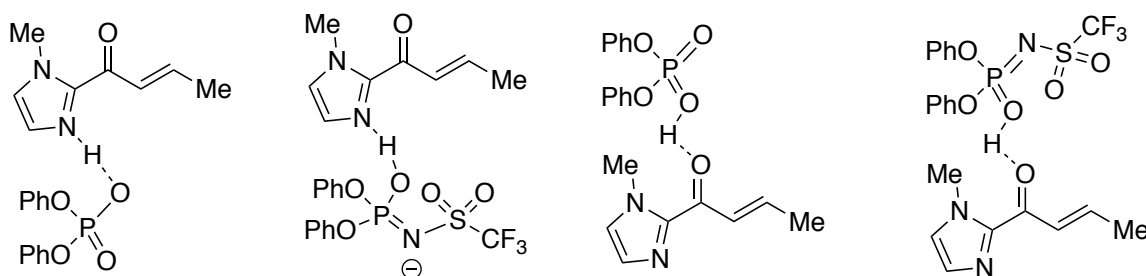
Scheme 4.7. Possible modes of activation of acylimidazoles by Brønsted acids.

Hence we synthesized doubly labeled acylimidazole **4.35** from ^{15}N labeled ammonium chloride according to Scheme 4.8. Ammonium chloride (^{15}N-labeled) on reaction with glyoxal and formaldehyde gave doubly labeled imidazole. The imidazole on reaction with *n*-BuLi/CH$_3$I gave doubly labeled N-methylimidazole. The doubly ^{15}N labeled N-methylimidazole on lithiation and reaction with Weinrebamide **4.38** gave acylimidazole **4.35** (Scheme 4.8).
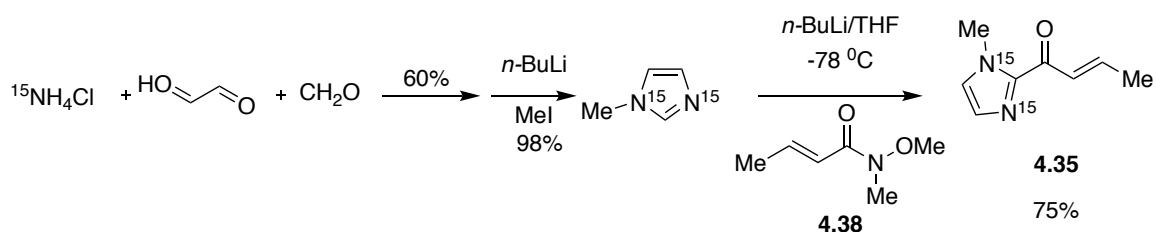
Scheme 4.8. Synthesis of doubly ^{15}N labeled acylimidazole.

Substrate **4.35** was used in NMR experiments. Since ^{15}N is nuclei with I = 1/2 similar to ^{1}H, if there is interaction between acid and **4.35** a doublet should be observed. The $^1J_{N-H}$ coupling constant should indicate the type of complex that is formed. The $^1J_{N-H} = 100$ Hz for complete

protonation. When the Brønsted acid used was **4.21a** the ^{1}H NMR showed no peaks corresponding to the protonation event but at -20 $^\circ$C a doublet with coupling constant of 96 Hz was observed. At -50 $^\circ$C doublets with good S/N ration was obtained (Figure 4.17).
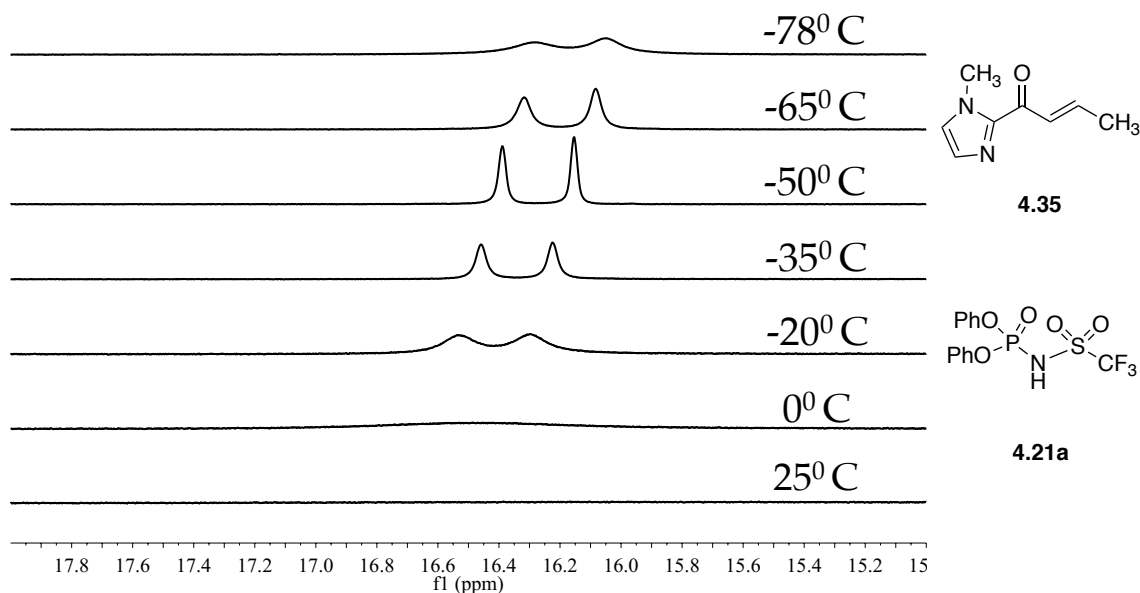
Figure 4.17. Acylimidazole-phosphoramide complex showing doublet (^{1}J$_{NH}$ = 96 Hz) in temperature range -20 to -78 $^\circ$C.

We also monitored the formation of **4.35-4.21a** complex by ^{15}N NMR. Acylimidazole **4.35** gave two signals ~ 168 ppm and ~284 ppm. Up on addition of **4.21a** to the acyl imidazole solution there is a shift in the position of the signal. The N-3 ^{15}N signal was shifted to ~185 ppm and the N-1 signal was moved to 178 ppm. This considerable shift on the ^{15}N NMR indicates protonation of N-3 of imidazole ring (Figure 4.18).

123
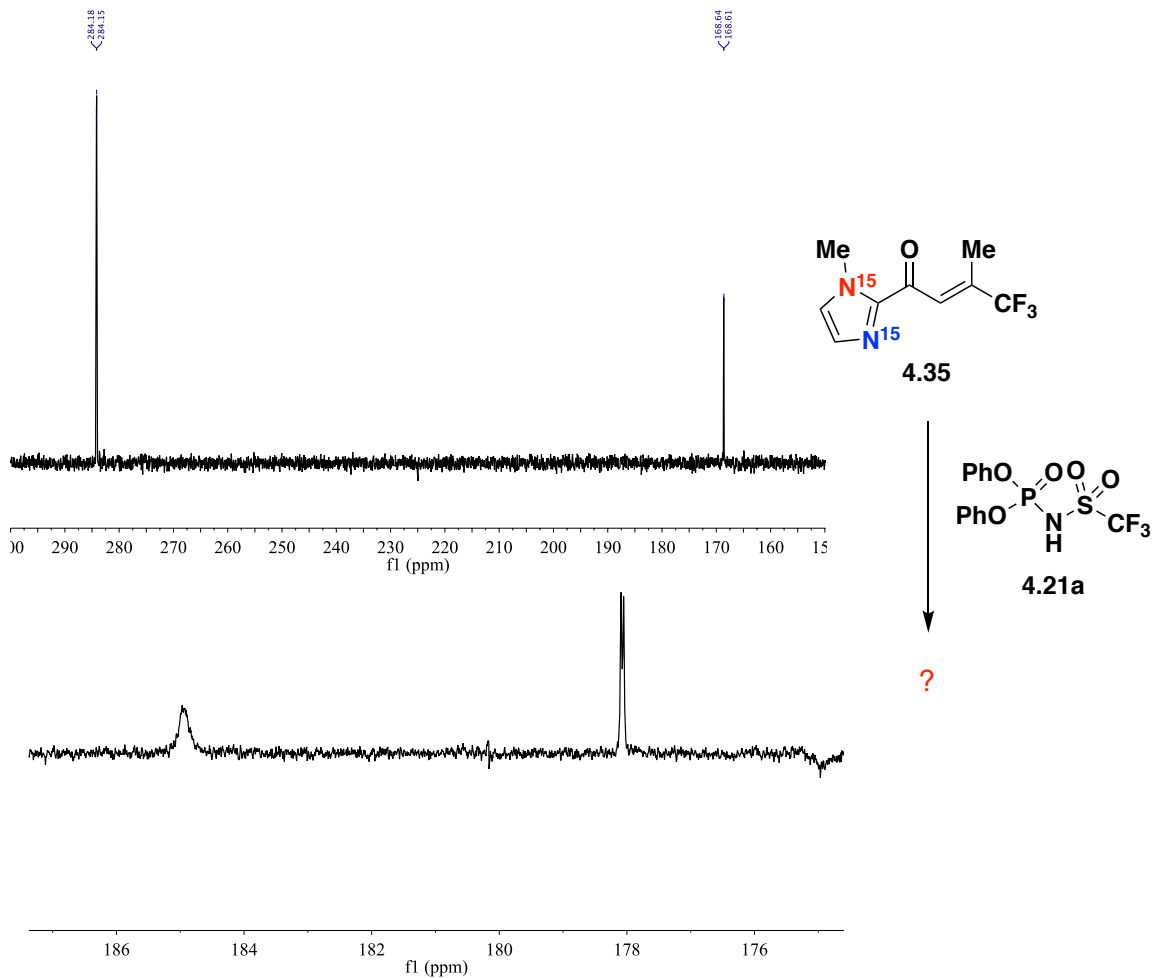
Figure 4.18. Monitoring the event of complexation by ^{15}N NMR.

We also confirmed the protonation of acylimidazole by ^{15}N-^{1}H HSQC (Figure 4.19). We observed a cross-peak between the doublet on the ^{1}H NMR and the ^{15}N NMR signal at 185 ppm.
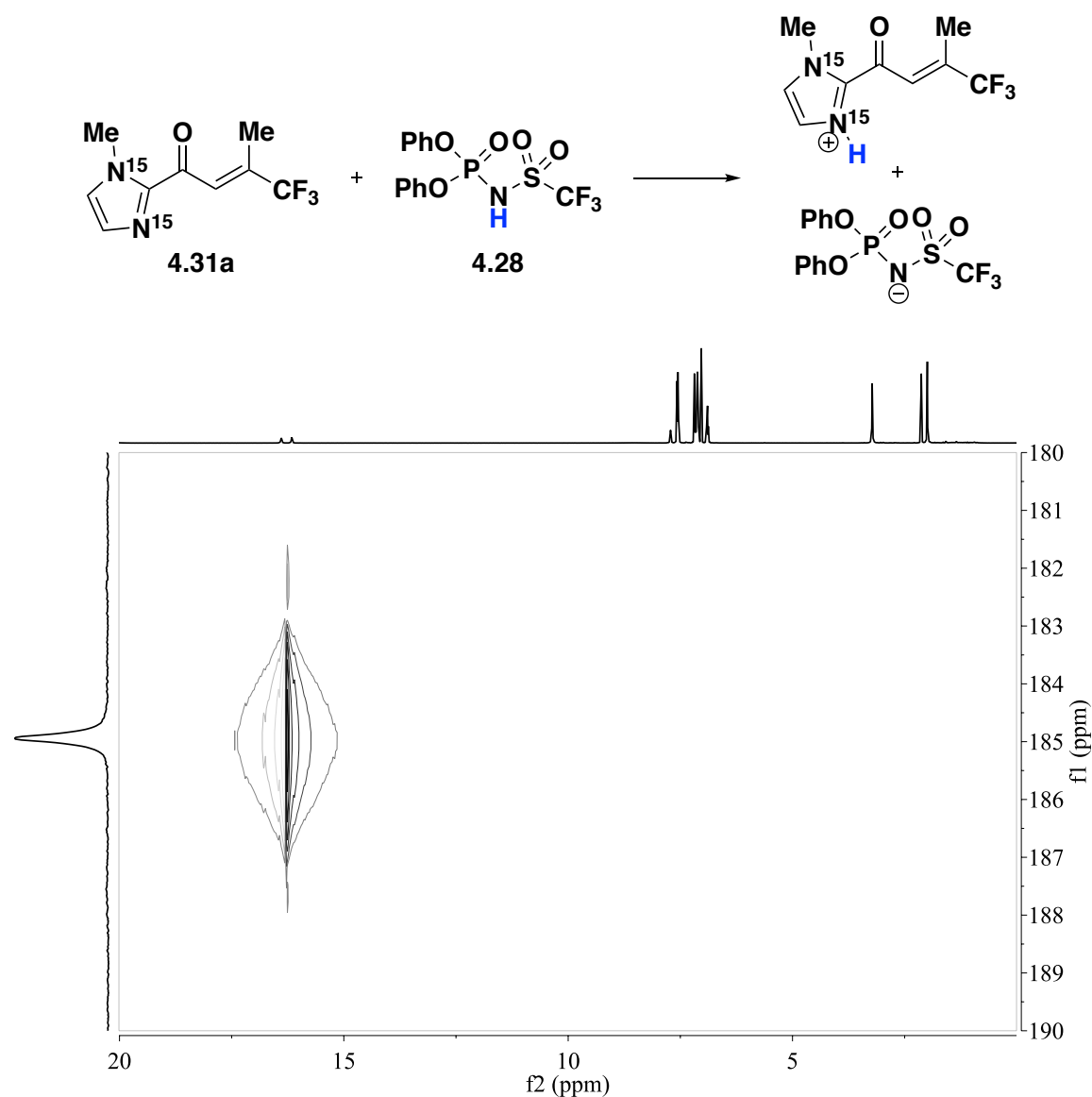
Figure 4.19. ^{15}N-^{1}H HSQC showing ^{1}J$_{NH}$ bond between acylimidazole phosphoramide.

After establishing the complexation event between the acylimidazoles **4.35** and achiral phosphoramide **4.21a**, we turned our attention to the complexation between **4.35** and chiral phosphoric acid **4.28** used in the exo-selective enantioselective [3+2] cycloaddition between azomethine imines and acylimidazoles (vide supra). Variable temperature ^{15}N NMR, ^{1}H NMR and ^{15}N-^{1}H HSQC indicate that the acylimidazole chiral phosphoramide **4.28** exist as an ion pair in solution.

4.5.1.8. Crystal structure of acylimidazole 4.31f chiral *N*-triflyl phosphoramide 4.28 complex and stereochemical model explaining exo-selectivity in the Brønsted acid catalyzed [3+2] azomethine imine cycloaddition reaction

Although solid-state structures of chiral phosphoric acids are known, the corresponding crystal structures of substrate–chiral phosphoric acid/chiral phosphoramide are relatively scarce.[44, 60] The X-ray crystal structure of acylimidazole-substrate complex **4.28.4.31f** is shown in Figure 4.20. This particular piece of evidence shows that the acylimidazoles are activated by the protonation of N-3 (pyridine-like nitrogen) of the acylimidazole during Brønsted acid catalyzed reactions. Furthermore, the acylimidazole **4.31f** adopts a s-*cis, syn* (*syn* relation between carbonyl and *N*-methyl group of imidazole) conformation. During the *endo* approach (Figure 4.20(C)), the dipole experiences unfavorable steric interactions of the R group and *N*-methyl group of the acylimidazole. Such interactions are absent during *exo* approach of the dipole (Figure 4.20(B)) and hence Brønsted acid catalyzed azomethine imine cycloadditions are *exo* selective in nature.
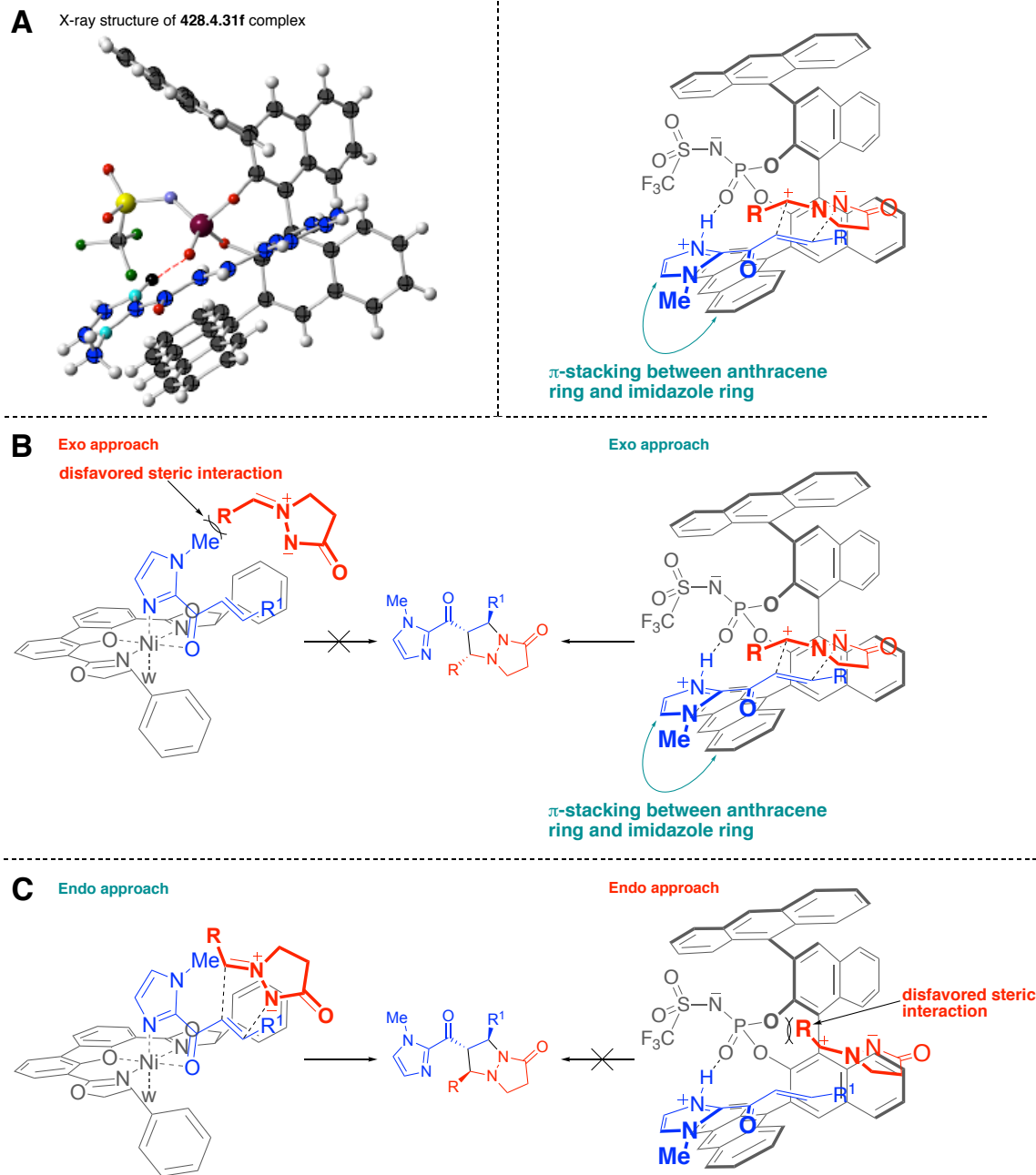
Figure 4.20. (A) X-ray crystal structure of acylimidazole (1g)–Brønsted acid (4d) complex showing s-*cis*, *syn* conformation adopted by acylimidazole. (B) Stereochemical model showing *exo* approach of the dipole in azomethine imine cycloadditions. (C) Stereochemical model showing *endo* approach of the dipole in azomethine imine cycloadditions.

4.6. Conclusions

We have developed a ^{19}F DOSY internal reference system for the successful prediction of formula weights in solution. The sharp, well-resolved signals and high sensitivity of ^{19}F NMR

facilitates DOSY usage. Plots of log D versus log FW show excellent linearity, and the agreement between DOSY-calculated and actual formula weights appears excellent. Fluorine labelling can be incorporated in the substrate, the acid, or both. In benzene-d_6 solvent, substrate **4.22a** forms 1:1 complexes with trifluoroacetic acid **4.18** and phosphoric acid **4.21**. In contrast, 2:2 complexes are formed with the strongly acidic bis(trifluoromethane)sulfonimide **4.20** and acylimidazoles **4.22a** and **4.22b**. Complexes show no indication of solvent-separated ion pairs. Continuing studies will apply ^{19}F DOSY in combination with other spectroscopic techniques to help characterize the solution structures of several asymmetric catalytic systems. Using a combination of ^{1}H NMR, ^{1}H NMR, ^{15}N-^{1}H-HSQC, DOSY NMR experiments and HRMS studies we were able to provide a stereochemical model to the exo-selective and enantioselective [3+2] azomethine imine cycloaddition reaction.

4.7. Experimental section

All reactions were carried out under inert atmosphere unless otherwise mentioned. Flash chromatography was performed using EM Science silica gel 60 (230-400 mesh). 1H-NMR was recorded on a Bruker Ascend$^{\text{TM}}$ 400 (400 MHz for ^{1}H) spectrometer. Chemical shifts δ are reported in parts per million (ppm) downfield from TMS, using residual CDCl$_3$ (7.26 ppm) as an internal standard. ^{13}C-NMR was recorded on Bruker Ascend$^{\text{TM}}$ 400 (100 MHz for ^{13}C) spectrometer, using broadband proton decoupling. Chemical shifts are reported in parts per million (ppm) downfield from TMS, using the middle resonance of CDCl$_3$ (77.00) as an internal standard. ^{19}F-NMR was recorded on Bruker Avance 400 (376 MHz for ^{19}F) using trifluoroacetic acid as an external standard. High Resolution Mass Spectra (HRMS) (ESI+) were recorded using Waters Synapt G2-SI.

4.7.1. Materials

The fluorinated hydrocarbons: benzotrifluoride **4.15**, 1,4-bis(trifluoromethyl)benzene **4.16** and 1,3,5-tris(trifluoromethyl)benzene **4.17** and the acids: trifluoroacetic acid **4.18**, trifluoromethanesulfonic acid **4.19** and bis(trifluoromethane)sulfonimide **4.20** were purchased from Sigma-Aldrich and used with out further purification. The amide (2E)-4,4,4-Trifluoro-N-methoxy-N-methyl-2-butenamide **4.23** was purchased from Sigma-Aldrich. The deuterated solvents were purchased from Cambridge Isotopes Laboratories. Tetrahydrofuran (THF) was freshly distilled from sodium benzophenone ketyl under nitrogen before the reaction.

4.7.2. Substrate synthesis

Acylimidazole substrate (**4.22b**): (*E*)-1-(1-Methyl-1*H*-imidazole-2-yl)-but-2-en-1-one) was synthesized using procedure reported in the literature.

Substrate **4.22a**: ((*E*)-1-(1-Methyl-1*H*-imidazole-2-yl)-4,4,4-trifluoro-but-2-en-1-one) was synthesized as follows: 1.2 mL of *n*-butyllithium in hexanes (2.5 M, 3.0 mmol) was added to a solution of N-methylimidazole (0.25 g, 3.0 mmol) in dry THF (10 mL) at -78 ^{0}C. The resulting solution was stirred at this temperature of 15 minutes followed by the addition of solution of amide **4.23** (0.5 g, 3.0 mmol) in THF. The mixture was gradually warmed up to room temperature over a period of 2 hours and then quenched using acetic acid. The excess acid was neutralized using saturated sodium bicarbonate solution. The mixture was extracted with ethyl acetate (2 x 100 mL) and the combined organic layers were washed with brine and dried over anhydrous sodium sulfate. The crude product thus obtained after the removal of solvent *in vacuo* was subjected to column chromatography using EtOAC/hexanes to yield (0.51 g, 79% yield) **4.22a**.
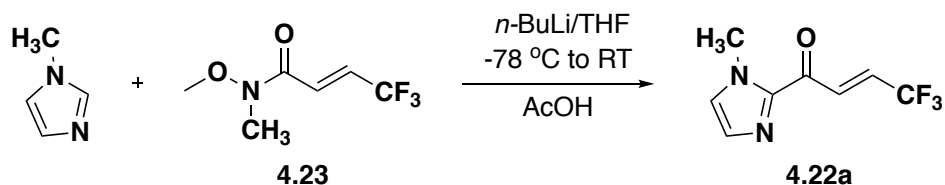
Scheme 4.9. Synthesis of β-trifluoromethyl-acylimidazole **4.22a**.

Analytical data of **4.22a**: ^{1}H NMR (400 MHz, CDCl$_3$) δ 7.99 (dd, J = 15.9, 1.9 Hz, 1H), 7.20 (s, 1H), 7.12 (s, 1H), 6.81 (dq, J = 15.7, 6.8 Hz, 1H), 4.03 (s, 3H); ^{13}C NMR (101 MHz, CDCl$_3$) δ 177.7, 142.9, 132.3 (q, J = 5.8 Hz), 130.3, 128.7 (q, J = 35 Hz), 128.4, 122.7 (q, J = 270.0 Hz), 36.1; ^{19}F NMR (376 MHz, CDCl$_3$) δ -64.96 (dd, J = 6.8, 2.0 Hz); HRMS (ESI): Exact mass calculated of C$_8$F$_3$H$_7$N$_2$O [M-H]$^+$: 205.0589. Found: 205.0638.

4.7.3. Diffusion NMR experiments

NMR samples were prepared in Norell NMR tubes (5mm O.D and 7" length) sealed with septum. The tubes were dried and filled with argon before use. The DOSY experiments were performed on Bruker Ascend^{TM} 400 spectrometer equipped with Multinuclear Broadband Fluorine Observe (BBFO^{PLUS}) probe with z-axis gradient coil. The standard Bruker pulse sequence (ledbpgp2s) incorporating longitudinal eddy current delay was used for ^{19}F DOSY experiments. For ^{19}F diffusion measurements, the delay δ was set to 700-1200 μs and Δ was set to 80-100 ms. The individual slices of pseudo-2D diffusion spectra were phased. The diffusion coefficients were obtained from the signal attenuation curves of individual DOSY peaks. The formula weights were obtained by the linear regression analysis of log D vs log FW where D is the experimentally calculated diffusion coefficients and FW is the formula weight of the compound.

4.8. Supporting information for DOSY experiments
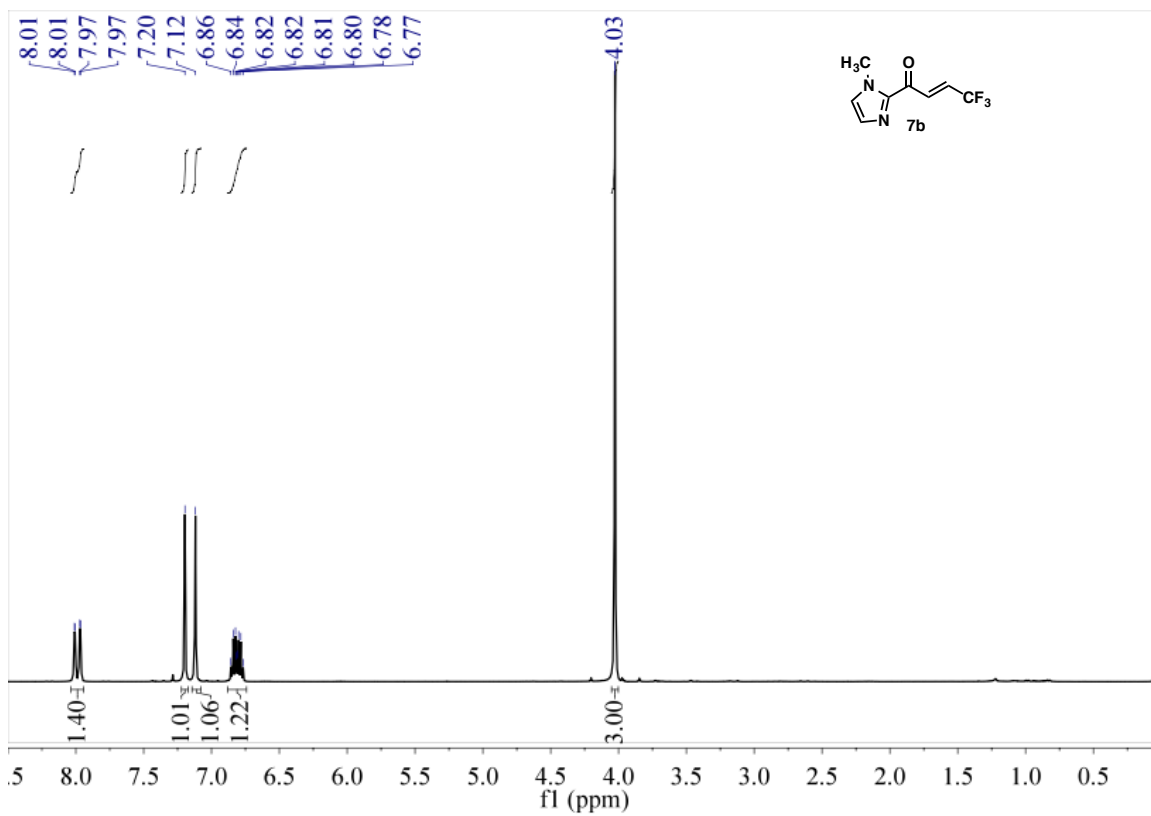
Figure 4.21. ^{1}H NMR spectrum of **4.22a** in CDCl$_3$.
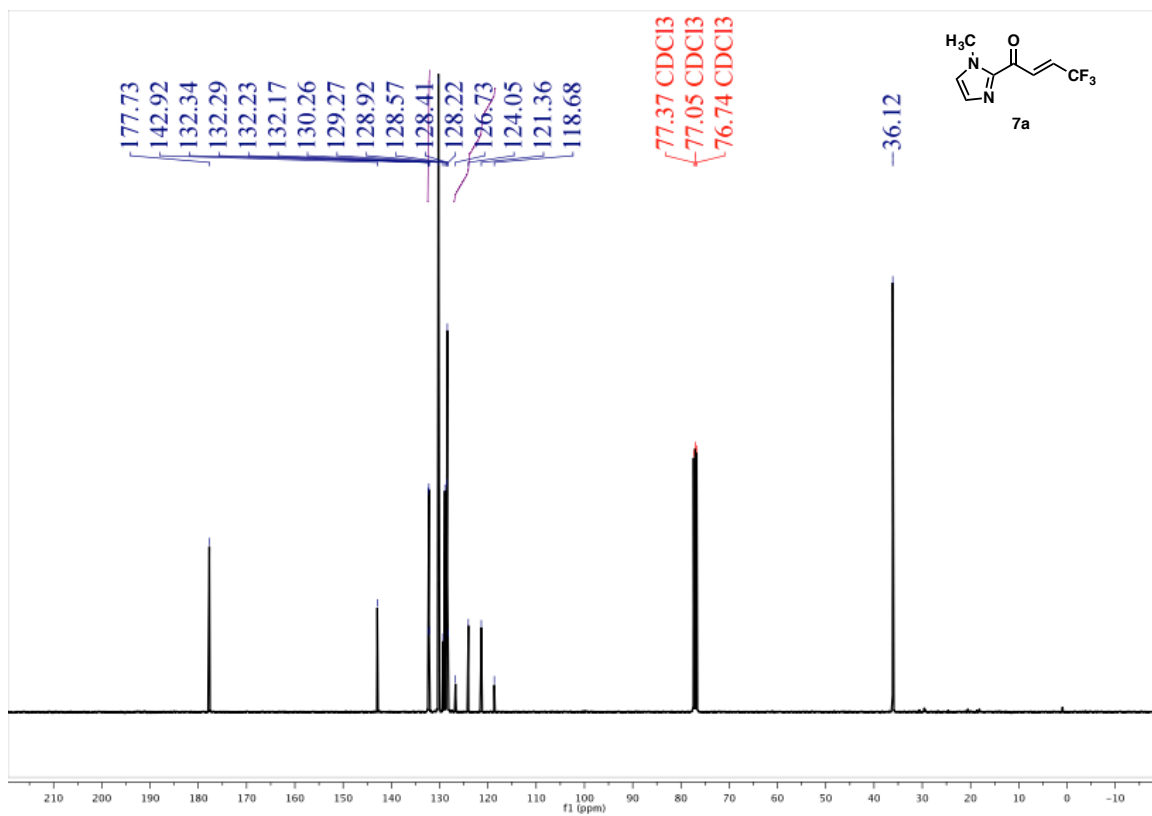
Figure 4.22. ^{13}C NMR spectrum of **4.22a** in CDCl₃.
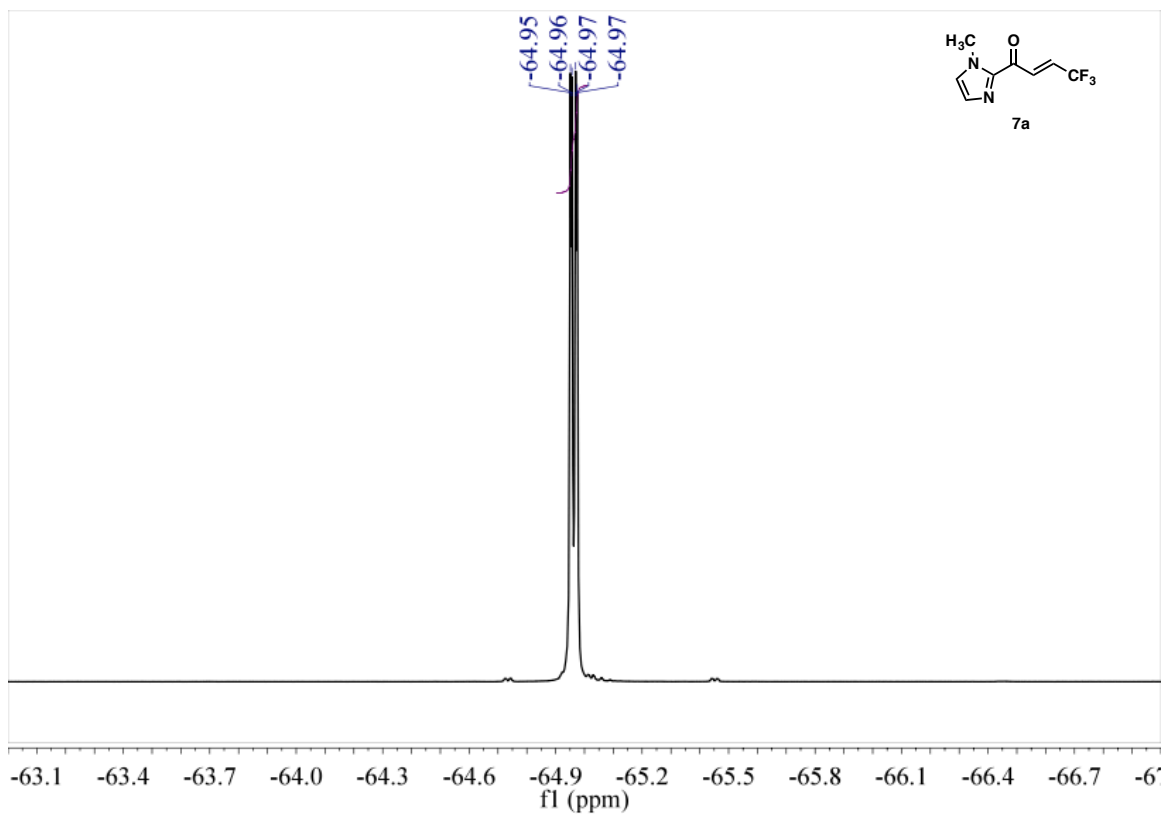
Figure 4.23. ^{19}F NMR spectrum of **4.22a** in CDCl$_3$.
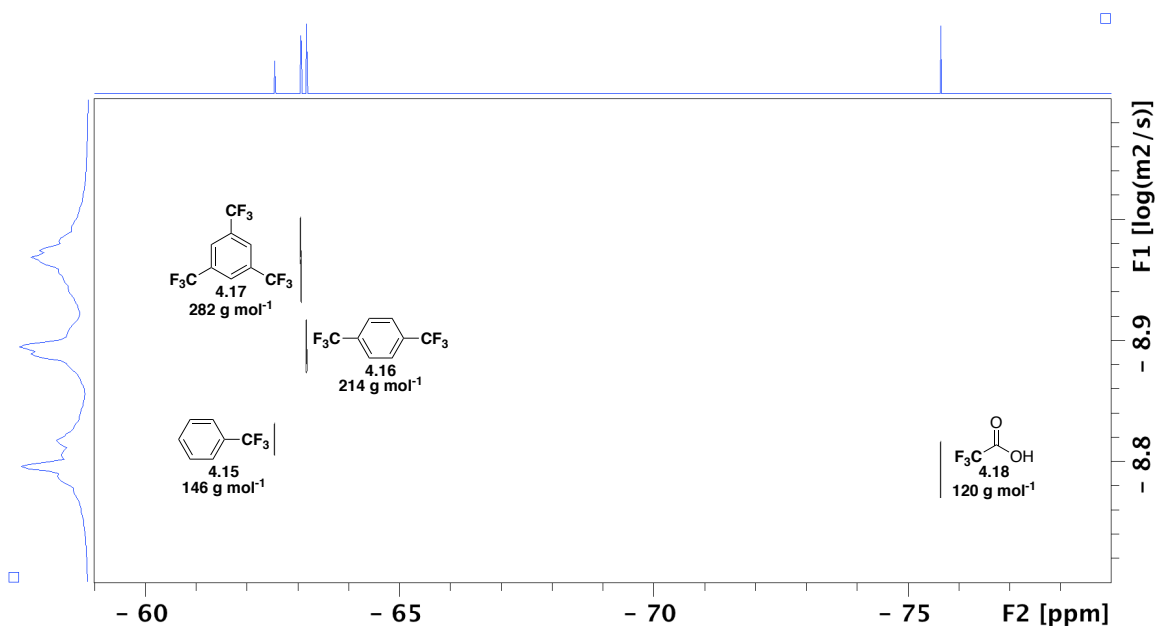
Figure 4.24. ^{19}F DOSY spectrum of a mixture of internal standards **4.15-4.17** and trifluoroacetic acid **4.18** in C$_6$D$_6$.

Figure 4.25. Signal attenuation curve of internal standard **4.15** in a mixture of compounds **4.15-4.18** in C_6D_6.

Figure 4.26. Signal attenuation curve of internal standard **4.16** in a mixture of compounds **4.15-4.18** in C_6D_6.

Figure 4.27. Signal attenuation curve of internal standard **4.17** in a mixture of compounds **4.15-4.18** in C$_6$D$_6$.

Figure 4.28. Signal attenuation curve of trifluoroacetic acid **4.18** in a mixture of compounds **4.15-4.18** in C$_6$D$_6$.
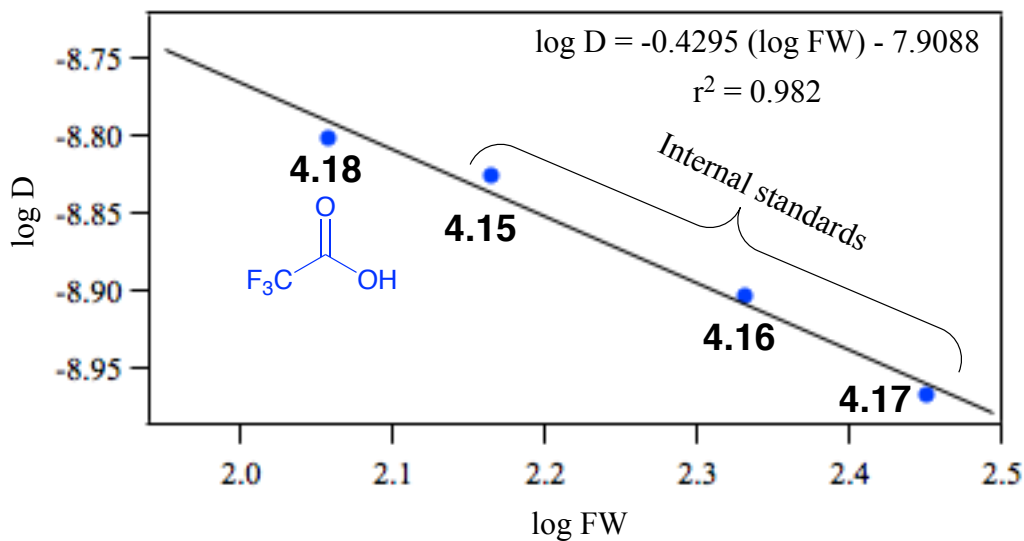
Figure 4.29. log D versus log FW analysis of ^{19}F DOSY of a mixture of **4.15-4.18** in benzene-d_6.

Table 4.9. D-FW analysis of ^{19}F DOSY spectrum of compounds **4.15-4.18** in C_6D_6.

Compound	FW (g mol^{-1})	$\delta(^{19}F)$ (ppm)	D (m^2 s^{-1})	FW$_{DOSY}$ (g mol^{-1})^a	% error
4.15	146	-62.5	1.491 x 10^{-9}	137	6.2
4.16	214	-63.1	1.246 x 10^{-9}	201	6.1
4.17	282	-63.0	1.076 x 10^{-9}	295	4.6
4.18	114	-75.7	1.575 x 10^{-9}	120	5.1

^{a} log D = -0.4295 (log FW) – 7.9088.

Figure 4.30. ^{19}F DOSY spectrum of compounds **4.15-4.17** and **4.19** in C_6D_6.

Figure 4.31. Signal attenuation curve of internal standard **4.15** in a mixture of compounds **4.15-4.18** and **4.19** in C_6D_6.

Figure 4.32. Signal attenuation curve of internal standard **4.16** in a mixture of compounds **4.15-4.18** and **4.19** in C_6D_6.
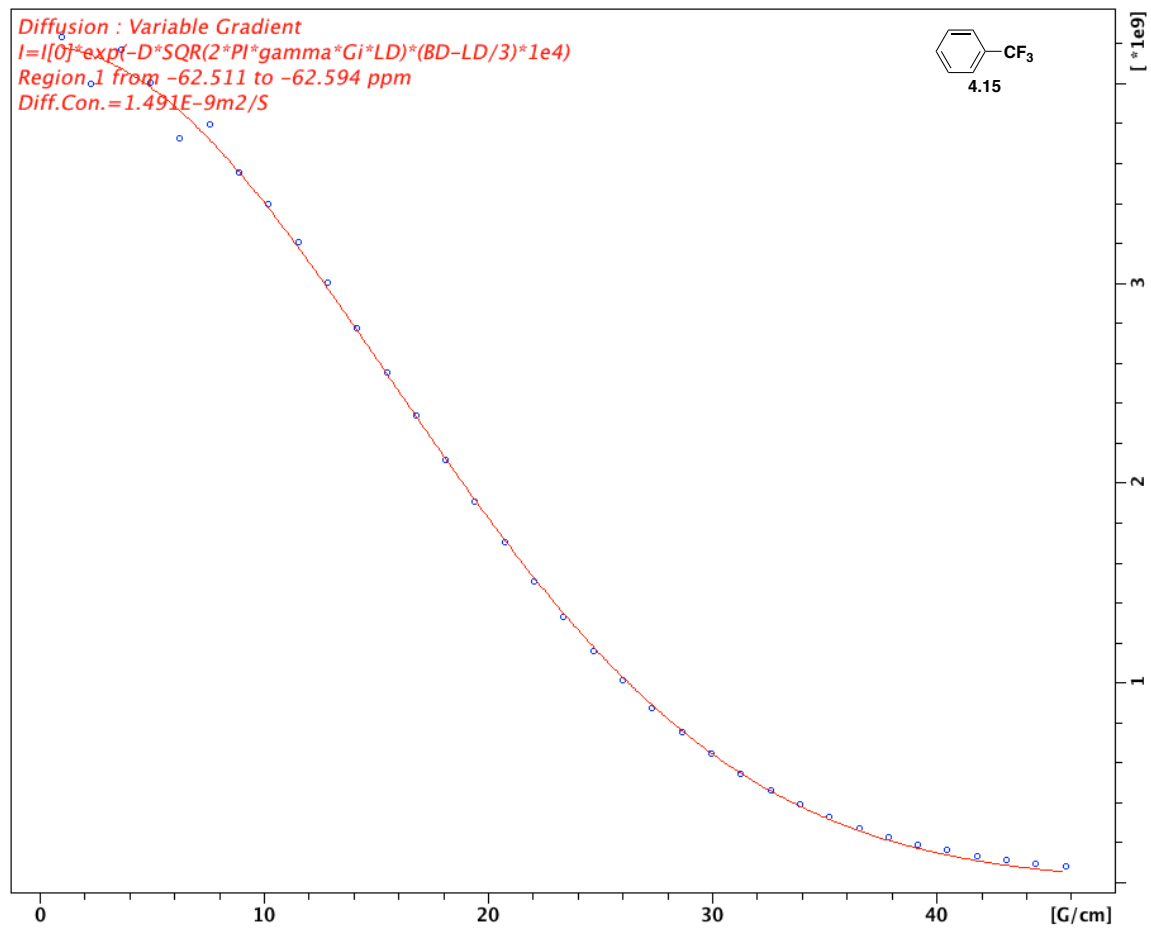
Figure 4.33. Signal attenuation curve of internal standard **4.17** in a mixture of compounds **4.15-4.18** and **4.19** in C_6D_6.

Figure 4.34. Signal attenuation curve of internal standard **4.19** in a mixture of compounds **4.15-4.18** and **4.19** in C_6D_6.
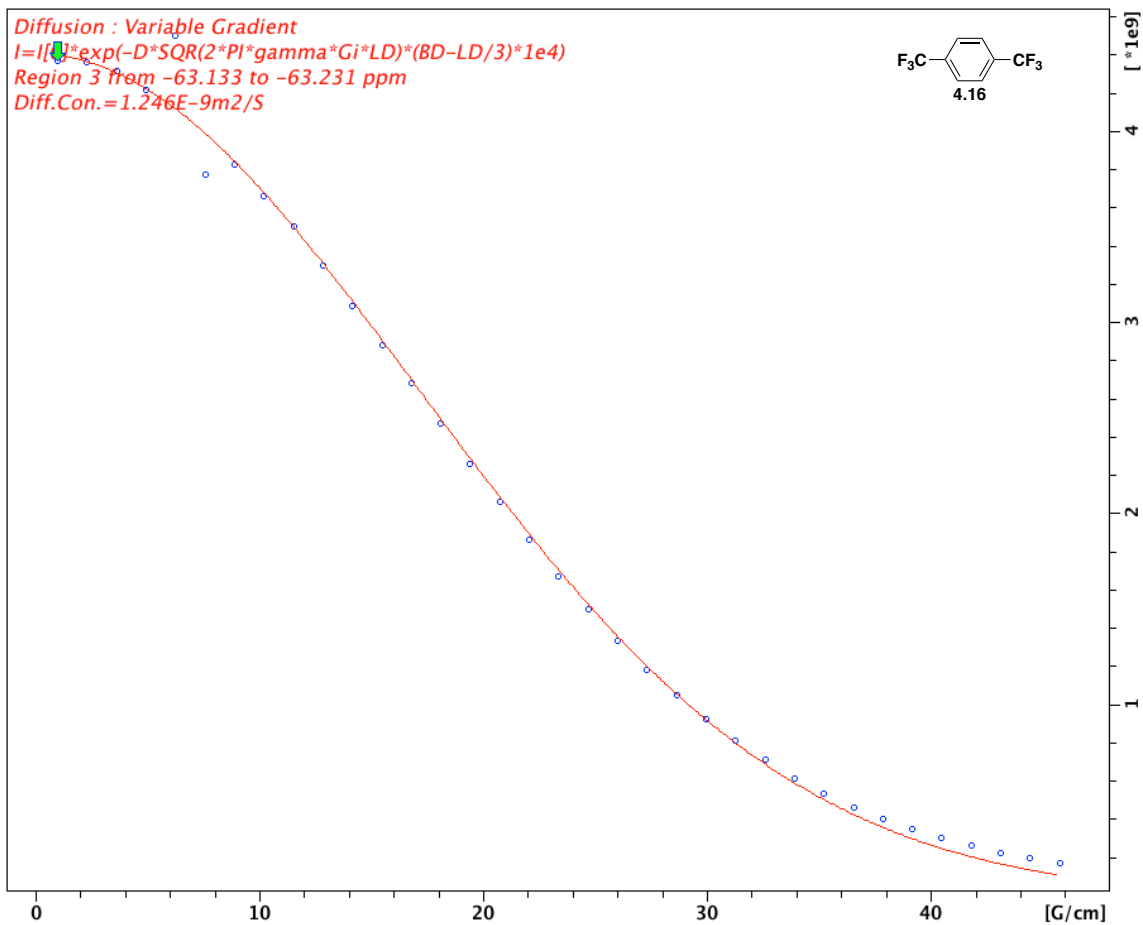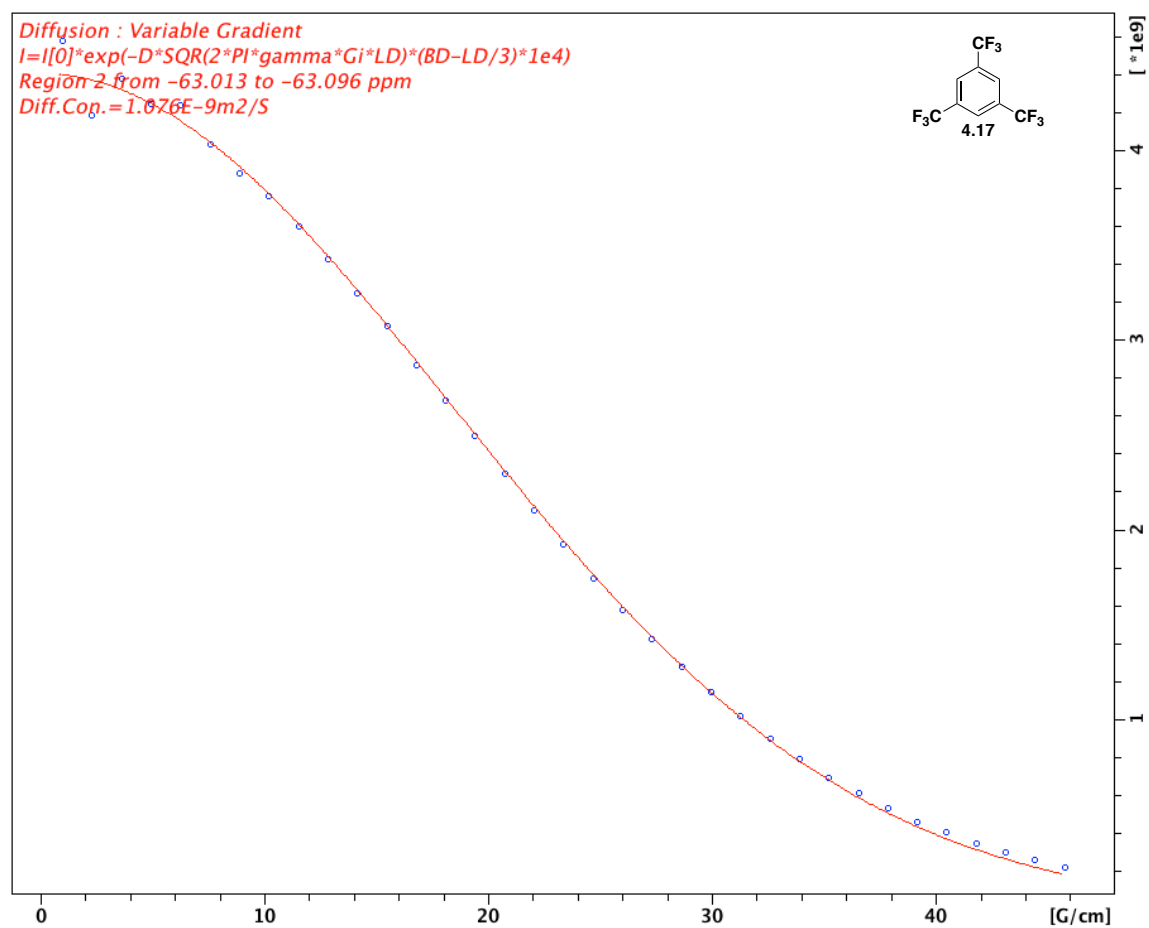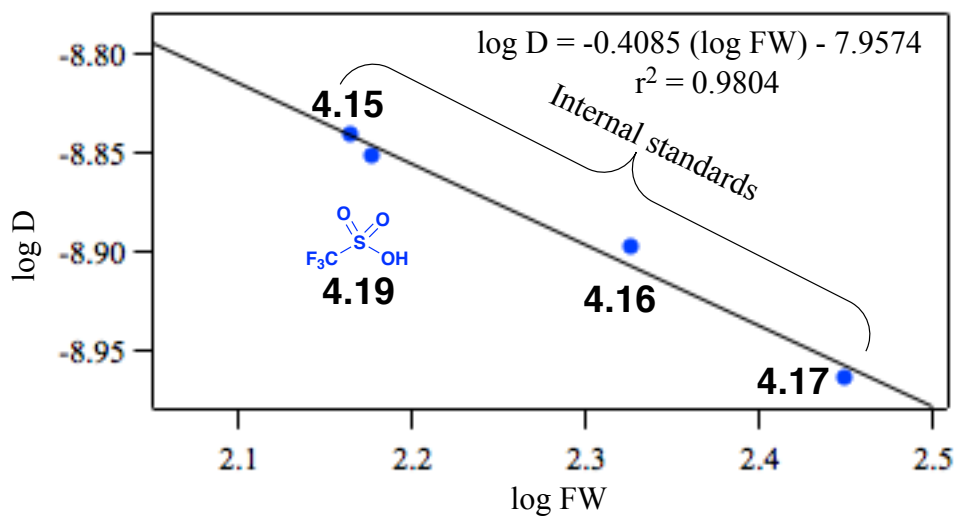
Figure 4.35. log D versus log FW analysis of ^{19}F DOSY of a mixture of **4.15-4.17** and **4.19** in benzene-d_6.

Table 4.10. D-FW analysis of ^{19}F DOSY spectrum of compounds **4.15-4.17** and **4.19** in C_6D_6

Compound	FW (g mol^{-1})	$\delta(^{19}F)$ (ppm)	D (m^2 s^{-1})	FW$_{DOSY}$ (g mol^{-1})[a]	% error
4.15	146	-62.5	1.441 x 10^{-9}	149	2.1
4.16	214	-63.1	1.265 x 10^{-9}	201	6.1
4.17	282	-63.0	1.087 x 10^{-9}	291	3.2
4.19	150	-76.7	1.405 x 10^{-9}	155	3.3

[a] log D = -0.4085 (log FW) – 7.9574.

145
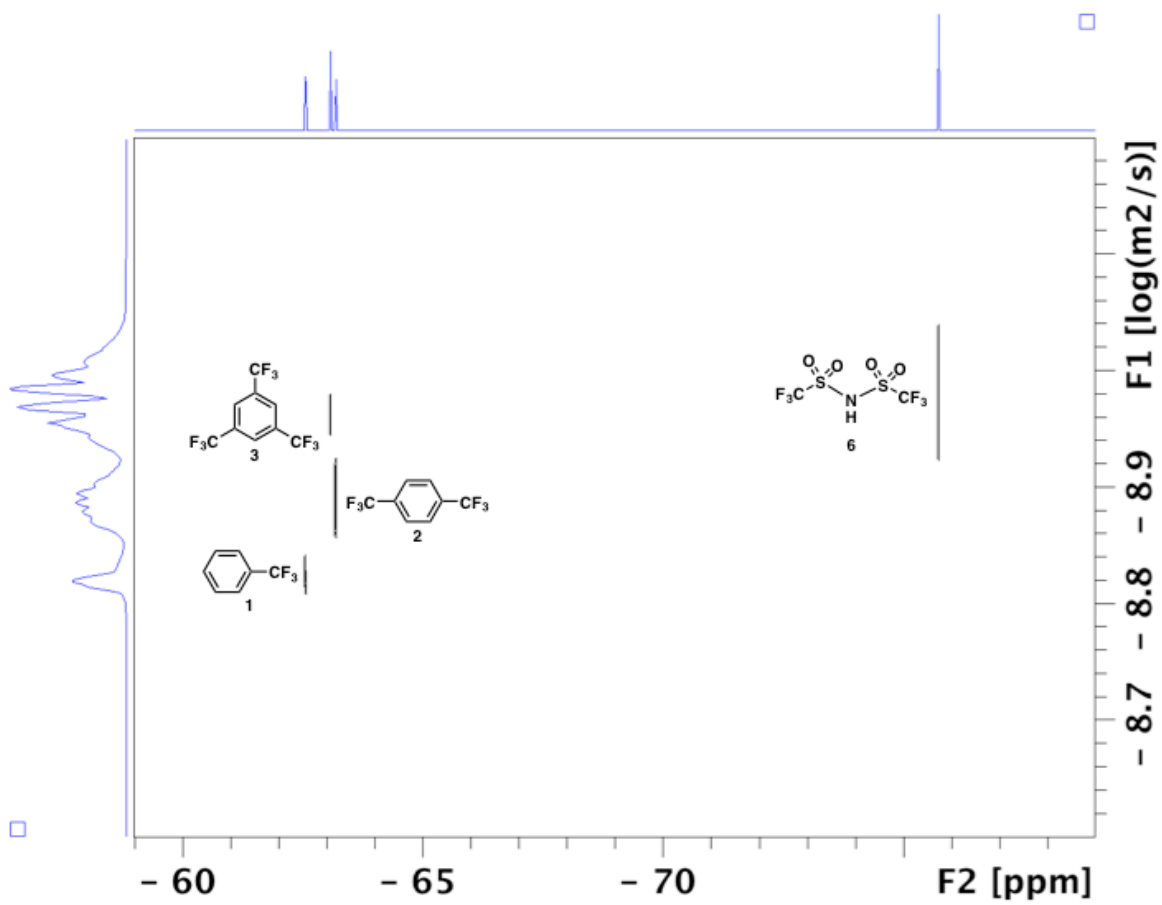
Figure 4.36. ^{19}F DOSY spectrum of compounds **4.15-4.17** and **4.20** in C$_6$D$_6$.

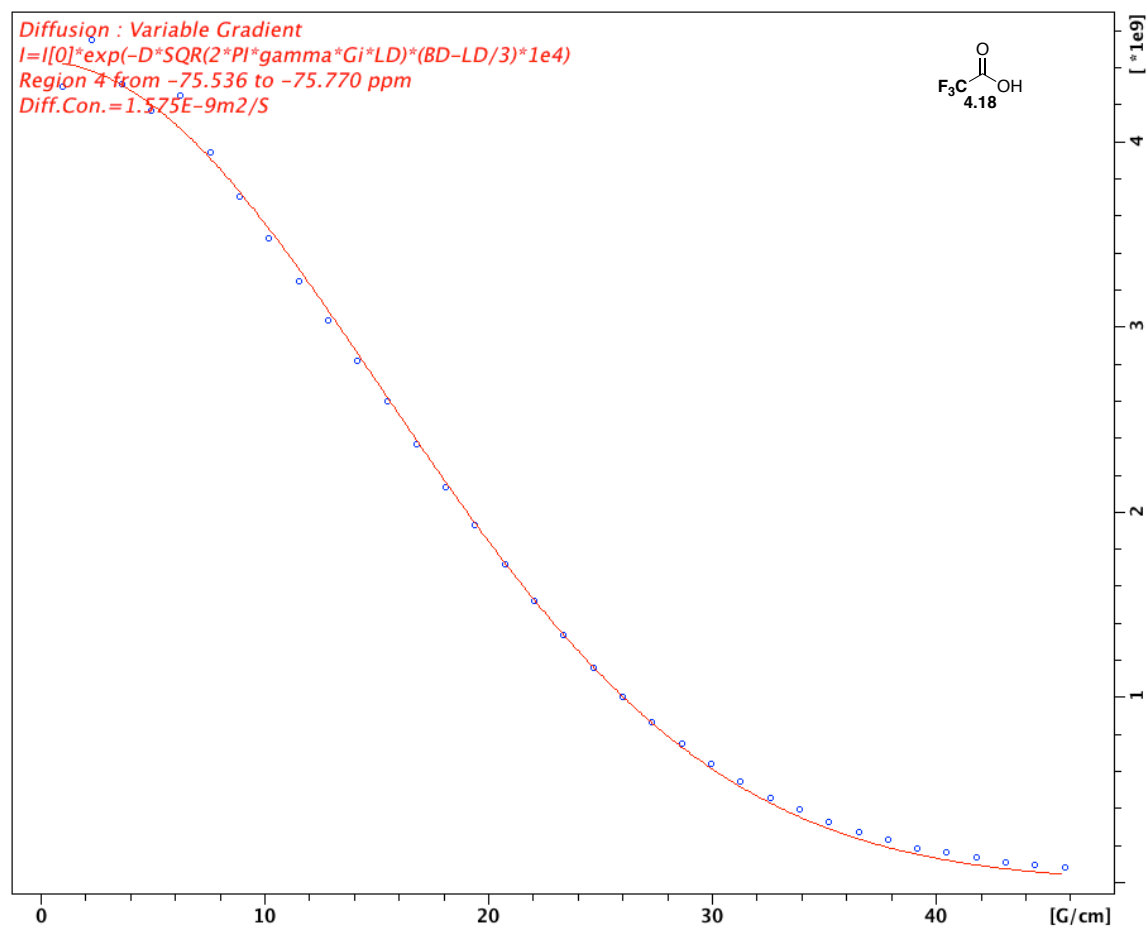Figure 4.37. Signal attenuation curve of internal standard **4.15** in a mixture of compounds **4.15-4.17** and **4.20** in C_6D_6.

Figure 4.38. Signal attenuation curve of internal standard **4.16** in a mixture of compounds **4.15-4.17** and **4.20** in C$_6$D$_6$.

Figure 4.39. Signal attenuation curve of internal standard **4.17** in a mixture of compounds **4.15**-**4.17** and **4.20** in C_6D_6.

Figure 4.40. Signal attenuation curve of bis(trifluoromethane)sulfonimide **4.20** in a mixture of compounds **4.15-4.17** and **4.20** in C_6D_6.
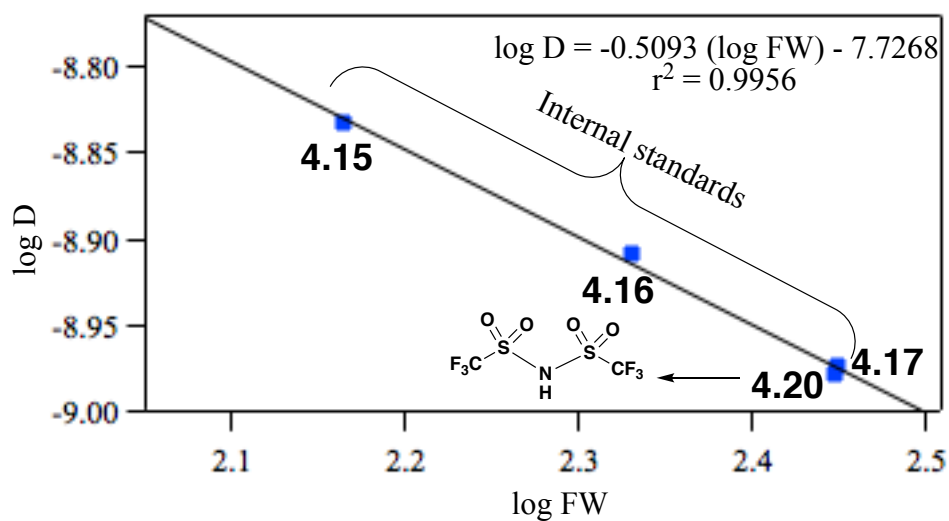
Figure 4.41. log D versus log FW analysis of ^{19}F DOSY of a mixture of **4.15-4.17** and **4.20** in benzene-d_6.

Table 4.11. D-FW analysis of ^{19}F DOSY spectrum of compounds **4.15-4.17** and **4.20** in C_6D_6.

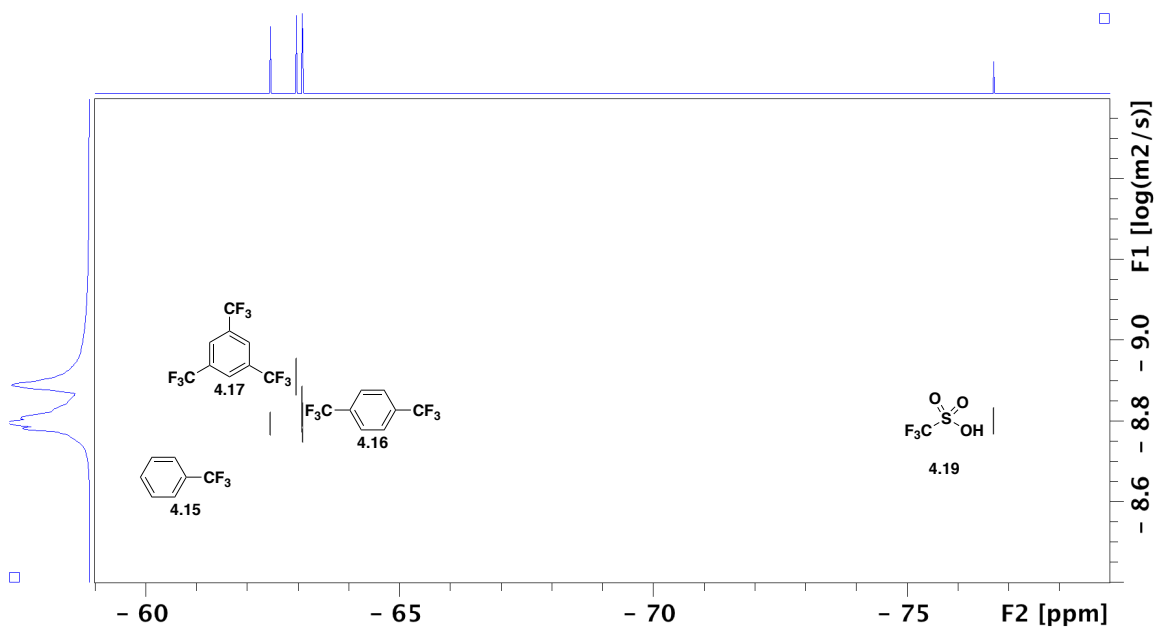| Compound	FW (g mol^{-1})	δ(^{19}F) (ppm)	D (m^2 s^{-1})	FW$_{DOSY}$ (g mol^{-1})[a]	% error
4.15	146	-62.5	1.473 x 10^{-9}	148	1.4
4.16	214	-63.1	1.237 x 10^{-9}	208	2.8
4.17	282	-63.0	1.062 x 10^{-9}	281	0.3
4.20	281	-76.7	1.051 x 10^{-9}	287	2.1

[a] log D = -0.5093 (log FW) – 7.7268.
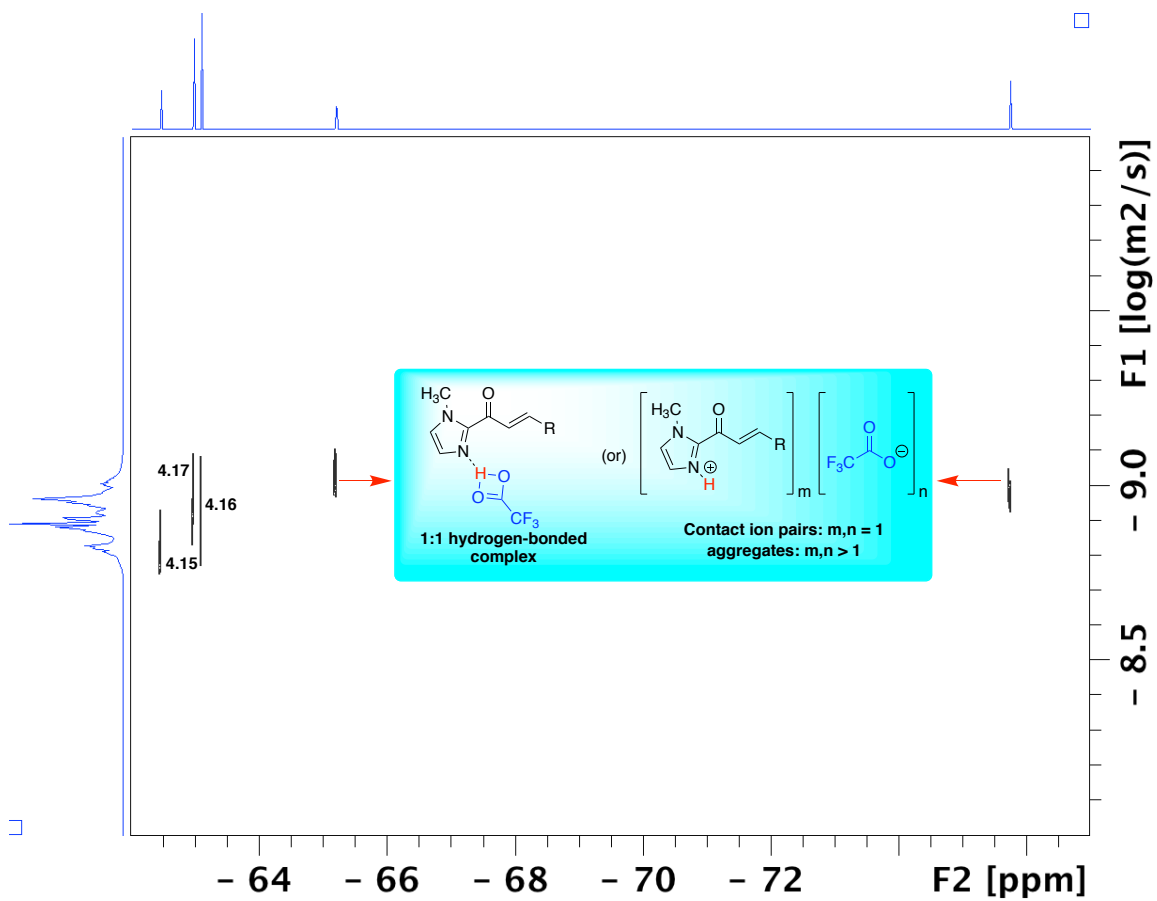
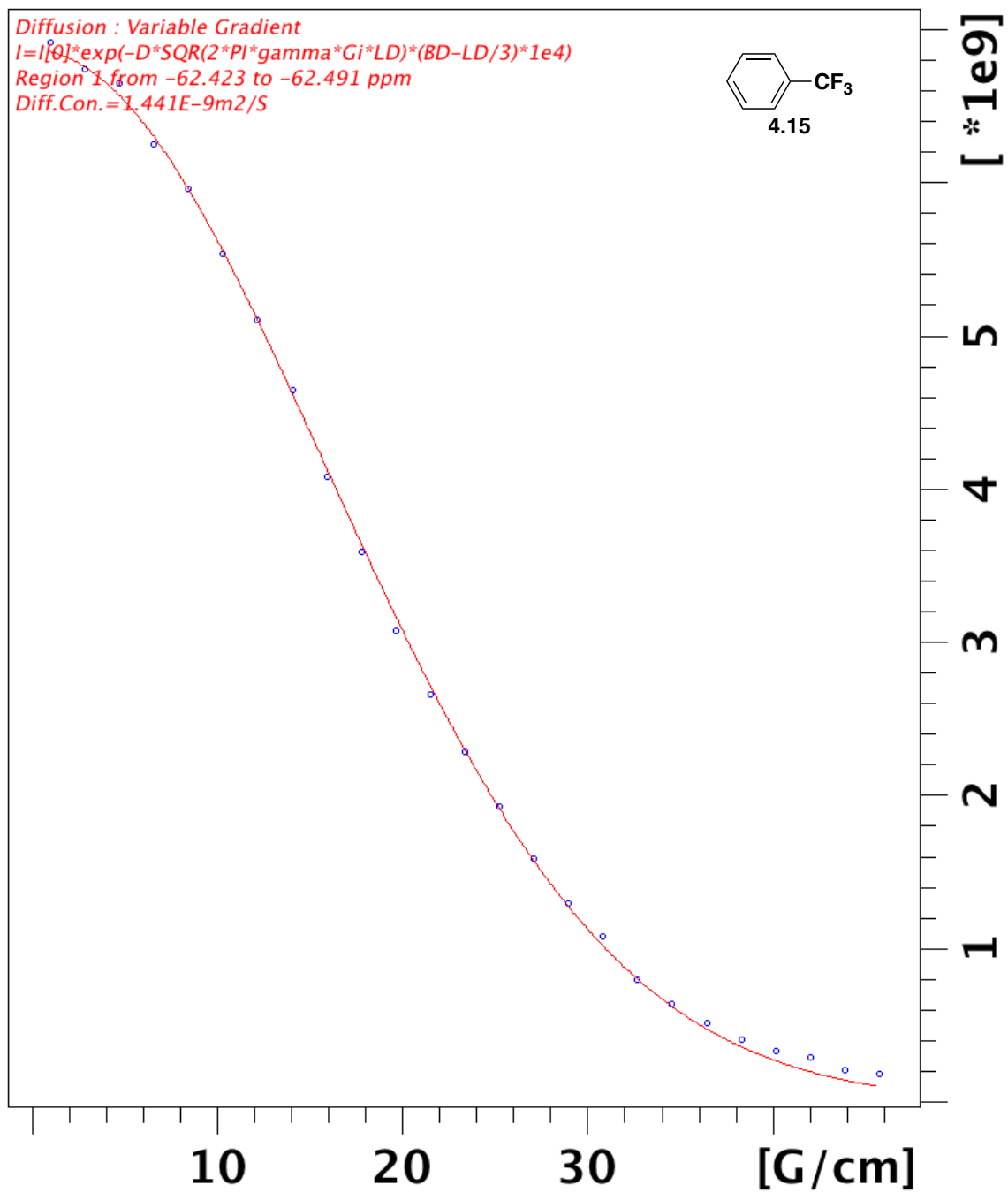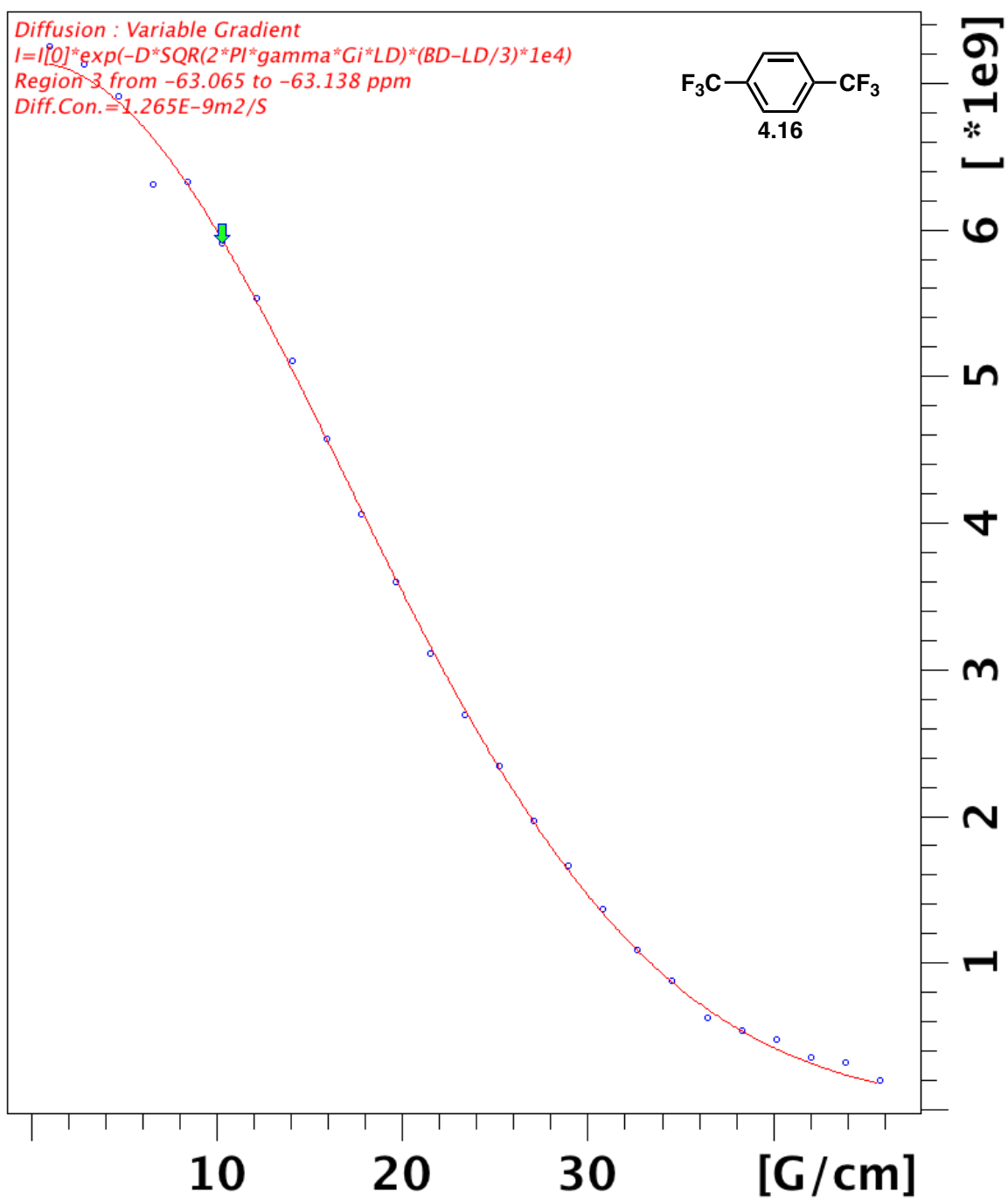Figure 4.42. ^{19}F DOSY spectrum of compounds **4.15-4.17** and **4.22a** in C$_6$D$_6$.
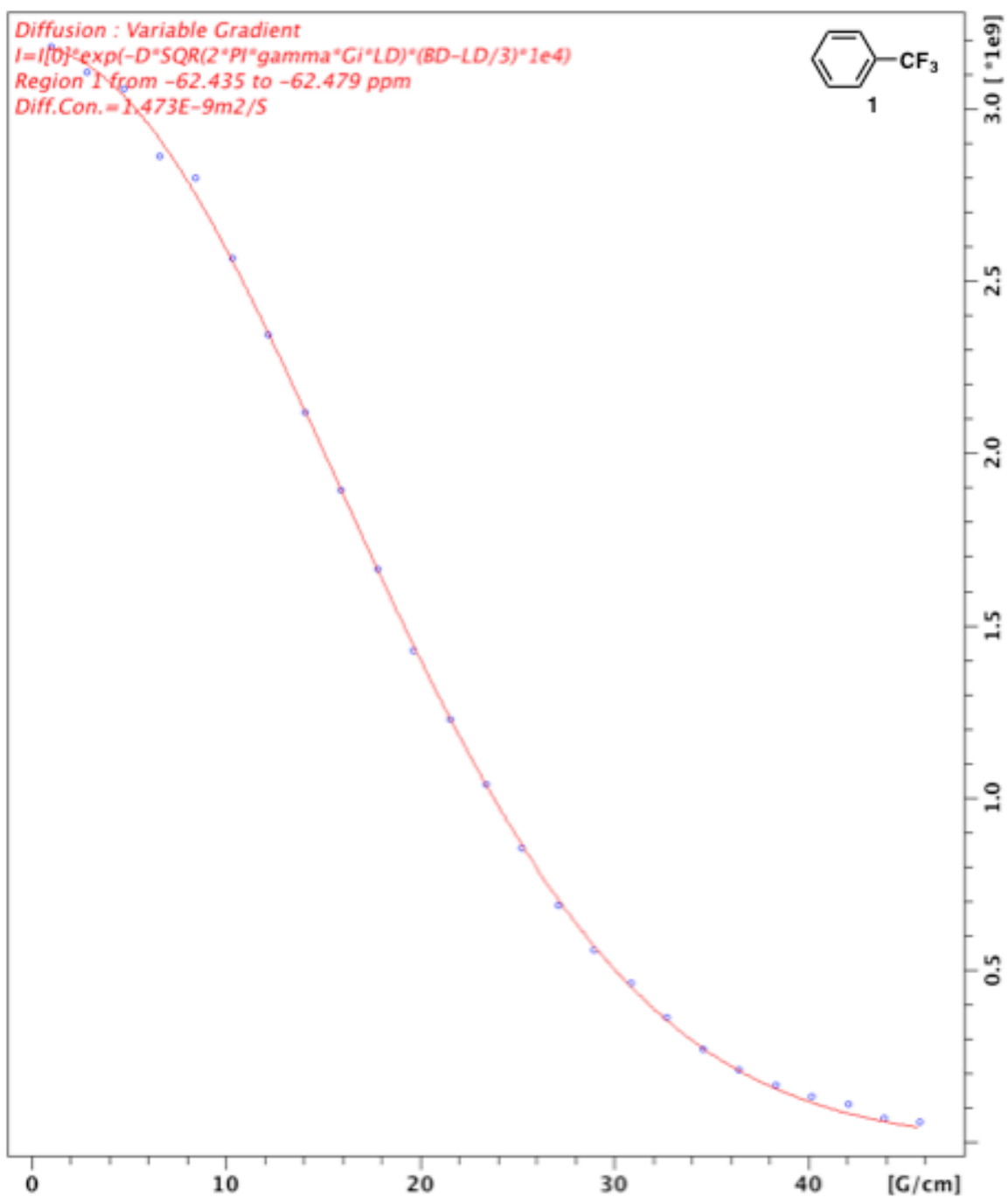
Figure 4.43. Signal attenuation curve of internal standard **4.15** in a mixture of compounds **4.15-4.17** and **4.22a** in C_6D_6.

Figure 4.44. Signal attenuation curve of internal standard **4.16** in a mixture of compounds **4.15-4.17** and **4.22a** in C₆D₆.
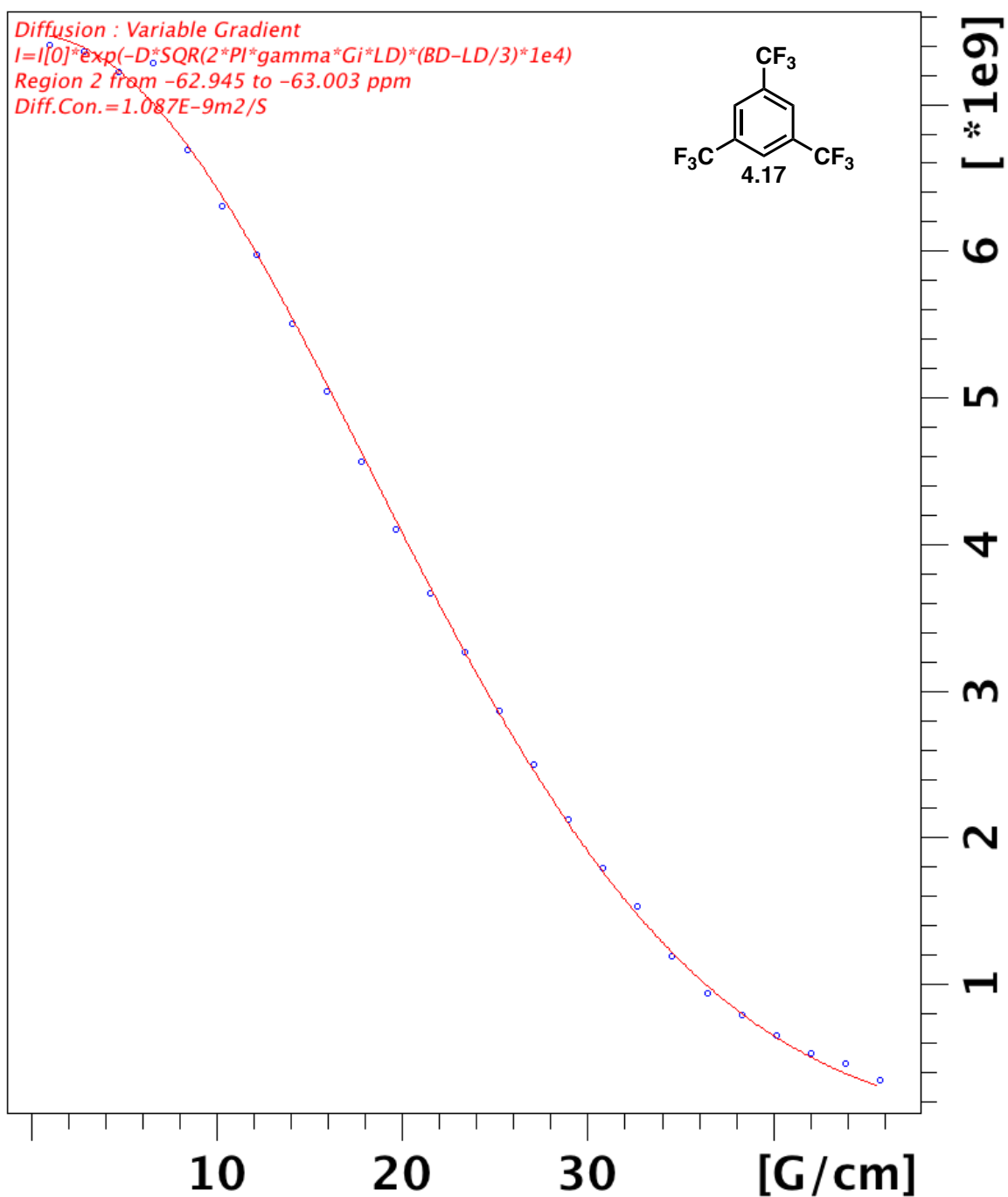
Figure 4.45. Signal attenuation curve of internal standard **4.17** in a mixture of compounds **4.15-4.17** and **4.22a** in C₆D₆.
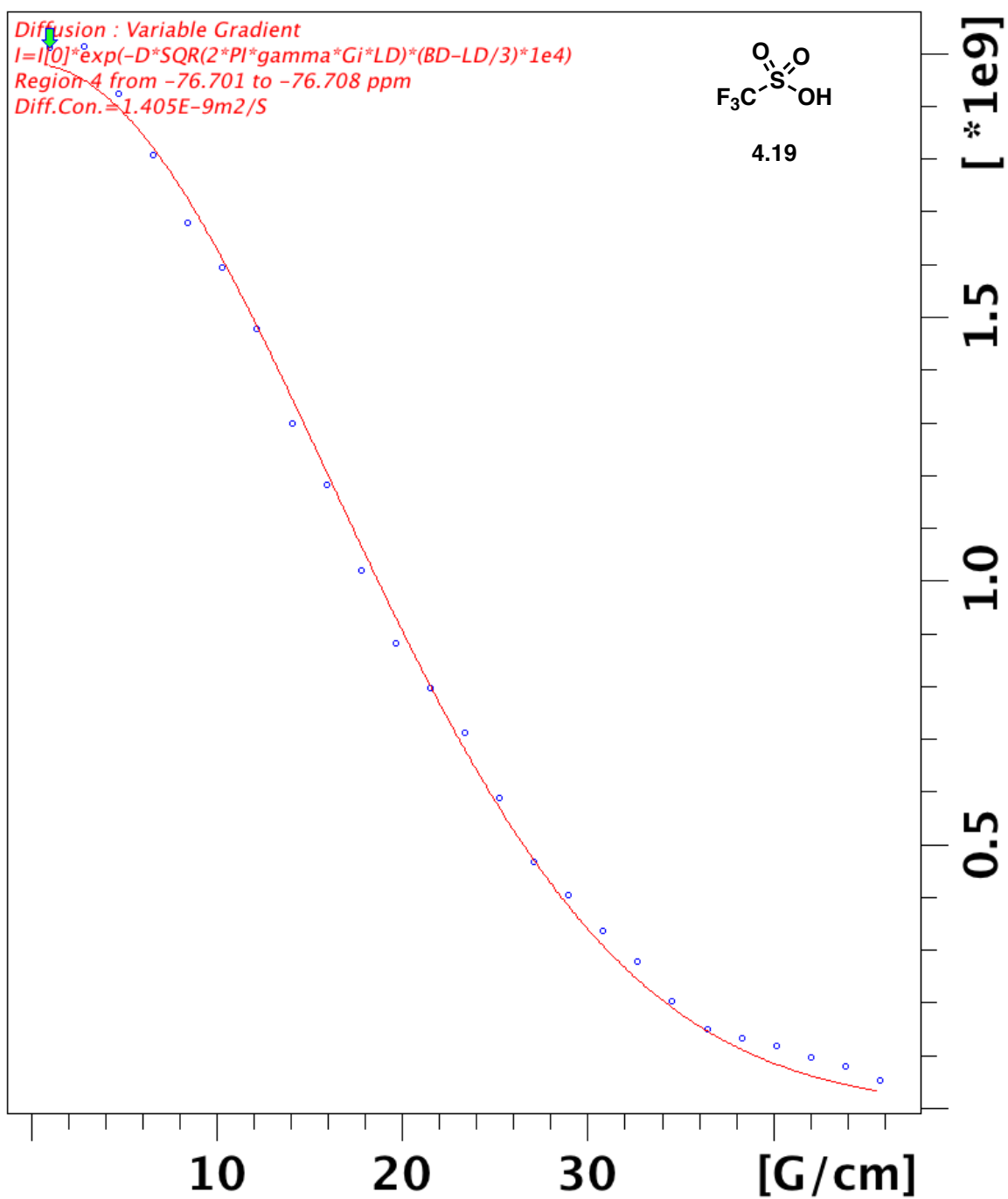
Figure 4.46. Signal attenuation curve of complex **(4.22a)$_m$.(4.15)$_n$** in a mixture of compounds **4.15-4.17** and **4.22a** in C_6D_6.

Figure 4.47. Signal attenuation curve of complex $(4.22a)_m.(4.17)_n$ in a mixture of compounds **4.15-4.17** and **4.22a** in C_6D_6.
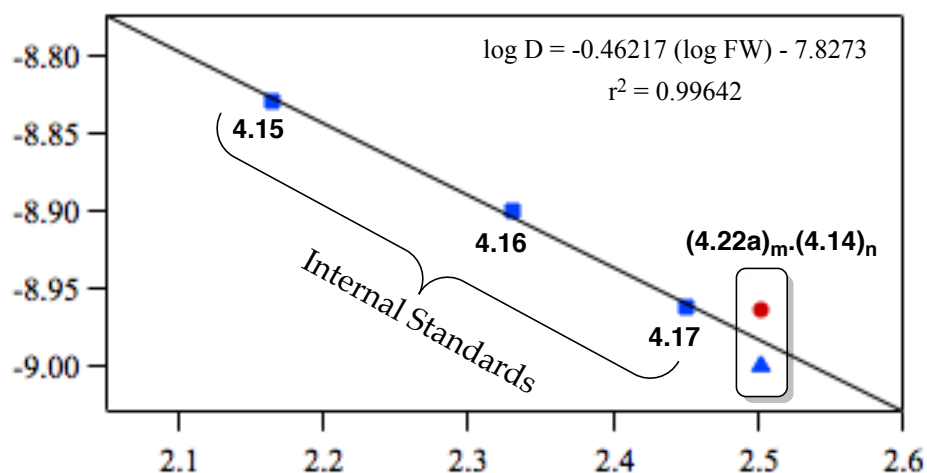
Figure 4.48. log D versus log FW analysis of ^{19}F DOSY of a mixture of **4.15-4.18**, **4.22a** in benzene-d_6. (•) correspond to diffusion constant of the trifluoroacetate anion and (▲) correspond to diffusion constant of the cation.

Table 4.12. D-FW analysis of ^{19}F DOSY spectrum of compounds **4.15-4.18** and **4.22a** in C_6D_6.

Compound	FW (g mol^{-1})	$\delta(^{19}F)$ (ppm)	D (m^2 s^{-1})	FW$_{DOSY}$ (g mol^{-1})[a]	% error
4.15	146	-62.5	1.473 x 10^{-9}	149	2.1
4.16	214	-63.1	1.259 x 10^{-9}	209	2.3
4.17	282	-63.0	1.097 x 10^{-9}	282	0.0
(4.22a)$_m$·(4.18)$_n$	318	-65.0	9.993 x 10^{-10}	345	7.8
(4.22a)$_m$·(4.18)$_n$	318	75.7	1.086 x 10^{-9}	288	9.4

[a] log D = -0.46217 (log FW) – 7.8273.

Figure 4.49. ^{19}F DOSY spectrum of a mixture of internal standards **4.15-4.17**, **4.20** and acylimidazole **4.22a** in C_6D_6.

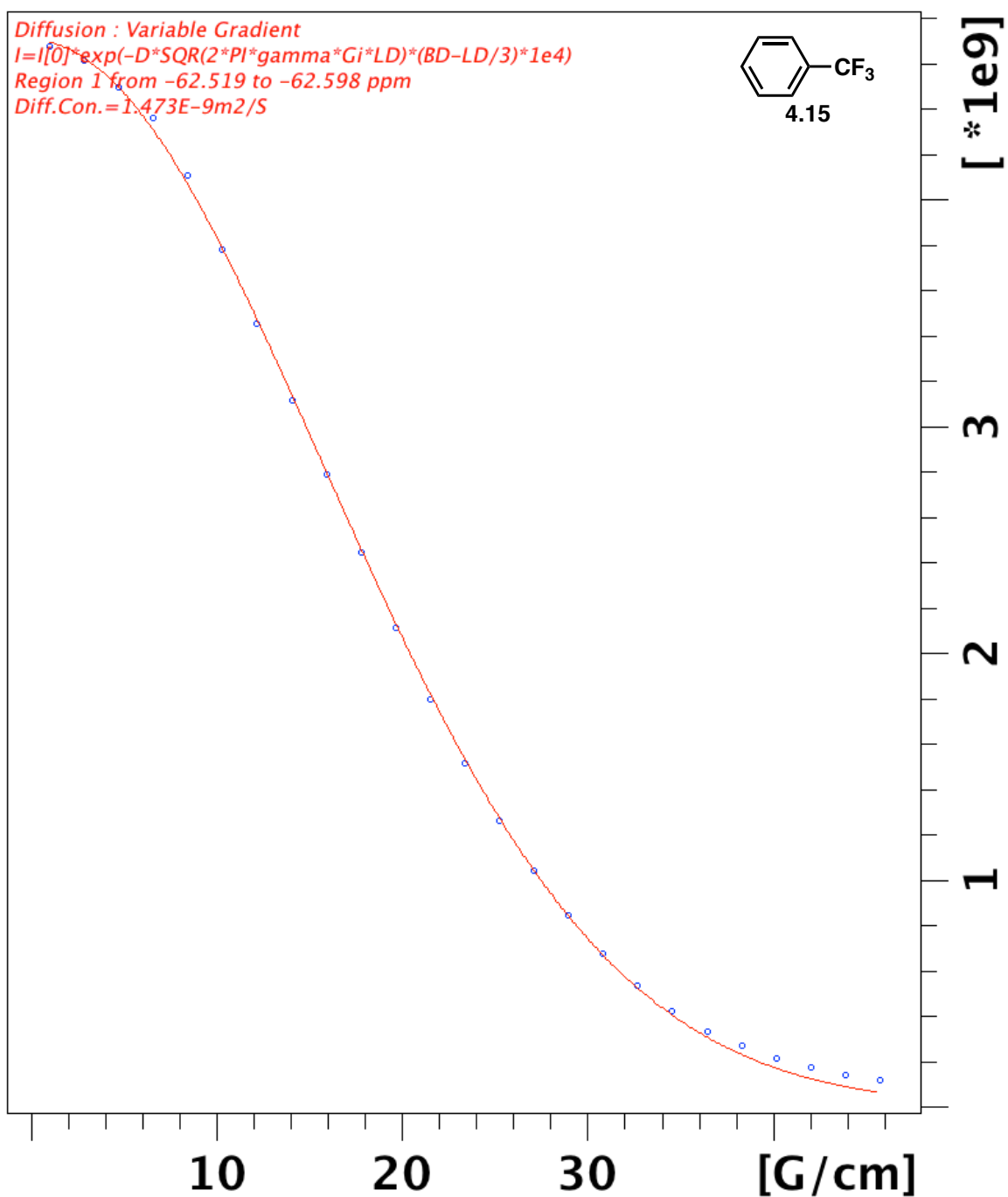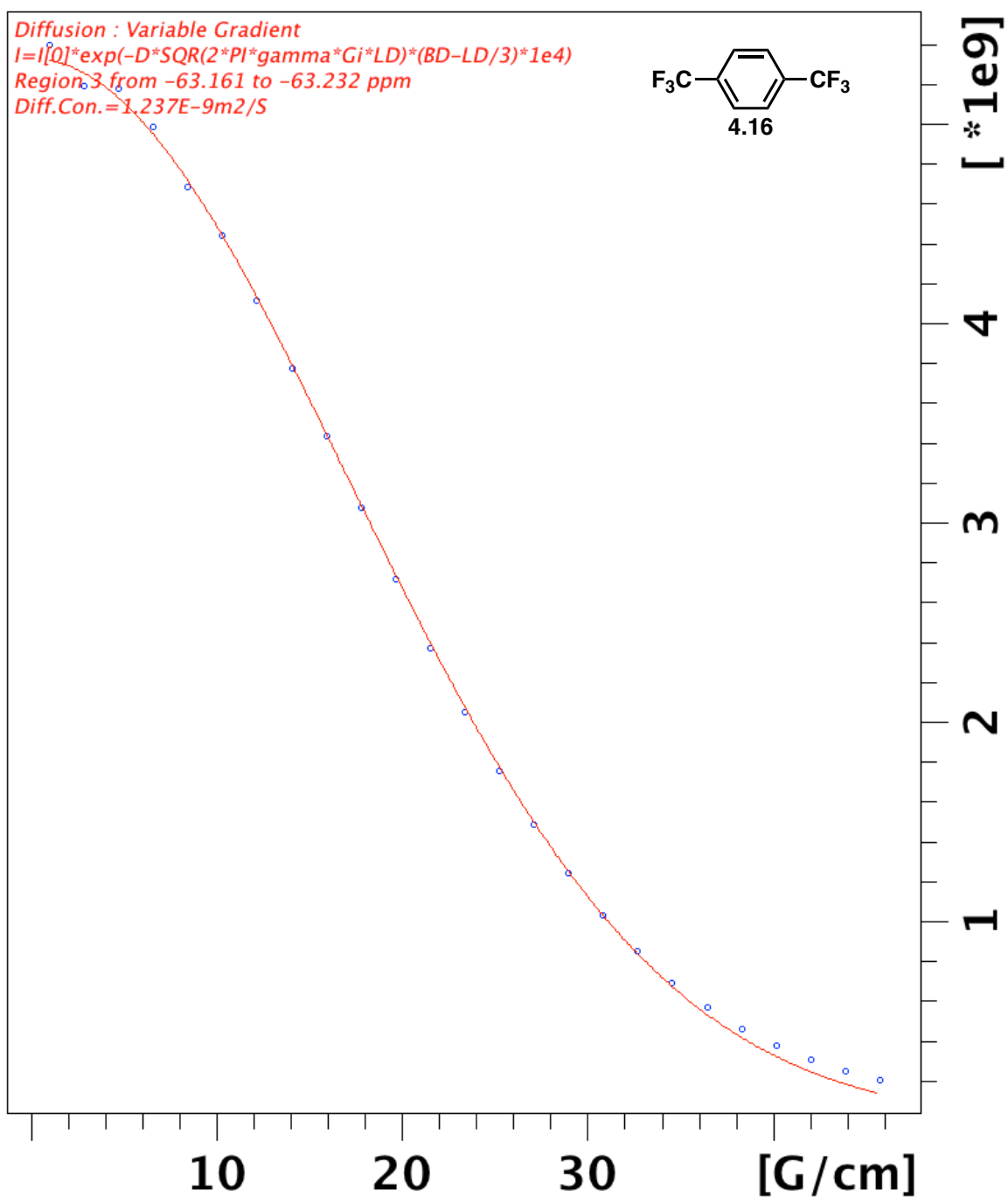Figure 4.50. Signal attenuation curve of internal standard **4.15** in a mixture of compounds **4.15-4.17**, **4.20** and acylimidazole **4.22a** in C$_6$D$_6$.

Figure 4.51. Signal attenuation curve of internal standard 4.16 in a mixture of compounds **4.15-4.17**, **4.20** and acylimidazole **4.22a** in C_6D_6.

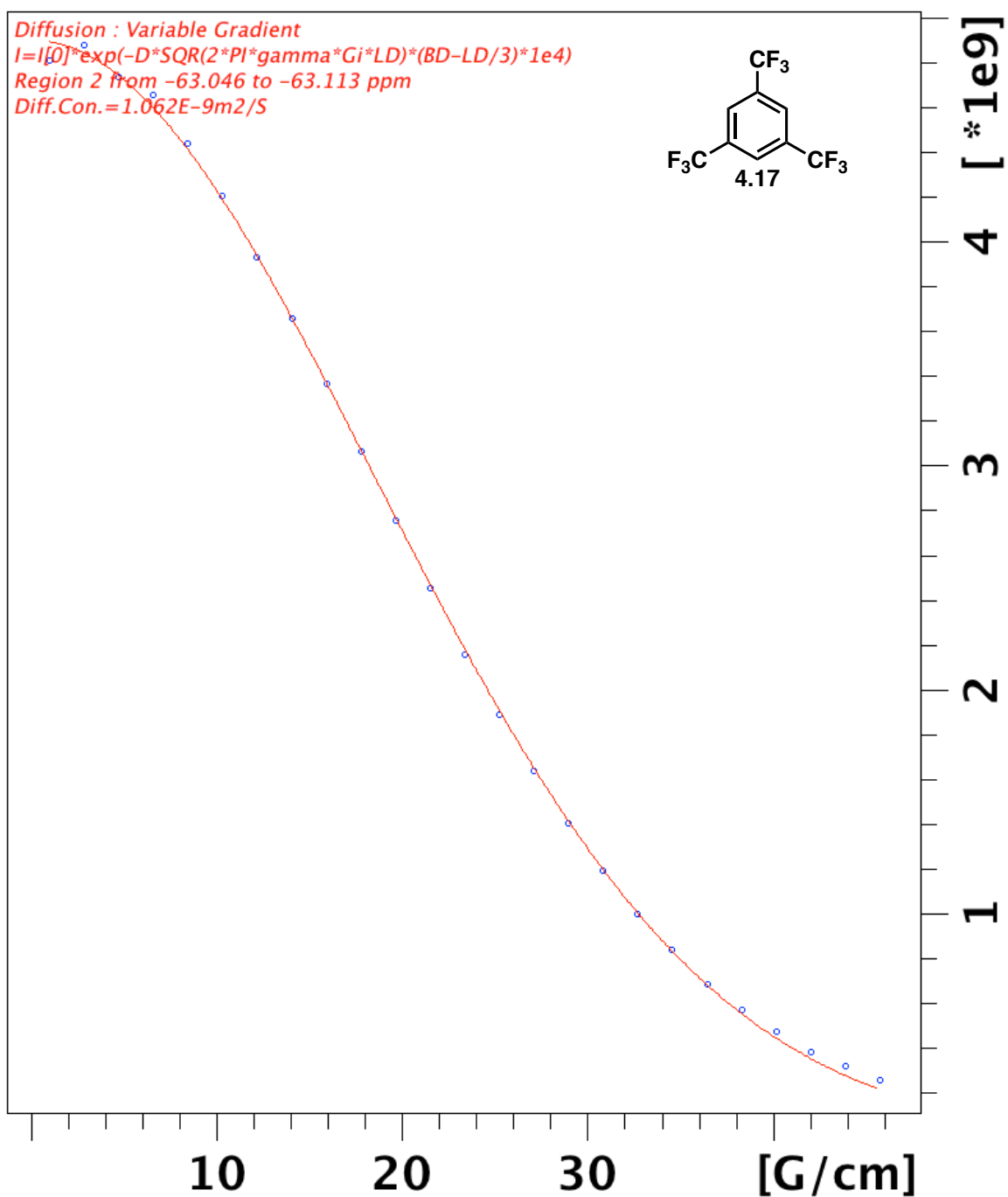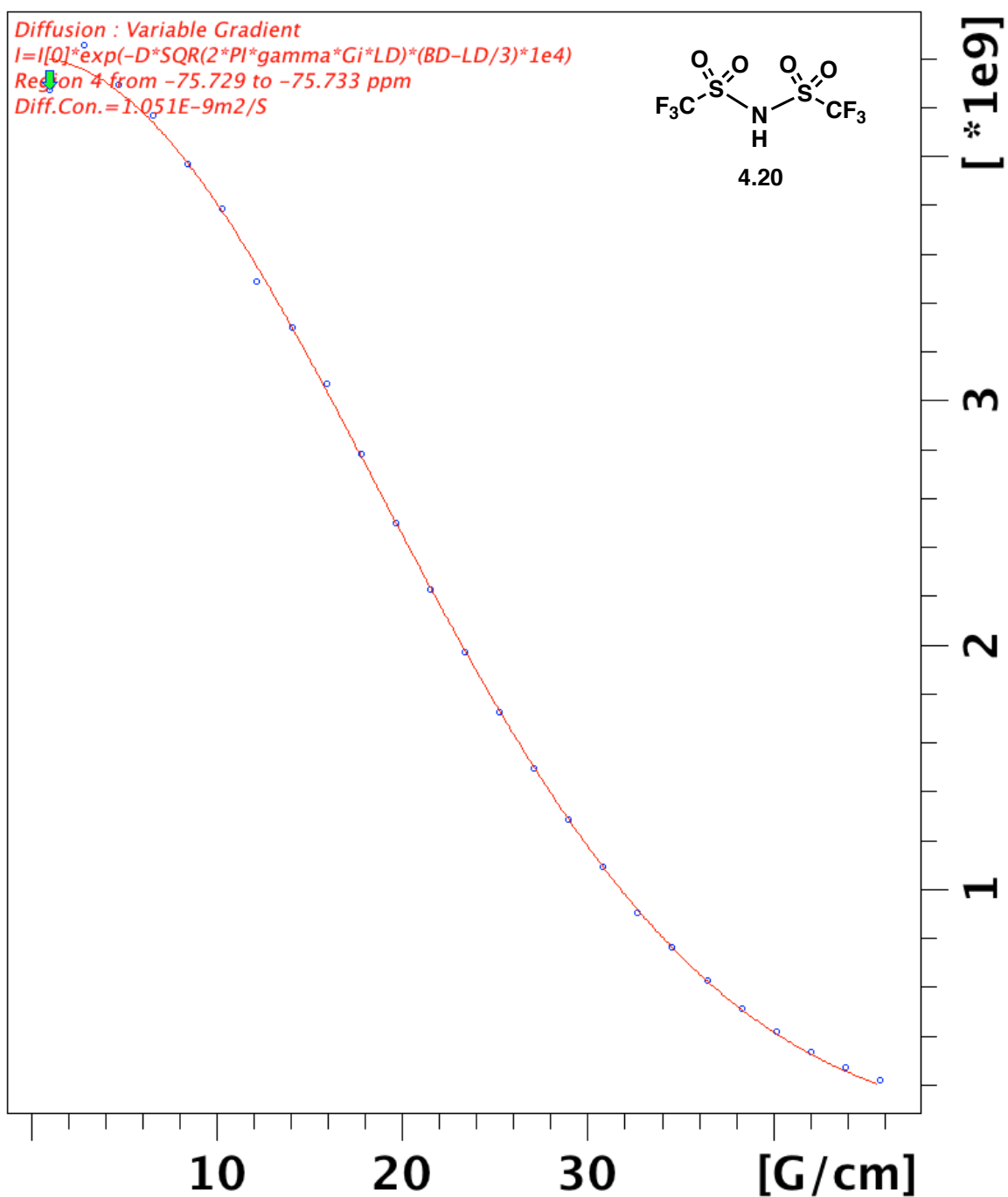Figure 4.52. Signal attenuation curve of internal standard **4.17** in a mixture of compounds **4.15-4.17**, **4.20** and acylimidazole **4.22a** in C_6D_6.

Figure 4.53. Signal attenuation curve of complex **(4.22a)$_m$.(4.20)$_n$** in a mixture of compounds **4.15-4.17**, **4.20** and acylimidazole **4.22a** in C_6D_6.
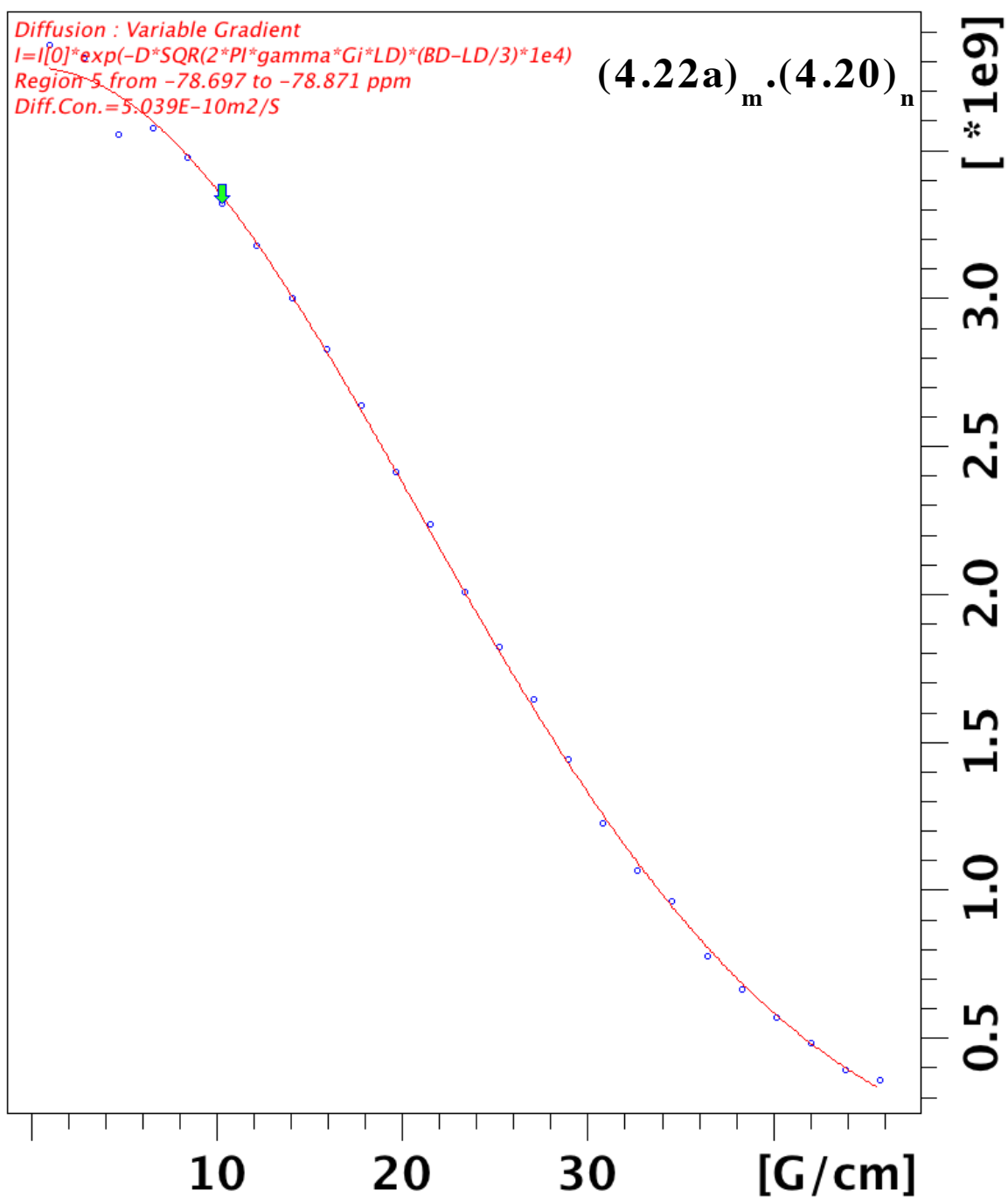
Figure 4.54. Signal attenuation curve of complex $(4.22a)_m.(4.20)_n$ in a mixture of compounds **4.15-4.17**, **4.20** and acylimidazole **4.22a** in C_6D_6.

Figure 4.55. log D versus log FW analysis of ^{19}F DOSY of a mixture of **4.15-4.17**, **4.20** and acylimidazole **4.22a** in benzene-d_6. (•) correspond to diffusion constant of the anion of trifluoromethanesulfonimide and (▲) correspond to diffusion constant of the cation.

Table 4.13. D-FW analysis of ^{19}F DOSY spectrum of compounds **4.15-4.17**, **4.20** and **4.22a** in C_6D_6

Compound	FW (g mol^{-1})	δ(^{19}F) (ppm)	D (m^2 s^{-1})	FW$_{DOSY}$ (g mol^{-1})^a	% error
4.15	146	-62.5	1.475 x 10^{-9}	149	0.7
4.16	214	-63.1	1.235 x 10^{-9}	202	5.6
4.17	282	-63.0	9.975 x 10^{-10}	292	3.5
(4.22a)$_m$.(4.20)$_n$	970	-65.6	5.074 x 10^{-10}	939	3.2
(4.22a)$_m$.(4.20)$_n$	970	-78.7	5.039 x 10^{-10}	950	2.1

^{a} log D = -0.57892 (log D) – 7.7539.
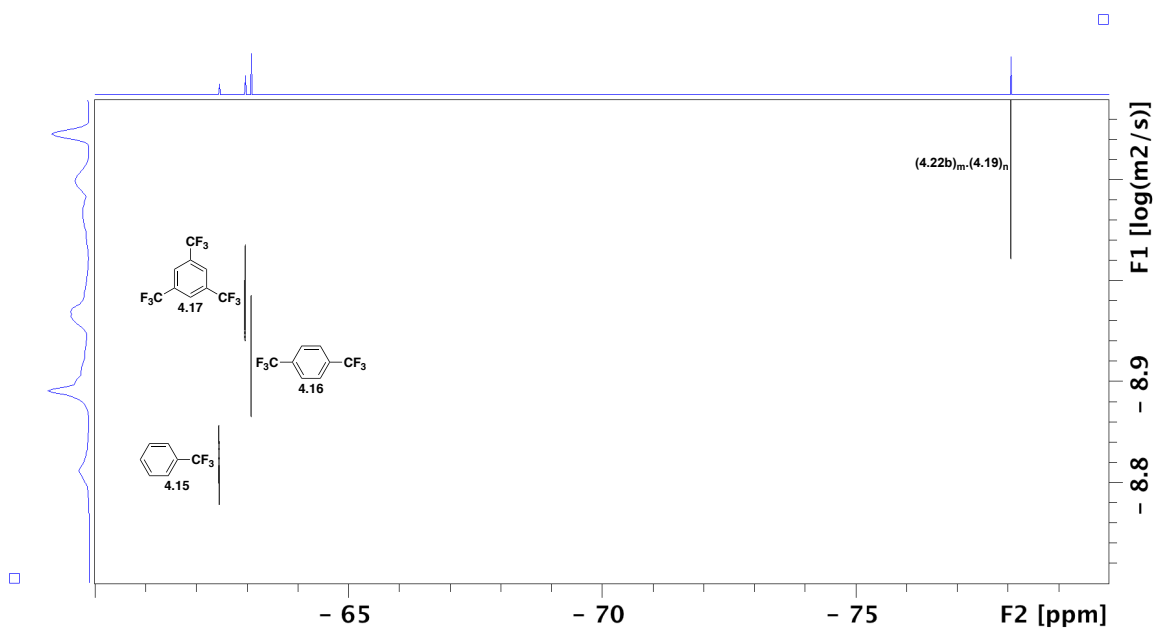
Figure 4.56. ^{19}F DOSY spectrum of a mixture of internal standards **4.15-4.17**, **4.19** and acylimidazole **4.22b** in C_6D_6.
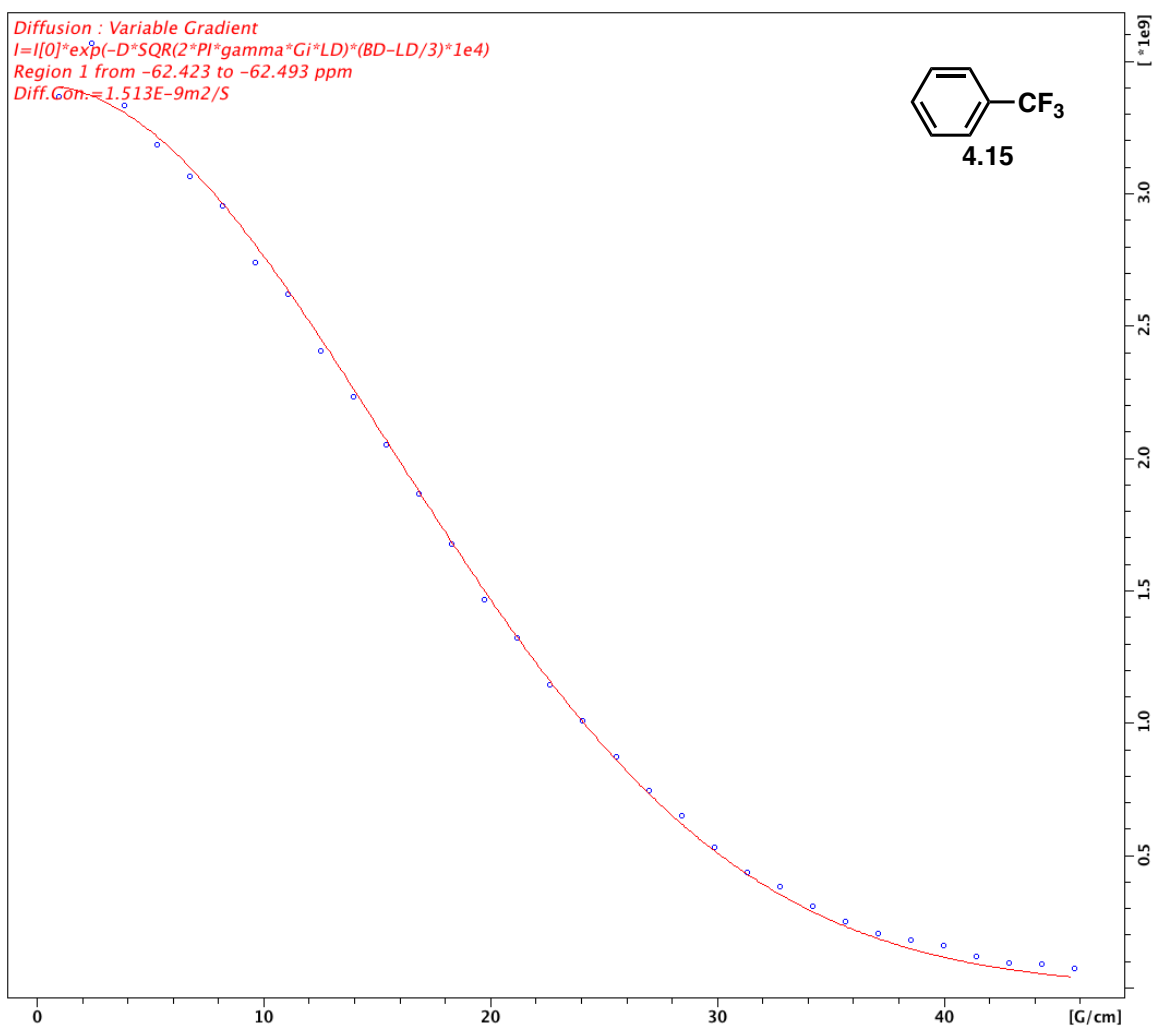
Figure 4.57. Signal attenuation curve of internal standard **4.15** in a mixture of compounds **4.15-4.17**, **4.19** and acylimidazole **4.22b** in C_6D_6.
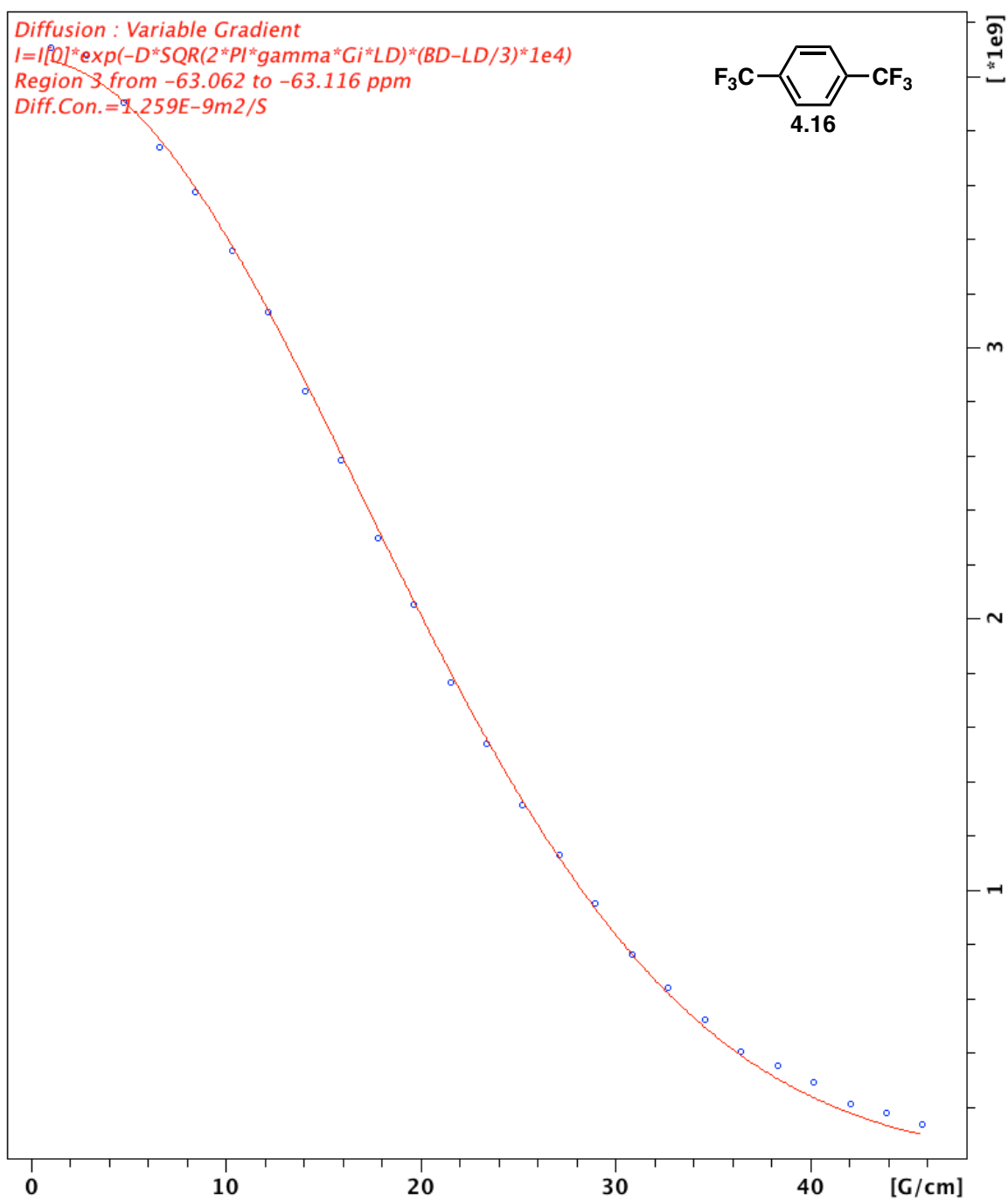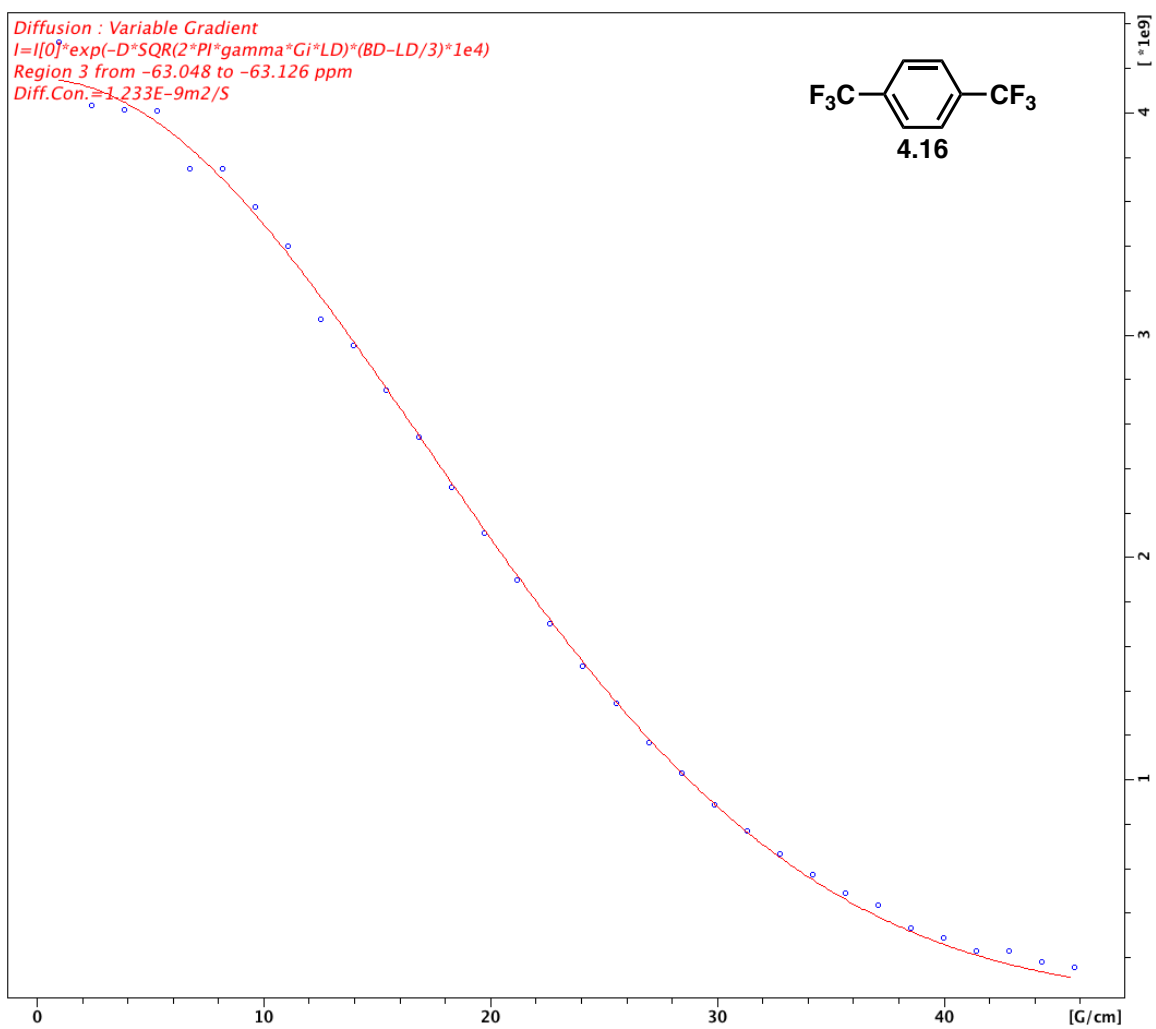
Figure 4.58. Signal attenuation curve of internal standard **4.16** in a mixture of compounds **4.15-4.17**, **4.19** and acylimidazole **4.22b** in C$_6$D$_6$.
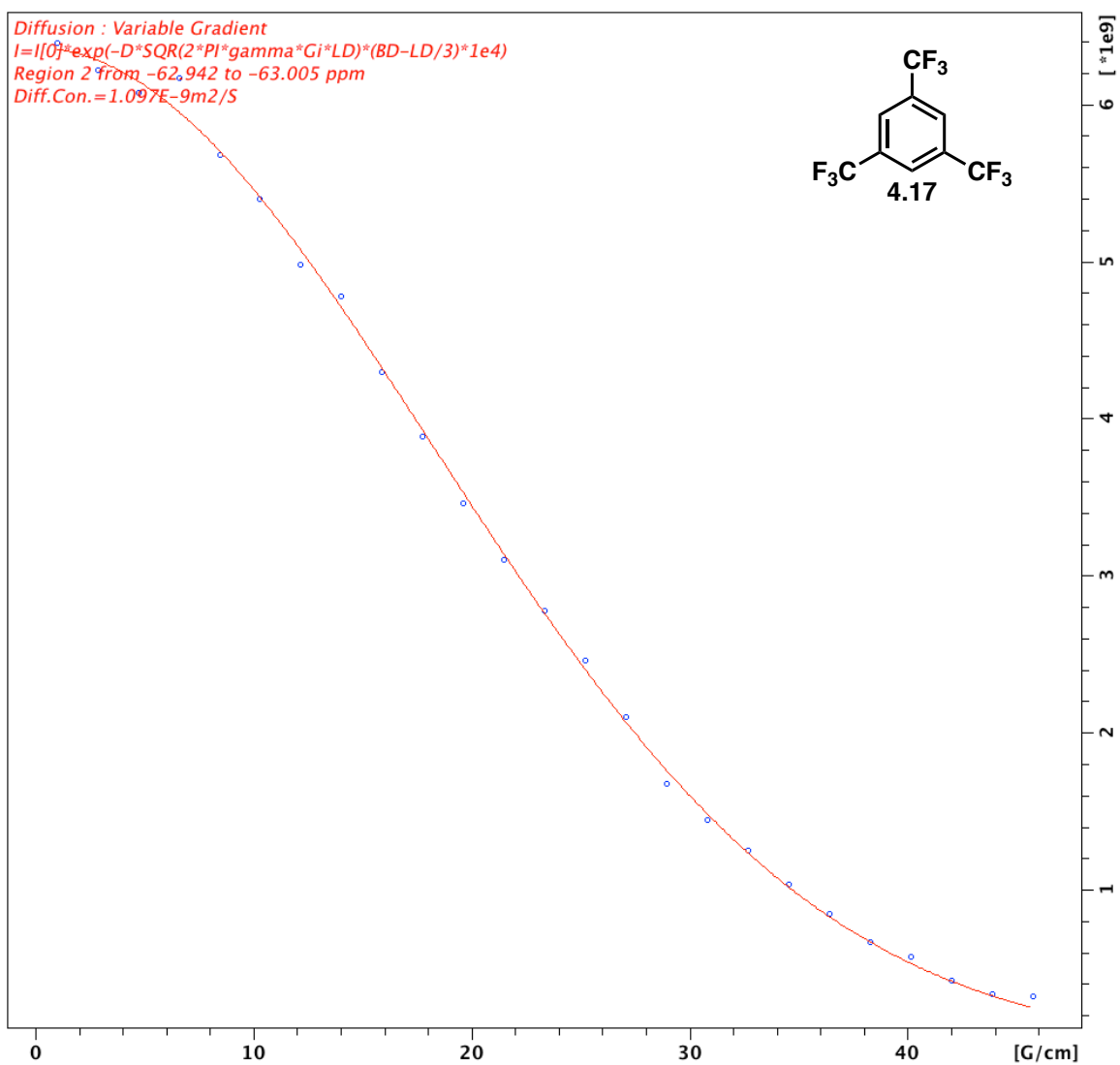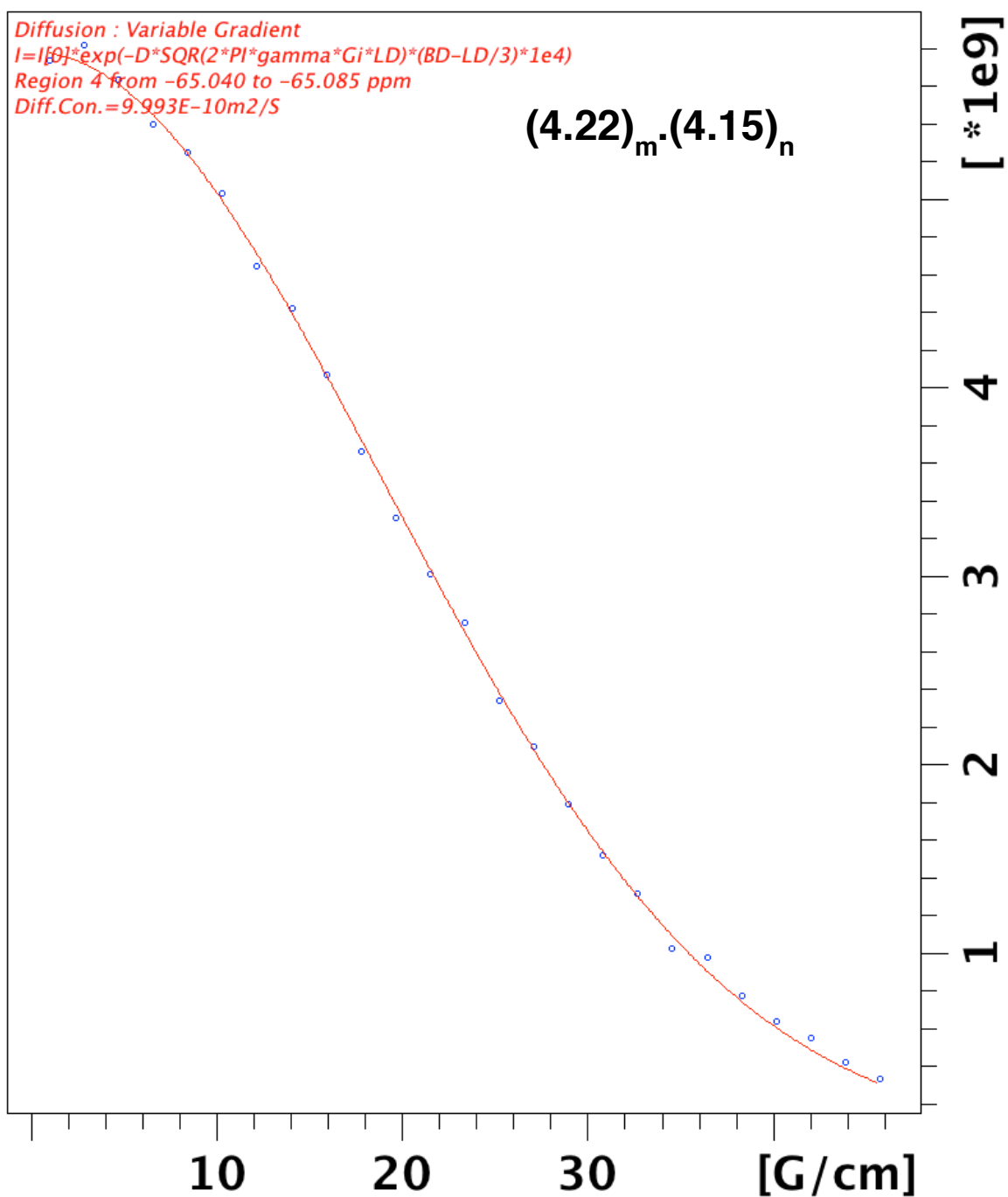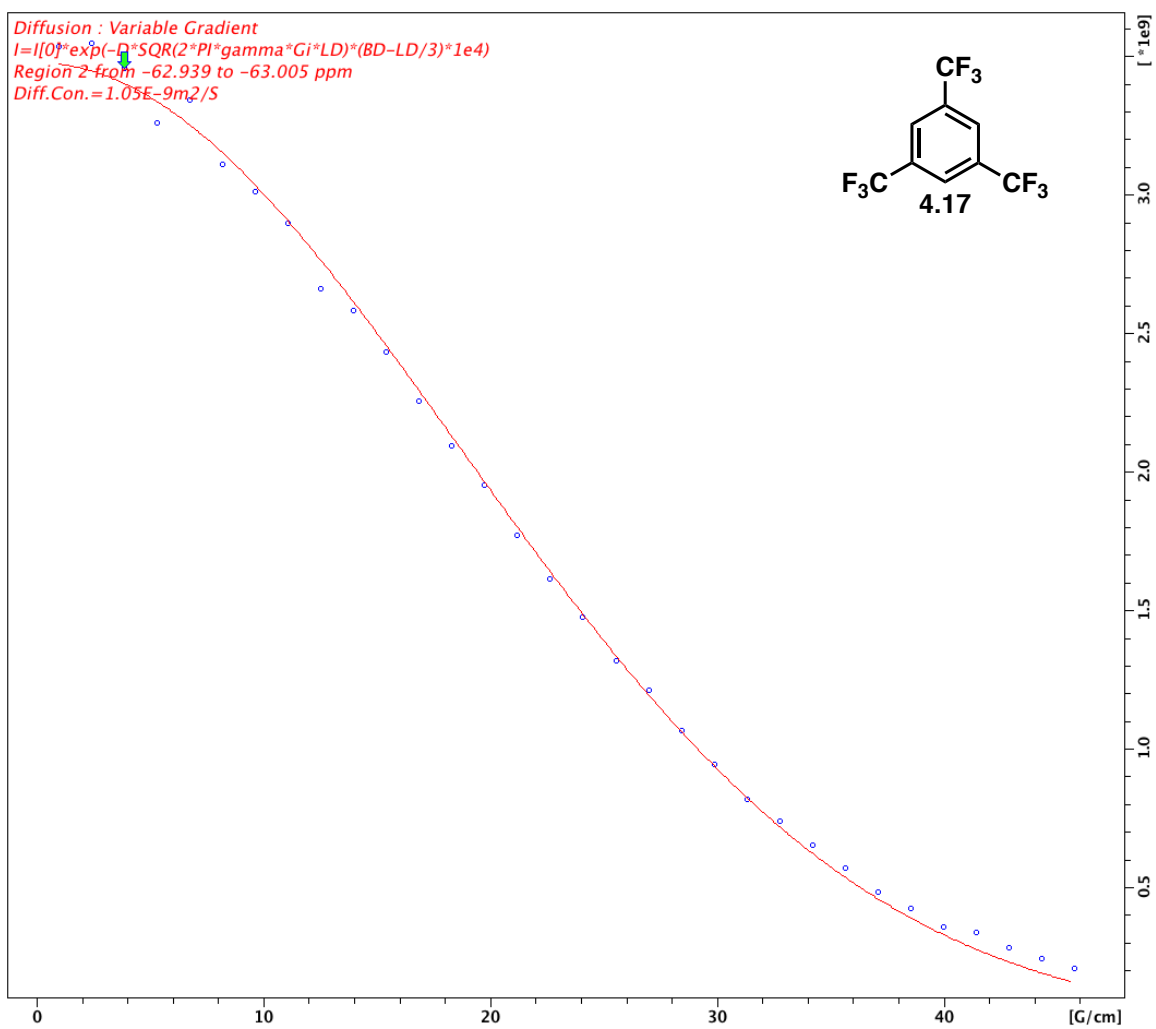
Figure 4.59. Signal attenuation curve of internal standard 2 in a mixture of compounds **4.15-4.17**, **4.19** and acylimidazole **4.22b** in C_6D_6.
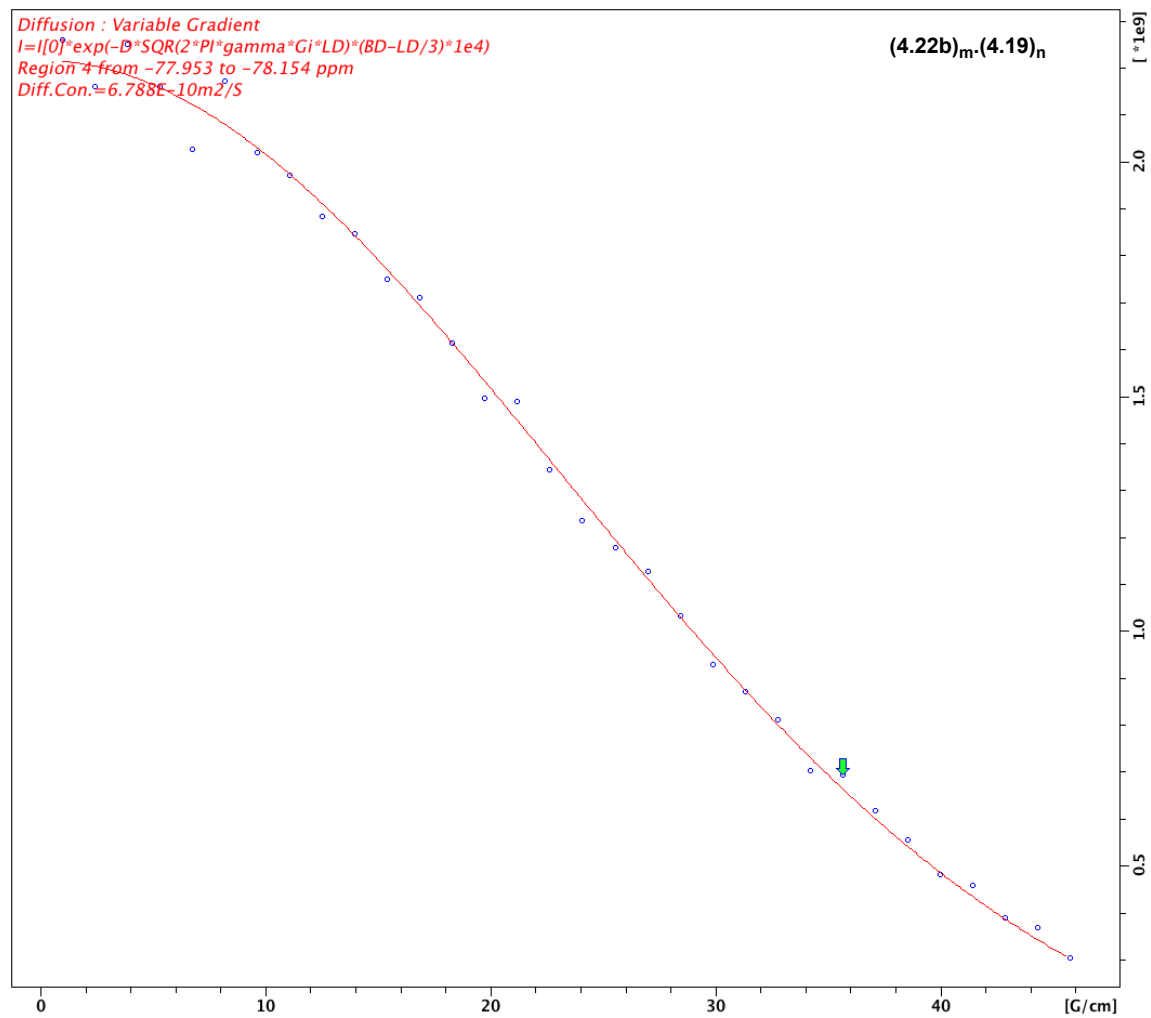
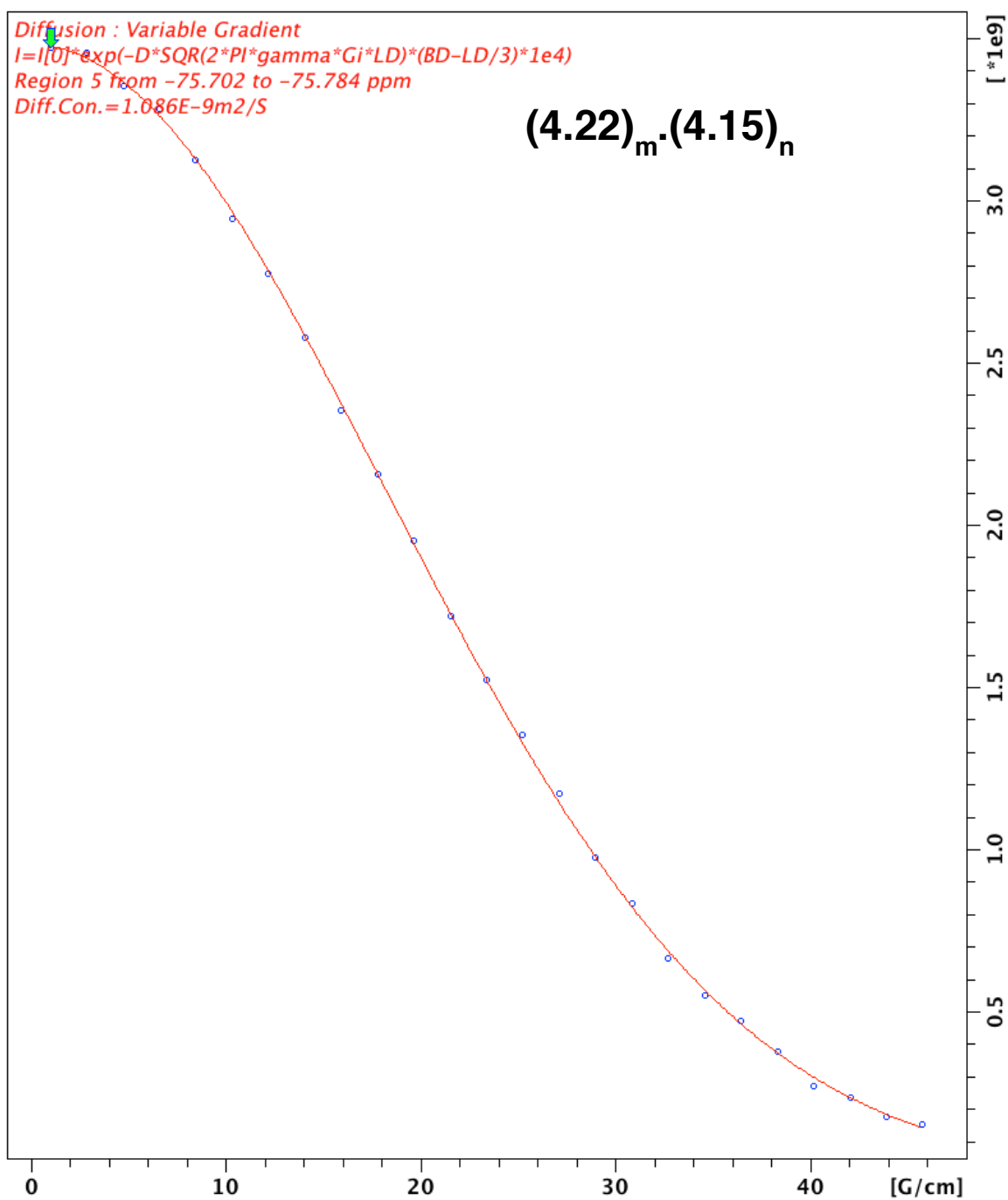Figure 4.60. Signal attenuation curve of complex **(4.22a)$_m$.(4.19)$_n$** in a mixture of compounds **4.15-4.17**, **4.19** and acylimidazole **4.22b** in C_6D_6.
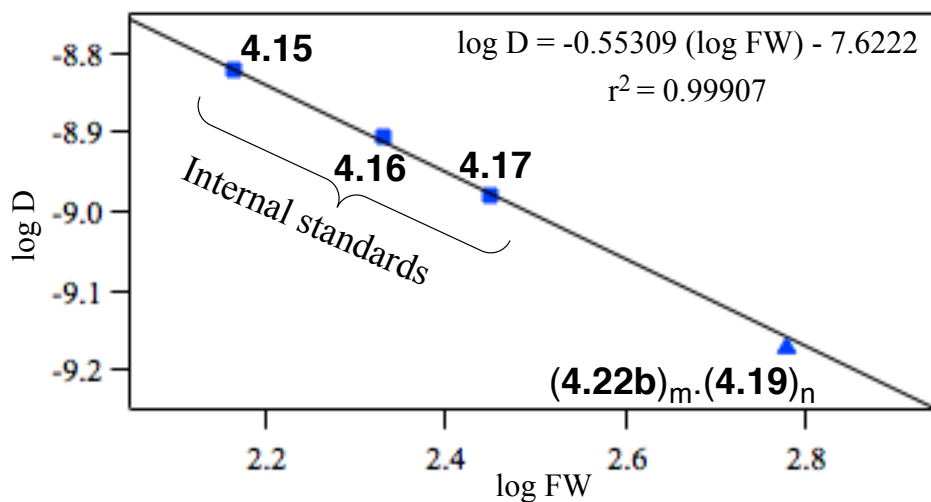
Figure 4.61. log D versus log FW analysis of ^{19}F DOSY of a mixture of **4.15-4.17**, **4.19** and acylimidazole **4.22b** in benzene-d_6.

Table 4.14. D-FW analysis of ^{19}F DOSY spectrum of compounds **4.15-4.17**, **4.19** and acylimidazole **4.22b** in C_6D_6.

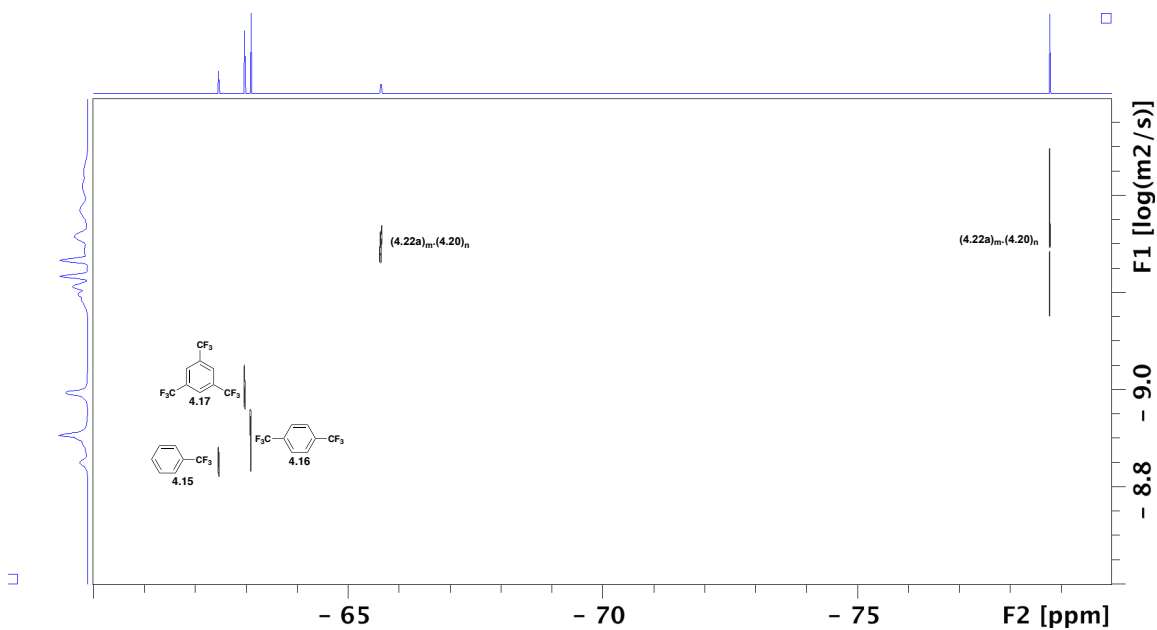| Compound	FW (g mol^{-1})	$\delta(^{19}F)$ (ppm)	D (m^2 s^{-1})	FW$_{DOSY}$ (g mol^{-1})^a	% error
4.15	146	-62.5	1.513×10^{-9}	147	0.70
4.16	214	-63.1	1.233×10^{-9}	212	0.93
4.17	282	-63.0	1.050×10^{-10}	284	0.71
(4.22b)$_m$.(4.19)$_n$	600	-78.0	6.788×10^{-10}	624	4.0

^{a} log D = -0.55309 (log FW) -7.6222.

171
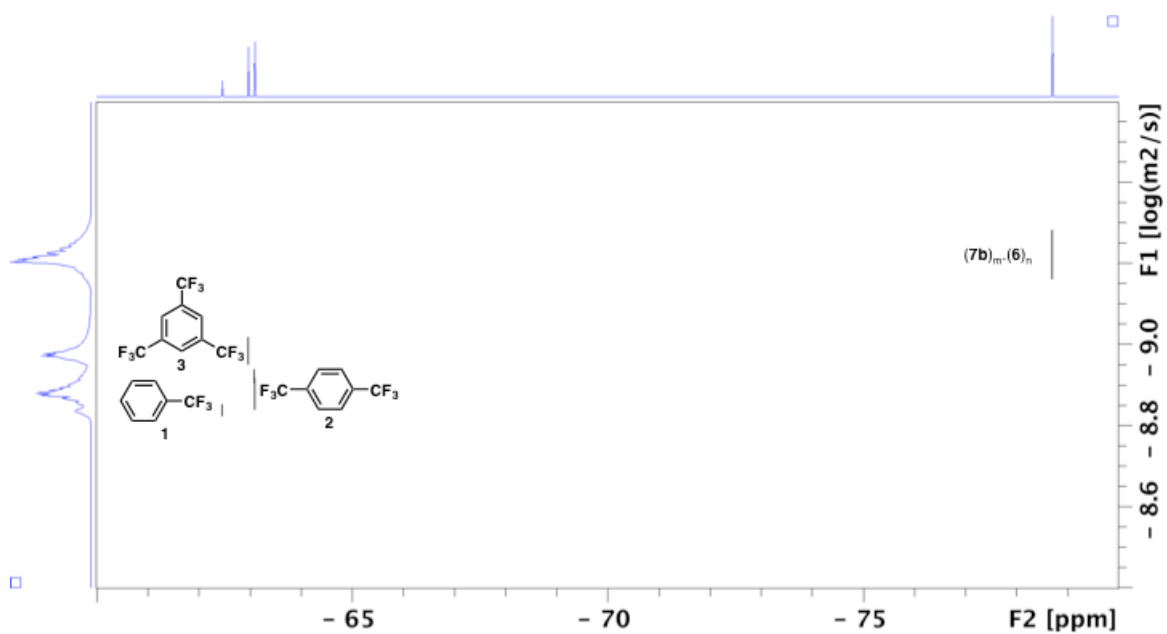
Figure 4.62. ^{19}F DOSY spectrum of a mixture of internal standards **4.15-4.17**, **4.19** and acylimidazole **4.22b** in C$_6$D$_6$.
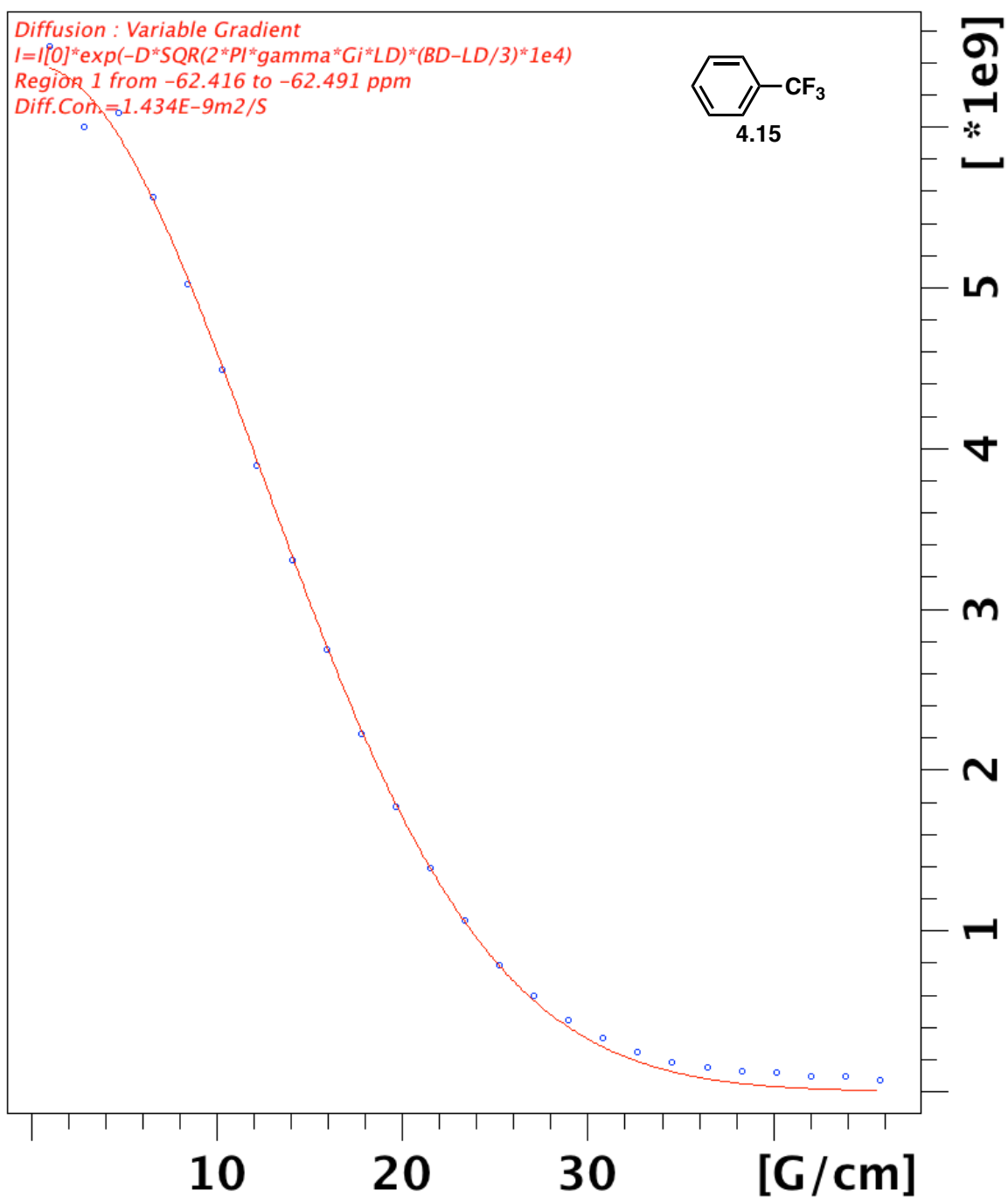
Figure 4.63. Signal attenuation curve of internal standard **4.15** in a mixture of compounds **4.15-4.17**, **4.19** and acylimidazole **4.22b** in C$_6$D$_6$.
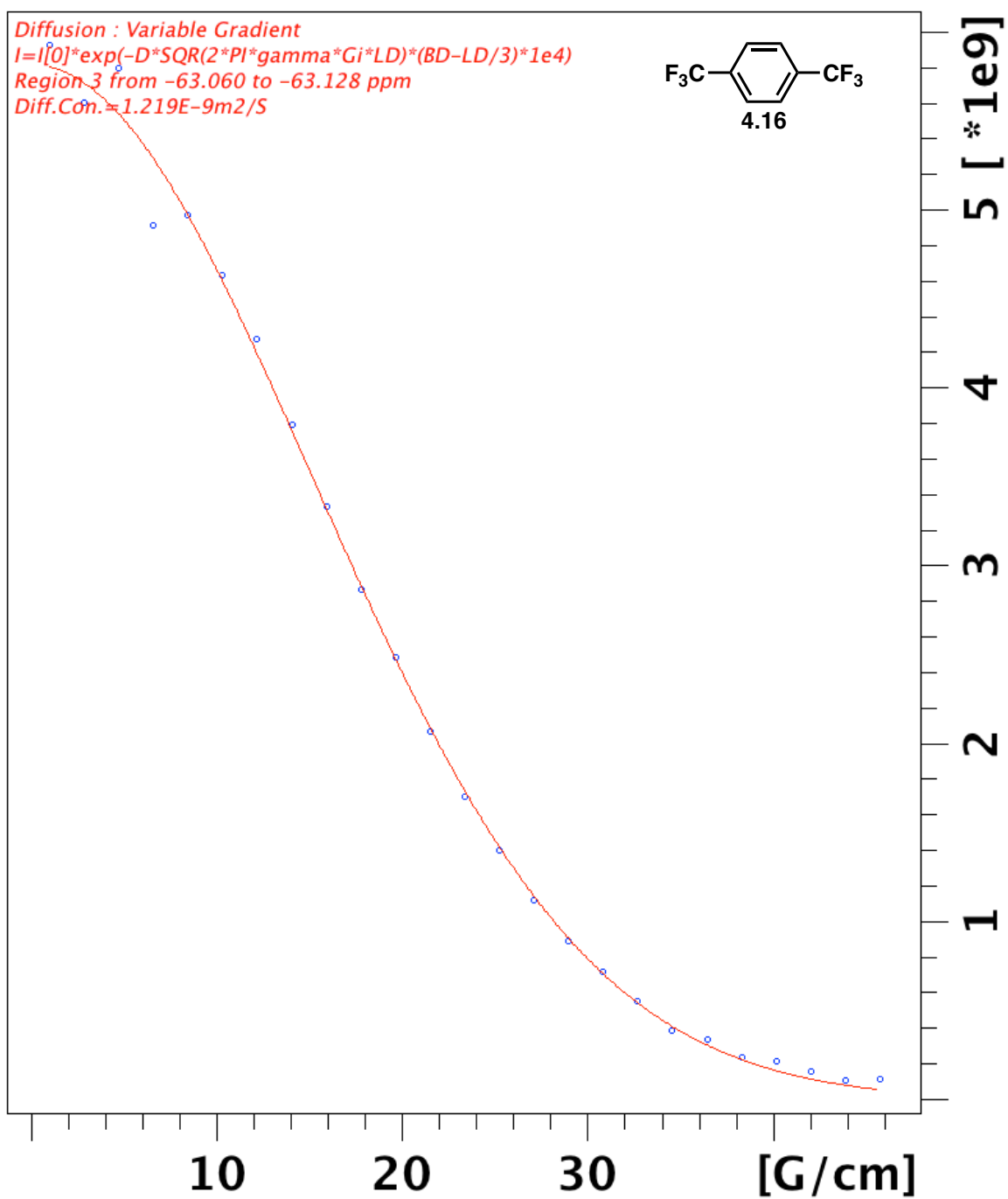
Figure 4.64 Signal attenuation curve of internal standard **4.16** in a mixture of compounds **4.15-4.17**, **4.19** and acylimidazole **4.22b** in C_6D_6.
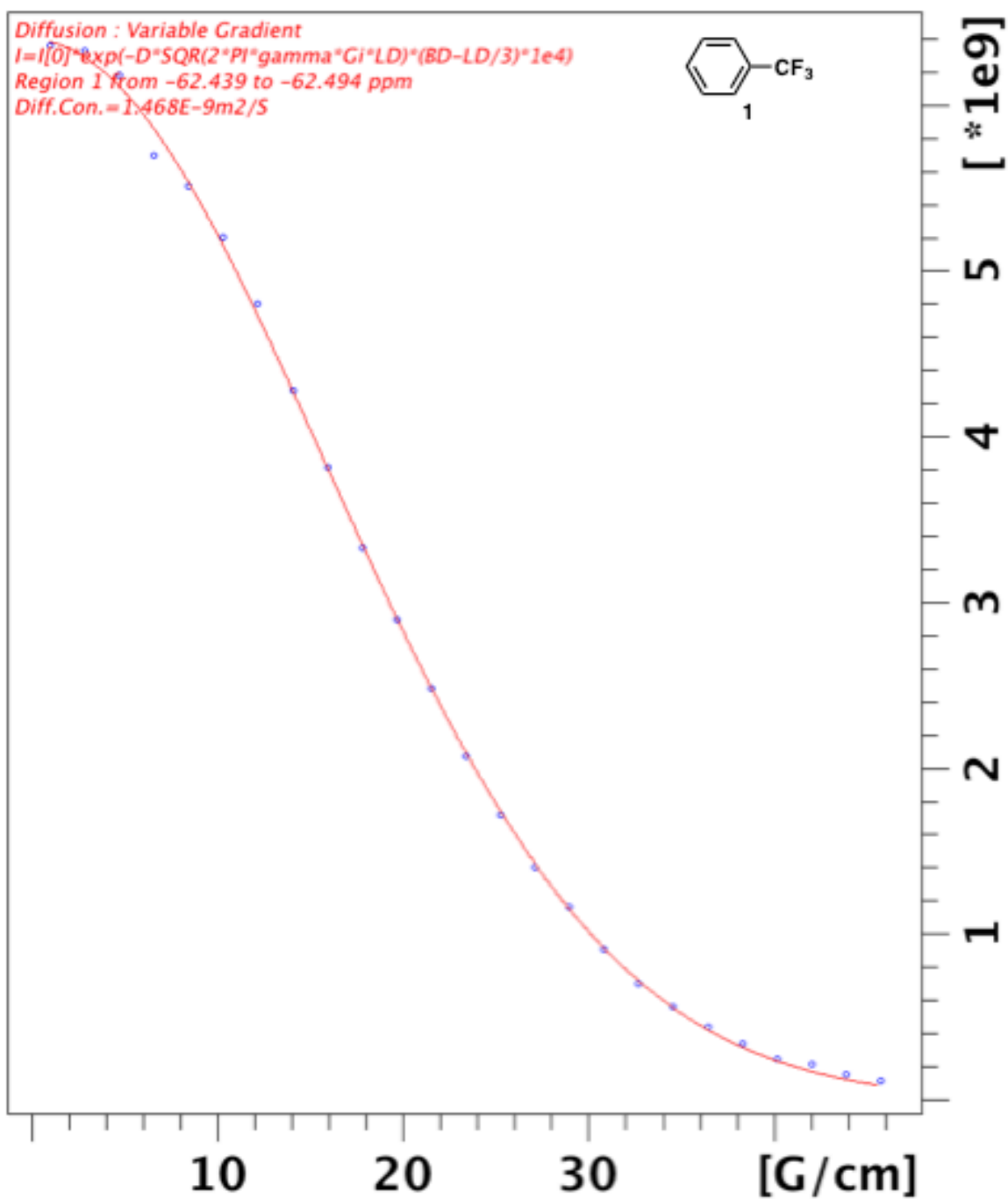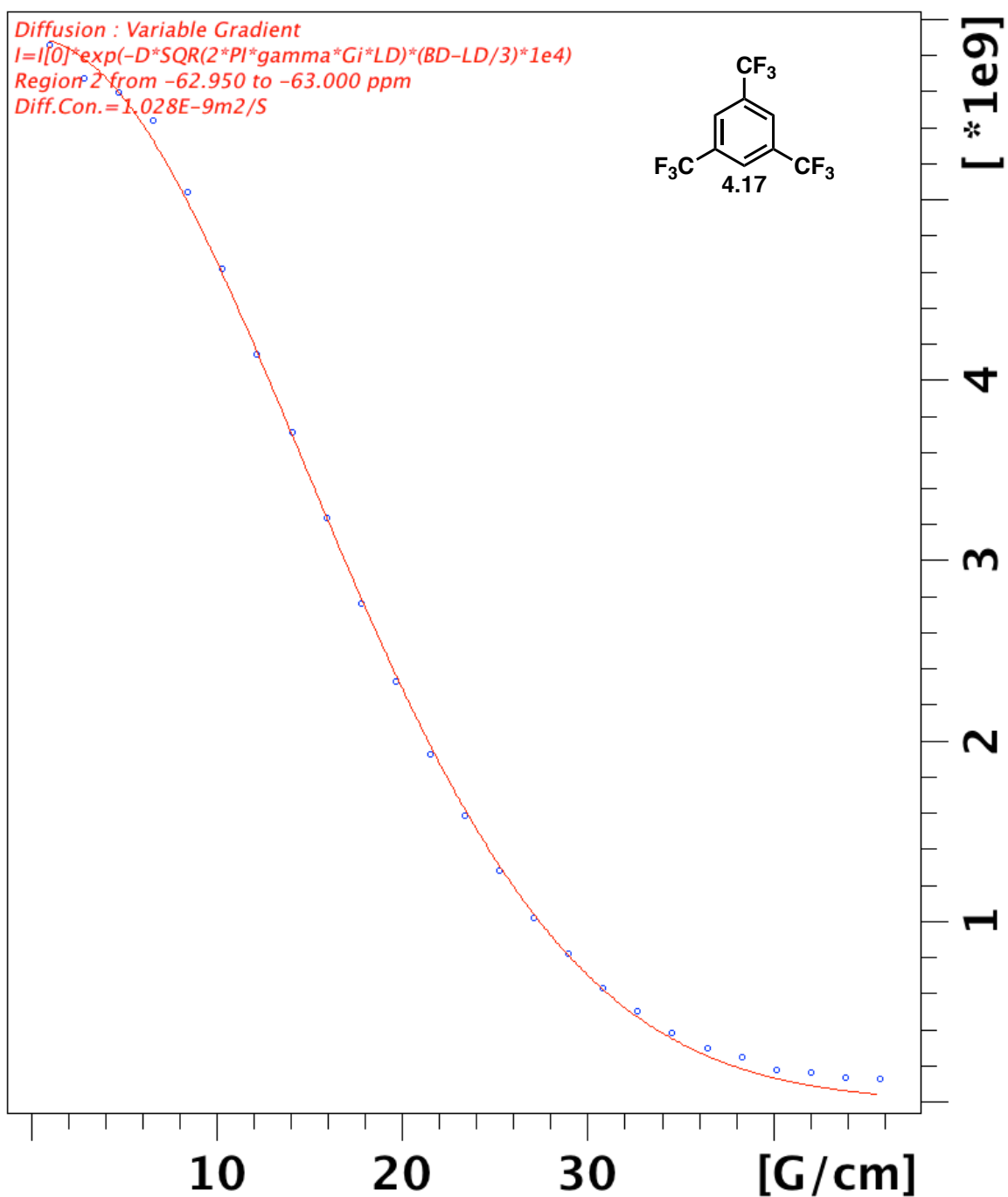
Figure 4.65. Signal attenuation curve of internal standard **4.17** in a mixture of compounds **4.15-4.17**, **4.20** and acylimidazole **4.22b** in C_6D_6.
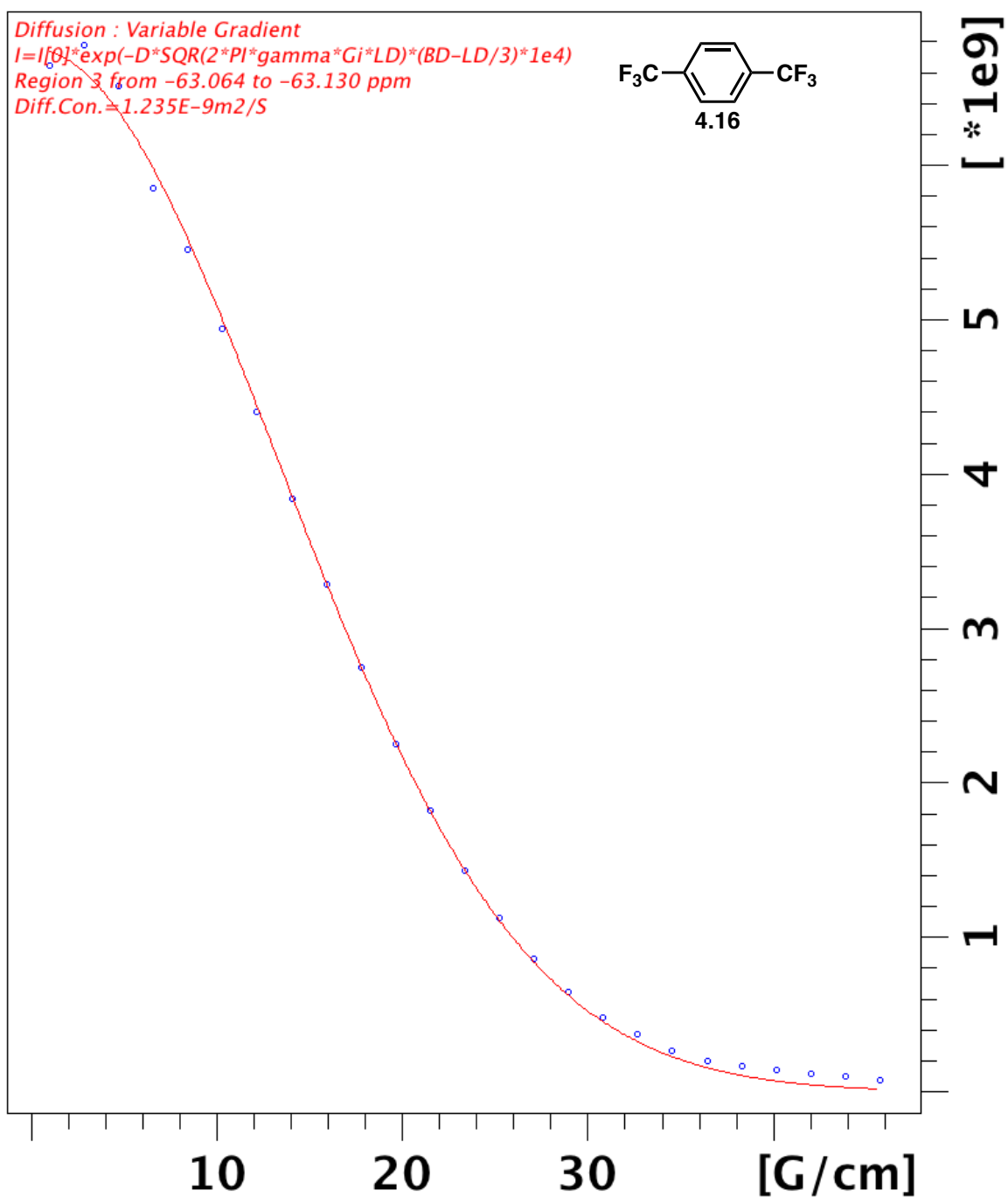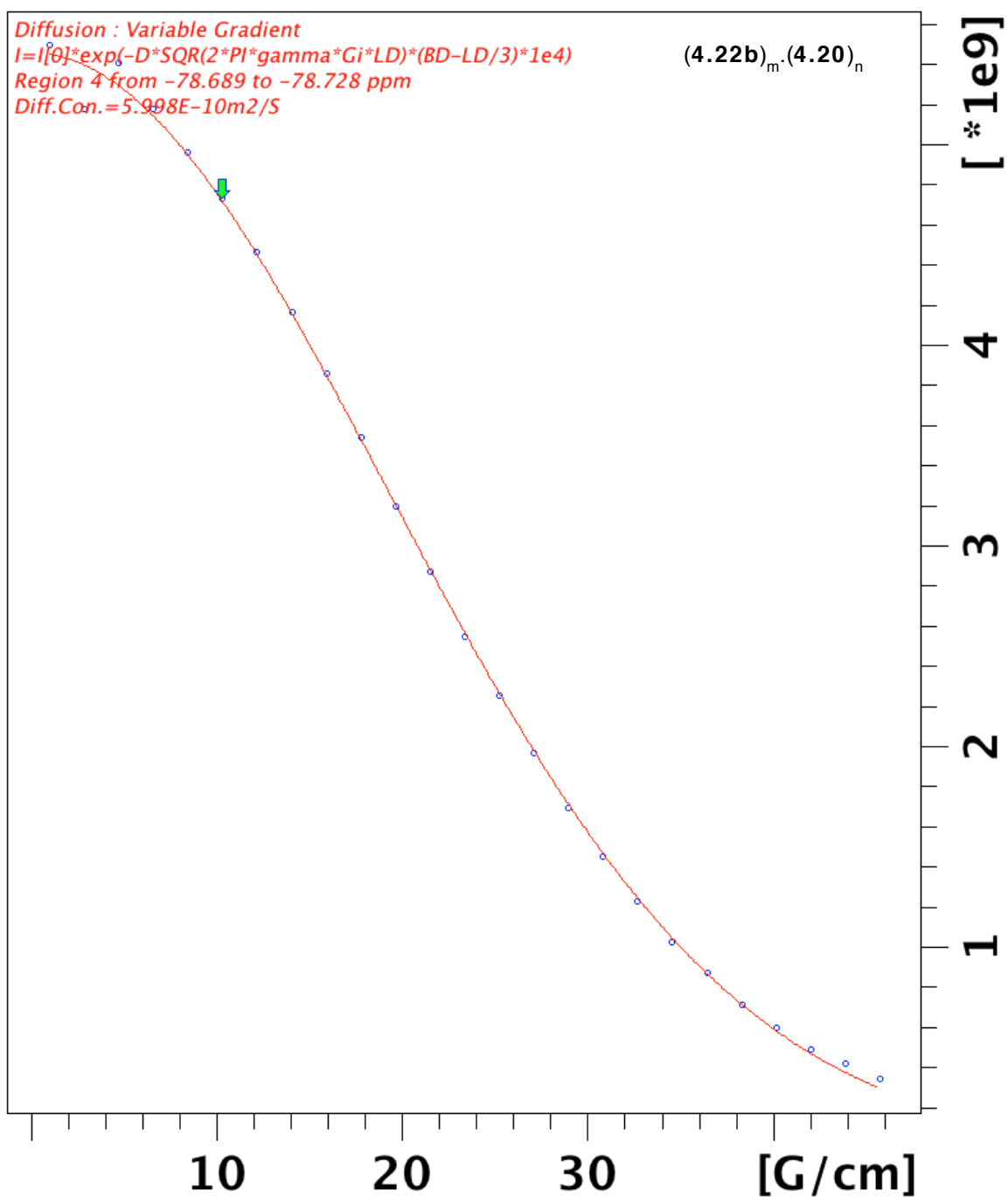
Figure 4.66. Signal attenuation curve of complex **(4.22b)$_m$.(4.20)$_n$** in a mixture of compounds **4.15-4.17**, **4.20** and acylimidazole **4.22b** in C_6D_6.
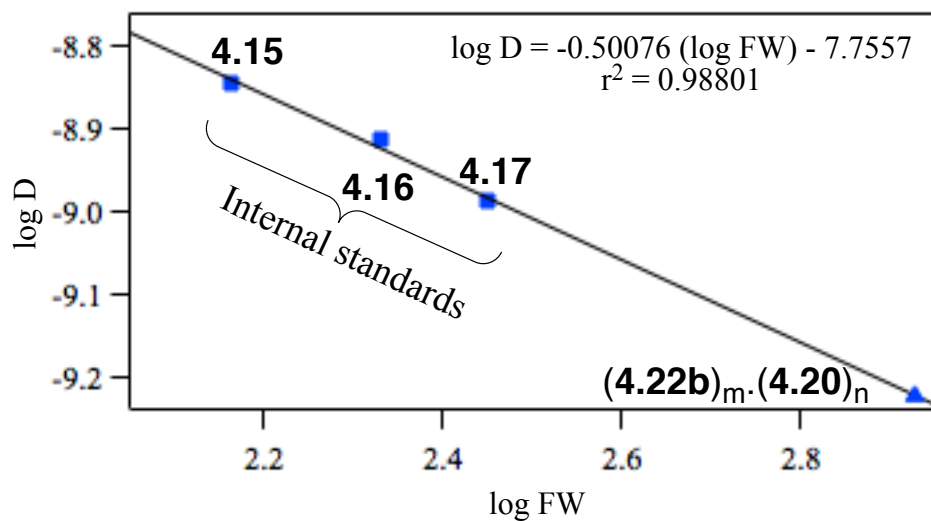
Figure 4.67. log D versus log FW analysis of ^{19}F DOSY of a mixture of **4.15-4.17**, **4.20** and acylimidazole **4.22b** in benzene-d_6.

Table 4.15. D-FW analysis of ^{19}F DOSY spectrum of compounds **4.15-4.17**, **4.20** and acylimidazole **4.22b** in C_6D_6.

Compound	FW (g mol^{-1})	$\delta(^{19}F)$ (ppm)	D (m^2 s^{-1})	FW$_{DOSY}$ (g mol^{-1})^a	% error
4.15	146	-62.5	1.434 x 10^{-9}	149	2.1
4.16	214	-63.1	1.219 x 10^{-9}	206	3.7
4.17	282	-63.0	1.028 x 10^{-10}	289	2.5
(4.22b)$_m$·(4.20)$_n$	862	-78.7	5.998 x 10^{-10}	847	1.7

^{a} log D = -0.50076 (log FW) -7.7557.
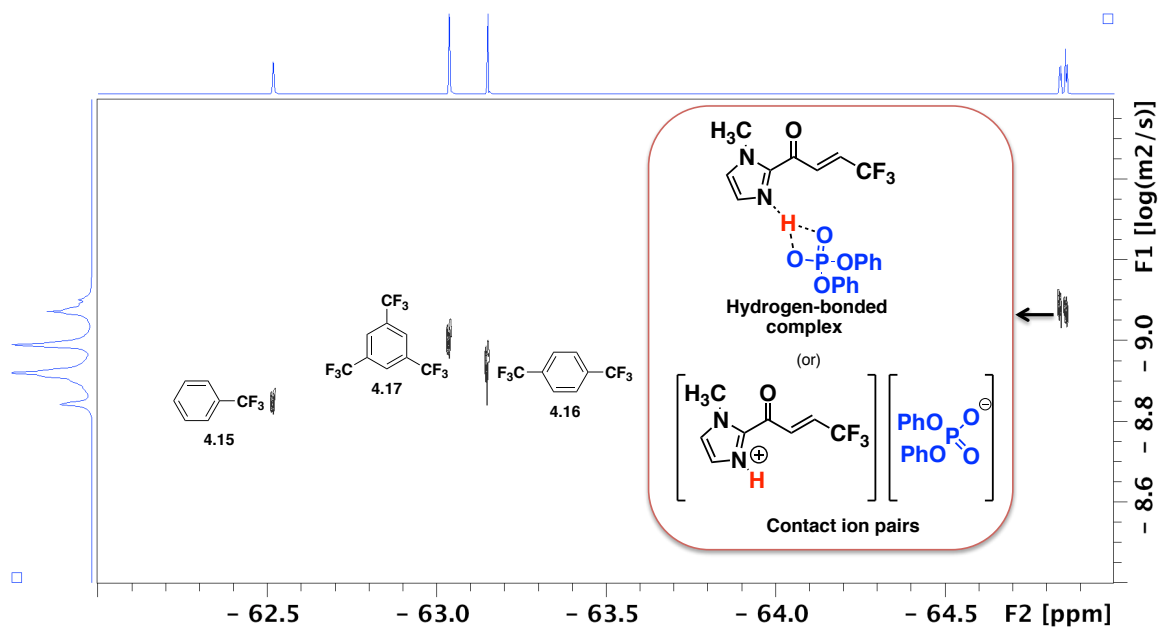
Figure 4.68. ^{19}F DOSY spectrum of a mixture of internal standards **4.15-4.17**, **4.21** and acylimidazole **4.22a** in C_6D_6.
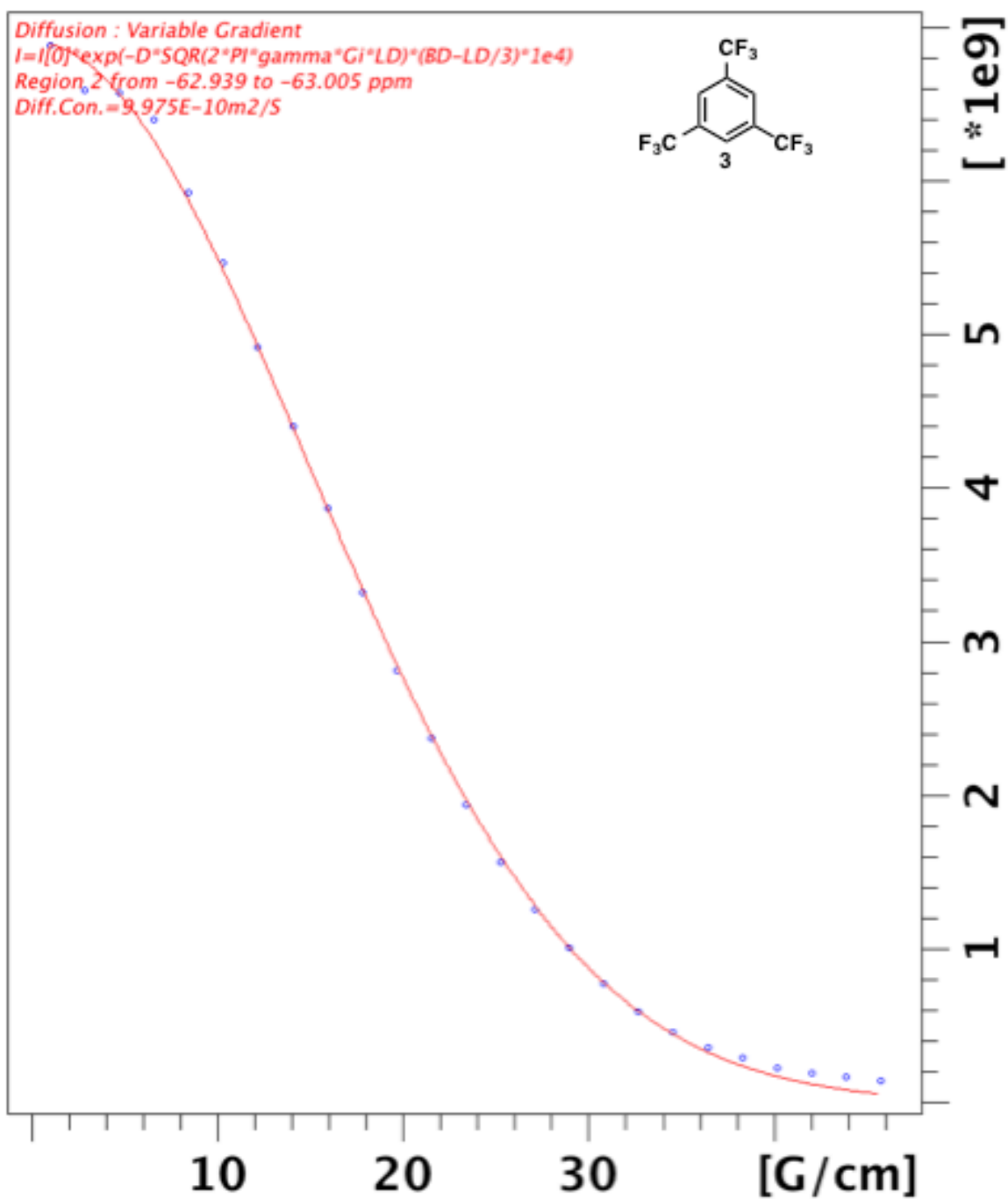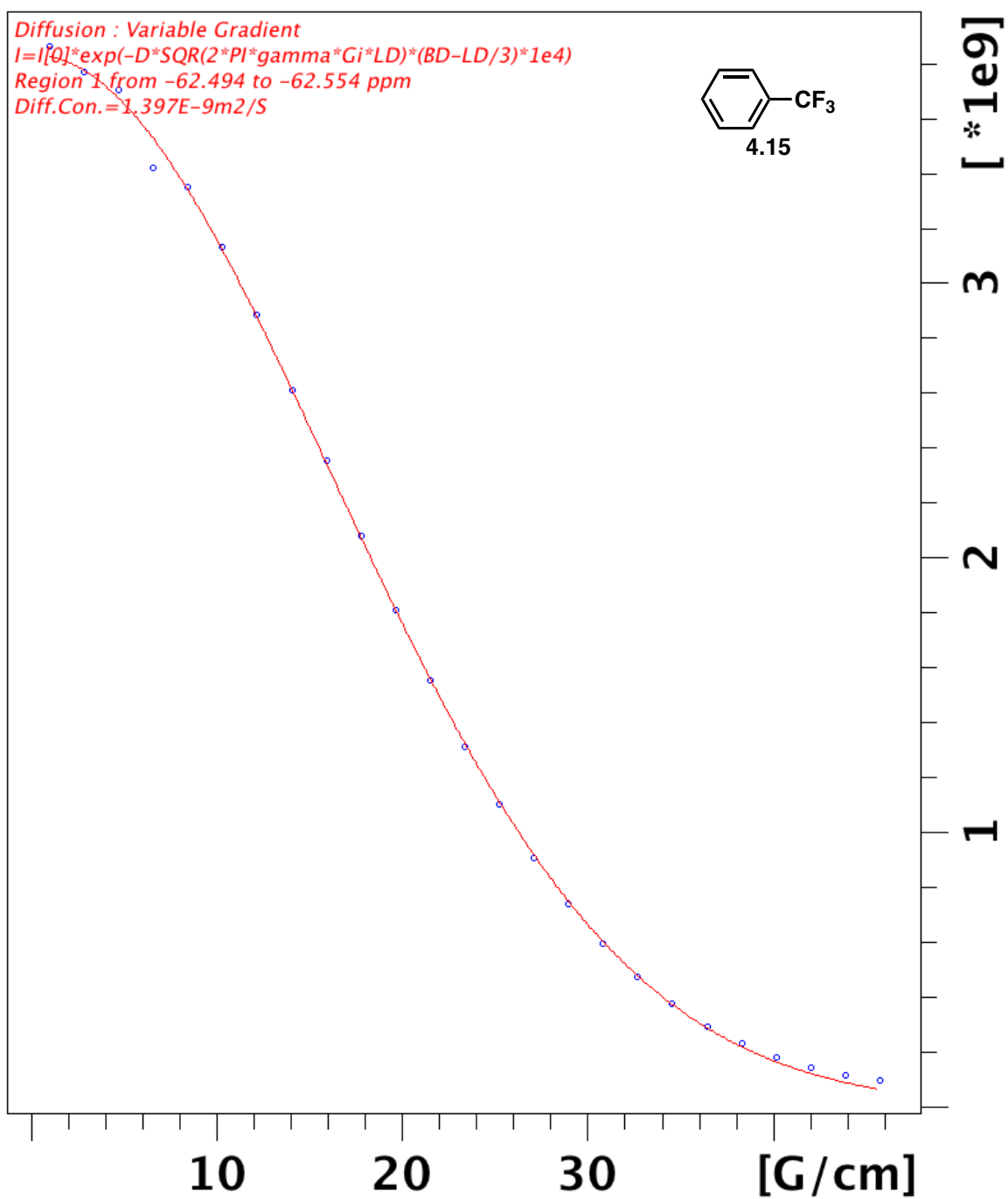
Figure 4.69. Signal attenuation curve of internal standard **4.15** in a mixture of compounds **4.15-4.17**, **4.21** and acylimidazole **4.22a** in C$_6$D$_6$.
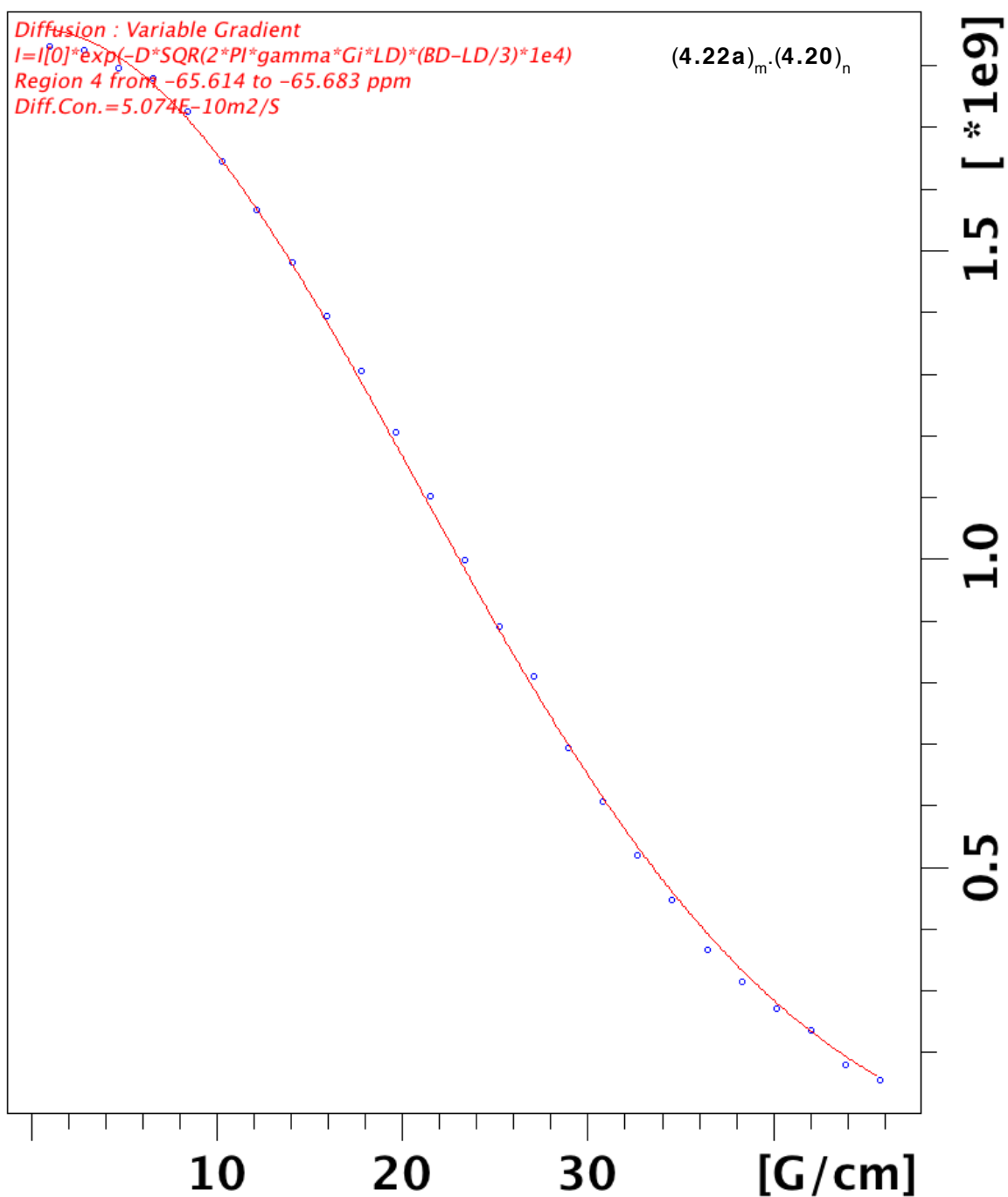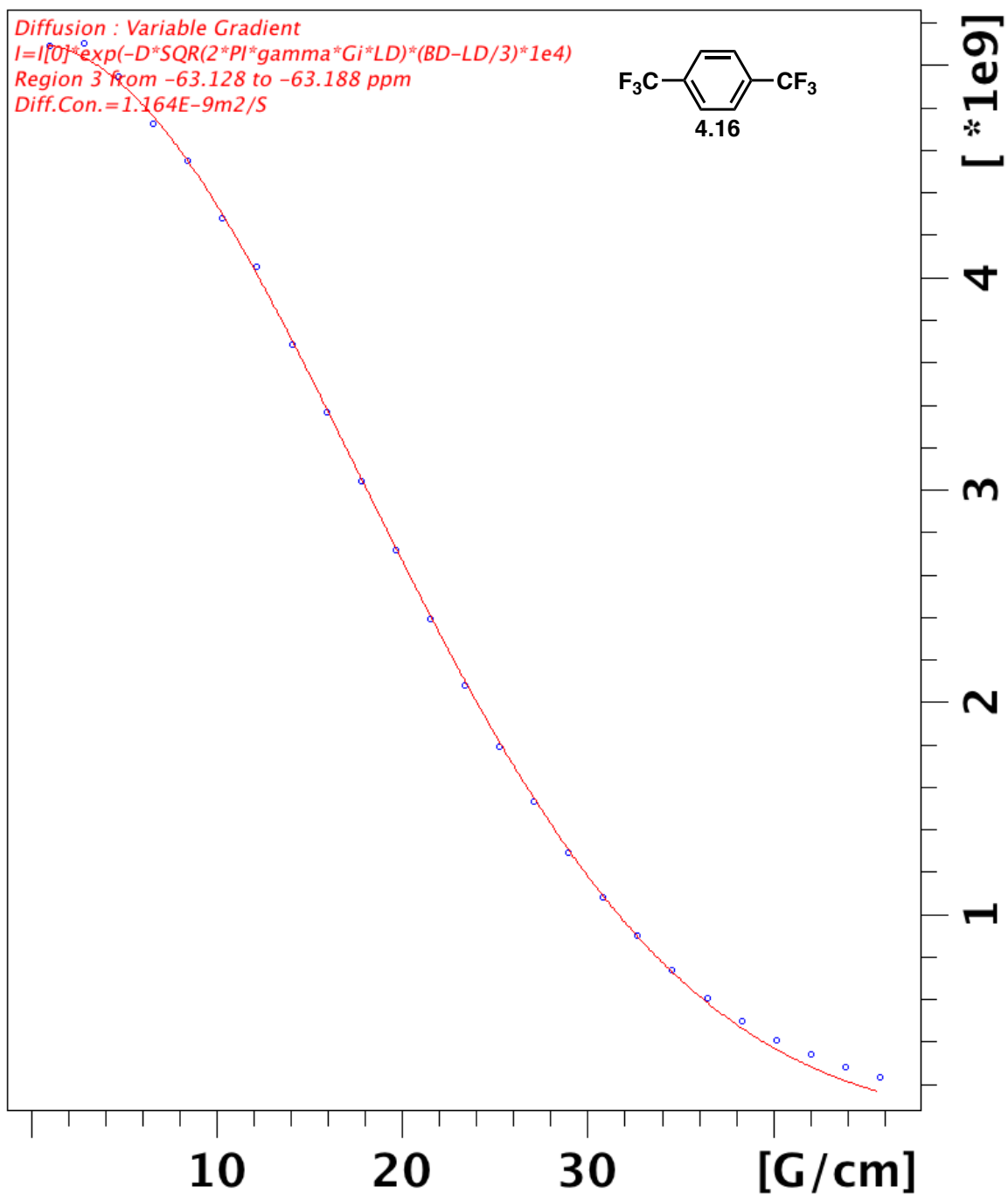
Figure 4.70. Signal attenuation curve of internal standard **4.16** in a mixture of compounds 4.**15-4.17**, **4.21** and acylimidazole **4.22a** in C_6D_6.
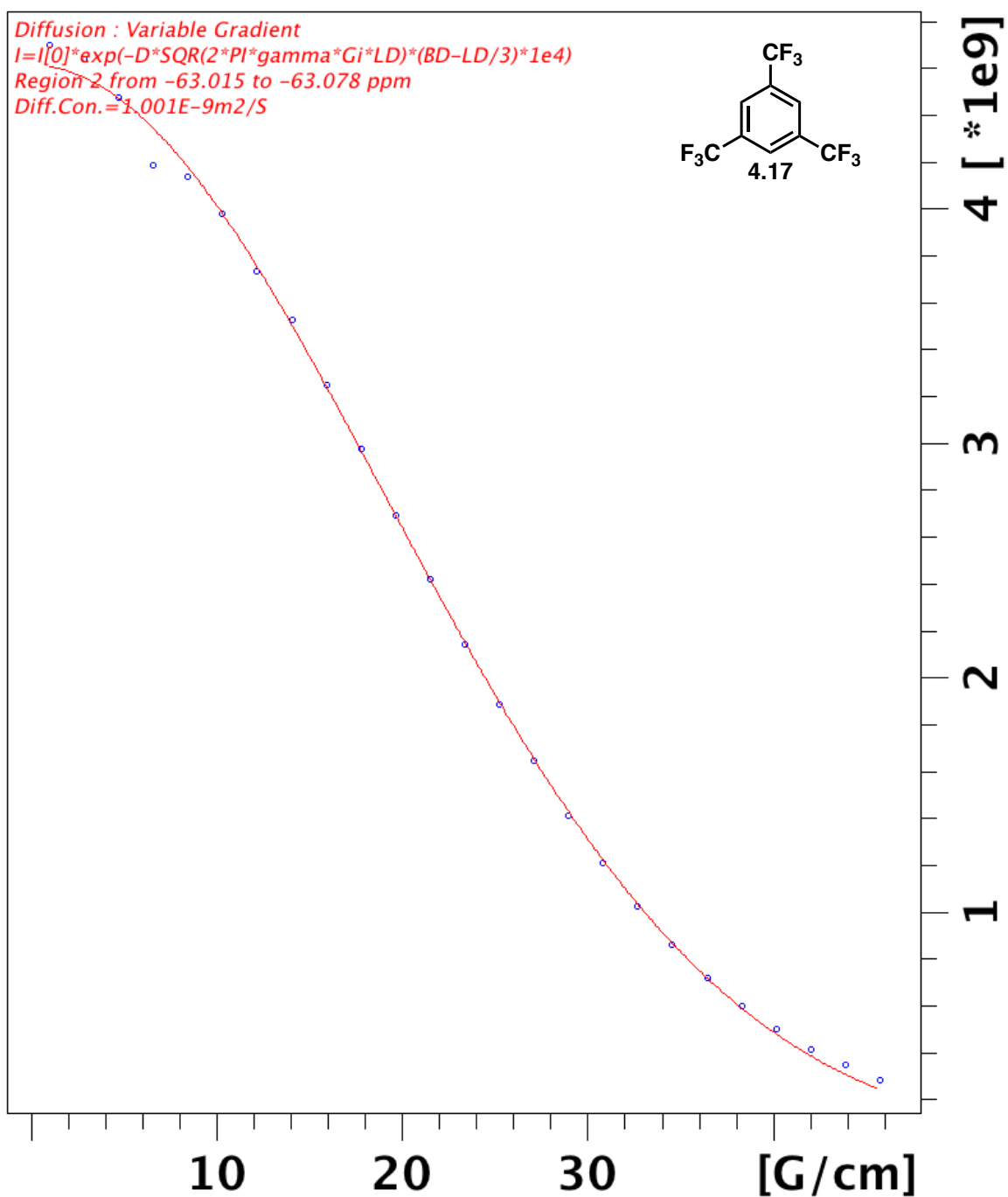
Figure 4.71. Signal attenuation curve of internal standard **4.17** in a mixture of compounds **4.15-4.17**, **4.21** and acylimidazole **4.22a** in C_6D_6.
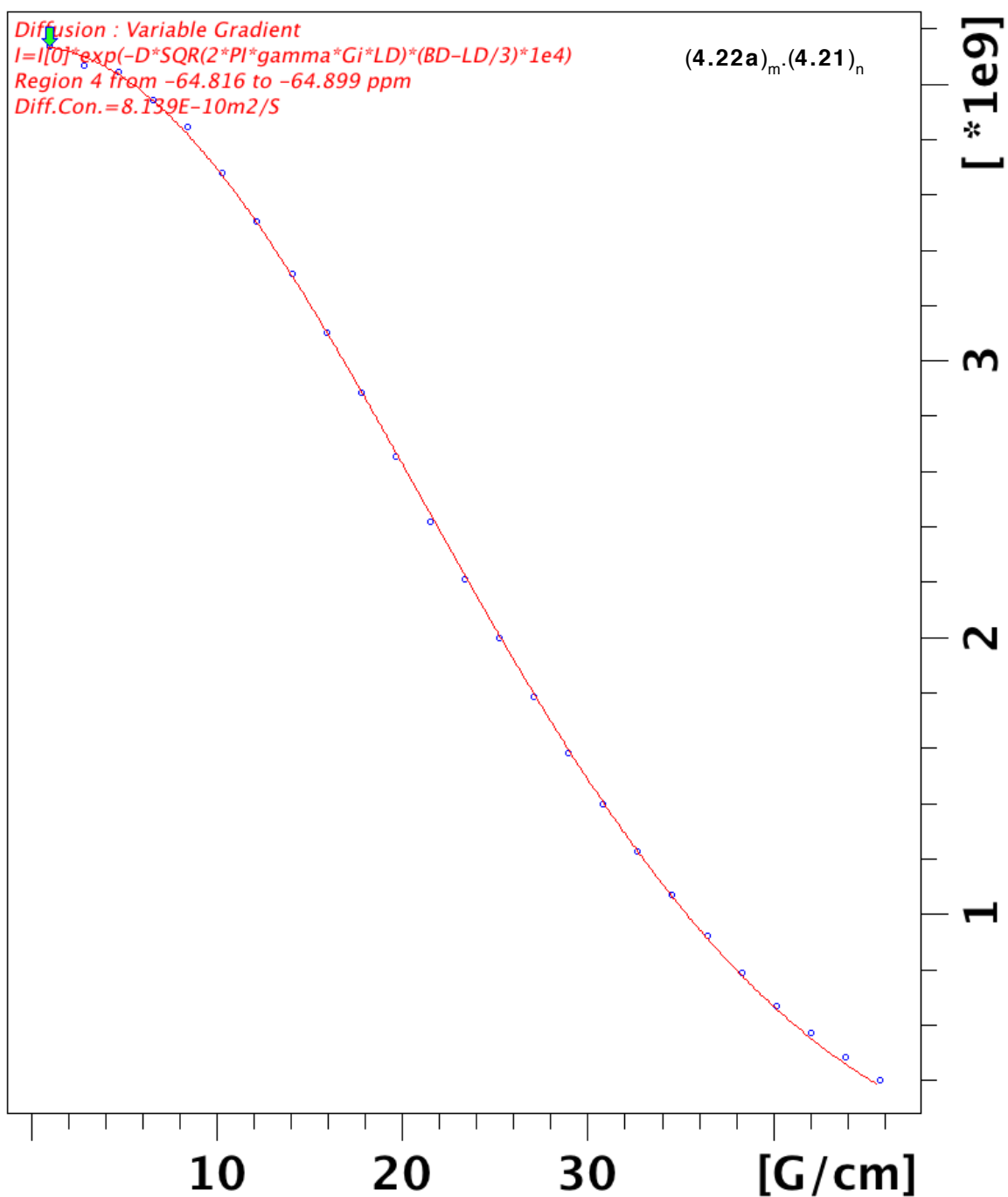
Figure 4.72. Signal attenuation curve of complex **(4.22a)$_m$.(4.21)$_n$** in a mixture of compounds **4.15-4.17**, **4.21** and acylimidazole **4.22a** in C_6D_6.
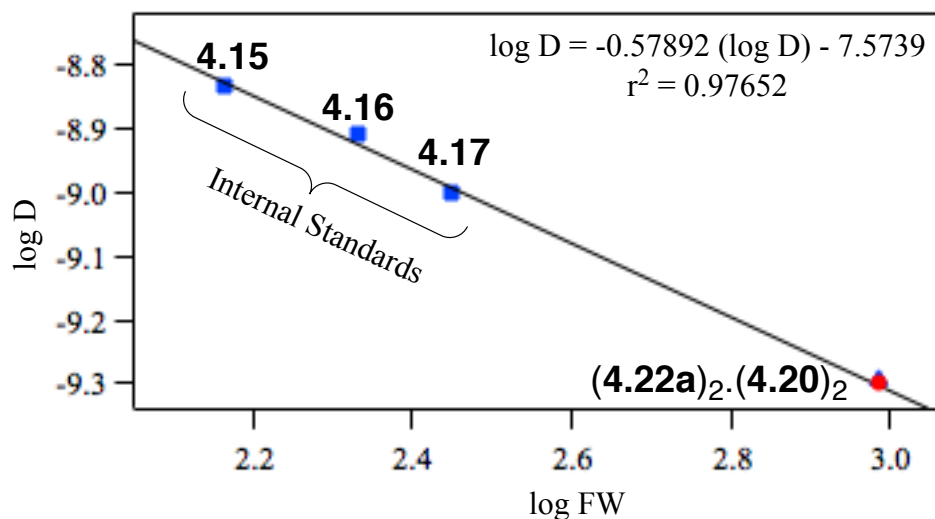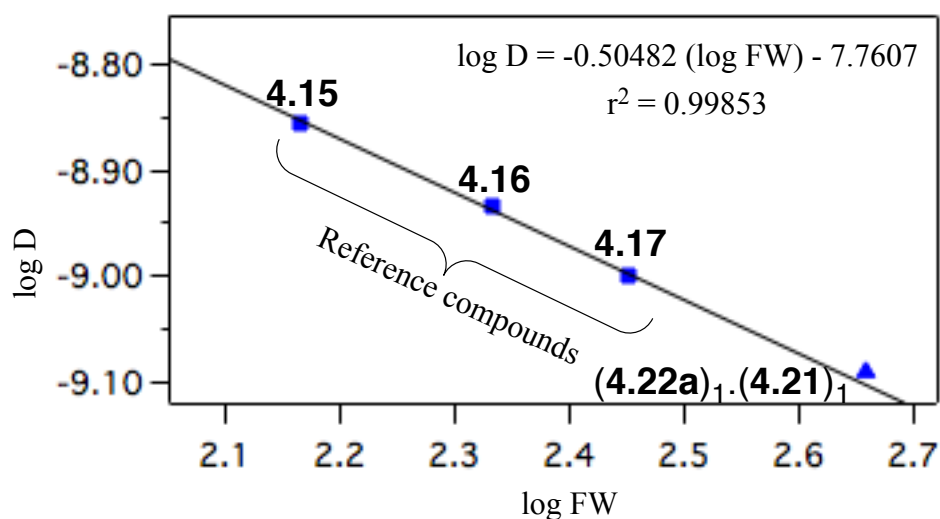
Figure 4.73. log D versus log FW analysis of ^{19}F DOSY of a mixture of **4.15-4.17**, **4.21** and acylimidazole **4.22a** in benzene-d_6.

Table 4.16. D-FW analysis of ^{19}F DOSY spectrum of compounds **4.15-4.17**, **4.21** and acylimidazole **4.22a** in C_6D_6.

Compound	FW (g mol^{-1})	$\delta(^{19}F)$ (ppm)	D (m^2 s^{-1})	FW$_{DOSY}$ (g mol^{-1})^a	% error
4.15	146	-62.5	1.397×10^{-9}	147	0.7
4.16	214	-63.1	1.164×10^{-9}	211	1.4
4.17	282	-63.0	1.001×10^{-10}	284	0.7
(4.22a)$_m$·(4.21)$_n$	454	-64.9	8.139×10^{-10}	429	5.5

^{a} log D = -0.50482 (log FW) -7.7607.

4.9. References

(1)   *Asymmetric Synthesis*; Morrison, J. D., Ed.; Academic Press: San Diego, 1985

(2)   *Catalytic Asymmetric Synthesis;* Ojima, I. Ed.; Wiley-VCH Verlag GmbH & Co. KgaA: Weinheim, 2010.

(3)   Comprehensive Asymmetric Catalysis; Jacobson, E. N.; Pfaltz, A.;Yamamoto, H. Eds. Springer-Verlag: Berlin, 2000.

(4) *Asymmetric Organocatalysis: From Biomimetic Concepts to Applications in Asymmetric Synthesis;* Berkessel, A.; Gröger, H. Eds.; Wiley-VCH Verlag GmbH & Co. KgaA: Weinheim, 2005.

(5) *Enantioselective Organocatalysis: Reactions and Experimental Procedures;* Dalko P. I. Ed.; Wiley-VCH Verlag GmbH & Co. KgaA: Weinheim, 2007.

(6) *Asymmetric catalysis on Industrial Scale: Challenges, Approaches and Solutions;* Blaser, H.; Schmidt, E. Eds.; Wiley-VCH Verlag GmbH & Co. KgaA: Weinheim, 2004.

(7) Nicolaou, K. C.; Sorensen, E. J. Classics in Total Synthesis; VCH: New York, 1996.

(8) Stejskal, E. O.; Tanner, J. E. *J. Chem. Phys.* **1965,** *42*, 288.

(9) Cohen, Y.; Avram, L.; Frish, L. *Angew. Chem., Int. Ed.* **2005,** *44*, 520.

(10) Morris, K. F.; Johson, C. S. *J. Am. Chem. Soc.* **1993,** *115,* 4291-4299.

(11) Johnson, C. S., Jr. *Prog. Nucl. Magn. Reson. Spectrosc.* **1999,** *34*, 203-256.

(12) Windig, W.; Antalek, B. *Chemom. Intell. Lab. Syst.* **1997,** 241-254.

(13) Van Gorkom, L. C. M.; Hancewicz, T. M. *J. Magn. Reson.* **1998,** 125-130.

(14) Delsuc, M. A.; Malliavin, T. E. *Anal. Chem.* **1998,** *70,* 2146-2148.

(15) Rita, S. C. O.; Pacheco, C. N.; Braga, J. P.; Pilo-Veloso, D. *J. Magn. Reson.* **2006,** *182,* 22-28.

(16) Chapman, B. E.; Kuchel, P. W. *Diffu. Fund.* **2007**, *4*, 1-15.

(17) Zhou, Y.; Zhuang, X., *Biophy. J. 91,* 4045-4053.

(18) Morris, K. F.; Johnson, C. S., Jr. *J. Am. Chem. Soc.* **1992,** *114,* 3139.

(19) Kadi, M; Dvinskikh, S. V.; Furo, I.; Almgren, M. *Langmuir* **2002**, *18*, 5015.

(20) Burini, A.; Fackler, J. P.; Galassi, R.; Macchioni, A.; Omary, M. A.; Rawashdeh-Omary, M. A.; Pietroni, B. R.; Sabatini, S.; Zuccacia, C. *J. Am. Chem. Soc.* **2002**, *124*, 4570.

(21)   (a) Zhang, Y.-P.; Lewis, R. N. A. H.; McElhaney, R. N. *Biophys. J.* **1997**, *72,* 779; (b) Bystrom, T.; Strandberg, E.; Kovacs, F. A.; Cross, T. A.; Lindblom, G. *Biochim. Biophys. Acta, Biomembr.* **2000**, *1509*, 335-345; (c) Chung, S. H.; Bajue, S.; Greenbaum, S. G. *J. Chem. Phys.* **2000**, *112*, 8515-8521; (d) Martinez-Viviente, E.; Rueegger, H.; Pregosin, P. S.; Lopez-Serrano, J. *Organometallics* **2002**, *21*, 5841-5846; (e) Martinez-Viviente, E.; Pregosin, P. S. *Helv. Chim. Acta* **2003**, *86*, 2364-2378; (f) Martinez-Viviente, E.; Pregosin, P. S.; Vial, L.; Herse, C.; Lacour, J. *Chem.--Eur. J.* **2004**, *10*, 2912-2918; (g) Fernandez, I.; Breher, F.; Pregosin Paul, S.; Fei, Z.; Dyson Paul, J. *Inorg. Chem* **2005**, *44*, 7616-23; (h) Fernandez, I.; Breher, F.; Pregosin, P. S.; Fei, Z.; Dyson, P. J. *Inorg. Chem.* **2005**, *44*, 7616-7623; (i) Fernandez, I.; Martinez-Viviente, E.; Breher, F.; Pregosin P. S. *Chemistry* 2005, *11*, 1495-506; (j) Fernandez, I.; Martinez-Viviente, E.; Breher, F.; Pregosin, P. S. *Chem.--Eur. J.* **2005**, *11*, 1495-1506; (k) Nama, D.; Anil Kumar, P. G.; Pregosin Paul, S. *Magn. Reson. Chem.* **2005**, *43*, 246-50; (l) Nama, D.; Kumar, P. G. A.; Pregosin, P. S. *Magn. Reson. Chem.* **2005**, *43*, 246-250; (m) Beves, J. E.; Chapman, B. E.; Kuchel, P. W.; Lindoy, L. F.; McMurtrie, J.; McPartlin, M.; Thordarson, P.; Wei, G. *Dalton Trans.* **2006**, 744.

(22)   Harris, R. K.; Kinnear, K. A.; Morris, G. A. Stchedroff, M. J.; Samadi-Maybadi, A. *Chem. Commun.* **2001**, 2422-2426.

(23)   Guang, J.; Hopson, R.; Williard, P. G. *J. Org. Chem.* **2015**, *80*, 9102.

(24)   (a) Fernandez, I.; Martinez-Viviente, E.; Pregosin Paul, S. *Inorg. Chem.* **2004**, *43* , 4555-7; (b) Fernandez, I.; Martinez-Viviente, E.; Breher, F.; Pregosin, P. S. *Chem.--Eur. J.* **2005**, *11*, 1495-1506.

(25)   Martinez-Viviente, E.; Ruegger, H.; Pregosin, P. S.; Lopez-Serrano, J. *Organometallics* **2002**, *21*, 5841-5843.

(26)   Nama, D.; Kumar, P. G. A.; Pregosin, P. S. *Magn. Reson, Chem.* **2005**, *43*, 246-250.

(27)   (a) Li, D.; Sun, C.; Williard, P. G., *J. Am. Chem. Soc.* **2008**, *130* (35), 11726-11736; (b) Oda, Y.; Matsuda, S.; Yamanoi, T.; Murota, A.; Katsuraya, K., *Supramol. Chem.* **2009**, *21* (7), 638-642.

(28)   Schlörer, N. E.; Cabrita, E. J.; Berger, S. *Angew. Chemie Intl. Ed.* **2002**, *41*, 107-109.

(29)   Guang, J.; Hopson, R.; Williard, P. G. *J. Org. Chemistry* **2015**, *80*, 9102-9107.

(30)   Jang, H. B.; Rho, H. S.; Oh, J. S.; Nam, E. H.; Park, S. E.; Bae, H. Y.; Song, C. E. *Org. & Biomol. Chem.* **2010**, *8*, 3918-3922.

(31)   (a) Sibi, M. P.; Itoh, K. *J. Am. Chem. Soc.* **2007,** *129*, 8064. (b) Sibi, M. P.; Ji, J.; Wu, J. H.; Gürtler, S.; Porter, N. A. *J. Am. Chem. Soc.* **1996,** *118*, 9200. (c) Sibi, M. P.; Kawashima, K.; Stanley, L. M. *Org. Lett.* **2009**, *11*, 3894. (d) Sibi, M. P.; Yang, Y.; Lee, S. *Org. Lett.* **2008,** *10*, 5349.

(32)   (a) Sibi, M. P.; Ji, J. *J. Am. Chem. Soc.* **1996,** *118*, 3063. (b) Sibi, M. P.; Stanley, L. M.; Xiaoping, N.; Venkatraman, L.; Liu, M.; Jasperse, C. P. *J. Am. Chem. Soc.* **2007,** *129*, 395.

(33)   (a) Akiyama, T. *Chem. Rev.* **2007,** *107*, 5744. (b) Parmar, D.; Sugiono, E.; Raja, S.; Rueping, M. *Chem. Rev.* **2014,** *114*, 9047.

(34)   Brønsted acids activate substrates through several modes: hydrogen bonding, simple acid-base interactions or ion pairing: Fleischmann, M.; Drettwan, D.; Sugiono, E.; Rueping, M. *Angew. Chem., Int. Ed.* **2011,** *50*, 6364.

(35) (a) Mayer, S.; List, B. *Angew. Chem., Int. Ed.* **2006,** *45*, 4193. (b) Hamilton, G. L.; Kang, E. J.; Mba, M.; Toste, D. F. *Science,* **2007,** *317*, 496. (c) Rueping, M.; Antonchick, A. P.; Brinkmann, C. *Angew. Chem., Int. Ed.* **2007,** *46*, 6903. (d) Brak, K.; Jacobsen, E. N. *Angew. Chem., Int. Ed.* **2013,** *52*, 534. (e) Mahlau, M.; List, B. *Angew. Chem., Int. Ed.* **2013,** *52*, 518.

(36) (a) Bellachioma, G.; Ciancaleoni, G.; Zuccaccia, C.; Zuccaccia, D.; Macchioni, A. *Coord. Chem. Rev.* **2008,** *252*, 2224. (b) Pregosin, P. S.; Anil Kumar, P. G.; Fernández, I. *Chem. Rev.* **2005,** *105*, 2977.

(37) (a) Anil Kumar, P. G.; Pregosin, P. S. *Organometallics* **2004,** *23*, 5410. (b) Martinez-Viviente, E.; Pregosin, P. S. *Inorg. Chem.* **2003,** *42*, 2209. (c) Beaulieu, L-P. B.; Roman, D. S.; Vallée F.; Charette, A. B. *Chem. Commun.* **2012**, *48*, 8249.

(38) Li, D.; Keresztes, I.; Hopson, R.; Williard, P. G. *Acc. Chem. Res.* **2009,** *42*, 270.

(39) Chen, A.; Wu, D.; Johnson, C. S., Jr. *J. Am. Chem. Soc.* **1995,** 117, 7965.

(40) (a) Li, D.; Kagan, G.; Hopson, R.; Williard, P. G. *J. Am. Chem. Soc.* **2009,** *130*, 11726. (b) Li, D.; Hopson, R.; Li, W.; Liu J.; Williard, P. G. *Org. Lett.* **2008,** *10*, 909. (c) Kagan, G.; Li, W.; Hopson, R.; Williard, P. G. *Org. Lett.* **2009,** *11*, 4818. (d) Li, W.; Kagan, G.; Hopson, R.; Williard, P. G. *ARKIVOC* **2011,** 180.

(41) Wu, D.; Chen, A.; Johnson, C. S., Jr. *J. Magn. Reson., Ser. A* **1995,** *115*, 123.

(42) Trifluoroacetic acid exists as a monomer in aromatic solvents: Kriszenbaum, M.; Corset, J.; Josien, M. L. *J. Phys. Chem.* **1971,** *75,* 1327.

(43) (a) Evans, D. A.; Fandrick, K. R.; Song, H. *J. Am. Chem. Soc.* **2005,** *127*, 8942. (b) Sibi, M. P.; Dunkle, K. L.; Rane, D. *Heterocycles* **2014,** *88*, 1639. (c) Yoshida, M.; Ohmiya, H.; Sawamura, M. *J. Am. Chem. Soc.* **2012,** *134*, 11896. (d) Trost, B. M.; Lam, T. M. *J. Am.*

Chem. Soc. **2012,** *134,* 11319. (e) Boersma, A. J.; Feringa, B. L.; Roelfes, G. *Org. Lett.*

2007, *9*, 3647. (f) Tyson, E. L.; Farney, E. P.; Yoon, T. P. *Org. Lett.* **2012,** *14*, 1110. (g)

Xu, X.; Hu, W-H.; Doyle, M. P. *Angew. Chem., Int. Ed.* **2011,** *50*, 6392. (h) Guan, X-Y.;

Yang, L-P.; Hu, W. *Angew. Chem., Int. Ed.* **2010,** *49*, 2190.

(44)   Storer, R. I.; Carrera, D. E.; Ni, Y.; MacMillan, D. W. C. *J. Am. Chem. Soc.* **2006,** *128,* 84.

(45)   Tang, W.; Johnston, S.; Iggo, J. a; Berry, N. G.; Phelan, M.; Lian, L.; Bacsa, J.; Xiao, J.

Angew. Chem., Int. Ed. **2013,** *52,* 1668.

(46)   Kim, H.; Sugiono, E.; Nagata, Y.; Wagner, M.; Bonn, M.; Rueping, M.; Hunger, J. *ACS*

Catal. **2015,** *5,* 6630.

(47)   Merten, C.; Pollok, C. H.; Liao, S.; List, B. *Angew. Chem., Int. Ed.* **2015,** *54,* 8841.

(48)   Fleischmann, M.; Drettwan, D.; Sugiono, E.; Rueping, M.; Gschwind, R. M. *Angew.*

Chem., Int. Ed. **2011,** *50,* 6364.

(49)   Sorgenfrei, N.; Hioe, J.; Greindl, J.; Rothermel, K.; Morana, F.; Lokesh, N.; Gschwind, R.

M. *J. Am. Chem. Soc.* **2016,** *138,* 16345.

(50)   Takeda, N.; Sibi, M. P. unpublished data.

(51)   Rane, D. S.; Sibi, M. P. unpublished data.

(52) Rane, D. S.; Yang, Y.; Subramanian, H.; Ugrinov, A.; Sibi, M. P. *Angew. Chemie., Intl. Ed.*

in preparation.

(53)   Dorn, H.; Otto, A. *Angew. Chem., Intl. Ed.* **1968,** *7,* 214.

(54)   (a) Holmes, R. E.; Neel, D. A. *Tetrahedron Lett.* **1990**, *31*, 5567. (b) Ternansky, R. J.;

Draheim, S. E.; Pike, A. J.; Counter, F. T.; Eudaly, J. A.; Kasher, J. S. *J. Med. Chem.* **1993**,

36, 3224.

(55)   a) Chen, W.; Du, W.; Duan, Y.-Z.; Wu, Y.; Yang, S.-Y.; Chen, Y.-C. *Angew. Chem., Int. Ed.* **2007,** *46,* 7667. (b) Suga, H.; Funyu, A.; Kakehi, A. *Org. Lett.* **2007,** *9,* 97. (c) Suárez, A.; Downey, C. W.; Fu, G. C. *J. Am. Chem. Soc.* **2005,** *127,* 11244. (d) Shintani, R.; Fu, G. C. *J. Am. Chem. Soc.* **2003,** *125,* 10778. (e) Sibi, M. P.; Rane, D.; Stanley, L. M.; Soeta, T. *Org. Lett.* **2008,** *10,* 2971. (f) Najera, C.; Sansano, J. M.; Yus, M. *Organic & Biomolecular Chemistry* **2015**, *13*, 8596.

(56) Stereodivergence in cycloadditions, selected examples: (a) Kim, H. Y.; Li, J.-Y.; Kim, S.; Oh, K. *J. Am. Chem. Soc.* **2011**, *133*, 20750. (b) Maroto, E. E.; Filippone, S.; Martín-Domenech, A.; Suarez, M.; Martín, N. *J. Am. Chem. Soc.* **2012**, *134*, 12936. (c) Abbasov, M. E.; Hudson, B. M.; Tantillo, D. J.; Romo, D. *J. Am. Chem. Soc.* **2014**, *136*, 4492. (d) Mei, L.-Y.; Wei, Y.; Tang, X.-Y.; Shi, M. *J. Am. Chem. Soc.* **2015**, *137*, 8131. (e) Qi, C.; Xiong, Y.; Eschenbrenner-Lux, V.; Cong, H.; Porco, J. A. Jr. *J. Am. Chem. Soc.* **2016**, *138*, 798.

(57)   Subramanian, H.; Jasperse, C. J.; Sibi, M. P. *Org. Lett.* **2015,** *17,* 1429.

(58)   Brønsted acids activate dipoles in inverse electron-demand [3+2] cycloadditions: (a) Jiao, P.; Nakashima, D.; Yamamoto, H. *Angew. Chem., Intl. Ed.* **2008,** *47,* 2411. (b) Hashimoto, T.; Omote, M.; Maruoka, K. *Angew. Chem., Intl. Ed.* **2011,** *50,* 3489. (c) Hong, X.; Küçük, H. B.; Maji, M. S.; Yang, Y. F.; Rueping, M.; Houk, K. N. *J. Am. Chem. Soc.* **2014,** *136,* 13769.

(59)   Hong, L.; Kai, M.; Wu, C.; Sun, W.; Zhu, G.; Li, G.; Yao, X.; Wang, R. *Chem. Commun.* **2013,** *49,* 6713.

(60) Sickert, M.; Abels, F.; Lang, M.; Sieler, J.; Birkemeyer, C.; Schneider, C. *Chem. – Eur. J.* 2010, *16*, 2806.

CHAPTER 5. FUTURE OUTLOOK ON 2-ACYLIMIDAZOLES: APPLICATIONS IN SYNTHETICALLY USEFUL ORGANIC TRANFORMATIONS

5.1. Introduction

Enantioselective catalysis is and always will be at the forefront of stereoselective organic synthesis.[1] A simple, but effective way of controlling the stereoselectivity of an organic transformation is through the use of templated acceptors. Sibi et al. have made several noteworthy contributions to the development of catalytic enantioselective methodologies applicable to acyclic systems based on achiral templates.[2] Over the past decade or so our group has developed novel imidazole (particularly N-alkoxyimidazole) based templates for asymmetric cataltic reactions (Chapter 3). Although highly enantioselective construction of all carbon quaternary center using imidazole templates using catalytic FC alkylation reaction is promising, there remain many promising avenues for future research.

5.2. Results and discussions

5.2.1. Evaluation of acylimidazoles in FC alkylation of N-methylpyrrole

The FC has been one of the most studied reactions. Although the scope and the utility of the reaction has been significantly expanded, the asymmetric FC reactions of tiglate type substrates such as **5.1** are virtually non-existent. In addition to enantioselective conjugate addition of FC nucleophile, the asymmetric reaction is complicated by diastereoselective protonation at the α-position (Scheme 5.1). During the process two contiguous stereocenters are formed. Hence control of relative as well as absolute stereochemistry is necessary for an efficient asymmetric catalytic process.
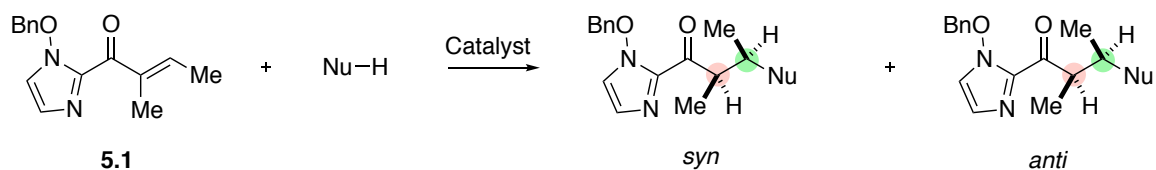
Scheme 5.1. Nucleophilic addition to tiglate-type substrates.

We have successfully demonstrated that FC nucleophiles could be added to β,β-disubstituted-α,β-unsaturatedacylimidazoles (Chapter 3) and enantioselective α-protonation could be achieved during FC alkylation using isoxazolidinone templates.[3] We hypothesize that these two processess (enantioselective conjugate addition and diastereoselective protonation) could be merged together to give highly diastereoselective (relative stereochemistry: *syn* Vs *anti*) and enantioselective (absolute stereochemistry) methodology using N-alkoxyimidazole templates.

We chose alkylation of N-methylpyrrole as a model reaction. A survey of chiral Lewis was performed for the FC alkylation of N-methylpyrrole. The results are summarized in Table 5.1. The chiral Lewis acid formed by the combination of Cu(OTf)$_2$/**5.5** does not catalyze the FC reaction (entry # 1, Table 5.1). The chiral Lewis acid formed by the combination of Sc(OTf)$_3$ and pyridine bisoxazoline ligands (**5.3** or **5.4**) did not effect the reaction (entry # 2 and # 3, Table 5.1). A combination of Yb(OTf)$_3$/**5.3** gave the alkylated product in very poor yield as a mixture of diasteromers (dr not determined, entry # 4, Table 5.1). A change of ligand to **5.4** was essential in realizing the FC alkylation of N-methylpyrrole (entry # 5, Table 5.1). The reaction was complete in 3 days. The alkylated product **5.2** was obtained as 3:1 mixture of diastereomers (entry # 5, Table 5.1). The relative stereochemistry of the major and minor diastereomers was not assigned. The ee of the two diastereomers were also not determined.

Table 5.1. Survey of chiral Lewis acids for diastereoselective and enantioselective FC alkylation of N-methylpyrrole.
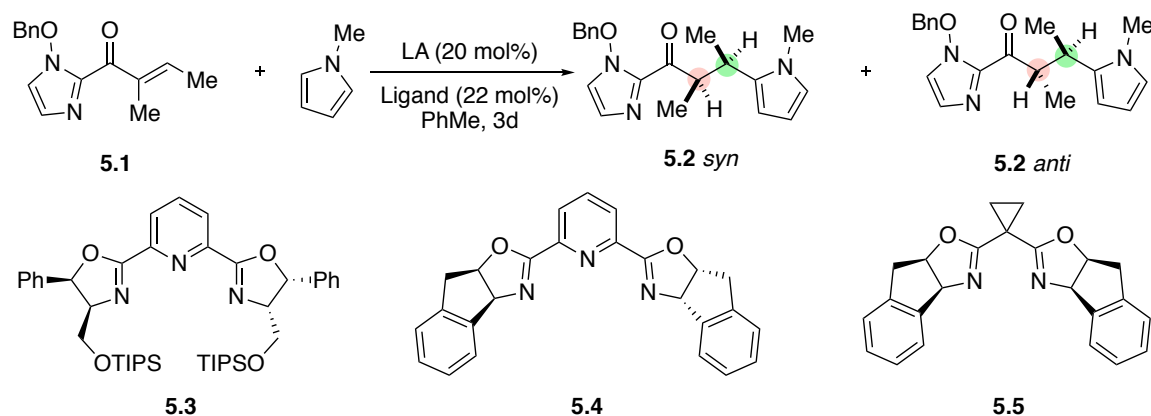
Entry	LA	Ligand	time	Yield (%)[a]	dr of 5.2[b]
1	Cu(OTf)$_2$	**5.5**	5d	-	-
2	Sc(OTf)$_3$	**5.4**	5d	-	-
3	Sc(OTf)$_3$	**5.3**	5d	-	-
4	Yb(OTf)$_3$	**5.4**	5d	10	nd
5	Yb(OTf)$_3$	**5.3**	3d	78	75:25

Reaction conditions: **5.1** (0.1 mmol), N-methylpyrrole (0.2 mmol), LA (0.02 mmol), **L** (0.022 mmol) toluene (2 mL) were stirred at rt. [a] isolated yield. [b] determined by ^{1}H NMR analysis of crude reaction mixture. nd = not determined.

In future we propose to determine the relative sterochemistry and %ee for the major and minor isomers. At present the diastereoselectivity of the alkylated product is only moderate. We plan to improve stereoselectivity of the FC alkylation by studying the effect of other parameters such as ligands, temperature and solvents. Once an optimized condition has been identified, acylimidazole scope (with different substituents on the α and β position of the acyl imidazoles) (Scheme 5.2) and pyrrole scope will be studied in detail.
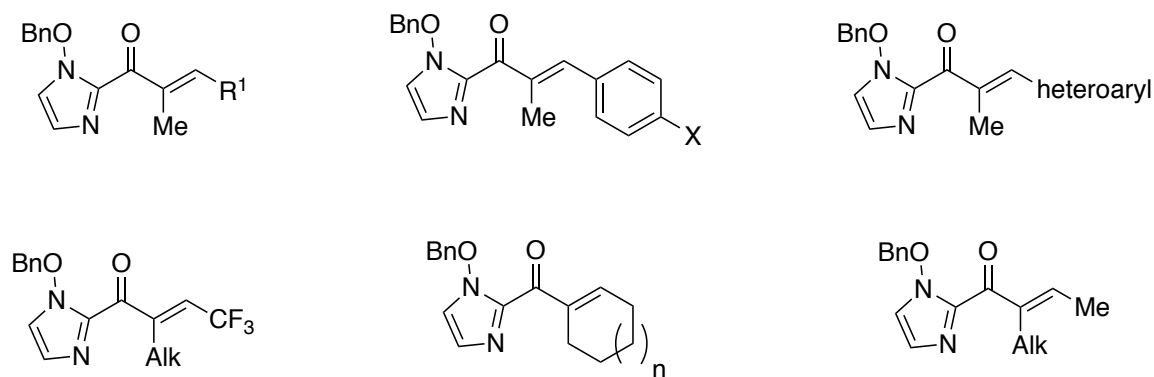
Scheme 5.2. Potential substrates for FC alkylation.

5.2.2. Diastereoselective and enantioselective Mukaiyama-Michael (MM) reaction

Enolate alkylation is a reaction of great significance in synthetic organic chemistry. Compounds such as silyl enol ethers and silyl ketene acetals are important synthetic intermediates in organic chemistry. These compounds are characterized by enolate bonded to an organosilicon group through the oxygen atom and are generally used as masked equivalents of enolates in organic transformations. Asymmetric conjugate addition of these pronucleophiles (silyl ketene acetals) is an alternate way of adding enolates.[4] Lactones and lactams are ubiquitous structural motifs present in several biologically active natural products. Owing to our interest in enantioselective construction of all carbon quaternary centers, we chose to investigate alkylation of lactone an important C-C bond forming reaction using silyl ketene acetals as pronucleophiles.

Initially, we screened several chiral Lewis acids in asymmetric Mukaiyama-Michael reaction of silyl ketene acetal of α-methyl-γ-butyrolactone **5.6** and acylimidazole β-substituted-α,β-unsaturated acylimidazole **5.7** (Table 5.2). The chiral Lewis acid formed by the combination of Cu(OTf)$_2$/**5.5** does not catalyze the MM reaction (entry # 1, Table 5.2). The combination of Ni(ClO$_4$).6H$_2$O/**5.9** also failed to catalyze the MM reaction between silyl ketene acetal **5.6** and and acyl imidazole **5.7** (entry # 2, Table 5.2). The chiral Lewis acid formed by the combination of Sc(OTf)$_3$ and pyridine bisoxazoline ligands (**5.3** or **5.4** or **5.10**) did not effect the reaction

193

(entry # 3, # 4 and # 5, Table 5.2). A combination of Yb(OTf)$_3$/**5.3** gave the alkylated product **5.8**

in high yield (90%) with very high diastereoselectivity (dr = 19:1) and low enantioselectivity (20

% ee; entry # 6, Table 5.2). A change of ligand to **5.10** gave the lactone alkylated product **5.8** in

very high yield, diastereoselectivity and excellent enantioselectivity for the major isomer (er =

90:10, entry # 7, Table 5.2).

Table 5.2. Chiral Lewis acids survey for diastereoselective and enantioselective MM reaction of silyl ketene acetal and β-substituted-α,β-unsaturated acylimidazole.
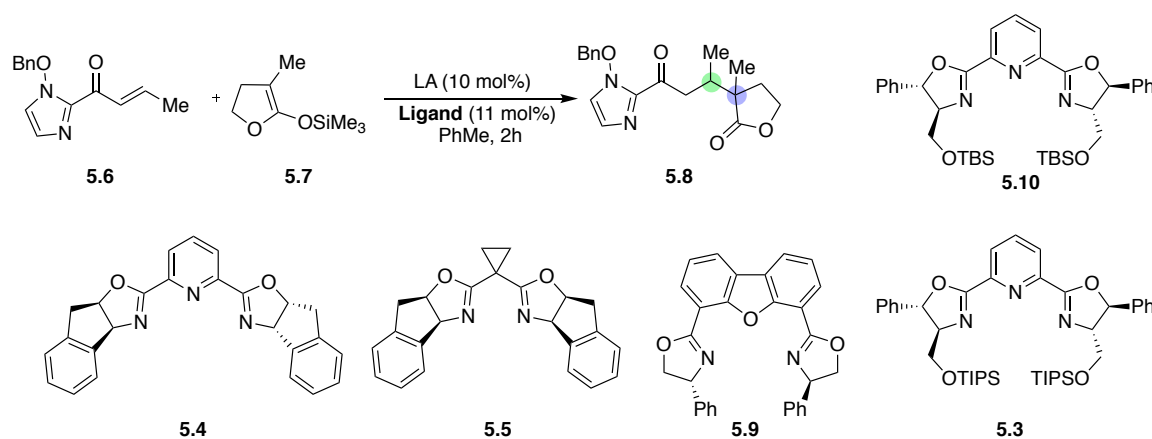
Entry	LA	Ligand	time (h)	Yield (%)[a]	dr of 5.8[b]	er of **5.8** (major isomer)[c]
1	Cu(OTf)$_2$	**5.5**	24	-	-	-
2	Ni(ClO$_4$).6H$_2$O	**5.9**	24	-	-	-
3	Sc(OTf)$_3$	**5.4**	24	-	-	-
4	Sc(OTf)$_3$	**5.3**	24	-	-	-
5	Yb(OTf)$_3$	**5.4**	2	90	19:1	60:40
6	Yb(OTf)$_3$	**5.10**	2	92	19:1	90:10

Reaction conditions: **5.6** (0.1 mmol), **5.7** (0.2 mmol), LA (0.01 mmol), **L** (0.011 mmol) toluene (2 mL) were stirred at rt. [a] isolated yield. [b] determined by ^{1}H NMR analysis of crude reaction mixture. [c] determined by chiral HPLC.

These initial results indicate the possibility of developing a chiral Lewis acid catalyzed

highly diastereoselective and enantioselective MM reaction. Two contiguous stereocenters (an

all carbon-quarternary center and a tertiary center) could be constructed with very high control

over relative and absolute stereochemistry.

We also investigated the possibility of nucleophilic addition of silyl ketene acetal **5.7** to

β,β-disubstituted-α,β-unsaturated acylimidazole **5.11** (Scheme 5.3). We adopted chiral Lewis

acid condition that is used for MM addition to β-substituted-α,β-unsaturated acylimidazoles.

Yb(OTf)$_3$/**5.10** combination effected the conjugate addition of pronucleophile **5.7** to **5.11**: the

alkylated lactone **5.12** was obtained in 78% yield with moderate diastereoselectivity (dr = 60:40).

The relative stereochemistry of the major and minor diastereomers was not assigned. The ee of

the two diastereomers were also not determined.
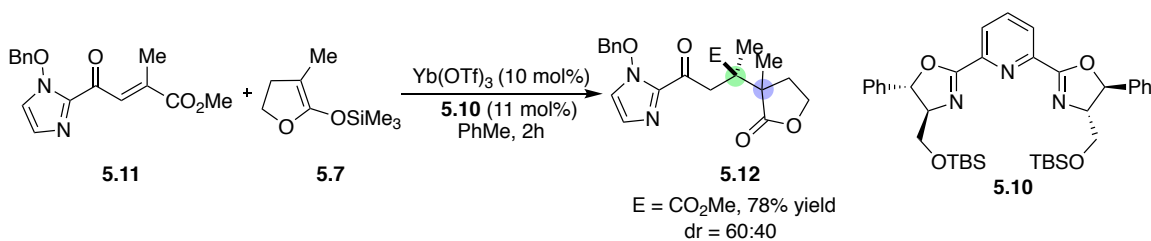
Scheme 5.3. Chiral Lewis acid catalyzed MM reaction for the construction of two contiguous all carbon-quaternary centers.

Future directions will include the determine the relative sterochemistry and %ee for the

of the major and minor isomers. At present the diastereoselectivity of the alkylated lactone

product **5.12** is only moderate. The stereoselectivity of MM reaction could be further improved

by studying the effect of other parameters such as ligands, temperature and solvents. Once an

optimized condition has been identified, acylimidazole scope (with different substituents on the

β position of the acylimidazoles) and silyl ketene acetal scope will be studied in detail.

Butenolides are another class of nucleophiles that is extensively studied in MM reactions.

The γ-butenolide addition to β-substituted-α,β-unsaturated carbonyl compounds are well

documented in the literature.[5] However, γ-butenolide addition to β,β-disubstituted-α,β-

unsaturated systems are not reported. We found that Yb(OTf)$_3$/**5.3** combination was effective in

catalyzing MM reaction of 2-(trimethylsilyloxy)furan and β,β-disubstituted-acylimidazoles

5.13a-c. The results are shown in Table 5.3. γ-alkylated butenolides **5.14a-c** were obtained in

high yield (>95%), good diastereoselectivity (dr = 4:1 to 92:08) and excellent enantioselectivity

for the major isomer (> 95% ee).[6]

Table 5.3. Acylimidazole scope in chiral Lewis acid catalyzed MM of 2-(trimethylsiloxy) furan
and β,β-disubstituted-acylimidazoles.
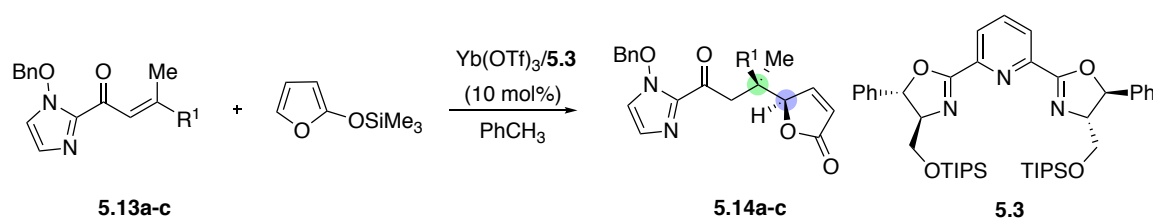
Entry	R^1	SM	Product	Yield (%)^a	dr^b	ee (%)^c
1	CF$_3$	**5.13a**	**5.14a**	98	4:1	98
2	Ph	**5.13b**	**5.14b**	98	96:04	98
3	Thienyl	**5.13c**	**5.14c**	95	92:08	99

Reaction conditions: **5.13a-c** (0.1 mmol), 2-(trimethylsiloxy)furan (0.2 mmol), Yb(OTf)$_3$ (0.01 mmol), **5.3** (0.011 mmol) MS 4Å (0.10 g) toluene (2 mL) were stirred at rt. ^{a} isolated yield. ^{b} determined by ^{1}H NMR analysis of crude reaction mixture. ^{c} determined by chiral HPLC.

5.2.3. Diastereoselective and enantioselective conjugate addition of azalactones to β-substituted-α,β-unsaturated acylimidazoles

Azalactones belong to a class of compounds known as oxazolones. These compounds are

important building blocks and they can be transformed to amino acids and other heterocycles.[7]

Conjugate addition of azalactones **5.15** to β-substituted-α,β-unsaturated acylimidazole **5.16**

could give two regioisomeric products **5.17** or **5.18** depending on if the conjugate addition of

azalactones takes place to either C-4 or C-2 carbon atoms respectively (Scheme 5.4).
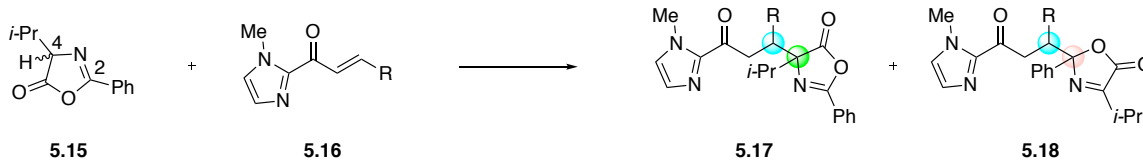
Scheme 5.4. Regioselectivity in azalactone addition.

Several catalytic conditions have been applied to the conjugate addition of azalactone

5.15 to acylimidazole **5.16a**. The results are summarized in Table 5.4. In the presence of

Pd(OAc)$_2$/**5.19** combination the conjugate addition of azalactone **5.15** (entry # 1, Table 5.4) did

not occur. Ni(OAc)$_2$ in combination with ligand (**5.9** or **5.19**) did not effect the conjugate

addition (entry # 2 and # 3, Table 5.4). When Cu(OAc)$_2$/**5.5** or **5.19** combination was used,

conjugate adduct **5.17** or **5.18** were not formed (entry # 4 and # 5, Table 5.4). Interestingly,

CuTC (TC = 2-thiophenecarboxylate)/**5.19** gave exclusively the regioisomer **5.17** as a single

diastereomer (relative and absolute stereochemistry of **5.17** was not determined).

Table 5.4. Regioselective and diastereoselective conjugate addition of azalactone to acylimidazole.
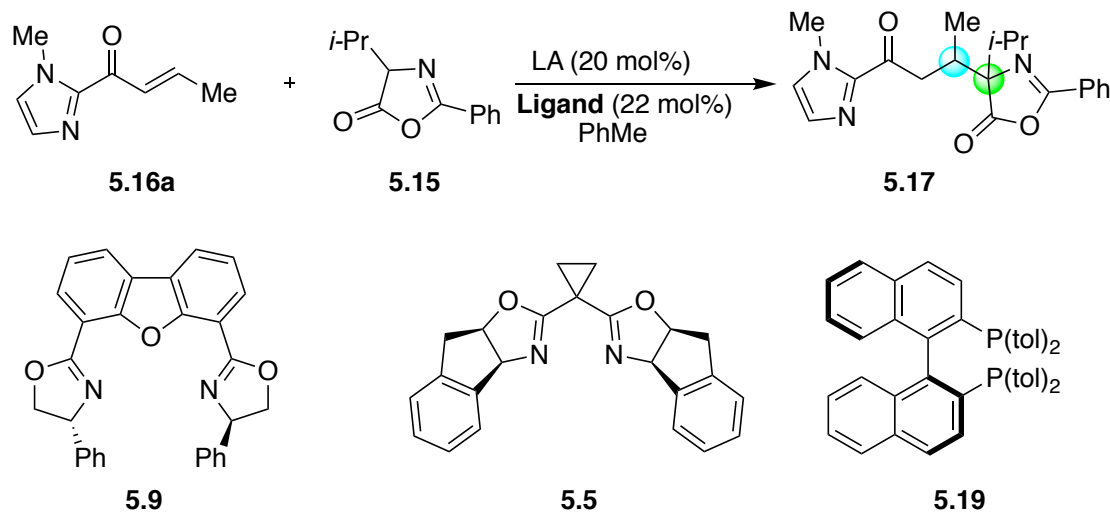
Entry	LA	Ligand	time	Yield (%)[a]	dr of **5.17**[b]
1	Pd(OAc)$_2$	**5.19**	5d	-	-
2	Ni(OAc)$_2$	**5.9**	5d	-	-
3	Ni(OAc)$_2$	**5.19**	5d	-	-
4	Cu(OAc)$_2$	**5.5**	3d	-	-
5	Cu(OAc)$_2$	**5.19**	3d	-	-
6	CuTC	**5.19**	3d	73	>40:1

Reaction conditions: **5.16a** (0.1 mmol), **5.15** (0.2 mmol), LA (0.01 mmol), Ligand (0.011 mmol) toluene (2 mL) were stirred at rt. [a] isolated yield. [b] determined by ^{1}H NMR analysis of crude reaction mixture. [c] determined by chiral HPLC.

5.3. Conclusions

Synthetic utility of 2-acylimidazoles have been discussed in this chapter. FC nucleophiles such as pyrroles have been added for the first time to tiglate type acylimidazoles with very high stereocontrol. The versatility of these substrates has been highlighted by its use in other reactions such as MM reaction for the construction of all carbon quaternary centers. Cyclic silyl ketene acetal with an α-substitution was added to β-substituted-α,β-disubstituted acylimidazole used to construct contiguous quaternary and tertiary centers with very high stereocontrol. On a similar note the same silyl ketene acetals have been successfully added to β,β-disubstituted-α,β-

disubstituted acylimidazole to form alkylated lactones bearing *two contiguous all carbon quaternary centers*. Other nucleophiles such as azalactone have been added with very high regio- as well as stereocontrol. The conjugate adducts of azalactones can be transformed to other useful synthetic building blocks.

5.4. Experimental section and supporting information

All solvents were dried and degassed by standard methods and stored under nitrogen. Flash chromatography was performed using EM Science silica gel 60 (230-400 mesh). ^{1}H NMR spectra were recorded on Varian Unity/Inova-400 NB (400 MHz) and Bruker (400 MHz) spectrometer. ^{13}C NMR spectra were recorded on Bruker (100 MHz) spectrometer. HPLC analyses were carried out with Waters 515 HPLC pumps and a 2487 dual wavelength absorbance detector connected to a PC with Empower workstation. Rotations were recorded on a JASCO-DIP-370 polarimeter. High-resolution mass spectra were obtained using Waters SYNAPT-G2-Si-HDMS spectrometer.

5.4.1. Synthesis of N-benzyloxy acylimidazole 5.1

Substrate **5.1** is synthesized according to Scheme 5.5.
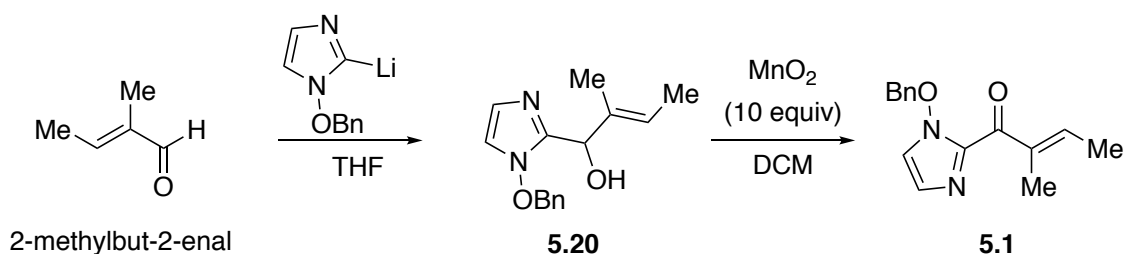
Scheme 5.5. Synthesis of β-substituted-α,α-disubstituted-α,β-unsaturated acylimidazole **5.1**.

BnO   OH

5.20

$C_{15}H_{18}N_2O_2$
Mol. Wt: 258.32
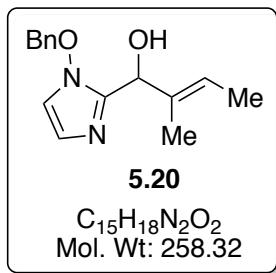
(2E)-1-[1-(Benzyloxy)-1H-imidazol-2-yl]-2-methylbut-2-en-1-ol (5.20): To a flame-dried flask N-benzyloxyimidazole (0.87 g, 5 mmol) and THF (20 mL) were added under Ar atmosphere. The reaction mixture was cooled to -78 °C and then *n*-BuLi (2.5 M in hexanes) (2 mL, 5 mmol) was added over 10 minutes and the mixture was stirred at -78 °C for 30 minutes. (E)-2-methylbut-2-enal (0.42 g, 5 mmol) dissolved in another 15 mL of THF was added slowly at -78 °C. The reaction was monitored by TLC. Upon completion of the reaction, the reaction was warmed to rt and then quenched using glacial acetic acid (6 equivalents). The reaction mixture was diluted with ethyl acetate and washed with saturated $NaHCO_3$ (3x100 mL), washed with brine (100 mL). The combined organic layers were dried over sodium sulfate, filtered and the filtrate was concentrated in vacuum to give alcohol **5.20** as crude brown oil, which was used without purification in the next step.

BnO   O

5.1

$C_{15}H_{16}N_2O_2$
Mol. Wt: 256.31
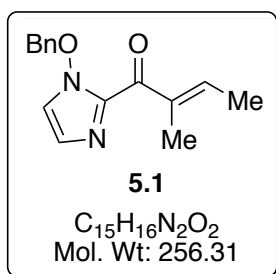
(2E)-1-[1-(benzyloxy)-1H-imidazol-2-yl]-2-methylbut-2-en-1-one (5.1): Compound **5.20** was dissolved in about 60 mL of dichloromethane. To this solution was added manganese dioxide (50 mmol) and the resulting suspension was stirred at room temperature for 48 h.

Dichloromethane was removed under vacuum and the residue was directly loaded on to a silica gel column and purified to give of a **5.1** as colorless oil (0.74 g, 58% yield).

^{1}H NMR (400 MHz, CDCl$_3$) δ 7.55 – 7.33 (m, 1H), 7.14 (dddd, J = 8.5, 7.1, 5.7, 1.5 Hz, 0H), 6.95 (dd, J = 6.2, 1.2 Hz, 0H), 5.36 (s, 2H), 2.06 – 1.83 (m, 1H). ^{13}C NMR (101 MHz, CDCl$_3$) δ 184.5, 144.7, 138.9, 137.2, 133.6, 130.1, 129.4, 128.7, 124.3, 120.2, 82.6, 15.2, 11.5. HRMS: Calcd for C$_{15}$H$_{16}$N$_2$O$_2$ [M+H^{+}]: 257.1285; Found: 257.1276.

5.4.2. General procedure for catalytic asymmetric alkylation of N-methylpyrrole

In a flame-dried 6-dram vial with magnetic stirbar was added Yb(OTf)$_3$ (0.01 mmol), ligand **5.3** (0.011 mmol) and tolune (4 ml). The mixture was stirred for 30 minutes after which appropriate acylimidazole substrate **5.1** (0.1 mmol) was added. After 5 minutes, N-methylpyrrole (0.2 mmol) was added and the mixture was stirred for 3 days. After the completion of reaction the mixture was directly loaded on to silica gel column and the product was separated.

5.4.3. General procedure for catalytic asymmetric MM reaction of silyl ketene acetal to α,β-unsaturated acylimidazole 5.6

In a flame-dried 6-dram vial with magnetic stirbar was added Yb(OTf)$_3$ (0.01 mmol), ligand **5.3** (0.011 mmol) and tolune (4 ml). The mixture was stirred for 30 minutes after which appropriate acylimidazole substrate **5.6** (0.1 mmol) was added. After 5 minutes, silyl ketene acetal **5.7** (0.2 mmol) was added and the mixture was stirred for 2h. After the completion of reaction, the solvent was evaporated, the residue was redissolved in CDCl$_3$ and crude NMR was taken to calculate the dr. After this CDCl$_3$ was removed under vacuum and the residue was purified by column chromatography.

5.8
C$_{19}$H$_{22}$N$_2$O$_4$
M. Wt.: 342.40
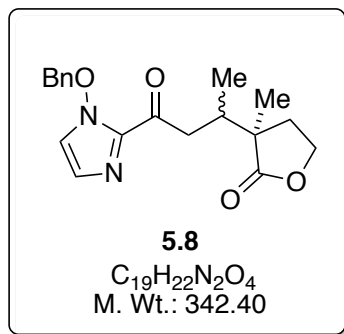
(3R)-3-{(2S)-4-[1-(Benzyloxy)-1H-imidazol-2-yl]-3-methyloxolan-2one (5.8): [1]H

NMR (400 MHz, CDCl$_3$) δ 7.50 – 7.35 (m, 5H), 6.95 (d, *J* = 1.1 Hz, 1H), 6.94 (d, *J* = 1.1 Hz,

1H), 5.25 (s, 2H), 4.41 – 4.06 (m, 2H), 3.16 (dd, *J* = 16.6, 10.2 Hz, 1H), 2.96 (ddd, *J* = 16.4, 3.0,

0.8 Hz, 1H), 2.71 – 2.53 (m, 1H), 2.49 – 2.29 (m, 1H), 2.01 – 1.85 (m, 1H), 1.31 (d, *J* = 4.6 Hz,

3H), 1.08 (s, 3H). ^{13}C NMR (101 MHz, CDCl$_3$) δ 187.3, 172.6, 154.0, 146.3, 138.4, 133.2,

130.0, 129.5, 128.7, 126.9, 125.1, 124.8, 124.3, 123.0, 122.3, 88.3, 82.1, 77.3, 77.0, 76.7, 47.7,

43.6, 20.6. HRMS: Calcd for C$_{19}$H$_{22}$N$_2$O$_4$ [M+H$^+$]: 343.1652; Found: 343.1666.

The ee value was determined by HPLC analysis using a CHIRALPAK AD3 column (1.0

mL/min, 10%, i-PrOH in hexane); retention times: 50.33 min (maj enantiomer) and 53.03 min

(min enantiomer).

5.4.4. Synthesis of substrates 5.13b and 5.13c

Substrates **5.13b** and **5.13c** are synthesized according to Scheme 5.6.
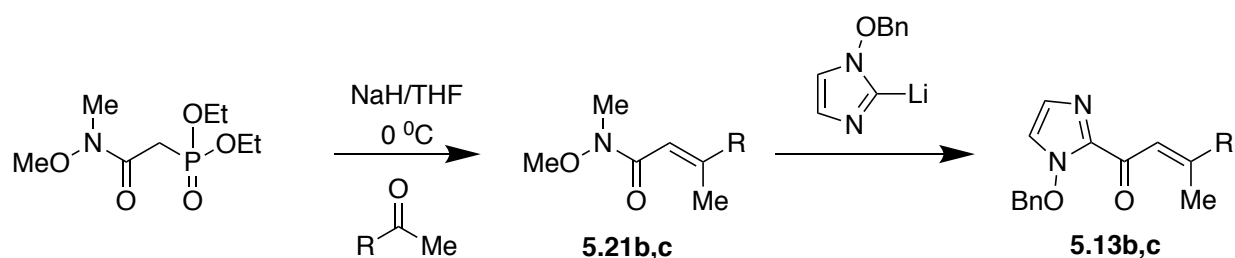
Scheme 5.6. Synthesis of substrates **5.13b**,**c**.

5.4.4.1. *Procedure for synthesis of 5.21b and 5.21c*

To a flame-dried 250 mL flask 250 mL round-bottom flask were addd NaH (20 mmol, 2.0 equiv) and THF (80 mL). The suspension was then coole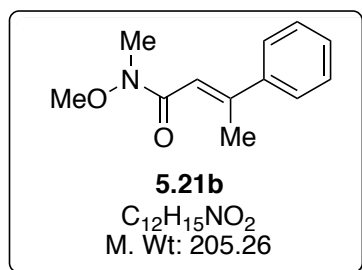d to 0 ^{0}C. Now, *N*-Methoxy-*N*-methyl-phosphonoacetamide diethyl ester (20 mmol, 2.0 equiv) dissolved in THF (10 ml) was added dropwise. The resulting mixture was allowed to stir at 0 ^{0}C for 15 minutes and at room temperature for 45 minutes. Then corresponding ketone (10 mmol, 1.0 equiv) was dissolved in THF (10 mL) was added. The solution was refluxed for 12 hours. The reaction was cooled to rt, quenched with NH$_4$Cl, extracted with ethyl acetate (3x100 mL). The combined organic layers were washed with brine, dried over MgSO$_4$, filtered and the solvent was removed in vacuo to give a crude product which, on purification by column chromatography gave 75 - 80% of **5.21**.

5.21b
C$_{12}$H$_{15}$NO$_2$
M. Wt: 205.26

(2E)-N-Methoxy-N-methyl-3-phenylbut-2-enamide (5.21b): ^{1}H NMR ((400 MHz, CDCl$_3$): δ 7.48-7.43 (m, 2H), 7.39-7.31 (m, 3H), 6.54 (s, 1H), 3.69 (s, 3H), 3.25 (s, 3H), 2.51 (d, J = 1.3 Hz, 3H). ^{13}C NMR (101 MHz, CDCl$_3$): δ 167.6, 154.8, 141.0, 128.1 (CH, 2C), 128.1 (CH, 2C), 125.7, 114.3, 61.0, 42.4, 33.6, 18.5. HRMS: Calcd for C$_{12}$H$_{15}$NO$_2$ [M+H$^+$]: 206.1181; Found: 206.1173.

5.21c
C$_{10}$H$_{13}$NO$_2$S
M. Wt: 211.28
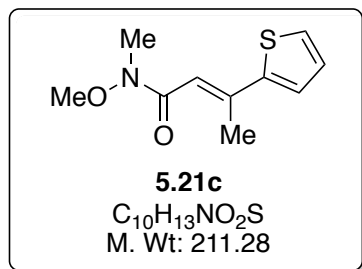
(2Z)-N-Methoxy-N-methyl-3-(thiophen-2-yl)but-2-enamide (5.21c): ^{1}H NMR (400 MHz, CDCl$_3$) δ 7.35-7.23 (m, 2H), 6.98 (dddd, J = 5.2, 3.7, 1.6, 0.8 Hz, 1H), 6.69 (s, 1H), 3.67 (s, 3H), 3.20 (s, 3H), 2.53 (s, 3H). ^{13}C NMR (101 MHz, CDCl$_3$) δ 167.8, 146.7, 145.3, 128.0, 126.4, 126.2, 113.3, 77.7, 77.3, 77.0, 61.8, 32.6, 17.6. C$_{10}$H$_{13}$NO$_2$S [M+H$^+$]: 212.0740; Found: 212.0753.

5.4.4.2. Synthesis of 5.13b,c

To a flame-dried flask N-benzyloxyimidazole (6 mmol) and THF (40 mL) were added under Ar atmosphere. The reaction mixture was cooled to -78 °C and then *n*-BuLi (2.5 M in hexanes) (6 mL, 25 mmol) was added over 10 minutes and the mixture was stirred at -78 °C for 30 minutes. Weinreb amide **5.21b,c** (6 mmol) dissolved in another 5 mL of THF was added slowly at -78 °C. The reaction was monitored by TLC. Upon completion of the reaction, the reaction was warmed to rt and then quenched using glacial acetic acid (6 equivalents). The reaction was diluted with ethyl acetate and washed with saturated NaHCO$_3$ (3x50 mL), washed with brine (50 mL). The combined organic layers were dried over sodium sulfate, filtered and the filtrate was concentrated in vacuum to give the crude solid, which was then purified by flash chromatography to give N-benzyloxyacylimidazoles **5.13b,c**.

5.13b
C$_{20}$H$_{18}$N$_2$O$_2$
M. Wt: 318.38
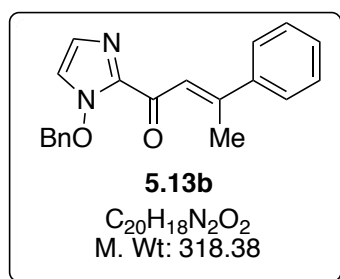
(2E)-1-[1-(Benzyloxy)-1H-imidazol-2-yl]-3-phenylbut-2-en-1-one (5.13b): Yellow solid. M.P: 65-68 °C. (0.30 g, 69%). ^{1}H NMR (400 MHz, CDCl$_3$): δ 7.73 (q, J = 1.3 Hz, 1H), 7.69-7.63 (m, 2H), 7.52-7.38 (m, 9H), 6.97 (d, J = 1.1 Hz, 1H), 6.90 (d, J = 1.1 Hz, 1H), 5.37 (s,

2H), 2.77 (d, J = 1.3 Hz, 3H). 13C NMR (101 MHz, CDCl$_3$): δ 179.7, 156.7, 142.5, 140.0, 133.5, 130.1 (CH, 2C), 129.4, 129.3, 128.7 (CH, 2C), 128.5 (CH, 2C), 126.7 (CH, 2C), 124.7, 121.7, 121.6, 82.2, 18.7. HRMS: Calcd for C$_{20}$H$_{19}$N$_2$O$_2$ [M+H$^+$]: 319.1447; Found: 319.1450.

5.13c
C$_{18}$H$_{16}$N$_2$O$_2$S
M. Wt: 324.40
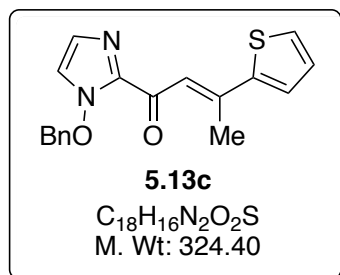
(2Z)-1-[1-(Benzyloxy)-1H-imidazol-2-yl]-3-(thiophen-2-yl) but-2-en-1-one (5.13c): ^{1}H NMR (400 MHz, CDCl$_3$) δ 7.42 – 7.28 (m, 5H), 7.25 – 7.20 (m, 1H), 7.17 (d, J = 5.1 Hz, 1H), 7.00 (d, J = 2.6 Hz, 1H), 6.96 – 6.90 (m, 1H), 6.87 (s, 1H), 6.82 (s, 1H), 6.07 (dd, J = 5.6, 1.7 Hz, 1H), 5.60 (s, 1H), 5.13 (s, 2H), 3.83 – 3.65 (m, 2H), 1.53 (s, 3H). ^{13}C NMR (101 MHz, CDCl$_3$) 187.3, 172.6, 154.0, 146.3, 138.4, 133.2, 130.0, 129.5, 128.7, 126.9, 125.1, 124.8, 124.3, 123.0, 122.3, 88.3, 82.1, 77.3, 77.0, 76.7, 47.7, 43.6, 20.6. HRMS: Calcd for C$_{20}$H$_{19}$N$_2$O$_2$ [M+H$^+$]: 325.1005; Found: 325.1009.

5.4.5. General procedure for catalytic asymmetric MM reaction of 2-(trimethylsiloxy)furan

In a flame-dried 6-dram vial with magnetic stirbar was added Yb(OTf)$_3$ (0.01 mmol), ligand **5.3** (0.011 mmol), MS 4Å (0.10 g) and tolune (4 ml). The mixture was stirred for 30 minutes after which appropriate acylimidazole substrate **5.1** (0.1 mmol) was added. After 5 minutes, 2-(trimethylsiloxy)furan (0.2 mmol) was added and the mixture was stirred for 1-2 days. After the completion of reaction, the solvent was evaporated, the residue was redissolved in CDCl$_3$ and crude NMR was taken to calculate the dr. After this CDCl$_3$ was removed under vacuum and the residue was purified by column chromatography.

5.14a

$C_{19}H_{17}F_3N_2O_4$

M. Wt.: 394.3502
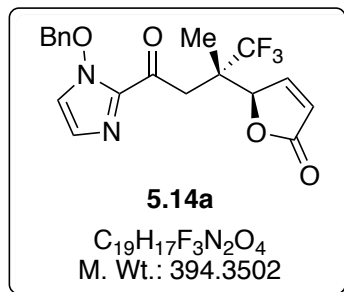
(S)-5-{(2S)-4-[1-(Benzyloxy)-1H-imidazol-2-yl]-1,1,1-trifluoro-2-methyl-4-oxobutan-2-yl}furan-2(5H)-one (5.14a): ^{1}H NMR (400 MHz, CDCl$_3$) δ 7.59 (dt, J = 5.8, 1.6 Hz, 1H), 7.45 – 7.32 (m, 5H), 6.93 (dd, J = 7.4, 1.1 Hz, 2H), 6.20 (dd, J = 5.9, 2.1 Hz, 1H), 5.76 – 5.70 (m, 1H), 5.28 – 5.19 (m, 2H), 3.76 (d, J = 15.5 Hz, 1H), 3.26 (d, J = 15.4 Hz, 1H), 1.30 (s, 3H). ^{13}C NMR (101 MHz, CDCl$_3$) δ 185.6, 171.5, 153.1, 138.1, 133.1, 131.1, 130.0, 129.6, 128.7, 128.3, 125.4, 122.9, 122.8, 82.3, 82.2, 77.3, 77.0, 76.7, 48.1, 47.8, 47.6, 47.3, 39.3, 34.2, 14.6, 14.6. HRMS: Calcd for $C_{19}H_{17}F_3N_2O_4$ [M+H^{+}]: 395.3577; Found: 395.3588.

The ee value was determined by HPLC analysis using a CHIRALPAK ASH column (1.0 mL/min, 10%, i-PrOH in hexane); retention times: 55.19 min (maj enantiomer) and 109.8 min (min enantiomer).

5.14b

$C_{24}H_{22}N_2O_4$

M. Wt.: 402.45
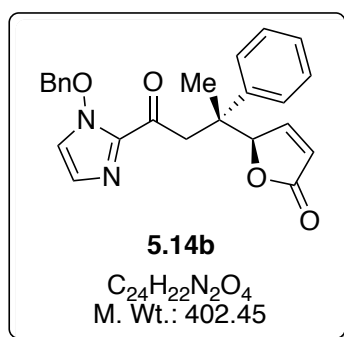
(S)-5-{(2S)-4-[1-(Benzyloxy)-1H-imidazol-2-yl]-4-oxo-2-(phenyl)butan-2-yl}furan-2(5H)-one (5.14b): ^{1}H NMR (400 MHz, CDCl$_3$) δ 7.45 – 7.39 (m, 2H), 7.38 – 7.27 (m, 5H), 7.26 – 7.18 (m, 3H), 7.01 (dd, J = 5.8, 1.5 Hz, 1H), 6.85 (d, J = 1.1 Hz, 1H), 6.76 (d, J = 1.1 Hz, 1H), 6.04 (dd, J = 5.8, 2.1 Hz, 1H), 5.55 – 5.44 (m, 1H), 5.08 – 4.96 (m, 2H), 3.93 (d, J = 16.0

Hz, 1H), 3.62 (d, $J = 16.0$ Hz, 1H), 1.49 (s, 3H). ^{13}C NMR (101 MHz, CDCl$_3$) δ 187.7, 172.7, 154.0, 141.5, 138.5, 133.2, 130.0, 129.4, 128.6, 128.6, 127.2, 126.3, 124.9, 123.0, 122.1, 89.1, 82.0, 77.3, 77.0, 76.7, 47.1, 44.4, 18.0. HRMS: Calcd for C$_{24}$H$_{22}$N$_2$O$_4$ [M+H$^+$]: 402.1580; Found: 402.1596.
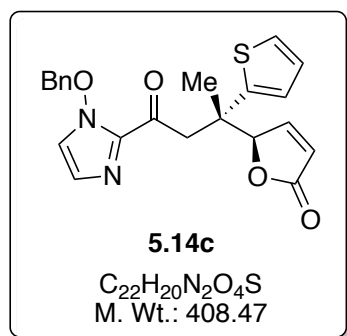
The ee value was determined by HPLC analysis using a CHIRALPAK IA column (1.0 mL/min, 10%, i-PrOH in hexane); retention times: 24.19 min (maj enantiomer) and 27.52 min (min enantiomer).

5.14c
C$_{22}$H$_{20}$N$_2$O$_4$S
M. Wt.: 408.47

(S)-5-{(2S)-4-[1-(Benzyloxy)-1H-imidazol-2-yl]-4-oxo-2-(thiophen-2-yl)butan-2-yl}furan-2(5H)-one (5.14b): ^{1}H NMR (400 MHz, CDCl$_3$) δ 7.42 – 7.28 (m, 5H), 7.26 – 7.14 (m, 2H), 7.00 (d, $J = 2.6$ Hz, 1H), 6.97 – 6.90 (m, 1H), 6.87 (s, 1H), 6.82 (s, 1H), 6.07 (dd, $J = 5.6$, 1.7 Hz, 1H), 5.60 (s, 1H), 5.13 (s, 2H), 3.84 – 3.62 (m, 2H), 1.53 (s, 3H). ^{13}C NMR (101 MHz, CDCl$_3$) δ 187.3, 172.6, 154.0, 146.3, 138.4, 133.2, 130.0, 129.5, 128.6, 126.9, 125.1, 124.8, 124.2, 123.0, 122.3, 88.3, 82.1, 77.3, 77.0, 76.7, 47.7, 43.6, 20.6. HRMS: Calcd for C$_{22}$H$_{20}$N$_2$O$_4$S [M+H$^+$]: 409.1217; Found: 409.1226.

The ee value was determined by HPLC analysis using a CHIRALPAK IA column (1.0 mL/min, 10%, i-PrOH in hexane); retention times: 100.14 min (maj enantiomer) and 127.54 min (min enantiomer).

5.5. References

1. *Comprehensive Asymmetric Catalysis;* Jacobsen, E. N., Pfaltz, A., Yamamoto, H., Eds.; Springer: Berlin, 1999; Vol I−III. (b) *Lewis Acids in Organic Synthesis;* Yamamoto, H., Ed.; Wiley-VCH: Weinheim, 2000, Vol 1−3. (c) Bauer, E. B. *Chem. Soc. Rev.* **2012**, *41*, 3153. (d) Heitbaum, M.; Glorius, F.; Escher, I. *Angew. Chem., Int. Ed.* **2006**, *45*, 4732. (e) A*symmetric catalysis on Industrial Scale: Challenges, Approaches and Solutions;* Blaser, H.; Schmidt, E. Eds.; Wiley-VCH Verlag GmbH & Co. KgaA: Weinheim, 2004. (f) Schmid, A.; Dordick, J. S.; Hauer, B.; Kiener, A.; Wubbolts, M.; Witholt, B. *Nature* **2001**, *409*, 258. (g) *Asymmetric Organocatalysis: From Biomimetic Concepts to Applications in Asymmetric Synthesis;* Berkessel, A.; Gröger, H. Eds.; Wiley-VCH Verlag GmbH & Co. KgaA: Weinheim, 2005. (h) Moisan, L. *Angew. Chem., Int. Ed.* **2001**, *40*, 3726. (i) *Enantioselective Organocatalysis: Reactions and Experimental Procedures;* Dalko P. I. Ed.; Wiley-VCH Verlag GmbH & Co. KgaA: Weinheim, 2007. (j) Bertelsen, S.; Jørgensen, K. A. *Chemical Society Reviews* **2009**, *38*, 2178. (k) *Catalytic Asymmetric Synthesis;* Ojima, I. Ed.; Wiley-VCH Verlag GmbH & Co. KgaA: Weinheim, 2010.

2. (a) Sibi, M. P.; Rane, D.; Stanley, L. M.; Soeta, T. *Org. Lett.* **2008**, *10*, 2971. (b) Sibi, M. P.; Stanley, L. M.; Nie, X.; Venkatraman, L.; Liu, M.; Jasperse, C. P. *J. Am. Chem. Soc.* **2007**, *129*, 395. (c) Adachi, S.; Takeda, N.; Sibi, M. P. *Org. Lett.* **2014**, *16*, 6440. (d) Sibi, M. P.; Itoh, K.; Jasperse, C. P. *J. Am. Chem. Soc.* **2004**, *126*, 5366.

3. (a) Sibi, M. P.; Coulomb, J.; Stanley, L. M. *Angew. Chem., Int. Ed.* **2008**, *47*, 9913. (b) Sibi, M. P.; Gustafson, B.; Coulomb, J. *Bull. Korean Chem. Soc.* **2010**, *31*, 541.

4. (a) Takenaka, N.; Abell, J. P.; Yamamoto, H. *J. Am. Chem. Soc.* **2007**, *129*, 742. (b) Rout, S.; Ray, S. K.; Singh, V. K. *Org. Biomol. Chem.* **2013**, *11*, 4537. (c) Li, H.; Wu, J. *Org. Lett.*

2015, *17*, 5424. (d) George, J.; Reddy, B. V. S. *Adv. Synth. Catal.* **2013**, *355*, 383. (e) Nagatani, K.; Minami, A.; Tezuka, H.; Hoshino, Y.; Nakada, M. *Org. Lett.* **2017**, *19*, 810.

5. (a) Veselovsky, V. V. *Russ. Chem. Rev.* **2009**, *78*, 337. (b) Barbosa, L. C. A.; Teixeira, R. R.; Amarante, G. W. *Curr. Org. Synth.* **2015**, *12*, 746. (c) Bassetti, M.; D'Annibale, A. *Curr. Org. Chem.* **2013**, *17*, 2654. (d) Zhang, Q.; Liu, X.; Feng, X. *Curr. Org. Synth.* **2013**, *10*, 764. (e) Mao, B.; Fananas-Mastral, M.; Feringa, B. L. *Chem. Rev.* **2017**, *117*, 10502.

6. (a) Li, X.; Lu, M.; Dong, Y.; Wu, W.; Qian, Q.; Ye, J.; Dixon, D. J. *Nat. Commun.* **2014**, *5*, 4479. (b) Brown, S. P.; Goodwin, N. C.; MacMillan, D. W. C. *J. Am. Chem. Soc.* **2003**, *125*, 1192-1194.

7. (a) Fisk, J. S.; Mosey, R. A.; Tepe, J. J. Chem. Soc. Rev. **2007**, *36*, 1432. (b) Ale´man, J.; Milelli, A.; Cabrera, S.; Reyes, E.; Jørgensen, K. A. Chem.- Eur. J. **2008**, *14*, 10958. (c) Uraguchi, D.; Ueki, Y.; Ooi, T. Science **2009**, *326*, 120.